Investigating the potential of therapeutically targeting the Insulin and Insulin-like Signalling Cascade in neurodegeneration

Joshua Paulin

UCL

Thesis submitted for partial fulfilment of the degree of Doctor of Philosophy

November 2016

Declaration

I declare that the work presented herein is my own, except where indicated below.

The processing of TG4510 tissue for protein analysis and RNA analysis, and subsequent western blotting and RT-qPCR was carried out by a BSc student in the lab; Barbora Ondrejickova. Subsequent analysis of the data and arrangement of data for presentation was carried out by me.

The preparation of organotypic hippocampal slices from GFP-S mice was carried out by Damian Cummings.

Intracerebroventricular injections were performed by Dervis Salih with surgical assistance from myself.

Acknowledgements

Firstly I would like to thank Dr Frances Edwards for allowing me to work in her lab for the past 5 years. I am immensely thankful for this opportunity, but most of all for the space to explore my own ideas and become a more independent researcher.

A special thank you must go to Dr Dervis Salih, who has taught me nearly all the practical skills I know. Without his help and patience I would not have been able to complete this PhD.

A huge amount of thanks go to my fellow lab members. The lab would not function without Damian, and my time would not have been half as enjoyable if not for every person who I had the pleasure of sharing the lab with over the years.

I would finally like to thank Eisai for funding this PhD, and Peter Atkinson and Lee Dawson for their guidance and advice.

Abstract

Decreasing signalling through the Insulin and Insulin-like Signalling (IIS) cascade by genetic and pharmacological means can increase the lifespan and healthspan of many organisms. Crucially, when long-lived animals are crossed with animal models of neurodegenerative disorders, the onset of pathology is slowed. Pharmacological inhibitors of the IIS cascade have also shown neurodegeneration delaying and neuroprotective properties. Furthermore, IIS is changed in neurodegenerative disorders; with increased astrocyte IGF1, localised increased ERK1/2 phosphorylation (p-ERK), and brain insulin and IGF1 resistance observed. The IIS cascade therefore seems critically implicated in neurodegeneration, and crucially via pharmacological means could yield disease-modifying interventions.

To investigate pharmacological IIS manipulation for therapeutic gain in neurodegeneration, I firstly characterised changes in IIS in human Alzheimer's Disease patient brain samples, and in brain samples of mice modelling rising amyloid beta and plaque levels, or rising hyperphosphorylated tau and tangle levels; finding increased IIS at early ages in these models. I subsequently designed a bilaminar neuron and astrocyte co-culture model of acute neurodegeneration, whereby I identified that increased astrocyte *Igf1* expression following a noxious stimulus is dependent on the presence of neurons during stress. I then manipulated IIS during the noxious stimulus by either knocking down increased *Igf1* expression, inhibiting p-ERK with the drug Trametinib, or both. I identified that increased astrocyte *Igf1* expression contributes to neuronal cell death, and that Trametinib was protective against neuronal cell death, but the mechanism of *Igf1* induced neuronal cell death was not due to increase p-ERK. This confirms IIS as a viable pharmacological target for intervening in neurodegeneration.

Table of contents

Chapter 1 – Introduction

Chapter 2 – Materials and Methods

Chapter 3 – Characterising endogenous changes to the Insulin an Insulin-like Signaling Cascade in Alzheimer's Disease

Chapter 4 – Implications of increased *Igf1* expression on acute neurodegeneration

Chapter 5 – Repurposing clinically approved IIS inhibitors to treat acute neurodegeneration

Chapter 6 – Discussion

Table of abbreviations

Abbreviation	Description	Synonym
ACSF	Artificial cerebral spinal fluid	
AD	Alzheimer's disease	
Akt	Protein kinase B	
AMPK	5' AMP-activated protein kinase	
ANOVA	Analysis of variance	
APP	Amyloid precursor protein	
APP-KI	Humanised amyloid beta knock-in mouse strain, specifically the NL-G-F/NL-G-F strain	
ATP	Adenosine triphosphate	
Aβ	Amyloid beta components - any pro-amyloidogenic amyloid beta cleavage fragments	
Aβ40	Amyloid beta 1-40 – amyloid beta fragment of 40 amino acids length	
Aβ42	Amyloid beta 1-42 – amyloid beta fragment of 42 amino acids length	
b-Raf	B-Raf proto-oncogene serine/threonine kinase	BRAF1
BACE1	Beta-secretase 1	
Bcrp	Breast cancer resistant protein	ABCG2
c-Abl	ABL proto-oncogene 1 non-receptor tyrosine kinase	
c-Raf	Raf-1 proto-oncogene serine/threonine kinase	RAF1, CRAF
C57BL/6J	C57 Black 6 mouse line	
CA1	Cornu Ammonis region 1	
CAMKIIα	Ca2+/ calmodulin dependent protein kinase II	
CC3	Cleaved caspase 3	
cDNA	Complementary deoxyribonucleic acid	
Daf2	Caenorhabditis elegans Igf1 receptor	
DAPI	4'6-diamidino-2-phenylindole	
DIV	Days in vivo	
DMSO	Dimethyl sulfoxide	
DOKS	Dok protein family	
ELK1	Ets domain-containing transcription factor family	
ERK1	Mitogen-activated protein kinase 3	ERK1, p44erk1, p44mapk
ERK1/2	Extracellular signal–regulated	

	kinases	
ERK2	Mitogen-activated protein kinase 1	ERK, ERK2, MAPK2, p41mapk
fAD	Familial Alzheimer's disease	
FOXO	Forkhead box family of transcription factors subtype O	
FPKM	Fragments per kilobase of transcript sequence per million mapped fragments	
FTD	Frontotemporal dementia	
FVB/N	Friend Virus B mouse strain	
Fyn	Proto-oncogene tyrosine-protein kinase Fyn	
GABS	Grb2-associated binder family adapter proteins	
GFP-S	Green fluorescent protein strain S	
GluA2	Glutamate ionotropic receptor AMPA type subunit 2	GRIA2
GluN2B	Glutamate ionotropic receptor NMDA type subunit 2B	GRIN2B
GSK3	Glycogen synthase kinase 3	
Hif2a	Hypoxia inducible factor 2 a	EPAS1
ICV	Intracerebroventricular	
IGF1	Insulin-like growth factor 1	IGF-I, IGF1A, IGFI, somatomedin C
IGF1R	Insulin-like growth factor 1 receptor	CD221, JTK13
IGF2	Insulin-like growth factor 2	FLJ44734, Somatomedic A
IGF2R	Insulin-like growth factor 2 receptor	CD222
IGFBP	Insulin-like growth factor binding proteins	
IIS	Insulin and insulin-like signalling	
IP	Intraperitoneal	
IR	Insulin receptor	
IRS1	Insulin receptor substrate 1	HIRS-1
IRS2	Insulin receptor substrate 2	
KD	Knock down	
MAPK	Mitogen-activated protein kinase	
MAPT	Microtubule associated protein tau	
MCAO	Middle cerebral artery occlusion	
MCI	Mild cognitive impairment	
MEK	Mitogen-activated protein kinase kinase family	

MEK1	Mitogen-activated protein kinase kinase 1	MAP2K1
MEK2	Mitogen-activated protein kinase kinase 2	MAP2K2
MND	Motor neuron disease – Lou Gerrings	
NFT	Neurofibrillary tangles	
NMDA	N-Methyl-D-aspartic acid	
NS	Not significant	
p-ERK	Phosphorylated ERK1/2	
P-gp	P-glycoprotein	ABCB1, Abcb1a
p-Tau	Phosphorylated microtubule associated protein tau	
PBS	Phosphate buffered saline	
PD	Parkinson's disease	
PDK1	3-phosphoinositide dependent protein kinase 1	PDPK1, PkB kinase
PFA	Paraformaldehyde	
PI3K	Phosphatidylinositol 3-kinase family	
PP2A	Protein phosphatase 2 A	
pS-Akt	Phosphoserine phosphorylated Akt	
PSEN1	Presenilin 1	
pT-Akt	Phosphotyrosine phosphorylated Akt	
PTPN5	Protein tyrosine phosphatase non-receptor type 5	STEP
PyK2	Protein tyrosine kinase 2 beta	PTK2B
Ras	Small GTPase superfamily	
RNA	ribonucleic acid	
RNA-seq	RNA sequencing	
RPS28	Ribosomal protein S28	S28
RT-qPCR	Real Time quantitative polymerase chain reaction	
sAD	Sporadic Alzheimer's disease	
SDS-PAGE	Sodium dodecyl sulfate polyacrylamide gel electrophoresis	
SEM	Standard error of the mean	
siRNA	Small interfering ribonucleic acid	
t-Akt	Total Akt	
t-ERK	Total ERK1/2	
TBI	Traumatic brain injury	
TBS	Tris buffered saline	
TBST	Tris buffered saline containing 0.1% Tween20	

	0.1% Tween20
TG4510	rTg(tauP301L)4510 transgenic mouse strain
Trametinib+KD	Trametinib and Igf1 siRNA joint treatment
TRE	Tetracycline operon-responsive element
WB	Western blotting
WT	Wild type

Chapter 1

Introduction

Neurodegenerative Diseases and their growing burden on humanity

Through the endeavours of biomedical research human life expectancy has been greatly increased. The success in limiting death from early and midlife causes of mortality has lead to diseases that were previously rare, as they mainly afflicted the old, now being the leading causes of death. Not only is the global prevalence of neurodegenerative diseases increasing rapidly, but also there are insufficient therapeutic options for treating them. In this thesis we address the urgent need for improved therapeutics for a family of diseases that are increasing in prevalence at a particularly rapid rate – the neurodegenerative diseases.

One molecular pathway seems uniquely poised to offer us the possibility of intervening in the neurodegenerative process. Signalling levels through the Insulin and Insulin-like Signalling (IIS) cascade have been shown to modulate the rate of ageing in organisms from worms to man, but also be able to modulate the rate of neurodegenerative disease development in experimental animal models of neurodegenerative disease. Furthermore, changes in the IIS cascade have been implicated as neuronal cell death signals, and endogenous alterations in IIS have been reported in a variety of neurodegenerative diseases. All of these features together implicate the IIS cascade as playing a central role in neuronal health and diseases, and therefore offer an alternative route to modulating neurodegeneration. Our overall aim therefore is to examine IIS in neurodegenerative disease, and investigate the possibility of modulating this cascade as a means of providing novel therapeutic approaches to ameliorating neuronal cell death.

Suitable neurodegenerative diseases for IIS therapeutic intervention

Neurodegenerative diseases are a wide and varied group, but all have the common feature of a progressive permanent loss of neurons. With adult neurogenesis being limited (Altman and Das, 1965; Lois et al., 1996), and with the overwhelming majority of adult neurons being made during embryogenesis, the neuronal cell loss in neurodegenerative diseases cannot be repaired and is therefore permanent. Considering that the oldest know living mammal, the bowhead whale, is estimated to have a lifespan of over 200 years, this means that individual neurons are capable of surviving for hundreds of years (Keane et al., 2015). Furthermore it seems that the host species limits the length of time that a neuron can survive for, not the neurons themselves (Magrassi et al., 2013). Given the potential lifespan of these neurons therefore, it seems sensible to view neurodegeneration as the premature death of neurons, with neurons having an extraordinary capacity to survive.

For such a prevalent group of diseases, the therapeutic interventions available are extremely limited. Most therapeutic interventions are disease pathology specific, with only Riluzole attempting to target a mechanism of neurodegeneration, in this case by preventing glutamate educed excitotoxicity (Doble, 1996). With many recent phase III trials for novel neurodegenerative therapies failing, and the burden of these diseases on society growing with the ageing population, the need for more effective therapies is great. With neuronal death being permanent, and being a ubiquitous feature in these diseases, it seems clear that therapies that target neuronal death itself have not been fully utilised in the attempted treatment of neurodegenerative diseases.

Neurodegenerative diseases can be demarcated into two groups based upon the length of time that neuronal cell death occurs over; with chronic neurodegenerative diseases experiencing neuronal loss over the duration of months and years, and acute neurodegenerative diseases showing neuronal loss over the duration of days to weeks. Typically the term neurodegenerative disease has only been applied to diseases which in this thesis I classify as chronic neurodegeneration, but I think the progressive loss of neurons also observed in acute neurodegenerative diseases, albeit over a shorter

time frame, makes grouping these diseases together useful. The reason behind this is that I think it seems more likely that the molecular underpinnings of neuronal cell death in these diseases will overlap, rather than there being distinct mechanisms of neurodegeneration for each disease.

We have focused our attentions in this thesis on the chronic neurodegenerative disease Alzheimer's disease (AD), and more generally acute neurodegenerative diseases such as stroke and traumatic brain injury (TBI). These diseases are the most prevalent neurodegenerative diseases, with both sets having insufficient therapies currently available, and therefore are the neurodegenerative diseases in most dire need to investigation with regards to unearthing new therapeutics. Most importantly, both have been shown to be susceptible to possible therapeutic intervention by IIS modulation (Ashabi et al., 2013; Cohen et al., 2009; Gladbach et al., 2014).

Alzheimer's disease

Dementia is a family of diseases primarily affecting people over the age of 60, clinically defined as a gradual decline in cognitive function and memory loss over the space of years. Progressive gradual memory loss is the most distinctive characteristic, but as the disease progresses cognitive ability reduces, with language and behavioural changes common (World Health Organisation, 1992). Dementias are estimated to have a global cost of US$ 818 billion, which equates to 1.09% of global GDP (Alzheimer's Disease International, 2015). This figure is expected to top US$ 2 trillion by 2030.

ADis the most common subtype of dementia, followed by vascular dementia, Lewy body dementia, and frontotemporal dementia (FTD). Whilst each type of dementia has distinct pathological hallmarks, the extent of an overlap of pathology between these types of dementia is substantial. Distinct from acute neurodegenerative diseases there is often not one clear initiating factor for dementia in patients, with the exception of autosomal dominantly inherited forms of dementia with high penetrance (>95%) such as familial Alzheimer's disease (fAD), or frontotemporal dementia with

a *MAPT* mutation (Bekris et al., 2010; Hutton et al., 1998). These inherited forms of dementia are by far in the minority however, with the vast majority of dementias being sporadic in nature. In these sporadic cases, whilst genetic contributing factors may be apparent, this does not solely dictate the emergence of the disease phenotype in a patient.

Sporadic AD (sAD) patients present with symptoms typically from 60 years, with the average disease duration from diagnosis being 8-10 years. Prior to this clinical stage is a long prodromal period however, with cognitive decline present for years before diagnosis (Amieva et al., 2008; Lim et al., 2013). When a patient presents with the early phenotype of mild amnesia, they are diagnosed with Mild Cognitive Impairment (MCI), with a distinguishable clinical phenotype from dementia (Petersen et al., 1999). MCI often progresses to dementia, with a conversion rate between 6-15% of MCI patients per year, of which 90% progress to sAD (Farias et al., 2009; Fischer et al., 2007; Solfrizzi et al., 2004). Therefore the neuronal loss present in the dementias and sAD takes place over decades, rather than weeks as in acute neurodegenerative diseases.

The neuropathological hallmarks of AD are the presence of extracellular protein accumulations in the form of senile plaques composed of aberrantly folded amyloid beta 42 (Aβ42) and intracellular neurofibrillary tangles (NFT's) of hyperphosphorylated microtubule associated protein tau, combined with a reduction in volume of the frontal and parietal cortices and increased ventricle size. Due to the defining properties of these hallmarks when separating AD from other dementias, they have justifiably attracted much attention as a source of potential therapeutic target.

With the causative factor of sAD being hard to ascertain, focus was placed on identifying what caused the emergence of fAD, and thereby involved characterisation of the genetic mutations that give rise to a patients developing fAD. This identified various mutations in the amyloid-processing pathway (Goate et al., 1991), which results in altered processing of amyloid precursor protein (APP) into Aβ fragments (figure 1.1, (Crews et al., 2010; Haass et al., 2012)). Usually APP is overwhelmingly sequentially cleaved by α-secretase and γ-secretase (a complex containing presenilin

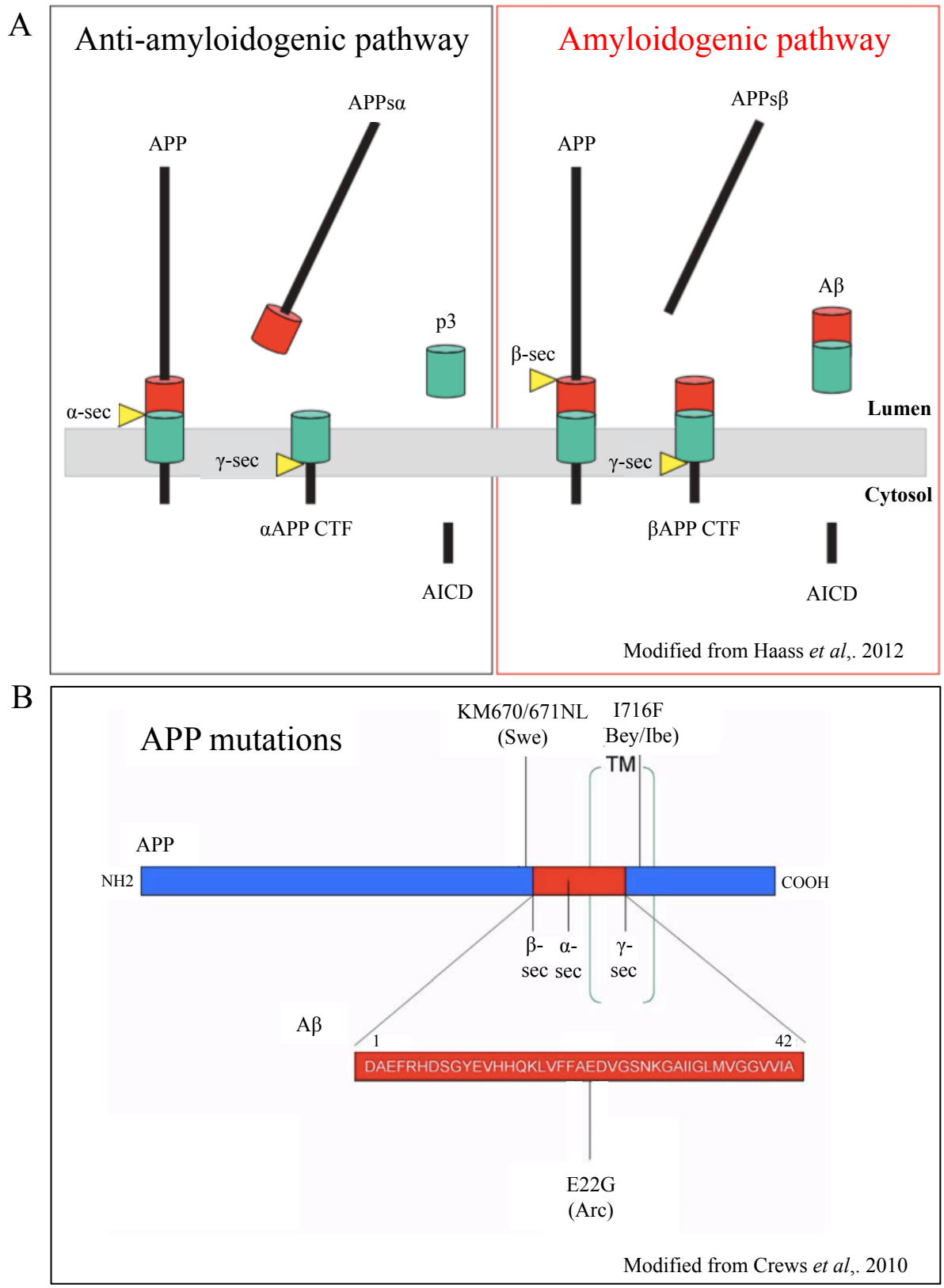

Figure 1.1. The amyloid processing pathway and position of APP mutations. Simplified diagrammatic representation of the processing of membrane bound APP, and the location of some APP mutations on the APP protein. (A) APP is cleaved either by α or β-secretase before being processed by γ-secretase. In the amyloidogenic pathway the sequential cleavage by β-secretase then γ-secretase produces amyloidogenic Aβ fragments. (B) The location of 3 APP fAD mutations. APP – amyloid precursor protein, α-sec – alpha secretase, β-sec – beta secretase, γ-sec – gamma secretase, CTF – carboxy-terminal fragment, AICD – APP intracellular domain, Swe – Swedish, Bey/Ibe - Beyreuther/Iberian, Arc – Arctic.

1), producing non-amyloidogenic components, but in fAD mutations at various points in the APP processing pathway lead to preferential cleavage of APP by β-secretase (BACE) leading to amyloidogenic Aβ fragments being produced. These mutations not only result in a higher ratio of Aβ42 to Aβ40, but also an increase in total Aβ level, with Aβ42 fragments forming oligomers and eventually plaques (Burdick et al., 1992; Chen and Glabe, 2006; Scheuner et al., 1996). This combined with the cerebrovascular amyloid protein accumulations present in late life dementia in people with Down's syndrome being very similar to beta amyloid in fAD, lead to the establishment of the Amyloid Hypothesis (Glenner and Wong, 1984; Hardy and Higgins, 1992), which puts amyloid accumulation as the central pathogenic mechanism of AD development, with all subsequent neurodegeneration and neurological changes a result of this.

Despite studies showing the deleterious effects of accumulated Aβ to various cells of the brain and their normal functioning, the Aβ toxicity observed seemed to be dependant on and facilitated by tau (Ittner et al., 2010; Jin et al., 2011; Rapoport et al., 2002; Roberson et al., 2007; Shipton et al., 2011). Furthermore, cognitive decline shown in AD patients did not correlate well with the increase in Aβ plaques, but did correlate well with NFT increase, neuronal loss, and synaptic loss (Arriagada et al., 1992; Giannakopoulos et al., 2003; Gomez-Isla et al., 1997; Gomez-Isla et al., 1996; Terry et al., 1991). Despite this correlation, whether these large insoluble NFT's or indeed Aβ plaques, represent a toxic species in themselves, or whether they represent a protective accumulation of smaller more toxic constituents, has recently come under fierce scrutiny.

It is becoming apparent that Aβ plaques are not the harmful species, but in fact the soluble oligomers cause a range of alterations in normal neuron physiology (Lambert et al., 1998; Shankar et al., 2007). It appears that this is also the case with NFT's, with small constituent oligomers the toxic species rather than the NFT itself (Lasagna-Reeves et al., 2011; Patterson et al., 2011). This is supported by human tauopathy patients showing high levels of neurodegeneration accompanied by high levels of tau phosphorylation, but only mild NFT formation (Bird et al., 1999). With the identification of what appears to be the specific species that give rise to toxicity in the

brains of dementia patients, efforts are now being undertaken to pharmacologically target these to elicit therapeutic gain.

Current therapeutics for Alzheimer's disease

Presently the extent of therapeutic intervention in AD is limited to symptomatic treatments that temporarily stem the decline in cognitive function in patients. Cholinesterase inhibitors (Donepezil, Galantamine, and Rivastigmine) are prescribed to mild and moderate AD patients to target the early degeneration and loss of long projecting cholinergic neurons in the forebrain, temporarily amplifying the dwindling signals from these pathways that contribute to memory and attention (Bird et al., 1983; Birks, 2006; Davies and Maloney, 1976; National Institute for Health and Clinical Excellence, 2011). Memantine, a NMDA receptor antagonist, is also prescribed for moderate and severe AD with limited clinical efficacy (McShane et al., 2006; National Institute for Health and Clinical Excellence, 2011). The effects of these drugs are short lived however, and make no attempt to target the cause of the disease or ameliorate the neurodegeneration present.

To disturb the accumulation of amyloid plaques, the drugs semagacestat and avagacestat were designed to inhibit the gamma secretase component of the amyloid-processing pathway. This branch is responsible for preferentially cleaving the amyloid precursor protein into the amyloidogenic Aβ42 rather than the non-amyloidogenic Aβ40 (Haass et al., 2012). These drugs showed little clinical efficacy however, with limited prevention of cognitive decline and side effects from the inhibition of the non-pathogenic functions of gamma secretase (Coric et al., 2012; De Strooper et al., 1999; Haapasalo and Kovacs, 2011). To bypass this, inhibitors of another member of the amyloidogenic branch of the APP processing pathway, BACE1, have been designed and show far more promising results in early clinical trials, although other protein targets of BACE1 mean off target effects are similarly a concern (Eisai, 2012; Forman et al., 2012).

Trials directly attempting to remove rather than prevent the build up of Aβ have also been attempted with the development of the passive Aβ immunotherapy drugs Bapineuzemab and Solineuzemab, both targeting the removal of Aβ oligomers from the central nervous system. Whilst the removal of Aβ was apparently achieved in these trials as measured by Pittsburg compound B imaging and peripheral Aβ oligomer levels, cognitive decline was not slowed in the Bapineuzemab trials, and was only slowed in the mild AD patients in the Solineuzemab trails (Doody et al., 2014; Farlow et al., 2012; Rinne et al., 2010; Salloway et al., 2014; Sperling et al., 2012). This positive result in the Solineuzemab trials has lead to on-going trials targeting patients earlier in the disease, either when they are likely to develop fAD as they have familial mutations in the DIAN trial, or in cognitively normal adults who show increased brain amyloid accumulation in the A4 trial (Alzheimer's Association, 2015; ClinicalTrials.gov, 2016a, b). Other Aβ clearance methods have also been employed in an attempt to stimulate the supposed natural clearance of Aβ, but with limited success at phase II trials for Crenezumab, or phase III trials for Gammagard (Adolfsson et al., 2012; Roche, 2014). Similarly to the Solineizemab trials, the Alzheimer's Prevention Initiative Trial using Crenezumab is currently underway, focusing on pre-emptively treating those likely to develop AD before the onset of symptoms, in this case in people with dominant presenillin mutations (Genentech, 2012).

Directly targeting tau species for therapeutic gain has not been a pharmaceutical priority given the predominance of amyloid processing mutations that give rise to fAD, and limited genetic indications of tau being an upstream factor in the pathogenesis of AD (Kauwe et al., 2008). Two main areas are now being explored however to try and treat AD by reducing the impact of toxic tau on the brain; either by reducing tau hyperphosphorylation, or by stopping the aggregation of tau tangles.

Very few tau kinase inhibitors have moved past preclinical trails. This is due to the vast number of phosphorylation sites on the tau protein and the promiscuity of the kinases that phosphorylate these sites (Pierre and Nunez, 1983), leading to off target effects when inhibiting these kinases. Even therapies that have progressed, for example the GSK3 inhibitors lithium and tideglusib, have failed to show sufficient benefit, or in doses where cognitive decline is slowed, have frequently shown off

target side effects (del Ser et al., 2013; Dominguez et al., 2012; Forlenza et al., 2011; Grogan, 2012; Hampel et al., 2009; Nunes et al., 2013).

Increasing the activity of phosphatases that dephosphorylate tau has also been explored as a pharmacological target. One of the mechanisms of action of selenium salts and the anti-diabetic drug metformin, is to potentiate the activity of protein phosphatase 2A (PP2A), which dephosphorylated many proteins including tau (Yamamoto et al., 1988). Despite potentially contradictory roles on metformin (dephosphorylating tau by PP2A activation, but potentially increasing tau phosphorylation via activating AMPK), positive preclinical data has been published, with a phase II trial treating patients with amnesic mild cognitive impairment completed in 2012 but awaiting publication, and a preliminary trial looking at cognition, imaging, and cerebrospinal fluid biomarker outcomes from metformin treatment in MCI and AD (ClinicalTrials.gov, 2016c, d; Mairet-Coello et al., 2013; Vingtdeux et al., 2010; Wang et al., 2012). Selenium salts also showed promising preclinical results, and a phase III trial looking to prevent AD development by selenium supplementation has recently been completed (ClinicalTrials.gov, 2016e; Corcoran et al., 2010; van Eersel et al., 2010).

The inhibition of tau aggregation has also been attempted using TRx0237, a methylene blue derivative, which has now completed various phase III trails. TRx0237's actions are not limited to disturbing tau aggregation, having been shown to inhibit Aβ fibrilisation, promoting tau degradation, and be neuroprotective by increasing cerebral blood flow and reducing reactive oxygen species (Lin et al., 2012; Taniguchi et al., 2005; Wischik et al., 1996). The clinical use of methyl blue is already well established for the treatment of malaria and methemoglobinemia, but despite positive results from phase II trials in AD patients, higher dosing having no effects, as well as an unorthodox use of control groups, means the phase III results are difficult to predict (Schirmer et al., 2011; Wischik et al., 2008).

Presently patients diagnosed with sAD can expect to receive treatment which temporarily ameliorates their symptoms and aims to temporarily slow their deteriorating quality of life.

Acute neurodegenerative diseases

Acute neurodegenerative diseases include ischaemic and haemorrhagic stroke, TBI, and cerebral hypoxia/ischemia. Although all of these disorders have an initial starting insult, neuronal loss not only occurs directly at the time of the said incident, but also is accompanied by a progressive further loss of neurons over the following period of weeks.

The most common acute neurodegenerative disorder is stroke, of which around 80% are ischaemic, and 20% are haemorrhagic. Cerebrovascular disease, of which stroke is the most common, accounts for approximately 10% of worldwide deaths, 85% of deaths due to neurological disorders, and 3.5% of Disability Adjusted Life Years (a measurement of the combined effect of disability and death on reducing the number of years of healthy life of an individual) lost worldwide ((Aarli, 2006) chapter 3). The incidence of stroke increases with age, with the risk of stroke roughly doubling every decade over 55. Whilst stroke incidence has dropped in recent decades in developed nations, there has been a remarkable leap in yearly incidence in middle and lower income nations (Feigin et al., 2009).

A stroke is defined as a rapid onset of focal or global cerebral deficit with no apparent cause other than a vascular one. Ischaemic stroke is the decrease in blood supply to an area or areas of the brain because of an occlusion to a blood vessel, or decrease in blood supply. This local ischemia leads to the area of brain deprived of oxygen and nutrients to die if blood flow is not re-established within minutes. The area surrounding this ischaemic area will also experience a decrease in blood flow, but may still be receiving partial blood flow from other vessels; this area is called the penumbra. Due to only the partial loss of blood flow to penumbra tissue, the death of these brain areas is not immediate, but depends upon the speed at which the blockage is rectified, the treatment the patient received, and the location and duration of the ischaemic incident. The subsequent delayed cell death occurs over the space of weeks following the ischaemic incident, but every further minute of ischemia without treatment essentially increased the amount of brain, and crucially neurons, that are lost as a consequence (Saver, 2006).

Haemorrhagic stroke is somewhat different in its neuronal cell death pattern, whereby it is often fatal to the patient, but if the ictus is survived the hematoma leads to progressive neuronal cell death radiating from the site of injury, for various proposed pathophysiological reasons, over the space of days to weeks (Aronowski and Zhao, 2011). Nonetheless, both variants of stroke have an immediate period of injury, followed by a more prolonged loss of neurons and brain tissue.

TBI is an externally generated impact to the head that results in injury to the brain and subsequent neuronal cell death. Although comprehensive data is lacking of the global burden of TBI's, it is estimated that 10 million people are affected annually, and it is often cited as the leading cause of disability in children and young adults in the world (Aarli, 2006; Hyder et al., 2007). Similarly to stroke, there is immediate cell death followed by delayed secondary cell death, with a variety of mechanisms proposed (Raghupathi, 2004).

Sharing this primary and secondary loss of neurons is cerebral hypoxia/ischemia (Huang and Castillo, 2008). Its cause overlaps greatly with ischaemic stroke insofar as it is a reduction in either oxygenated blood or blood in general that is received by the brain, but the fact that cerebral hypoxia affects the whole brain, rather than local areas distinguishes the two. The cause of cerebral hypoxia is a sudden decrease in oxygenation of the blood, most frequently caused by an obstruction of breathing, and cerebral ischaemia is the sudden decrease in blood in general to the brain, often due to the reduced blood flow to the brain.

Current therapeutic options for acute neurodegenerative diseases

In all of these acute neurodegenerative diseases the immediate therapeutic course of action is to identifying the exact cause of the incident, and immediately combat the acute source of pathology, with the speed of correct therapeutic intervention being of paramount importance (Fan et al., 2012; Marler et al., 2000). This intervention can be by removing the source of ischemia with thrombolytic and anticoagulant medication

or surgical intervention for ischaemic stroke (Gupta et al., 2003; The National Institute of Neurological Disorders and Stroke rt-PAStroke Study Group, 1995), or reducing the intracranial pressure following a bleed and removing the haemorrhage in some instances of haemorrhagic stroke (Hemphill et al., 2015). Once the acute incident has been treated, appropriate medication is then used to mitigate the redevelopment of pathology, and then the long-term neuropathological treatment of the patient essentially involves leaving the brain to recover on its own. The prevention of the reoccurrence of ischaemic stroke is achieved by prescribing anticoagulants and thrombolytics to prevent the reoccurrence of vessel occlusion, however this may increase the short-term incidence of haemorrhagic stroke (Adams et al., 2007).

The mitigation of long-term pathology in all of these acute diseases is done with secondary therapies such as physiotherapy to try and preserve motor function, or speech therapy to try and preserve speech. Crucially, in all of these cases, whilst patients can generally expect excellent and swift treatment, no current therapeutic interventions are available to try and stop the progressive neurodegeneration following the incident that results in such profound disability in these diseases. The prognosis of these diseases varies from patient to patient therefore, but if therapies could be devised to mitigate the post-incident neuronal loss, a novel and crucial new therapeutic strategy may be possible for treating acute neurodegenerative disease.

Insulin and insulin-like signalling in neurodegenerative disorders – a potential therapeutic target

Whilst there are substantial differences in neuropathology between the different neurodegenerative diseases, one molecular pathway has been repeatedly shown to be endogenously altered in its signalling level in neurodegenerative disorders, and seems uniquely poised to impact on the general health and survival of neurons. This pathway is of substantial interest to us because it is implicated in the ageing process itself, and is therefore directly involved in the longevity and healthspan of organisms and tissues, as well as directly being implicated in neuronal cell death mechanisms. All

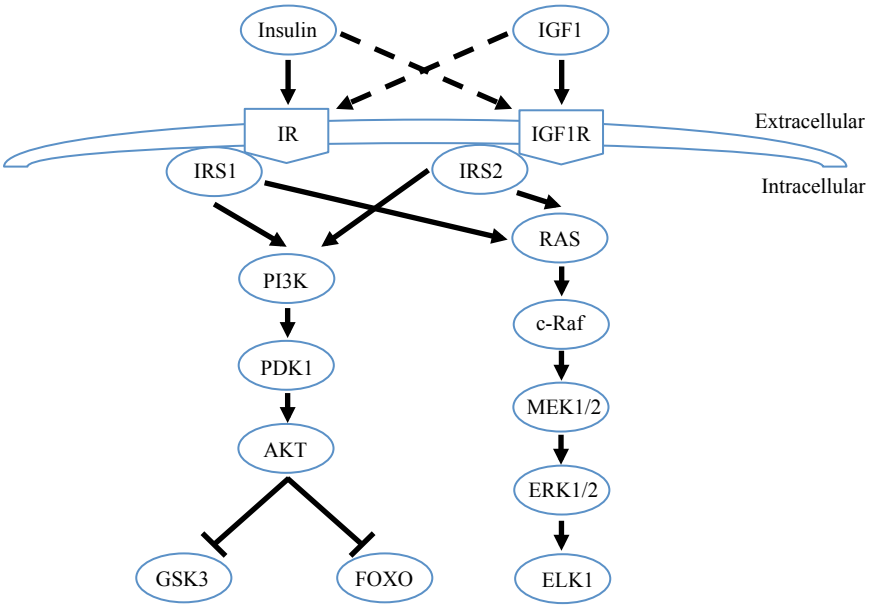

Figure 1.2. The canonical insulin and insulin-like growth factor signaling pathway. Simplified diagrammatic representation of the canonical IIS cascade. The soluble ligands IGF1 and insulin bind and activate IGF1R and IR respectively, as well as IR and IGF1R with less affinity. This causes autophosphorylation of the receptor tyrosine kinases IGF1R and IR, and the subsequent downstream signaling through the PI3K-AKT and RAS-MAPK pathways. Crosstalk between pathways, and input onto these pathways from other signaling cascades is apparent. Common protein names used; see key in appendix for official/alternate protein and gene names.

these factors make the IIS cascade an ideal candidate for the type of pro-health interventions that we desire.

The IIS cascade in the brain in health and disease

The IIS cascade is an ancient and well-conserved molecular signalling pathway, which in essence is a nutrient sensing pathway, implicated in a multitude of key cellular processes in nearly all tissues in the human body. The signalling pathway can be seen in figure 1.2, and is activated in its signalling via three hormone ligands;

insulin, insulin-like growth factor 1 (IGF1) and insulin-like growth factor 2 (IGF2). Whilst the effects of insulin and IGF2 are undoubtedly very important in human brain physiology, it is the signalling of IGF1 specifically that we are interested in this thesis. IGF1 predominantly signals through the IGF1 receptor (IGF1R), although IGF1R is still receptive to both IGF2 and insulin, albeit with 10 and 100 fold lower affinity (Czech, 1989). Similarly IGF1 can activate both the insulin receptor (IR), and IGF2 receptor (IGF2R), but with less affinity than their namesake ligands (Czech, 1989). With IGF1R and IR both being comprised of two subunits forming a heterodimer (Hubbard, 1999), and sharing great homology (Ullrich et al., 1986), it is also the case that IGF1R/IR heterodimer can form with a high affinity for IGF1 and low for insulin (Soos et al., 1993), but the exact significance and prevalence of these hybrid receptors, especially in the brain, are yet to be fully determined.

The downstream effects of receptor activation are mainly conveyed via the Insulin Receptor Substrates 1 and 2 (IRS1 and IRS2) and Shc, whereby activation of IGF1R and IR directly phosphorylates these proteins and thereby allows the binding of SH2 domain proteins to these large receptor substrates. This leads to the activation of two molecular pathways; the phosphatidylinositol 3-kinase (PI3K)–AKT pathway, and the Ras–mitogen-activated protein kinase (MAPK) pathway (Avruch, 1998). It is highly likely that there is tissue specific signalling through these cascades, and therefore we must specifically examine IIS signalling in the brain.

By adding IGF1 and insulin to post-mortem brain tissue and then measuring the changes in phosphorylation levels in downstream components of the IIS cascade, Talbot *et al* showed that insulin signalled predominantly through IRS1 to the PI3K branch of the IIS cascade, whereas IGF1 signalled predominantly through IGF1R and IRS2 through the MAPK (ERK1/2) branch in the brain (Talbot et al., 2012). This therefore represents the two divergent yet interacting signalling cascades that make up canonical IIS: the PI3K, and MAPK branches. These two branches go on to signal to various transcription factors such as the ELK1 and FOXO families. These signalling cascades seem to have distinct functions in the brain that is only now beginning to be fully elucidated (Broughton and Partridge, 2009).

So far this is only a simplistic overview of the canonical IIS cascade. Other non-canonical branches of IR/IGF1R signalling do exist, for example there is evidence to suggest that IR/IGF1R phosphorylates proteins such as Gabs (Nishida and Hirano, 2003) and DOKS (Mashima et al., 2009). Also IGF1 and insulin have been shown to be activators of other non-receptor kinases such as the Janus kinases (Gual et al., 1998), and c-Abl kinase (Genua et al., 2009). These associations are yet to be thoroughly investigated however, and how they may impact on IIS specifically in the brain is far from known.

In the periphery the most significant action of IGF1 is via the mediation of the growth promoting effects of growth hormone by acting as a growth and differentiation factor on many tissue types (Laron, 2001). This is achieved by growth hormone being released into the blood from the pituitary gland where it stimulates the synthesis and release of IGF1 into the blood from the liver (Daughaday et al., 1972). Therefore IGF1, by being a trophic factor in the periphery, is seen overwhelmingly as a pro-growth factor. Indeed, it is this pro-growth property that is implicated in some cancers, leading to IGF1R inhibitor development as chemotherapy agents (Weroha and Haluska, 2008).

The bioavilability of IGF1 in the blood is regulated by its high affinity binding to IGF binding proteins (IGFBPs), with various IGFBPs having differing affinities for IGF1 (Duan, 2002). Whilst the pro-growth effects of IGF1 in the periphery are well defined, cell types in the periphery are mitotic and therefore capable of undergoing cell division and replication. The brain is a unique organ containing neurons that are post mitotic and extremely long lived, and also astrocytes which are likely long lived with a low cell turnover, as well as containing cell types capable of proliferation such as microglia. Therefore the effects that IGF1 has in the brain are worthy of special consideration, as abundant evidence suggests atypical properties for what is classically assumed to be a proliferative pathway.

IIS signaling is integral in brain development, with IGF1 and IGF1R mutations causing microcephaly (Netchine et al., 2009; Walenkamp et al., 2005), and the lack of humans with a total genetic loss of IGF1R implies its lethality. Insulin and IGF1 are expressed abundantly in the periphery, with increased levels in the blood causing an

increase in levels in the brain (Baura et al., 1993). The work of Liu *et al* showed that the liver was not the only organ capable of expressing IGF1 (Liu et al., 2000), and although IGF1 and insulin are actively transported into the brain from the periphery, cells in the brain also express IGF1.

Developmental studies show that under healthy conditions this IGF1 expression is predominantly in neurons (Bondy, 1991; Bondy et al., 1990), and this pattern is confirmed in online expression databases (Zhang et al., 2014)(figure 1.3). The expression of IGF1 and the IGF1 receptor (IGF1R) in the brain is highest during development, with IGF1 expression decreasing significantly in the adult brain (Bondy and Lee, 1993; Han et al., 1988; Sandberg et al., 1988). IGF1 acts during all the major phases of brain development, with IGF1R's expressed as early as the formation of the ventral floor plate, as well as in major brain regions such as the hippocampus, neocortex and cerebellum during later stages of development, acting to promote the proliferation of neuronal precursor cells and the differentiation of neurons to form complex networks (Bondy et al., 1992; Bondy et al., 1990; Ozdinler and Macklis, 2006; Sosa et al., 2006).

These patterns of expression change profoundly during injury however, with increased IGF1 production in astrocytes observed in TBI, hypoxia, and sAD (Beilharz et al., 1998; Connor et al., 1997; Madathil et al., 2013), although a reduction has been observed when *IGF1* expression is measured in the AD brain via RT-qPCR (Steen et al., 2005). The increase in IGF1 expression in such a wide variety of diseases suggests that it is a response to damage in the brain, with the proximity of IGF1 expressing astrocytes to the site of head injury in TBI supporting this. What is of interest here is that the IGF1R is expressed in nearly all cells of the brain, but crucially in neurons and astrocytes (figure 1.3, B). Given the non-mitotic properties of astrocytes and neurons, and the pro-growth and differentiation signals that IGF1 usually conveys, it is clear that increased IGF1 signaling in these cells must have different cellular effects to those characterized in the periphery.

It is possible that this increase in IGF1 production in glial cells is stimulating growth not in terms of cell division, but in terms of synapses and neuronal processes to compensate for damage, as IGF1 has been shown to affect neuronal transmission and promote synapse formation (Gazit et al., 2016; Shcheglovitov et al., 2013). With

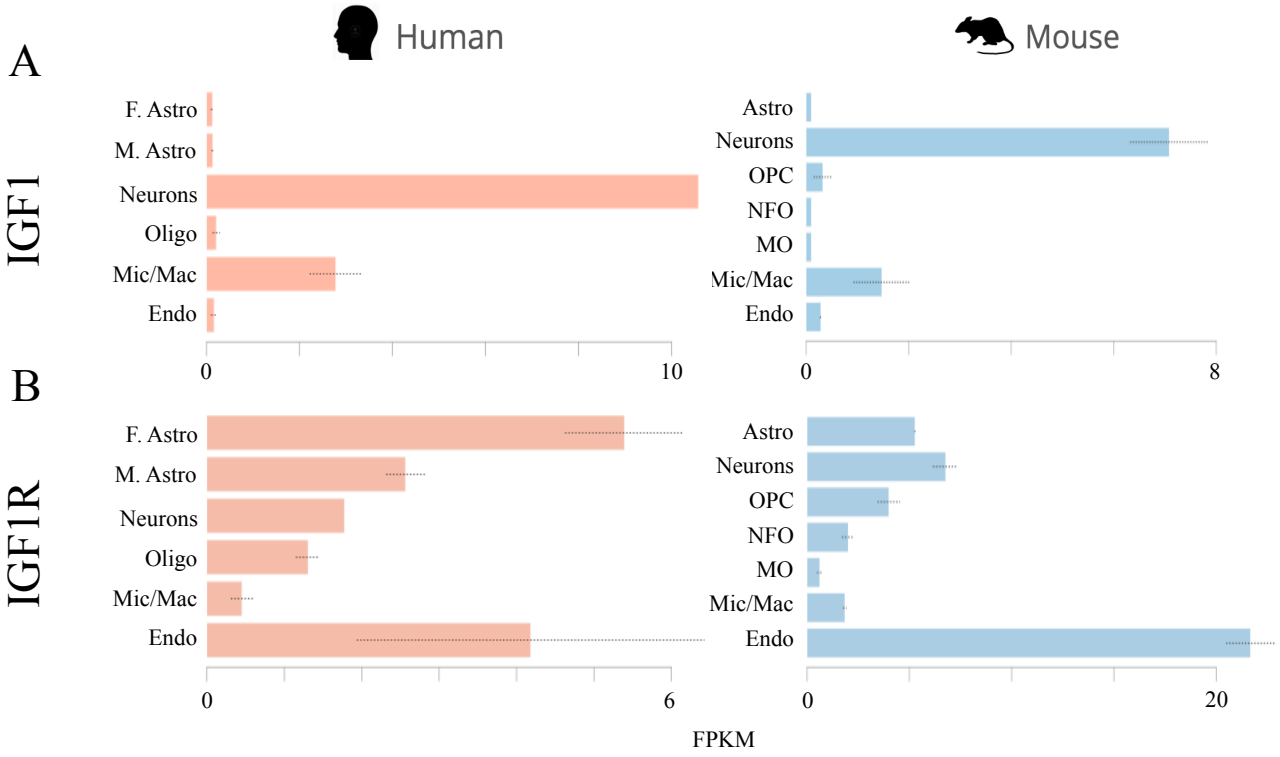

Figure 1.3. Expression levels of IGF1 and IGF1R in the mouse and human brain. (A) IGF1 in the adult human and mouse brain is nearly exclusively expressed in neurons, but also to a lesser extent in microglia. (B) IGF1R however is more generally expressed across all cell types of the brain, with high levels apparent in the endothelial cells of the adult brain. Panels modified from http://www.brainrnaseq.org. F. Astro - Fetal Astrocytes, M. Astro – Mature Astrocytes, Oligo – Oligodendrocytes, Mic/Mac – Microglia/Macrophages, Endo – Endothelial, OPC – oligodendrocyte Precursor Cells, NFO – Newly Formed Oligodendrocytes, MO – Mature Oligodendrocytes. FPKM - Fragments per kilobase of transcript sequence per million mapped fragments.

synaptic loss proximal to the damaged area of the brain well documented, this is a distinct possibility.

Another more worrying possibility is that increased IGF1 levels cause an increase in signaling downstream of IRS2, and in particular at ERK1/2. Neuronal cell death has been associated with ERK1/2 activation, and in multiple experiments neuronal cell death in neuronal cultures has been reduced using the specific inhibitors of MEK1 and MEK2 U0126 and PD98059 (Bhat and Zhang, 1999; Canals et al., 2003; de Bernardo et al., 2004; Lesuisse and Martin, 2002; Stanciu et al., 2000). PD98059 was also shown to be neuroprotective *in vivo*, by reducing hippocampal neuronal loss

following TBI in rats (Lu et al., 2008). It seems though that the duration of ERK1/2 activation is relevant as to whether the signal is protective or indicative of neuronal cell death, with prolonged ERK1/2 activation proving neurodegenerative, and transient increases being neuroprotective (Almeida et al., 2005; Luo and DeFranco, 2006; Subramaniam et al., 2005). Crucially Subramaniam *et al* showed that exogenous IGF1 application to a cell culture model of neuronal cell death showed a transient increase in ERK1/2 and neuroprotection. How this translates to the endogenous IGF1 increase in neurodegenerative disorders however is unclear, especially in the chronic neurodegenerative disease sAD, where presumably the IGF1 increase is for a far longer time.

Changes in IIS with regards to ERK1/2 phosphorylation levels in disease states have also been shown, with ERK1/2 activity being directly attributed to key pathological changes in AD. In AD patients, increased phosphorylated ERK1/2 has been shown to co-localise with tau tangle containing hippocampal neurons, with the sequential presence of phosphorylated and therefore activated forms of ERK1/2 and its kinase MEK in pretangle neurons in parallel with Braak staging (Pei et al., 2002; Perry et al., 1999). The sizes of cytosolic granular accumulations of these activated kinases in this sequential progression increased with the accumulation of hyperphosphorylated tau within the neurons (Pei et al., 2002). One of the many substrates of ERK1/2 is tau, implying that ERK1/2 signalling increase could contribute to tau hyperphosphorylation (Guise et al., 2001; Harris et al., 2004). Considering that Aβ accumulation precedes tau phosphorylation, and tau phosphorylation increase seems to be increasingly implicated as the source of neurotoxicity in AD, the direct action of Aβ in inducing prolonged activation of ERK1/2 resulting in tau phosphorylation in neuronal cell cultures provides a possible crucial link between these two pathological hallmarks of AD (Rapoport and Ferreira, 2000).

Increased ERK1/2 activation is not unique to AD however, with neurons containing Lewy bodies in the substantia nigra of Parkinson's disease patients being shown to contain the same granular accumulations of phosphorylated ERK1/2 as those apparent in tau tangle containing neurons in AD patients (Zhu et al., 2002). Similarly alpha synuclein itself increases p-ERK levels in microglia, inducing the release of pro-inflammatory cytokines (Klegeris et al., 2008). Furthermore the gradual loss of

neurons in the weeks following an ischaemic event has been shown to be dependent of increased ERK1/2 phosphorylation, with increased phosphorylated ERK1/2 observed in middle cerebral artery occlusion (MCAO) models of ischemia, permanent MCAO models, and in other hypoxia ischemia and pure ischemia animal models of stroke (Alessandrini et al., 1999; Irving et al., 2000; Kitagawa et al., 1999; Lennmyr et al., 2002; Namura et al., 2001; Wang et al., 2003). Therefore with the above mentioned changes in ERK1/2 phosphorylation in multiple neurodegenerative diseases, and its implications in neuronal cell death, it would seem that not only is IIS clearly implicated in pathogenesis in neurodegeneration, but ERK1/2 represents a focal point of signalling through which neuronal cell death signalling is present.

ERK1/2 is not the only part of the IIS cascade that is endogenously changed in neurodegenerative diseases however. Substantial IIS resistance, whilst normally associated with peripheral disorders such as diabetes mellitus and polycystic ovary disease, has been observed in the brains of sAD patients, with the level of resistance correlating with the cognitive decline of these patients (Talbot et al., 2012). This resistance has been shown to occur as a decrease in expression of proteins in the IIS cascade (Steen et al., 2005), and also at the phosphorylation level. This resistance importantly is most profound in the hippocampus (Talbot et al., 2012), with the hippocampus being one of the brain regions most profoundly degenerated in AD (West et al., 1994). As with the p-ERK change detailed above, this change in IIS signaling is not apparent in all cell types of the hippocampus, with histological staining of a phosphorylation site on IRS1 that reduces IIS (pS616 IRS1) highlighting pyramidal neurons of the CA1 region (Talbot et al., 2012). The correlation between AD progression, cognitive decline, and the development of IIS resistance all coinciding in the hippocampus of AD patients, has inevitably led to many inferring that IIS resistance in AD is a contributing factor to the development of pathology and neurodegeneration in the disease. This has led to an abundance of research into treatments to prevent or alleviate the IIS resistance seen in AD (Bomfim et al., 2012; Long-Smith et al., 2013; Talbot and Wang, 2014). It is possible to interpret this resistance in another way however, with decreases in signaling through the IIS cascade having been shown to have very different effects on diseases pathology.

Ageing and neurodegeneration

Ageing can be defined as the deterioration of the physiological functions of an organism in a time dependant manner that affects the correct functioning and ultimately survival of that organism. This is a distinguishable process from age-related diseases, and it is this deterioration of physiological function that is one of the theories of how ageing affects the probability of developing age-related diseases. Although long thought of as an unregulated natural stochastic process in an organism's life, the regulatory pathways that determine the rate of ageing in organisms have begun to be defined. By far the most thoroughly researched of these regulatory pathways is the IIS cascade. It has been shown that by altering the level of signalling through this pathway, the rate of ageing of an organism can be modulated. By systemically decreasing signalling through the IIS pathway, a lifespan of over double what is normally seen can be achieved in *daf-2* (a hormone receptor similar to that of insulin and IGF1) mutants in *Caenorhabditis elegans* (*C. elegans*) (Kenyon et al., 1993). This has been demonstrated robustly in many experimental animals with increasing supportive evidence in higher organisms, including humans (Barbieri et al., 2010; Holzenberger et al., 2003; Kojima et al., 2004; Milman et al., 2014; Suh et al., 2008; Tatar et al., 2001).

The most remarkable aspect of this lifespan extension is not just that these animals live longer, but that they live healthier for longer. The amount of time that an organism spends in a healthy non-diseased state is termed its healthspan, and it is the increase in healthspan that makes this lifespan extension very relevant for understanding the affects of ageing on the increased risk of neurodegenerative disease development. It has been shown that decreasing IIS signalling in animal models of AD can prolong the healthspan of these animals, and slow the onset of the AD phenotype when compared to non-IIS reduced AD mutant mice, as well as crucially decreasing neuronal cell death (Cohen et al., 2009). Processes known to lower systemic IGF1 levels such as fasting have also been shown to delay the onset of AD in AD model mice (Halagappa et al., 2007).

This ability to manipulate an ageing regulatory pathway and show delays in the development of neurodegenerative disease pathology, therefore represents tangible proof that neurodegeneration can be delayed by ageing delaying therapies. Precisely how the onset of these diseases is delayed by slowing ageing, and how this change is manifest at a cellular level, is currently the focus of rigorous research, with pathways and molecules downstream of the IGF1 receptor and its orthologs being scrutinised (Baird et al., 2014; Pierce et al., 2013). If this link can be better understood then there would be potential to develop therapies that would manipulate this process for therapeutic gain. Whilst genetic manipulation to lower signalling through the IIS cascade does not seem plausible, the identification of drugs that inhibit this pathway opens up the possibility of pharmacological manipulation of this pathway. This is a far more clinically applicable concept.

Modulating IIS in the brain as a therapeutic target – our aims

With the IIS cascade appearing to be a pharmacologically modifiable molecular pathway capable of influencing neuronal cell death and brain health, we have identified an approach to directly target neuronal cell death in neurodegenerative diseases that is yet to be fully explored. Attempts have already been made to utilise the IIS pathway in the brain for therapeutic gain, with varying success.

Therapeutically targeting chronic neurodegeneration

The window for neuroprotective therapeutic intervention in acute neurodegenerative disorders is fairly straightforward, neuronal cell death occurs in the weeks following the initial noxious insult, so therapeutically opposing neuronal cell death in this time period seems the obvious intervention strategy. For chronic neurodegenerative diseases the picture is far more complex.

Certain aspects of AD pathology make designing IIS based therapeutics for this disease very difficult. The first difficulty is the substantial prodromal period and extent of neuronal loss and disease development before clinical presentation of AD symptoms, with substantial hippocampal atrophy present by diagnosis (Fox et al., 1996). Ideally disease intervention would be before substantial neuronal loss and cognitive impairment has occurred, and indeed substantial effort is being put into devising improved pre-cognitive impairment diagnostic tests (Humpel, 2011). Due to this concerted effort to diagnose AD earlier in the disease progression, the search for improved therapeutics should not limit itself to post-diagnosis interventions, and therefore our search for optimal IIS modulating therapy intervention will include pre and post-diagnosis AD stages.

The second difficulty in IIS modulating therapies being considered for disease intervention in AD is that endogenous IIS changes have been reported in the AD brain (Steen et al., 2005; Talbot et al., 2012). These changes could undermine our proposed interventions. For example, the profound IIS resistance in the diagnosable AD brain could limit the efficacy of both inhibitors and stimulators of the IIS pathway. IIS inhibitors would have reduced effect as the pathway is already lessened in its signalling, and the efficacy of applications of stimulators such as IGF1 would be lessened as the extent to which it can stimulate signalling would be reduced by the resistance. Understanding the endogenous changes in IIS at different points in AD progression is therefore essential in order to aid the appropriate timing of our proposed IIS based interventions.

In order to identify the most appropriate time point for disease intervention in the chronic neurodegenerative disease AD via IIS modulation, the first aim in this thesis was to examine how IIS changes at different time points during disease pathogenesis in AD.

To examine IIS changes at earlier disease stages in the AD brain we chose from the wide range of mouse models available that model different pathological components of AD. Given the heritability of fAD, animal models have been made by incorporating fAD mutations such as those in the *PSEN1* and *APP* genes into the genomes of the model animal of choice (Goate et al., 1991; Sherrington et al., 1995).

With a profound overlap in the clinical and neuropathological presentation of fAD and sAD, these fAD models of AD can be used as a means to study sAD and AD in general. These models lead to animals with increasing levels of Aβ pathology and plaque formation, but lacked the complete tau pathology seen in clinical AD, with hyperphosphorylated tau occasionally observed but never producing tau tangles (Howlett et al., 2008; Kurt et al., 2003; Sturchler-Pierrat et al., 1997).

To be able to model hyperphosphorylated tau and tau tangles, mutations in the *MAPT* gene were incorporated into animal genomes (Santacruz et al., 2005; Terwel et al., 2005). These are not mutations found in AD patients however, but mutations that give rise to frontotemporal dementia (FTD), thereby utilising the overlap in tau pathology between these diseases to form a mouse model of tau pathology, and thereby examine the effects of tau pathology on the brain. Animal models of AD that only contain Aβ pathology or tau models are not accurate portrayals of AD in humans however, and therefore should not be viewed as "models of AD" as they only model one pathological component of the disease. Whilst this is often seen as a downside to animal models of AD, it provides the opportunity to tease apart the effect of these two neuropathological components on IIS signalling.

Mouse models of amyloid and tau pathology in AD

The amyloid pathology mouse model that was chosen was the APP knock-in model developed by Saito and Saido (Saito et al., 2014). Both strains developed by this group are an improvement on previous APP based amyloid transgenic mouse models, as they avoid the problems of APP overexpression common in other models. This was achieved by using a humanised Aβ sequence in the mouse APP gene; meaning human Aβ is produced in mouse neurons at a physiologically correct level. This improvement on previous overexpression transgenic APP models was the main reason why the APP knock-in model was used for our experiments, as this will allow a far more physiological response to misfolded Aβ to be studied. This is in sharp contrast

to overexpression models, where the variable of increased protein load was also present.

With these mice having a human Aβ sequence, the addition of specific fAD mutations therefore produces misfolded aggregating Aβ, with the two APP-KI strains differing in the number of fAD mutations present. The NL-F/NL-F strain harbours only the Spanish Beyreuther/Iberian mutations, whereas the NL-F-G/NL-F-G strain also contain the Arctic mutation (Saito et al., 2014). The Swedish KM670/671NL mutation increases Aβ40 and Aβ42 creation, the Beyreuther/Iberian I716F mutation increases the Aβ42 to Aβ40 ratio, and the Arctic mutation caused the mice to exhibit greater neuroinflammation and a swifter pathology (Citron et al., 1992; Guardia-Laguarta et al., 2010; Saito et al., 2014; Tsubuki et al., 2003).

Whilst both strains show progressive amyloid pathology, the addition of the arctic mutation greatly increases the speed of its development. In the APP-KI$^{NL\text{-}G\text{-}F/NL\text{-}G\text{-}F}$ mouse model, there is an age dependant development of Aβ pathology beginning at 2 months of age in the cortex hippocampus and subcortex, with Aβ accumulation saturating by 7 to 9 months (Saito et al., 2014). This is accompanied by extensive neuroinflammation with increased astrogliosis and microgliosis by 9 months. Memory impairment was observable by 6 months of age as measured by deficits in the Y-maze test. Crucially this model also has no distinguishable neuronal cell loss. In the APP-KI$^{NL\text{-}F/NL\text{-}F}$ strain however, Aβ deposition only began at around 6 months, progressing to around 8% cortical plaque coverage by 20 months – a plaque burden observed by 7 months when the Arctic mutation is present (Saito et al., 2014). Furthermore comparatively less neuroinflammation is observed in APP-KI$^{NL\text{-}F/NL\text{-}F}$ mice.

Due to our APP-KI$^{NL\text{-}F/NL\text{-}F}$ colony only being young at the time of my experiments, all my experiments were performed on the more aggressive APP-KI$^{NL\text{-}G\text{-}F/NL\text{-}G\text{-}F}$ strain using tissue sent from our collaborators Saito and Saido (see chapter 2). Based upon this pathology development in the APP-KI$^{NL\text{-}G\text{-}F/NL\text{-}G\text{-}F}$ mice, we examined IIS signalling at 2, 4, and 8 months of age, which corresponds to the very beginning of amyloid pathology at 2 months, midrange amyloidosis at 4 months, and maximal amyloid deposition at 8 months.

The rising tau model that was chosen is the TG4510 model (Santacruz et al., 2005). This model expresses human tau containing a P301L mutation which in humans leads to a type of familial FTD called frontotemporal dementia and parkinsonism linked to chromosome 17 (FTDP-17)(Hutton et al., 1998). In this model pretangles develop by 2.5 months and progressed rapidly with full tangles observable by 4 month in the cortex and 5.5 months in the hippocampus (Santacruz et al., 2005). This was accompanied by extensive neuronal cell loss, with substantial brain weight reduction, and a 60% reduction in hippocampal CA1 pyramidal neurons by 5.5 months. This profound neurodegeneration continue with only 23% of these neurons still present in 8.5-month-old mice. Whilst this model is very aggressive, we wanted a model that showed pretangle pathology, tangle pathology, and also showed extensive neuronal cell loss. This aggressive pathology development can also be seen as a disadvantage however, as more subtle changes in IIS may be lost given the speed of progression. However, as neuronal cell loss defines neurodegenerative diseases, the presence of a substantial level of neurodegeneration in this model was seen as an advantage given our aims.

With such a rapidly progressing pathological progression, we chose to examine the IIS cascade in 2-month-old animals to see how the development of pretangle pathology affected IIS in the brain, and 8-month-old animals to see how IIS is changed in the brain during neurodegeneration. This model therefore allowed us to examine very early AD events, and also very late, post diagnosis events, in relation to the level of IIS.

As human AD contains both amyloid and tau pathology, to gain insight into how our IIS characterisations in just amyloid and tau containing mice compared with the IIS changes in the AD brain, we also carried out a preliminary investigation into IIS levels in a small number of human brain samples from the UCL Queen Square brain bank. These samples were from fAD and sAD patients, as well as from non-demented controls for comparison. Depending on this initial human brain tissue study, more samples can be requested for further analysis.

Using these two mouse models, we can therefore assess changes in IIS signalling at a range of time points during AD pathology development that is not possible in human brains.

IGF1 and neurodegeneration

There is evidence to suggest that exogenous insulin and IGF1 administration in various forms has positive effects on cognition and proteostasis in animal models of AD. Infusions of IGF1 have been shown to improve Aβ clearance from the brain in aging rats, and decrease behavioral impairments seen in AD mouse models (Carro et al., 2006; Carro et al., 2002). This combined with evidence showing that intranasal administration of insulin improves memory in healthy humans, has lead to considerable attention being given to the prospect of insulin administration being a viable therapy for treating, or at least providing alternative symptomatic relief for sAD patients (Benedict et al., 2004; Benedict et al., 2007; Wadman, 2012).

IGF1 administration or increasing IGF1 has had positive effects in animal models of motor neuron disease (MND) and stroke. Following ischemia and stroke IGF1 has proven to be neuroprotective in rats and sheep, but has yet to be translated into clinical benefit. In these models both administering, and genetically overexpressing astrocyte *IGF1* was neuroprotective following hypoxia ischemia, albeit in a dose response relationship, with only higher levels providing neuroprotection (Bergstedt and Wieloch, 1993; Carro et al., 2006; Guan et al., 2000; Guan et al., 1993; Johnston et al., 1996; Li et al., 2010; Madathil et al., 2013). Overexpressing IGF1 in the brains of MND model mice has also proved beneficial for disease symptoms in those animals (Dodge et al., 2008). These studies all suggest a neuroprotective role for IGF1 in neurodegenerative conditions.

As mentioned above, endogenous IGF1 increase has been observed in astrocytes in traumatic head injury, hypoxia, and sAD (Beilharz et al., 1998; Connor et al., 1997; Madathil et al., 2013). Based on the neuroprotective findings of IGF1 administration, this endogenous increase would appear to be a neuroprotective response to damage in

the brain. However, as described earlier a reduction in IIS signaling by genetic and pharmacological means has shown to be able to postpone neurodegenerative disease progression and be neuroprotective. With IGF1 being a potent activating factor of signalling through the IIS cascade (Laviola et al., 2007), there are directly opposing views as to the role IIS signaling plays in the pathogenesis of neurodegenerative disease. Furthermore, with a dose-response relationship shown in the IGF1 neuroprotection papers (Bergstedt and Wieloch, 1993; Johnston et al., 1996), where low levels of IGF1 administration elicited no neuroprotection against injury, the role of endogenously changed IGF1 levels in neurodegenerative diseases is difficult to predict.

With the complications of IIS intervention timing in chronic neurodegenerative disease, and the identification of a brain resistant state in sAD (Talbot et al., 2012), we cannot assume that the effect of endogenous IGF1 increase is the same in chronic and acute neurodegenerative diseases. We therefore focused only on the effects of endogenously increased IGF1 in acute neurodegenerative disease.

The second aim in this thesis was to clarify the role of endogenously increased IGF1 in acute neurodegenerative diseases, especially with regards to neuronal cell loss.

To investigate this, we chose to develop an *in vitro* model of acute neurodegeneration, which showed neuronal cell loss accompanied by increased astrocyte Igf1 levels. Our model was based on the bilaminar co-culture protocol of Shimizu *et al*, where primary astrocyte and neuron cultures from mice are generated, and then combined in a single well by suspending a coverslip with primary neurons attached above an astrocyte culture grown in the bottom of the well (Shimizu et al., 2011). This allowed the sharing of the medium between these cultures, but the separation of each cell type for separate analysis. To induce neurodegeneration we applied a short-term hypoxic insult.

Inhibiting the IIS pathway as a therapeutic target

Probably the strongest support for using IIS inhibitors to treat neurodegenerative diseases in mammals comes from the separate work of Echeverria *et al*, Gladbach *et al*, and Ashabi *et al*. Whilst recent further supportive evidence for the therapeutic benefit of inhibiting IIS to slow neurodegenerative disease progression has been shown using *Caenorhabditis elegans* (El-Ami et al., 2014), the work of the above groups is closer to progression to the clinic in virtue of being carried out in intact mammalian systems. Echeverria *et al* showed that by administering the clinically approved c-Raf inhibitor Sorafenib, neuronal cell death was ameliorated in culture, and successfully rescued memory deficits in a mouse model of AD (Echeverria et al., 2008; Echeverria et al., 2009). What was lacking from this was a direct quantification of whether this c-Raf inhibitor prevented neuronal cell death, or had more general effects on the disease pathology, such as rescuing alterations in neuronal plasticity. Direct evidence of neuronal cell protection in a neurodegenerative disease animal model treated with an IIS inhibitor was shown in studies that administered the MEK inhibitors U0126 and PD169316 to mice following an ischemic incident, or mice injected with Aβ fibrils into their brains (Ashabi et al., 2013; Gladbach et al., 2014). In both of these studies neuronal cell loss was substantially reduced by IIS inhibitor administration. The progress of IIS inhibitors to the clinic to treat neurodegeneration is yet to happen however.

On a mechanistic level as mentioned above, a prolonged increase in signalling through this cascade specifically at ERK1/2, has been shown to be indicative of a neuronal cell death cascade, and this increased ERK1/2 signalling has been shown in multiple neurodegenerative disorders specifically in the areas of brain that are undergoing neurodegeneration (Alessandrini et al., 1999; Almeida et al., 2005; Lu et al., 2008; Luo and DeFranco, 2006; Pei et al., 2002; Perry et al., 1999; Subramaniam et al., 2005; Zhu et al., 2002). With neuronal cell death such an integral feature of neurodegenerative disorders, the neuroprotective effects of IIS inhibitor administration could be through interference in these increased ERK1/2 neuronal cell death signals.

Whilst most work using IIS inhibitors to modulate neuronal cell death has focused on experimental inhibitors such as U0126 and PD169316, or novel preclinical inhibitors such as NT219 (El-Ami et al., 2014), many inhibitors of the IIS cascade have already been approved for human use to treat many forms of cancer.

The third and final aim of this thesis is therefore to investigate the possible repurposing of clinically approved IIS inhibitors to ameliorate neurodegeneration in acute neurodegenerative diseases.

Whilst there is undoubtedly use in trialing novel inhibitors of this pathway, the abundance of already clinically approved inhibitors, albeit for different diseases, could greatly facilitate the transition of our hypothesis to the clinic. For this reason already clinically approved inhibitors, or inhibitors in late stage clinical trials, were prioritized over preclinical compounds. Furthermore, with the impressive mammalian work of Echeverria *et al*, Gladbach *et al*, and Ashabi *et al*, focusing at the Ras and ERK1/2 stage of the IIS, we chose to focus at specifically this level of the pathway rather than higher or lower. This also provided a wide range of clinically approved inhibitors to choose from.

Once more acute neurodegenerative diseases were chosen in preference over chronic neurodegeneration, this time due to the time frame of the possible drug administration, and the common side effects of IIS inhibitors.

Figure 1.4 lists inhibitors of the IIS cascade that are already approved for use in humans or are in later stages of clinical trials, the diseases they target, and the pharmaceutical companies that own them. Clinically approved inhibitors with low IC50's were preferred, with inhibitors of MEK and Ras specifically being a focus as discussed above. Priority was given to investigating the MEK inhibitor Trametinib (Mekinist), with the B-Raf inhibitor Dabrafenib (Tafinlar) chosen as an alternative option. The work by Slack *et al* established Trametinib as a pharmacological intervention that decreased signalling in the IIS pathway leading to lifespan extension in Drosophila (Slack et al., 2015). With reduced pathology in animal models of neurodegeneration when crossed with animal models of lifespan extension or treated with experimental IIS inhibitors, and Trametinib administration leading to lifespan extension, this drug was chosen over others that lacked this direct link.

Official name	Trade name	Stage	Disease prescribed/ in testing for	Daily dose	IC50	Company
IGF1R inhibitors						
Picropodophyllin (AXL1717)		Phase I/II (NCT01721577)	Astrocytoma	300-520mg twice daily orally	1nM[1]	Axelar AB
BMS-754807		Phase I/II (NCT01225172) (NCT00898716)	Breast cancer; neoplasms	100mg daily orally	1.8nM[2]	Bristol-Myers Squibb
Linsitinib (OSI-906)		PhaseII/III (NCT00924989) (NCT02546544) (NCT02057380)	Adrenocortical Carcinoma; Erwing sarcoma; Advanced solid tumours		35nM[3]	Astellas Pharma Inc
Raf inhibtors						
Vemurafenib (PLX4032)	Zelboraf	Approved	V600E melanoma	960mg twice daily orally	100nM[4]	Roche
Sorafenib	Nexavar	Approved	Renal cell carcinoma; Hepatocellular carcinoma; Thyroid cancer	400mg twice daily orally	6nM[5]	Bayer/Onyx Pharmaceuticals
Dabrafenib	Tafinlar	Approved	V600E melanoma	150mg twice daily orally	3.2nM[6]	GlaxoSmithKline
Raf265 (Chir265)		Phase I/II (NCT00304525) (NCT01352273)	Metastatic melanoma; Solid tumours	83.6mg daily	60nM[7]	Novartis
RXDX-105 (CEP-32496)		Phase I/II (NCT01877811)	Solid tumours	275mg once daily orally	36nM[8]	Ignyta Inc.
Encorafenib (LGX818)		Phase III (NCT02109653)	V600E melanoma	300mg daily orally	N/A[9]	Array BioPharma
LY3009120		Phase I (NCT02014116)	Neoplasms; Melanoma		47nM[10]	Eli Lilly
RO5126766 (CH5126766)		Phase I (NCT02407509) (NCT00773526)	Solid tumours; Multiple myeloma; Neoplasms		19nM[11]	Roche
MEK inhibitors						
Selumetinib (AZD6244)		Phase III (NCT01974752) (NCT01843062) (NCT01933932)	Metastatic melanoma; Thyroid cancer; Non small cell lung cancer	75mg twice daily orally	14nM[12]	AstraZeneca
PD0325901		Phase I/II (NCT02022982) (NCT02096471)	KRAS mutant non small cell lung cancer; Neurofibramatosis	4mg twice daily orally	0.33nM[13]	Pfizer

Trametinib (GSK1120212)	Mekinist	Approved	V600E melanoma	2mg once daily orally	1.8nM[14]	GlaxoSmithKline
PD184352 (CI-1040)		Phase II (NCT00033384)	Breast cancer; Colorectal	Twice daily orally	17nM[15]	Pfizer
Pimasertib (AS-703026)		Phase II (NCT01936363) (NCT01693068)	Ovarian cancer; Cutaneous melanoma	60mg once daily orally	20nM[16]	Merck Serono
Binimetinib (MEK162)		Phase III (NCT01763164) (NCT01849874)	Cutaneous melanoma; Ovarian cancer	45mg twice daily orally	12nM[17]	Array BioPharma
Refametinib (RDEA119)		Phase II (NCT02168777) (NCT01915589)	Neoplasms; Carcinoma	50mg twice daily orally	19nM[18]	Bayer
GDC-0623		Phase I (NCT01106599)	Solid cancers		0.13nM[19]	Genentech
Cobimetinib	Cotellic	Approved	V600E melanoma	60mg once daily orally	4.2nM[20]	Genentech
ERK1/2 inhibitors						
Ulixertinib (BVD-523, VRT752271)		Phase I/II (NCT02608229) (NCT02296242)	Pancreatic cancer; Leukemia		0.3nM[21]	BioMed Valleys Discoveries
GDC-0994		Phase I (NCT01875705)	Solid cancers		0.3nM[22]	Genentech

Figure 1.4. Inhibitors of the IIS signalling pathway that are currently approved for human use, or currently in Phase trials. ClinicalTrails.gov identifier numbers are given for on-going trials. IC50 figures refer to inhibition of wild type protein only, and can be far more sensitive for specific mutated versions of the proteins. (1- (Girnita et al., 2004), 2- (Carboni et al., 2009), 3- (Mulvihill et al., 2009), 4- (Bollag et al., 2010), 5- (Wilhelm et al., 2004), 6- (Laquerre et al., 2009), 7- (Mordant et al., 2010), 8- (Rowbottom et al., 2012), 9 - (Stuart et al., 2012), 10- (Henry et al., 2015), 11- (Ishii et al., 2013), 12- (Huynh et al., 2007), 13- (Barrett et al., 2008), 14- (Yamaguchi et al., 2011), 15- (Sebolt-Leopold et al., 1999), 16- (Kim et al., 2010), 17- (Pheneger et al., 2006), 18- (Iverson et al., 2009), 19- (Hatzivassiliou et al., 2013), 20- (Hoeflich et al., 2012), 21- (Ward et al., 2015), 22- (Robarge et al., 2014)).

Trametinib is currently approved for use in terminal metastatic melanoma with a V600E B-Raf mutation, but these patients have a high chance of developing secondary metastases in the brain (Amer et al., 1978; Infante et al., 2012). Inhibitors showing specificity for mutated B-raf rather than wild-type B-raf, such as Dabrafenib and Vemurafenib, have shown efficacy in inhibiting secondary brain metastases in clinical trials, whilst no evidence exists of clinical efficacy of Trametinib treating brain metastases (Dummer et al., 2014; Long et al., 2012). Experiments in mice further suggest poor brain bioavailability of Trametinib (Vaidhyanathan et al., 2014). With this being the organ we are aimed to target, this could severely limit Trametinib's effectiveness as an IIS inhibitor for diseases of the brain.

Several limitations of Dabrafenib as a sole agent for treating melanoma, including acquired resistance to Dabrafenib and the increased incidence of squamous cell carcinoma with treatment, which was reduced when paired with a MEK inhibitor, lead to Trametinib being paired with Dabrafenib as a combination therapy for treating metastatic melanoma with a B-Raf V600E mutation (Anforth et al., 2012; King et al., 2013; Robert et al., 2015; Solit and Rosen, 2011). Whilst many neurodegenerative disorders are accompanied by damage to the blood brain barrier and neurovasculature that may well increase the brain bioavailability of Trametinib (Obermeier et al., 2013), it seems prudent to also examine Dabrafenib as a secondary pharmacological option given its apparent brain bioavailability (Mittapalli et al., 2013). It is for this reason that Dabrafenib has been chosen as a secondary agent in our investigations.

To establish the susceptibility of brain cells to inhibition by Trametinib and Dabrafenib, we first considered expression levels of the proteins being targeted in these cell types in the brains of humans and mice. Considering the transcriptomes of brain cell types using online databases, all types of brain cells express B-Raf and MEK1, which are the proteins that Dabrafenib and Trametinib inhibit (figure 1.5)(Hawrylycz et al., 2012; Zhang et al., 2014). We would therefore predict that our two drugs of choice would inhibit the IIS cascade in the cell types we are interested in.

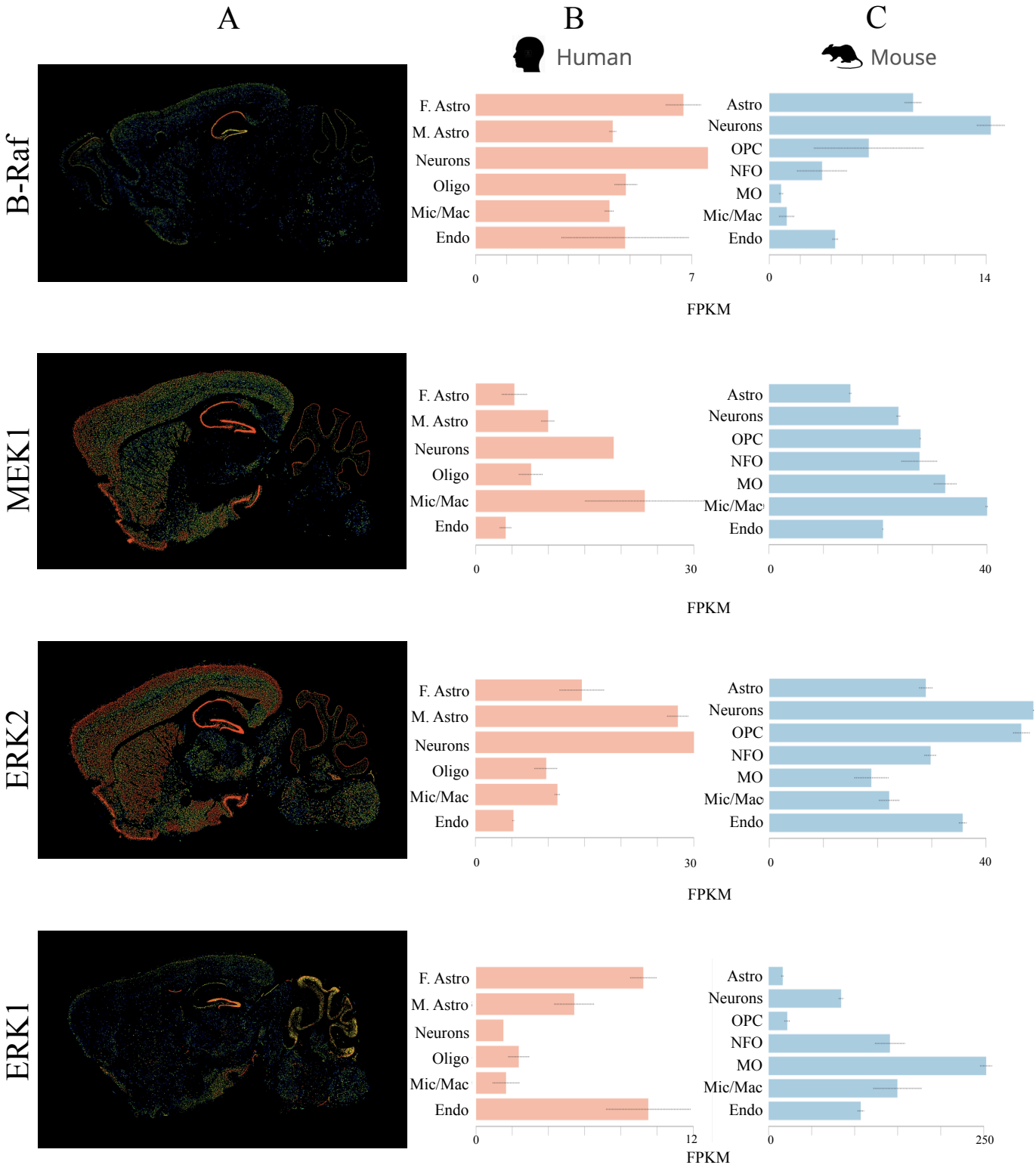

Figure 1.5. Expression levels of members of Insulin and Insulin-like Signaling Cascade in the mammalian brain. (A) RNAseq images of the 4 genes showing high levels of expression in the hippocampus, but with the CA3 cells showing comparatively less ERK1 and IGF1R expression. (B) (C) RNAseq graphs showing relative expression. Panels in A modified from http://mouse.brain-map.org/, B from http://web.stanford.edu/group/barres_lab/brain_rnaseq.html, and C from http://www.brainrnaseq.org. F. Astro - Fetal Astrocytes, M. Astro – Mature Astrocytes, Oligo – Oligodendrocytes, Mic/Mac – Microglia/Macrophages, Endo – Endothelial, OPC – Oligodendrocyte Precursor Cells, NFO – Newly Formed Oligodendrocytes, MO – Mature Oligodendrocytes. FPKM - Fragments per kilobase of transcript sequence per million mapped fragments

With two suitable clinically approved IIS inhibitors identified, we investigated the repurposing of Trametinib and Dabrafenib by testing these drugs in primary neuronal and astrocyte cultures, before testing for neuroprotective effects in our developed model of acute neurodegeneration, and finally investigated the efficacy of using these drugs to inhibit IIS in the mammalian brain.

Summary

The most common diseases limiting human life expectancy and healthspan in developed nations are testimony to the success of biomedicine at reducing early life causes of mortality. The diseases responsible for early life mortality were overwhelmingly communicable, and predominantly had a clear exogenous initiating factor. Currently the diseases that are limiting human life expectancy and healthspan in developed nations are non-communicable diseases, which lack clear initiating factors, meaning that adequate treatment has proved difficult to identify. With this change in the type of disease has also come a change in the types of organs affected also. Neurodegenerative disorders are a wide family of diseases affecting the brain and characterised by progressive neuronal loss, and have rapidly grown in prevalence with the increase in human life expectancy. Currently very limited adequate therapies are available to treat these disorders, with treatments often limited to symptomatic therapies. A crucial feature of neurodegenerative disease is that the neurons lost are irreplaceable. Very limited therapies have been developed that in any way target this neurodegeneration, and this presently unrestricted loss of neurons in these diseases will severely limit the patient outcome for those diagnosed with these diseases.

This thesis investigates the IIS pathway as a potential source of novel therapeutics that could directly modulate neuronal cell death, with the aim of unearthing new therapeutic targets and drugs. Endogenous alterations in the IIS pathway have been observed in multiple neurodegenerative diseases, and decreasing IIS signalling by genetic and pharmacological means has been shown to reduce neurodegeneration. This puts the IIS cascade as a pharmacologically targetable molecular pathway that is implicated in neuronal cell death and neurodegeneration and is yet to be exploited for

therapeutic gain. By investigating endogenous changes of the IIS cascade in AD, the effect of endogenously increased IGF1 in acute neurodegeneration, and the potential for repurposing currently available IIS inhibitors, we hope to uncover novel therapeutic possibilities to target the neuronal cell loss that is so central to neurodegenerative diseases.

Chapter 2

Materials and methods

All mice experiments were conducted according to UK Home office regulations under the Animals (Scientific Procedures) Act 1986, as well as UCL local ethical guidelines.

Experimental animals

APP-KI$^{NL\text{-}G\text{-}F/NL\text{-}G\text{-}F}$ mice were generated by Saito and Saido by knocking in a humanised Aβ sequence with three specific fAD mutations on a C57BL-6J background (Saito et al., 2014). The Swedish KM670/671NL mutation increases Aβ40 and Aβ42 creation, the Beyreuther/Iberian I716F mutation increases the Aβ42 to Aβ40 ratio, and the Arctic mutation caused the mice to exhibit greater neuroinflammation and a swifter pathology (Citron et al., 1992; Guardia-Laguarta et al., 2010; Saito et al., 2014; Tsubuki et al., 2003). These mice therefore do not overexpress APP, but express wild type levels of APP from the endogenous mouse promoter with three fAD mutations, which gives progressive amyloid plaque deposition.

All APP-KI mice used were housed and maintained in the RIKEN Brain Science Institute (Japan) by the Saido lab. Mice were housed 12 per cage (26 cm x 37 cm x 19 cm), kept under standard housing condition in 12 hour light dark cycles, and allowed *ad libitum* access to food and water. Mice were sacrificed in Japan, and snap frozen tissue sent to us for analysis. All mice used were male. Wild type littermates were kept in identical conditions, and sent for comparison.

TG4510 mice were generated by the Ashe lab (University of Minnesota) (Ramsden et al., 2005; Santacruz et al., 2005). These mice express a repressible form of human tau containing the P301L mutation (4R0N tau P301L), which in humans causes familial frontotemporal dementia (Hutton et al., 1998). The transgene is downstream of a

tetracycline operon–responsive element (TRE) under the Ca^{2+}/ calmodulin dependent protein kinase II (CaMKII-α) promoter, with expression restricted to the forebrain (Ramsden et al., 2005; Santacruz et al., 2005). The mice used were the bitransgenic F1 progeny of responder transgene (TRE promoter upstream of mutated tau) and activator transgene (CaMKII-α upstream of tet-off open reading frame) mice, and expressed approximately 13 times the level of wild type murine tau. They are therefore an F1 mix of equal proportions of FVB/N (from one parental line), and C57BL-6 (from the other parental line).

All TG4510 mice used were housed and maintained by Eisai Inc (Massachusetts). Mice were housed under standard conditions, under standard housing condition in 12 hour light dark cycles, and allowed *ad libitum* access to food and water. Mice were sacrificed in the USA, and snap frozen tissue sent to us for analysis. All mice used were female. Wild type littermates were kept in identical conditions, and sent for comparison.

Wild type animals used for testing Trametinib and GFP-S strain mice for organotypic slice preparation were from C57BL/6J colonies (Feng et al., 2000), kept in the University College London Biological Services Unit. Mice were housed 6 per cage from weaning, kept under standard housing condition in 12 hour light dark cycles, and allowed *ad libitum* access to food and water. All mice used were male. Processing of GFP-S mice for organotypic slices, and wild type mice following Trametinib treatment is discussed below.

Primary cell cultures and organotypic brain slices

Primary neuronal cultures

Primary neuronal cultures were generated from C57BL/6J mice following a modified protocol from the protocol used by Dresbach *et al* (Dresbach et al., 2003). Postnatal mice between 0-1 days old (P0-P1) were killed by decapitation, with the brain quickly removed and placed in ice-cold dissection media (160mM NaCl, 5mM KCl, 1mM

$MgSO_4$, 4mM $CaCl_2$, 5mM HEPES, 5.5 mM glucose, 5µM phenol red, pH 7.4). Swiftly following brain removal, cortices and hippocampi were dissected under a light microscope in dissection media, and kept on ice in fresh dissection media. When all brains had been dissected, cortices and hippocampi were removed from dissection media diced, and incubated at 37^{o}C for 30 minutes in enzymatic digestion media (dissection media, 1.5mM L-cysteine, 0.5mM EDTA, 5mM $CaCl_2$, 30mM NaOH, 100V papain, 1% DNaseI), with occasional agitation. Digested tissue was allowed to settle, digestion media removed, and inactivation media added (serum media (MEM w/Earle's w/o l-glutamine, 5% fetal bovine serum (FBS), 0.4g/l glucose), 0.25%w/v bovine serum albumen (BSA)), for 2 minutes before removal, and then serum media was added. Cells were liberated from digested tissue via trituration, with the resulting cell suspension pipetted off from settled debris, pelleted at 1,000RPM for 5 minutes at room temperature, and then the pellet re-suspended, and plated at a density of either 130,000/cm^2 or 325,000/cm^2 in poly-d-lysine coated 24 well plates, in neuron media (Neurobasal Media (ThermoFisher), 4% B27 with vitamin A, 1% Glutamax-I (ThermoFisher)).

Half the neuron media was changed after 1 day and 7 days, and 10µM FUDR was added after 4 days to inhibit non-neuronal cell growth. From around 18-20 days, gradual cell death occurred in the cultures, so all experiments were performed on neurons between 10-17 days in vitro (10-17 DIV).

Primary astrocyte cultures

Primary astrocyte cultures were generated from C57-BL6 mice following the protocol of Schildge *et al* (Schildge et al., 2013). P2-P4 mice were killed via decapitation, with the brain quickly removed and placed in ice-cold HBSS. Following the removal of all brains, cortices and hippocampi were dissected and added to fresh ice cold HBSS. Dissected cortices and hippocampi were then diced, before being incubated at 37^{o}C for 30 minutes with occasional agitation in digestion media (HBSS, 0.25% Trypsin). Following centrifugation at 300g for 5 minutes at room temperature, the supernatant was discarded, the pellet dissociated in glial media (high glucose DMEM, 10% FBS,

50 units Penicillin, 50µg Streptomycin), and mixed glia plated at 120,000/cm^2 in a poly-d-lysine coated flask. Glial media was changed every 3 days.

These mixed glial cultures were purified for astrocytes after 7 days by shaking at 240RPM at 30^oC in a heated shaker for 5 hours. This dislodged non-astrocyte glial cell allowing their removal, allowing pure astrocytes to be isolated via trypsinisation, and re-plated at a density of 120,000 cells/cm^2 in 24 well plates. After a further 3-5 days of incubations, a nearly confluent layer of astrocytes was present, which could then be used for our experiments.

Forming bilaminar co-cultures

To create bilaminar co-cultures, we modified the protocol of Shimizu *et al* (Shimizu et al., 2011). Primary neuronal and astrocyte cultures were grown separately as detailed above, with neuronal cultures grown on glass cover slips and astrocyte cultures grown on the bottom of 24 well plates. To facilitate cell death analysis, in some wells of the plate, astrocytes were grown at the same density but on glass cover slips. This was done to allow removal of astrocytes and neurons for PFA fixation, without negatively impacting on the other wells on the plate that were to be taken for protein or RNA. When neurons were 9-12 DIV, and astrocytes 11-20 DIV, the neuronal cover slips were suspended above the astrocyte cells by the addition of a small 3mm length of autoclaved plastic tubing to the bottom of each well of the 24 well plate, before cover slips were inverted and placed on top (figure 4.1). The media in each well was changed from mixed glial media to neuronal media, with half the media (500µl) being from the well of the neuronal cover slip added, and half being fresh warmed neuron media.

Organotypic brain slices

Organotypic slices of the hippocampal formation were made from P5-7 C57BL-6 GFP-S transgenic mice. Mice were decapitated and the brain swiftly removed into

cold slicing media (EBSS, 5mM HEPES). Removed brains were bisected down the midline, before angled sections 15% off midline were made from the dorsal surface, and this surface attached to the vibratome stage (Campden). This slice orientation preserved CA1 pyramidal neurons making these slices useful for examining these cells.

Both hemispheres were glued to the vibratome stage and 300µm slices taken. The hippocampus was dissected out and transferred via glass pipette to 13mm filter paper (LCR 0.5µm; Millicell), sitting in inserts in 6 well culture plates (Millipore), three to a well. Each well contained 1 ml culture medium (50% MEM with Glutamax-1, 25% horse serum, 23% EBSS, 36.1 mM glucose, 50 units penicillin, 50 µg streptomycin and 6.25 units nystatin) that was changed three times a week.

Culture treatments

Dabrafenib and Trametinib treatment of primary neuronal and astrocyte cultures

Once mature, primary neuronal and astrocyte cultures were treated with various concentrations of either Dabrafenib, Trametinib (Both Selleckchem), or the same volume of DMSO vehicle control. This was achieved by diluting 10µl of solution into 40µl of fresh media, and adding this to the wells of treated cultures.

Igf1 knockdown of bilaminar co-cultures

Once bilaminar co-cultures were made, following 3-4 hours acclimatisation, the cultures were then treated with either siRNA against *Igf1* (ThermoFisher, catalogue number 4390771) or non-targeting siRNA (Ambion, catalogue number 4457287). To transfect these cultures, 3µl/well Lipofectamine® RNAiMAX was diluted in 50µl/well Opti-MEM®, with 5pM/well siRNA against either *Igf1* or non-targeting siRNA was diluted in 50µl/well Opti-MEM®, before these dilutions were combined and incubated at room temperature for 5 minutes (all reagents from

LifeTechnologies). 50µl of Lipofectamine®-siRNA complex was then added to each well of treated cultures.

Trametinib and dual Igf1 knockdown and Trametinib treatment of bilaminar cultures

For sole Trametinib treatment, once bilaminar co-cultures were made, following 1 hours acclimatisation, the cultures were then treated with either 10µM Trametinib dissolved in DMSO (1% final concentration DMSO), or 10µl of DMSO vehicle (1% final concentration DMSO), with both diluted by adding to 40µl neuron media before adding to the wells of treated cultures.

For dual Trametinib and siRNA treatment, the outlined protocols for the sole administration of each treatment were both administered to the wells to be treated with both, with control wells being treated with both non-targeted siRNA and DMSO.

Inducing cell stress via hypoxic condition exposure

To apply a stressful hypoxic incident to our cultures, we modified the protocol outlined by Wang *et al* (Wang et al., 2014). Following the addition of Trametinib, siRNA, or vehicle, plates that were to be exposed to hypoxic condition were allowed to settle for 1 hour before being placed in hypoxic conditions. Plates were placed in between two sheets of heat sealable plastic, sealed using a heat sealer, and flushed for 1 minute with 100% argon gas to displace oxygen. The bag was then sealed in an inflated state to allow easy observation of the preservation of a successful seal to the outside gaseous environment. Hypoxic bags were then placed within a cell culture chamber to maintain the cultures at 37^{o}C. Cultures were exposed to hypoxic conditions for 5 hours, with the chamber purged of containing gas with argon once more after 2 ½ hours, and resealed. This purging step accounts for any dissolved gas coming out of solution during the previous two hours, therefore maintaining optimal

hypoxic conditions. At the end of the 5 hours in hypoxic conditions, plates were cut out of the sealed bag and placed back in the incubator.

Molecular Biology and microscopy

Mouse brain dissection

For molecular biology examination of wild type mice treated with either Trametinib or vehicle, male wild type mice were decapitated and brains swiftly removed and dissected on ice. Following the isolation of cortex or hippocampus, tissue for protein and RNA analysis was immediately snap frozen on dry ice and stored at -80^{o}C until required.

For APP-KI and their relevant controls, brain samples sent from our collaborators were cut into segments whilst frozen and processed separately for protein or RNA. To achieve this, tissue was placed on a sterile petri dish on dry ice and one hemisphere of cortex was quartered from each sample. One quarter was then processed for protein, and another for RNA, with half of the brain kept at -80^{o}C for future use if required. Samples were never allowed to thaw during this process.

TG4510 samples had two hippocampal samples from each mouse separate, allowing analysis of either sample separately for protein or RNA.

Human brain samples came in an eppendorf tube containing pieces of tissue, with one piece taken for protein and another for RNA.

Brain tissue homogenisation for protein and gene expression analysis

Mouse cortex, or hippocampus were sonicated (Branson sonifier, 450) for 30s at 9W

in ice cold RIPA buffer (1% Triton X-100, 1% sodium deoxycholate, 0.1% SDS, 0.15M NaCl, 20mM Tris.HCl (pH 7.4), 2mM EDTA (pH 8.0), 50mM sodium fluoride, 40mM β-glycerophosphate, 1mM EGTA (pH 8.0), 2mM sodium orthovanadate, 1mM PMSF, protease inhibitor tablet (Roche), 0.055 units aprotinin (Sigma), 1% phosphatase inhibitor cocktail (Sigma)). Samples were centrifuged at 13,000RPM for 10 minutes twice, with supernatants kept each time and insoluble pellets disposed of. Half the volume of the resulting homogenate was separated and diluted with half the volume of 3X Laemmli buffer (188 mM Tris-Cl [pH 6.8], 3% SDS, 30% glycerol, 0.01% bromophenol blue, 15% β-mercaptoethanol) and boiled for 3 minutes before being stored at -20^{o}C until required. Non-laemmli diluted homogenate was used for protein concentration quantification for each homogenate using the Bio-Rad Bradford protein assay by comparison to a standard curve generated from serial dilutions of bovine serum albumin.

For gene expression analysis, mouse cortex or hippocampus samples were homogenised using a homogeniser for 30 seconds on ice using RNA lysis buffer (QIAGEN). Following homogenisation samples were aliquoted and stored at -80^{o}C.

Culture lysis to measure gene expression, cell signalling, and cell death changes in bilaminar cultures

In solo astrocyte and neuronal cultures for protein and gene expression analysis, cultures were grown on the bottom of either 6 well or 24 well plates. To lyse wells for RNA and protein in bilaminar co-cultures, astrocytes were grown on the bottom of each well, with neurons suspended above on a glass coverslip. Coverslips were removed for lysis. For wells to be processed for fixation, astrocytes were also grown on coverslip and placed at the bottom of the well, with neurons once more suspended above them. These coverslips were removed to a new plate for fixation.

To lyse for protein or RNA, neuronal cover slips were removed from above the astrocyte layer into different wells, and plates put on ice. Neuron and astrocyte cultures were then washed with ice-cold PBS 3 times, before 500µl RNA lysis buffer

(QIAGEN), or 75 µl of 2X Laemmli dye was pipetted onto the cultures. Cultures were then scraped with a pipette tip, incubated on ice for five minutes, scraped again, and then removed into 1.5ml eppendorf tubes. Duplicate wells had samples pooled, with RNA homogenate stored at -80^{0}C and protein homogenate boiled for 2 minutes in a heat block, and stored at -20^{0}C.

For cell number counting in bilaminar co-cultures, cultures were fixed by adding 500µl of 4% PFA to cultures containing 500µl media, and incubating for 15 minutes. Cultures were then washed 5 times with PBS, with PBS containing DAPI at a concentration of 1:10,000 used for the 4th wash. Cover slips were stored in PBS with 0.02% sodium azide until imaged.

Western blotting

Protein samples were resolved by sodium dodecyl sulfate polyacrylamide gel electrophoresis (SDS-PAGE) using 10% polyacrylamide gels with 15 well combs. For brain protein samples, proteins were diluted to a given weight, whereas culture homogenates were loaded blind onto the gel. A molecular weight ladder was also loaded to aid band identification (BioRad). Proteins were subsequently transferred to 0.45µm nitrocellulose membrane (BioRad) by wet electrotransfer overnight at 30V.

Following transfer, membranes were washed in Tris-buffered saline (30 mM NaCl, 30mM Tris pH7.4)(TBS), blocked in 5% milk for 1 hour at room temperature, washed in TBS with 0.1% Tween-20 (TBST)(Sigma) 3 times for 5 minutes, and incubated in primary antibody in 5% milk/BSA in TBST overnight at 4°C (figure 2.1). Membranes were then washed in 0.1% TBST 3 more times for 5 minutes each, and then incubated in Horseradish peroxidase-conjugated secondary antibody specific to the species of the primary antibody (1:10000; Jackson ImmunoResearch) diluted in 5% milk in TBST for 1 hour at room temperature. Membranes were washed 3 more times for 5 minutes in TBST before enhanced chemiluminescence detection kit (ECL, BioRad) was applied to the membrane for 4 minutes. Image acquisition and densitometric analysis was performed using ImageLab (v5.2, BioRad).

Target	Supplier and product code	Dilution
Phospho-Akt (Ser473)	CST 4060	1:1000
Phospho-Akt (Thr308)	CST 2965	1:1000
Total Akt	CST 4691	1:1000
Phospho-ERK1/2 (Thr202/Tyr204)	CST 9101	1:1000
Total ERK1/2	CST 9102	1:1000

Figure 2.1. Antibodies used for western blotting. A table of the specific antibodies used during western blotting, the supplier and product code, and the dilution they were used at. CST – Cell Signaling Technologies.

For phospho-protein density values, bands of interest were normalized against density values for total protein (e.g. pSer473-Akt normalized to total Akt). Total protein density values were normalized against total lane protein using the Ponceau S (Sigma Aldrich) stain.

To immunoblot a membrane for both the phosphorylated and total protein, membranes were first probed for the phospho-protein, then stripped following chemiluminescence detection by agitating at 50^{o}C in stripping buffer (60µM Tris base, 70µM Sodium dodecyl sulfate, 0.7% 2-Mercaptoethanol), before washing 6 times for 5 minutes in TBST. The membrane was then ready for blocking, and re-probing with primary antibody.

Primer design and testing

Primers for *Igf1, IGF1, Rps28, and RPS28* were designed to span exon boundaries with PrimerBLAST (NCBI). Sequences were ordered with salt-free purification from Eurofins MWG Operon. Primers were tested in RT-PCR by incubating cDNA from 4-

week-old wild type cortex with 0.25μM forward and reverse primers and SsoAdvanced PCR Mix (BioRad) (cycling conditions 95°C-3 minutes, [95 °C-10s; 58 °C-30s; 72 °C-30s] x40, 95 °C -1 minute), before running in a 3% agarose gel containing ethidium bromide and visualising using a Bio-Rad ChemiDoc MP imaging system.

A single band of the correct size was observed for all primers, with bands being absent in controls where no reverse transcriptase was added to the reaction. Melt curve analysis was run on the product of a dilution series of cDNA, with qRT-PCR reactions containing SYBR green (Bio-Rad) allowing optimal cDNA concentrations to be used for each primer pair. A single peak corresponding to one product size was seen also for all primer pairs.

RNA purification and cDNA conversion

The mRNA samples were disrupted using a 21-gauge syringe and purified with the Qiagen miRNA easy mini kit treated with DNAse. cDNA was then made for each sample using the ThermoFisher High-Capacity cDNA reverse transcriptase kit, with a negative control reaction without reverse transcriptase also made to use as a control in RT-qPCR reactions.

RT-qPCR

To measure *Igf1* expression levels in mouse brain homogenates, RT-qPCR was performed using 0.125 and 0.033 times dilutions of cDNA (0.05mg/ml stock concentration) for *Igf1* and *Rps28* respectively, using SYBR Green PCR Mix (BioRad) with the above cycling conditions in the CFX96 touch qRT-PCR detection system (Bio-Rad), and the same concentration of forward and reverse primers. For *IGF1* expression in human brain samples identicle conditions were used, with the

exception of cDNA dilutions of 0.33 and 0.033 dilutions were used for *IGF1* and *RPS28* primers respectively. For cell culture lysates there was no dilution of cDNA.

Samples were tested in triplicate with a no-RT control in a 96 well plate, with raw cycle threshold (CT) expression values normalised to Rps28 expression values.

DAPI cell counting

PFA fixed cover slips were imaged for DAPI staining in 4 areas of each coverslip at 10X magnification on an EVOS® FL Auto Cell Imaging System (Life technologies). Images were then processed for counting using ImageJ (v1.48) by converting images to 8-bit format and counting using the Analyse Particles function.

Dendritic spine imaging

Organotypic slices were transferred to the chamber of a confocal microscope (Olympus Fluoview), and 30°C carbogen aerated artificial cerebral spinal fluid (ACSF)(125mM NaCl, 2.5mM KCl, 1.25mM NaH_2PO_4, 26mM $NaHCO_3$, 2mM $CaCl_2$, 1mM $MgCl_2$, 25mM glucose) was circulated over the slice at a rate of 1ml/minute. Using a mercury lamp fluorescent CA1 pyramidal cells of the hippocampus were located and suitable dendritic processes identified. Using the confocal microscope and the FluoView software (Olympus), dendritic processes were imaged at 60X magnification (water immersion Zeiss objective, NA 0.9) by taking images of a selected x y area at 3X mechanical zoom, and imaging at 0.2µm z axis steps until the complete dendrite was imaged.

Dendritic spines were then counted manually by scrolling through image stacks using the ImageJ software, and the spine density calculated by dividing by the dendrite length.

Statistical analysis

All statistical analysis was performed using Prism v6.2 (Graphpad Software Inc). Testing for significance between means was done using the Student's t-test when individual comparisons were made, when multiple comparisons were made (e.g. within a plate of bilaminar co-cultures), 2-way ANOVA was performed.

Chapter 3

Characterising endogenous changes to the Insulin and Insulin-like Signalling Cascade in Alzheimer's disease

Introduction

The level of signalling through the Insulin and Insulin-like signalling (IIS) cascade can modulate the rate of ageing, with reductions in IIS by genetic and pharmacological means producing organisms with substantially increased life spans (Bjedov et al., 2010; Harrison et al., 2009; Holzenberger et al., 2003; Kenyon et al., 1993; Slack et al., 2015; Tatar et al., 2001). Crucially this increase in lifespan is accompanied by an increase in healthspan, meaning a longer duration of healthy disease free life for these long-lived organisms. When genetically long-lived organisms are crossed with animal models of Alzheimer's disease (AD) and Parkinson's disease (PD), the progression of the neurodegenerative pathology is slowed, and neuronal cell loss is reduced (Cohen et al., 2006; Cohen et al., 2009; Cooper et al., 2015). This protection against neurodegeneration has also been demonstrated using pharmacological IIS inhibitors applied to animal models of neurodegenerative disease (Ashabi et al., 2013; Echeverria et al., 2009; Gladbach et al., 2014). This suggests that IIS inhibitors could be used therapeutically to ameliorate neurodegeneration, and this forms our overall hypothesis.

With acute neurodegenerative diseases such as stroke and traumatic brain injury (TBI), the therapeutic window for intervention is small and well defined, and therefore the timing of potential IIS modulating therapies is straightforward. This is not so for chronic neurodegenerative diseases however, as disease pathogenesis and neuronal cell loss occurs over a far more extended time frame. Before IIS modulating therapies can be investigated in chronic neurodegenerative diseases therefore, the appropriate time point for IIS modulator application must be ascertained. We chose to do this for AD specifically, as this is the most prevalent chronic neurodegenerative disease.

AD has a long disease time course, including a long prodromal period with substantial neuronal cell loss present by diagnosis (Fox et al., 1996). Improved therapeutics are grossly lacking for this disease, with IIS modulating therapies therefore representing a novel approach to AD therapeutics. Endogenous alterations in IIS have been observed in the AD brain however (Ferrer et al., 2001; Steen et al., 2005; Talbot et al., 2012), and these alterations could interfere with or directly oppose any intended pharmacological IIS intervention. For example, brain IIS resistance could limit the efficacy of IIS stimulating therapies. Similarly, if these changes contribute to the pathological progression of these diseases, identifying the time point of these changes can aid the correct timing of IIS intervention therapies. Current characterisations of endogenous IIS changes in AD have focused on post mortem brain tissue, but these samples are from the very end stage of disease progression (Ferrer et al., 2001; Steen et al., 2005; Talbot et al., 2012). As it seems likely that successful AD therapies will have to be applied earlier in disease progression, it is crucial to consider IIS alterations earlier as well as later in the disease. A more extensive characterisation will therefore aid us in avoiding the application of IIS modulating therapies at time points where endogenous IIS alterations may limit the efficacy of our proposed interventions.

In order to best test our overall hypothesis in AD, we have therefore established how the IIS cascade is endogenously changed at different stages of AD pathogenesis, meaning that we have examined earlier pathological stages in AD than has previously been reported.

Aims

The aim of this chapter is to characterise the endogenous changes in the IIS cascade at different pathological components of AD, to aid the future testing of our main hypothesis; that IIS modulating therapies can ameliorate neuronal cell loss in neurodegeneration. This characterisation will include pathological stages of AD that are yet unexamined, that being early stages of disease development, which correspond

to pre-diagnosis AD. By identifying endogenous IIS changes that could interfere with our proposed IIS interventions, this characterisation will allow the optimisation of the timing for future IIS modulating therapies in AD.

Methods

To characterise IIS changes at multiple points in the disease time course we utilised two different mouse models of pathological components of dementia, representing different pathological stages of disease development in relation to human pathology. Given the temporal distinction in the development of these neuropathological hallmarks in human AD, with amyloid pathology preceding tau pathology, we examined IIS changes in response to amyloid and tau pathology individually, and finally measured IIS changes in post mortem human brain samples to characterise IIS changes at the end stage of AD development. We were therefore able to characterise endogenous IIS changes at different pathological stages of AD development.

To model progressive amyloid pathology, we used the APP-KI$^{NL\text{-}G\text{-}F/NL\text{-}G\text{-}F}$ (APP-KI) mouse model showing a progressive increase in $A\beta_{40}$ and $A\beta_{42}$ levels and subsequent progressing amyloid plaque deposition (Saito et al., 2014). We examined IIS changes at 2, 4, and 8 months of age in cortical tissue from male animals, which corresponds to the very beginning of amyloid pathology (increasing $A\beta_{40}$ and $A\beta_{42}$ and the first small amyloid plaques) at 2 months, midrange amyloidosis (increasing plaque number) at 4 months, and heavy amyloid pathology at 8 months (maximal plaque deposition)(Saito et al., 2014). To model progressive tau pathology we used the TG4510 mouse model, which shows progressive tau hyperphosphorylation and tangle accumulation, accompanied by extensive neuronal cell loss (Ramsden et al., 2005; Santacruz et al., 2005). This is a rapidly progressing disease model, with over 75% of hippocampal pyramidal neurons lost by 8 months of age. We examined IIS changes at 2.5 months and 8 months in the hippocampus of female animals, corresponding to early tau pathology (increased p-Tau levels and pretangle development) and very late stage tau pathology (heavy tangle formation and substantial neuronal cell loss). These

IIS changes were all made in comparison to wild type age matched mice of the same gender and mouse strain. Finally, as a preliminary means of examining final stage endogenous IIS changes, we examined post mortem human frontal cortex samples from fAD and sAD patients and non-demented controls, the patient details which can be seen in figure 3.1. In the future, further experimentation of this type will take place with a larger number of patient samples. Thorough descriptions of mouse models and how they correspond to human AD neuropathology, as well as the source of tissue used, is covered in chapter 1.

To assess the levels of IIS signalling in these tissues, we examined multiple points in the IIS cascade. As changes in IGF1 level have been repeatedly observed in neurodegenerative disorders (Beilharz et al., 1998; Connor et al., 1997; Madathil et al., 2013; Steen et al., 2005), we measured both *IGF1* and *Igf1* expression in the

Disease state	Age	Gender
Familial AD	66	Male
Familial AD	58	Female
Familial AD	59	Female
Sporadic AD	68	Female
Sporadic AD	76	Female
Sporadic AD	79	Female
Control	56	Female
Control	69	Male
Control	68	Female

Figure 3.1. Details of the human brain samples used. Human frontal cortex samples from fAD, sAD, and non-demented control brain were used for analyzing the IIS cascade, with these samples coming from varying age and gender donors.

human and mouse brain tissue via RT-qPCR. To examine signalling through both branches of the IIS cascade, we carried out western blotting using antibodies for the activation phosphorylation sites pS473 and pT308 on Akt (pS-Akt and pT-Akt) in the PI3K-Akt pathway (Alessi et al., 1996), and pT202/pY204 and pT185/pY187 on ERK1/2 (p-ERK) in the Ras-MAPK pathway (Canagarajah et al., 1997; Payne et al., 1991). The level of phosphorylation at these sites was normalised by using total Akt and ERK1/2 protein antibodies, to account for possible changes in total Akt and ERK1/2 level in response to AD pathology. To establish if levels of total Akt or ERK1/2 were changed, we normalised Akt and ERK1/2 levels against total loaded protein using the Ponceau S stain. Levels of phosphorylation at Akt and ERK1/2 gave an indication of the level of signalling through each branch of the IIS cascade under different AD pathological conditions.

Hypotheses

1. The primary hypothesis underlying the experiments in this chapter is that as amyloid and tau pathology increase in the AD brain, the IIS cascade will be endogenously changed, and that the changes will differ at different stages of AD pathogenesis.
2. Given the previous changes observed in the IIS cascade in neurodegeneration and AD, we hypothesised that increased *IGF1* will be observed in human AD brains as well as increased *Igf1* in the APP-KI and TG4510 models, with expression increasing with pathological progression in these models.
3. With the implications of increased p-ERK levels in neuronal cell death, we also hypothesised that increased p-ERK levels will be observable in 2.5-month TG4510 tissue as neurotoxic tau species are beginning to occur. With extensive neuronal cell death present in the 8 month TG4510 and human AD brain, and neuronal cell death associated p-ERK increases likely lost once neurons die, significant increases in p-ERK levels were not predicted to be detectable in these samples. With limited neuronal cell loss reported in the APP-KI mouse model, we do not expect to see changes in p-ERK level in the brains of these animals.

Results

Effects of progressive amyloid beta pathology on brain IIS signalling

Igf1 expression levels as measured by RT-qPCR, showed a significant increase in expression in the cortex of APP-KI mice at 2 and 8 months, but not at 4 months, with an 84% increase at 2 months, and 160% increase at 8 months (fig 3.2, 2-months p=0.0481, 8-months p=0.0090). This therefore shows that *Igf1* expression is raised in response to early increases in amyloid-beta elevation, and at late stage maximal plaque deposition, but not in intermediate stages of amyloid pathology. With increased *Igf1* in 2 and 8 months we would expect to see a corresponding increase in signalling in the IIS cascade.

Examining the levels of pS-Akt, pT-Akt and p-ERK by western blotting in the cortex of APP-KI and wild type mice allowed us to examine changes in signalling in both branches of the IIS cascade. In the cortex of 2-month APP-KI mice, there was

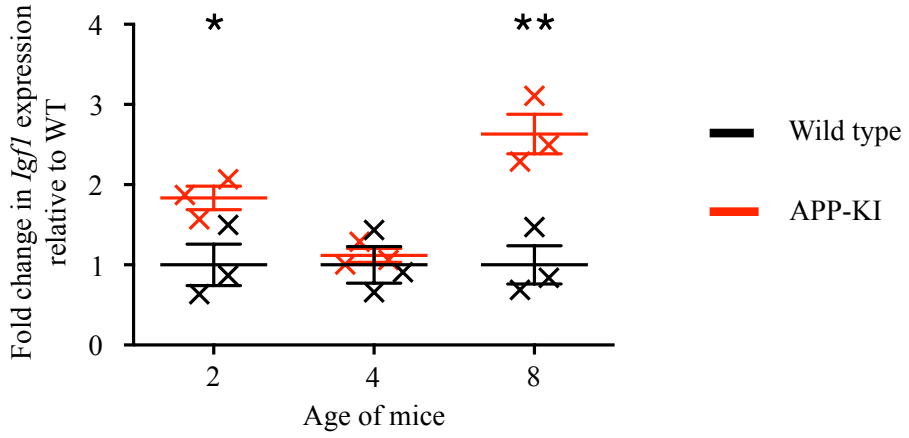

Figure 3.2. Cortical *Igf1* expression in APP-KI and wild type mice at 2, 4, and 8 months of age. *Igf1* is significantly increased in its expression in the cortex of APP-KI mice at 2 and 8 months, as measured by RT-qPCR. n=3 in all groups. Data shown is the mean +/- SEM. Student's t-test * $p<0.05$ ** $p<0.01$ *** $p<0.001$.

significantly increased phosphorylation at both Akt and ERK1/2 compared to that seen in wild type mice, with both activating phosphorylation sites on Akt increased in their level of phosphorylation (figure 3.3, p-ERK p=0.0008, pS-Akt p=0.0201, pT-Akt p=0.0437). A 12-fold increase was seen in p-ERK levels, and a 2.8 fold increase in both pS-Akt and pT-Akt levels. This indicates that not only is *Igf1* significantly increased in expression, but also that this may be increasing signalling through the IIS cascade in the cortex of the APP-KI mice.

In the 4 month and 8 month mice however, the levels of phosphorylation at Akt and ERK1/2 did not significantly differ between the APP-KI and wild type mice (figure 3.4). In the 4-month samples this was consistent with the lack of increase in the upstream activator *Igf1*'s expression. In the 8-month sample however, a very large increase in *Igf1* expression is observed whilst there is a lack of increase in activation in the IIS cascade. This implies that the *Igf1* increase is not activating the cascade. This is noteworthy as this may be supportive evidence for acquired Igf1 resistance as observed in previous studies (Talbot et al., 2012), although without testing on *ex vivo* tissue as was carried out in the Talbot *et al* paper, we cannot confirm whether this is the case. There was no change in total Akt or ERK1/2 protein level in any samples compared to wild type controls. These data suggest that early amyloid-beta elevation induces an increase in *Igf1* expression accompanied by a substantial increase of signalling through both branches of the IIS cascade. By the time plaque deposition has reached saturation and the brain has a high number of plaques however, whilst *Igf1* expression is again increased, the accompanying increased IIS signalling is not observable in either branch of the pathway suggesting resistance.

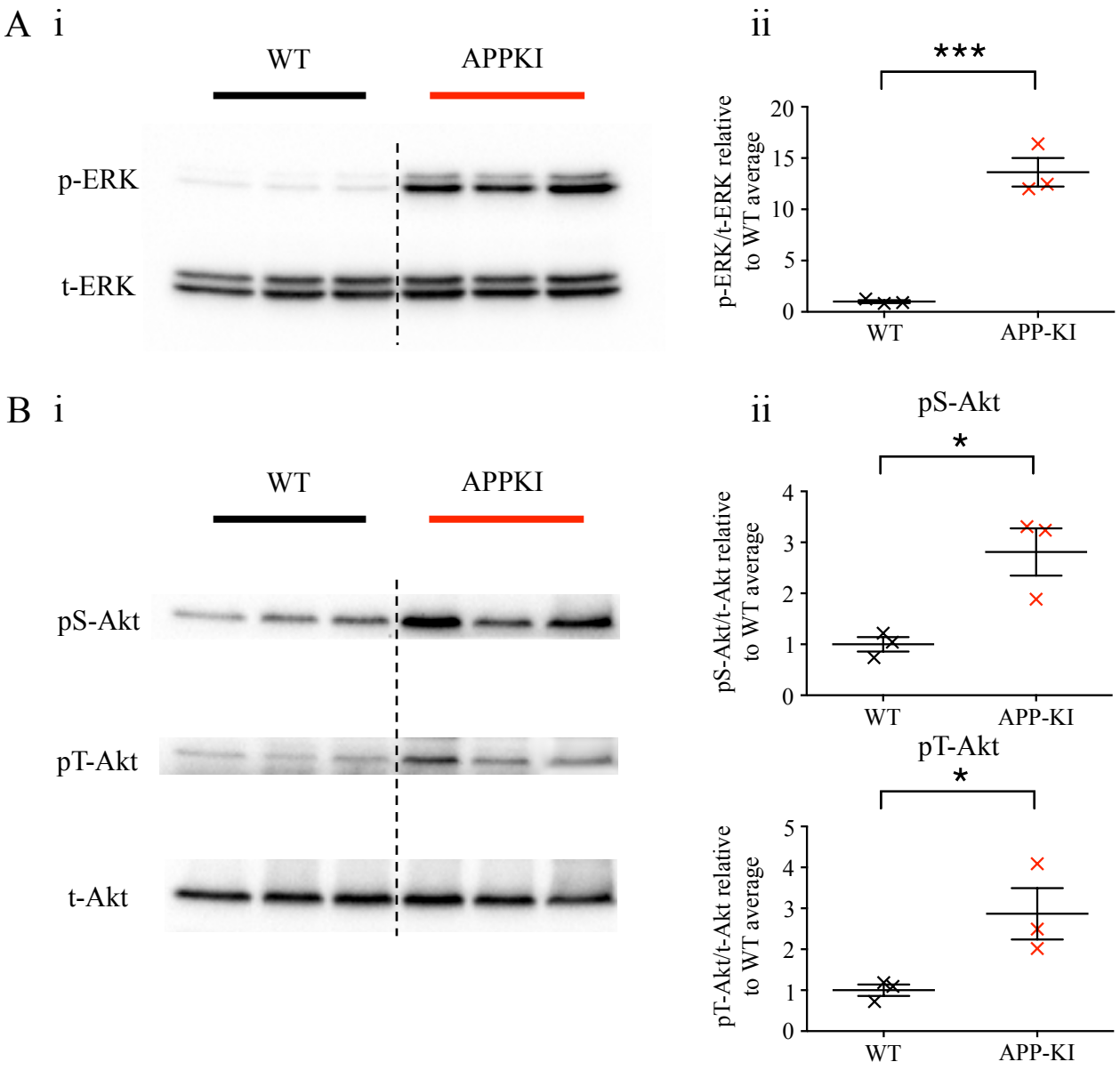

Figure 3.3. Changes in ERK1/2 and Akt phosphorylation in the cortex of 2 month old APP-KI mice. Significantly higher phosphorylation at ERK1/2 and Akt is observable in the cortex of 2 month old APP-KI mice compared with age matched wild type controls. In all (i) Representative western blot images (ii) Graphical representation of western blot data. (A) Significantly higher p-ERK levels are present in APP-KI tissue (B) Levels of phosphorylation are significantly higher at both activating sites on Akt. n=3 in all groups. Data shown is the mean +/- SEM. Student's t-test * $p<0.05$ ** $p<0.01$ *** $p<0.001$.

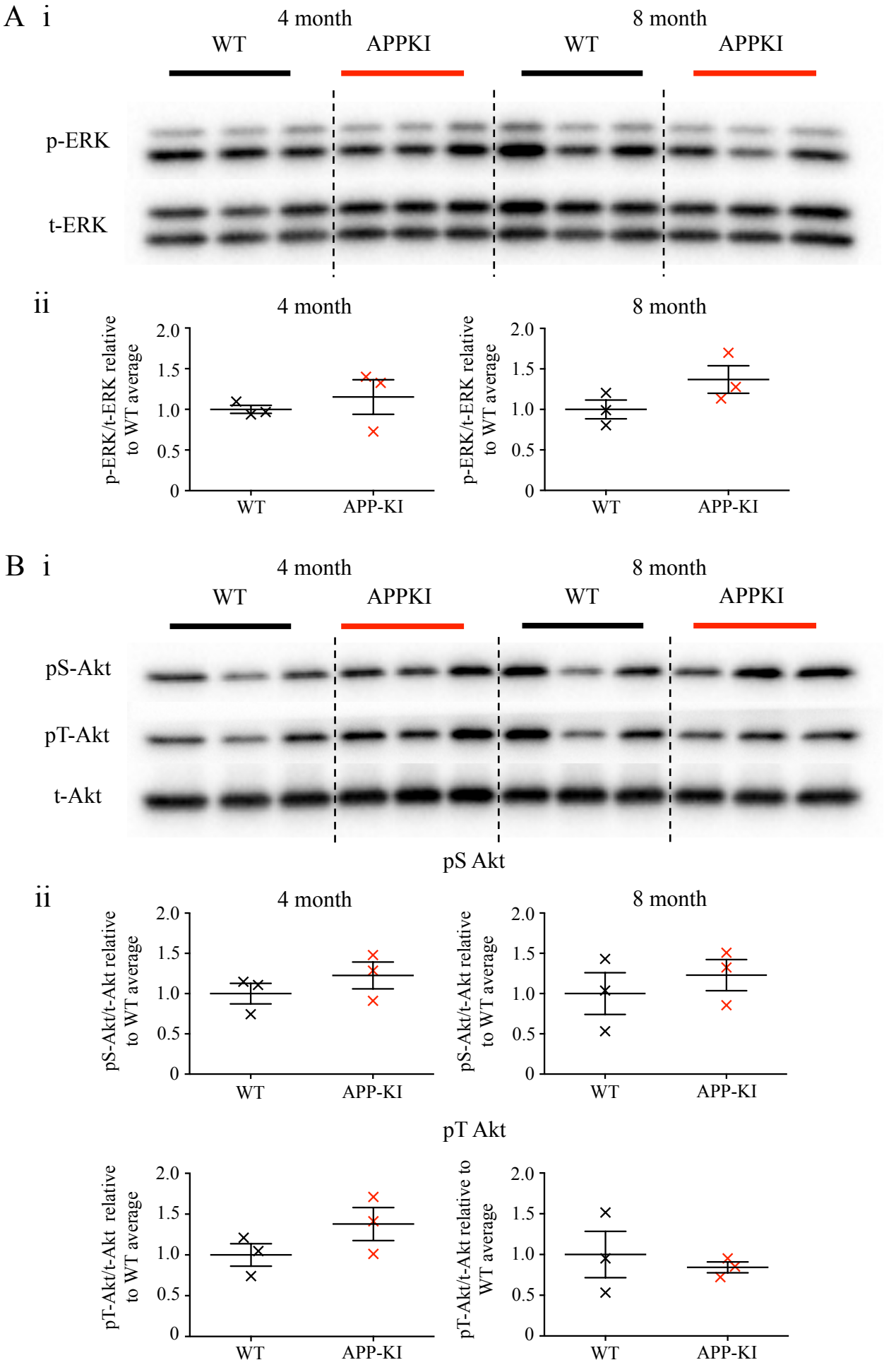
A i
4 month
8 month
WT
APPKI
WT
APPKI
p-ERK
t-ERK
ii
4 month
8 month
p-ERK/t-ERK relative to WT average
2.0
1.5
1.0
0.5
0
WT
APP-KI
B i
4 month
8 month
WT
APPKI
WT
APPKI
pS-Akt
pT-Akt
t-Akt
pS Akt
ii
4 month
8 month
pS-Akt/t-Akt relative to WT average
pT Akt
pT-Akt/t-Akt relative to WT average
pT-Akt/t-Akt relative to WT average

Figure 3.4. There are no changes in ERK1/2 and Akt signaling in the cortex of 4 and month old APP-KI mice. No significant change in IIS signaling is seen at ERK1/2 or Akt in the cortex of 4 or 8 month old APP-KI mice compared with age matched wild type controls. In all (i) Representative western blot images (ii) Graphical representation of western blot data. (A) p-ERK levels are not significantly changed in APP-KI tissue (B) Levels of phosphorylation at both activating sites on Akt are not significantly altered in APP-KI mice. n=3 in all groups. Data shown is the mean +/- SEM. Student's t-test * $p<0.05$ ** $p<0.01$ *** $p<0.001$.

Effects of rising hyperphosphorylated tau and neuronal cell loss of brain IIS signalling

Using RT-qPCR, *Igf1* expression was found to be significantly higher in the 8-month TG4510 hippocampus as compared to wild type tissue, but *Igf1* expression was not significantly altered in 2.5-month TG4510 animals (fig 3.5, p=0.0005). This suggests that pretangles and tau hyperphosphorylation is not accompanied by increased *Igf1* expression, but the severe tau pathology and neurodegeneration seen by 8 months is accompanied by a substantial increase in expression, with a 70% increase observed in TG4510 tissue at this age.

When signalling through the IIS cascade was measured, a significant increase in p-ERK levels was observed between wild type and TG4510 tissue at 2.5-months but not 8-months (fig 3.6, p=0.0035). A pattern of decreased Akt phosphorylation was observable at 2.5 and 8 months in TG4510 hippocampus (fig 3.6, pS-Akt 2.5-months p=0.0137. pT-Akt 8-months p=0.0099). There was a significant reduction in pS-Akt levels in 2.5-month TG4510 hippocampal samples (30% reduction), and a significant reduction in pT-Akt levels in 8-month TG4510 hippocampal samples (75% reduction). There was no change in total Akt or ERK1/2 protein level in any samples compared to wild type controls. Therefore whilst *Igf1* expression is not changed at 2.5 months but is increased at 8 months in TG4510 tissue, a significant reduction in Akt phosphorylation is observable at both time points albeit at different activating phosphorylation sites, with an early increase in p-ERK levels also present.

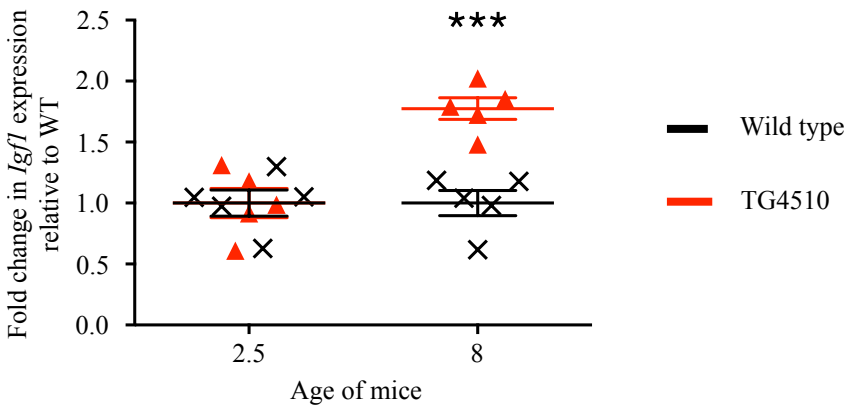

Figure 3.5. Hippocampal *Igf1* expression in TG4510 and wild type mice at 2.5 and 8 months of age. *Igf1* is significantly increased in its expression in the hippocampus of TG4510 mice at 8 months but not at 2.5 months, as measured by RT-qPCR. n=5 in all groups. Data shown is the mean +/- SEM. Student's t-test * $p<0.05$ ** $p<0.01$ *** $p<0.001$.

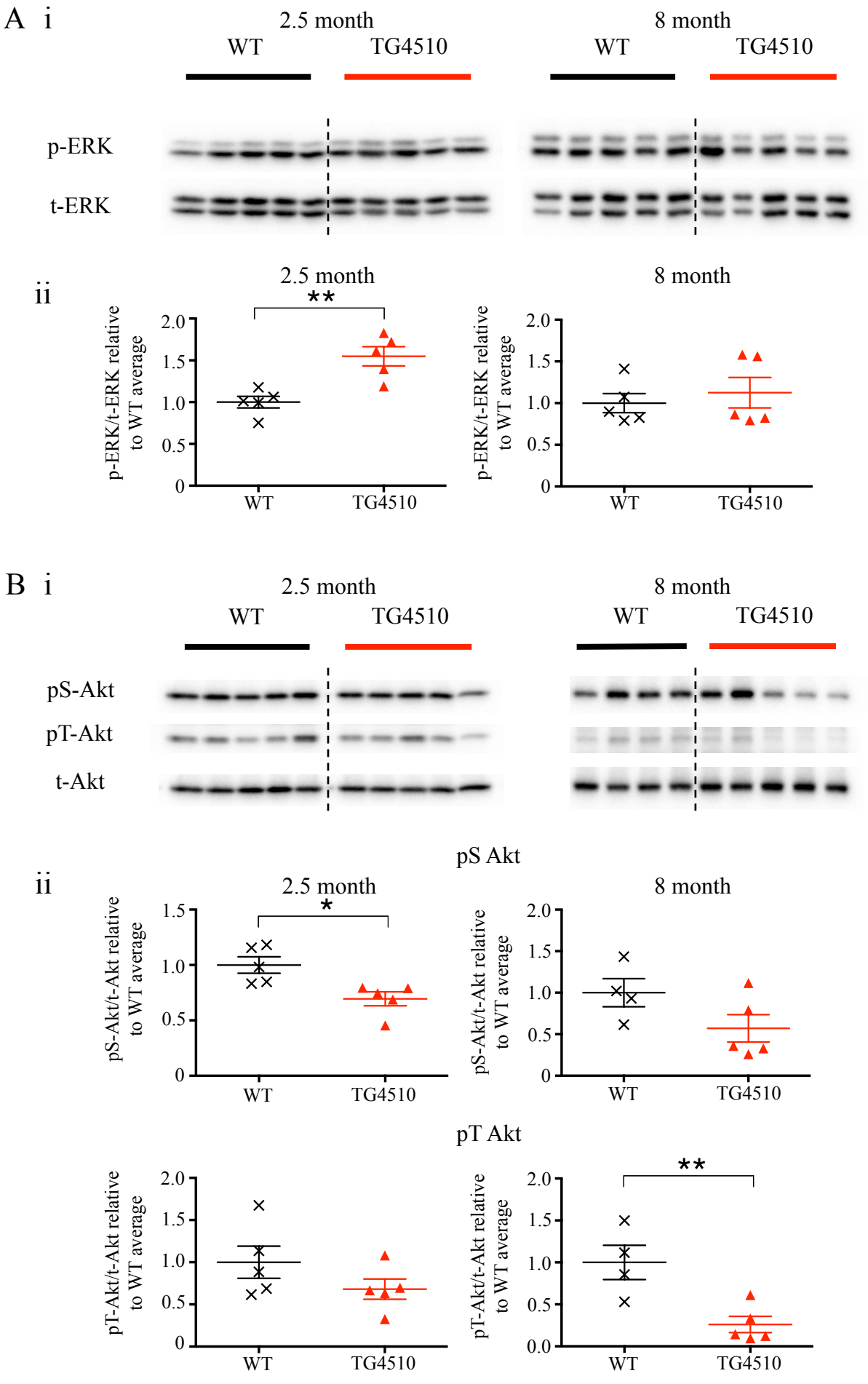
A i
2.5 month
WT
TG4510
8 month
WT
TG4510
p-ERK
t-ERK
ii
2.5 month
8 month
**
p-ERK/t-ERK relative to WT average
2.0
1.5
1.0
0.5
0
WT
TG4510
B i
2.5 month
WT
TG4510
8 month
WT
TG4510
pS-Akt
pT-Akt
t-Akt
pS Akt
ii
2.5 month
*
8 month
pS-Akt/t-Akt relative to WT average
1.5
1.0
0.5
0
WT
TG4510
pT Akt
**
pT-Akt/t-Akt relative to WT average
2.0
1.5
1.0
0.5
0.0
WT
TG4510

Figure 3.6. Phosphorylation levels of ERK1/2 and Akt in the hippocampus of 2.5 and 8 month old TG4510 mice. Significant changes in Akt and ERK1/2 phosphorylation are seen in the hippocampus of TG4510 mice compared with age matched wild type controls. pS-Akt levels were significantly reduced at 2.5 months in TG4510 animals, with pT-Akt levels significantly reduced at 8 months. p-ERK levels are significantly increase in the 2.5 month TG4510 hippocampus. In all (i) Representative western blot images (ii) Graphical representation of western blot data. (A) p-ERK levels (B) pS-Akt and pT-Akt levels. n=5 in all groups. Data shown is the mean +/- SEM. Student's t-test * $p<0.05$ ** $p<0.01$ *** $p<0.001$.

Changes in the IIS cascade in post mortem human brain tissue

IGF1 mRNA levels were measured in fAD, sAD and non-demented control frontal cortex samples by RT-qPCR. Although we hypothesised that *IGF1* levels would be increased in human AD brain tissue, there was no significant difference in *IGF1* expression levels between non-AD samples and either AD group (fig 3.7). If data from fAD and sAD samples was pooled as a single AD group increasing the power of the analysis, there was still no significant difference in *IGF1* expression compared to non-demented controls.

Levels of signalling through the IIS cascade in frontal cortex sample from fAD and sAD human patients were largely not significantly different compared to non-AD control samples, but in contrast to late stage TG4510 tissue, a significant increase in pT-Akt was seen in fAD (fig 3.8, $p=0.0181$,). If considered as a pooled AD group once more, there was no significant change in phosphorylation level at Akt or ERK1/2, with the previous significant increase in pT-Akt level in fAD tissue only showing a trend towards significance in the pooled AD group ($p=0.0637$). Whilst levels of phosphorylation at ERK1/2 and at pS-Akt were very steady in all samples, the pT-Akt levels varied widely in AD samples, with 2 out of 3 sAD samples increasing substantially, and all 3 fAD samples increasing in phosphorylation level.

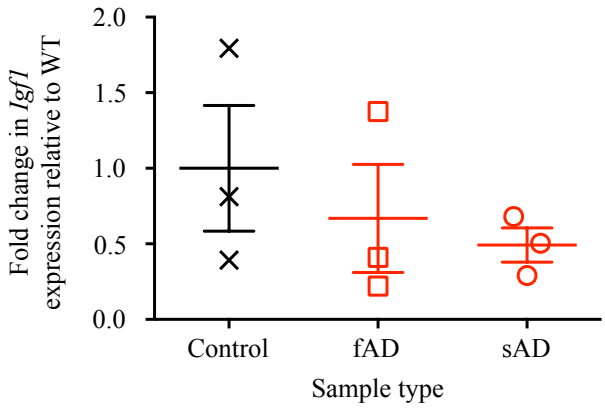

Figure 3.7. Frontal cortex *Igf1* expression in human brain samples from fAD, sAD and non-demented control patients. *Igf1* is not significantly increased in its expression in the frontal cortex in either the fAD or sAD brain samples tested, as measured by RT-qPCR. n=3 in all groups. Data shown is the mean +/- SEM. Student's t-test * $p<0.05$ ** $p<0.01$ *** $p<0.001$.

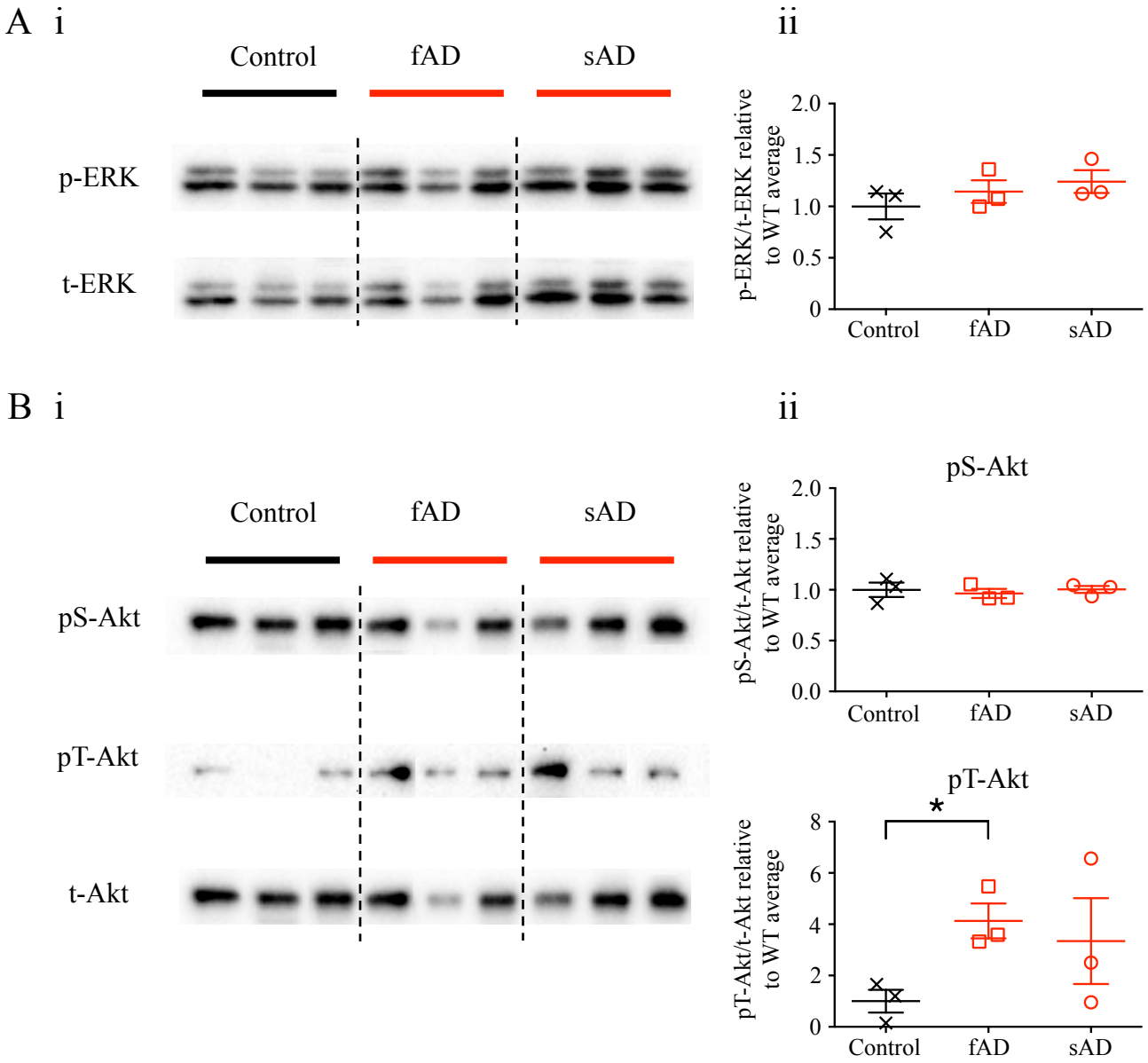

Figure 3.8. ERK1/2 and Akt phosphorylation levels in the frontal cortex of human fAD, sAD, and non-demented controls. Significantly higher levels of phosphorylation at pT-Akt is observable in the frontal cortex of fAD patient brain samples compared with non-demented controls, although p-ERK and pS-Akt levels are not significantly altered. In all (i) Representative western blot images (ii) Graphical representation of western blot data. (A) No changes in p-ERK levels are present in fAD or sAD tissue (B) Levels of pT-Akt are significantly higher in fAD samples but not sAD, with pS-Akt levels being unchanged between groups. n=3 in all groups. Data shown is the mean +/- SEM. Student's t-test * $p<0.05$ ** $p<0.01$ *** $p<0.001$.

Summary

The overall aim of this thesis is to investigate the potential for IIS modulating interventions to be used as a means of positively modulating neuronal cell loss in neurodegeneration. In chronic neurodegenerative disorders the development of disease pathology occurs over a very protracted time frame, and endogenous IIS alterations have previously been reported in human post mortem AD brain tissue. In order to eventually successfully investigate our overall hypothesis in AD, we sought to characterise endogenous IIS changes in response to different pathological components of AD, that being progressive amyloid and tau pathology. This allows us to identify the appropriate time point in AD development for future testing of IIS based interventions, and therefore lays the foundation for future experimentation. In particular, by examining amyloid pathology alone in mice, it allowed an examination of earlier stages of AD development than is possible if just examining post mortem human tissue. The results of this chapter identified three points in AD pathology where a significant alteration in IIS is present, as well as identifying a more general pattern of increased *Igf1* expression with pathological development of amyloid and tau (fig 3.9).

The greatest change in IIS in the pathological stages of AD examined was during early rising amyloid pathology, as modelled by 2-month APP-KI mice (fig 3.9, A). At this point there is an increase in $A\beta_{40}$ and $A\beta_{42}$ levels as well as the first observable small amyloid plaques (Saito et al., 2014). This pathology is most similar to amyloid pathology decades before diagnosis, as by diagnosis far greater plaque deposition is present in the brains of patients. This early amyloid pathology induced an increase in *Igf1* expression, and also a strong increase in phosphorylation at Akt and ERK1/2, with a particularly dramatic increase in p-ERK. This was unexpected. We hypothesised that *Igf1* expression would increase with pathology accumulation, and yet at a disease stage with minor pathology, and no neuronal cell loss, a significant increase in *Igf1* expression was observed. Similarly, whilst IGF1 is known to increase IIS signalling, such a strong increase in ERK1/2 signalling was hypothesised to occur when neuronal cell death was occurring, yet there is no neuronal cell death at this time point in this model. This suggests that whilst increased p-ERK has been

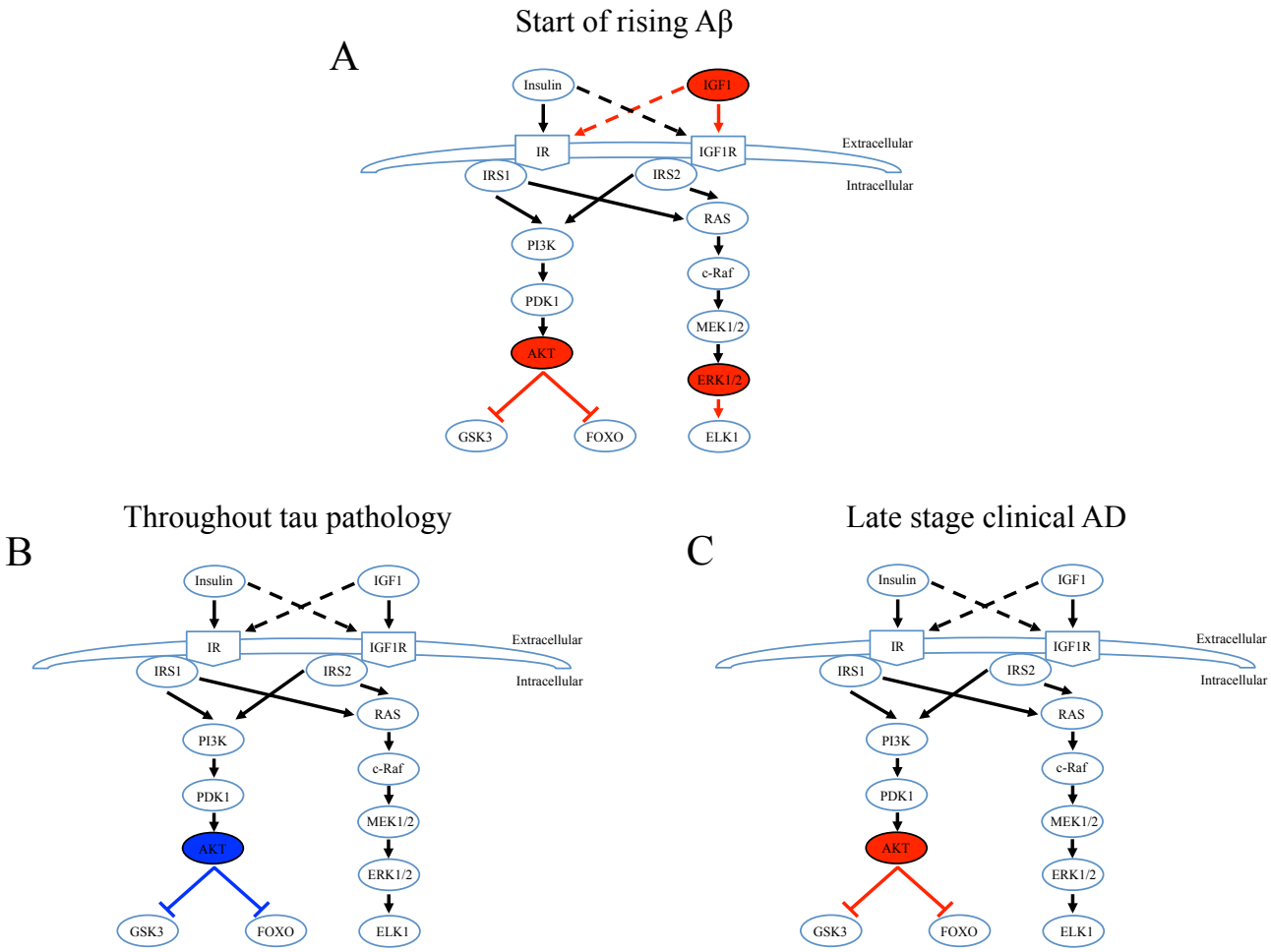

Figure 3.9. Changes in IIS at different pathological stages of AD. Diagrammatic representation of the changes in the IIS cascade at different points in AD pathogenesis. (A) Early rising Aβ has the most substantial effect on IIS with increased p-Akt, p-ERK, and increased *Igf1* expression (B) At both early and late tau pathology, a decrease in p-Akt is observable, albeit at pS-Akt in early pathology, and pT-Akt in late (C) At late stage AD in post mortem human tissue, increased pT-Akt is observable in fAD frontal cortex samples, but not sAD. Red represents increased signalling, blue represents a decreased signalling.

associated with neuronal cell death (Subramaniam and Unsicker, 2010), and increased p-ERK has been shown in the late stage human AD brain (Perry et al., 1999), substantial increases are also present at far earlier stages in pathological AD development, at least in the mouse. The physiological impact of these changes on AD disease progression is impossible to currently tell, but it seems that there is a strong response in IIS to the very early stages of amyloid pathology.

IIS change was also observed when the first tau pretangle pathology developed in the 2.5-month TG4510 mice, and also when advanced tau pathology and neuronal cell loss was present in 8-month TG4510 mice (fig 3.9, B). Whilst there was no increase in *Igf1* expression at 2.5 months, there was a significant reduction in Akt phosphorylation and a significant increase in ERK1/2 phosphorylation, implying a reduction in signalling through this branch of IIS. This reduced Akt signalling was observed at late stage tau pathology also, but this was also accompanied by increased *Igf1* expression. It is interesting to note that there was an increase in ERK phosphorylation levels but a decrease in Akt phosphorylation levels, showing that the branches of the IIS cascade can be independently modulated in their levels of signalling. Our hypothesis of increase p-ERK level with the start of neuronal loss in 2.5-month TG4510 mice was correct, and also there was no p-ERK increase during more advanced tau pathology in 8-month TG4510 mice. With tangle containing neurons previously being shown to contain high p-ERK staining in human tissue (Perry et al., 1999), our 8-month TG4510 findings are at odds with previous data.

Whilst examining phosphorylation levels of key IIS members as well as expression levels, gives an idea as to the level of signalling through this cascade, a future confirmation experiment should be carried out looking at changes in downstream expression levels of genes whose expression is affected by IIS level. For example, measuring expression levels of genes encoded by the FOXO transcription factors, such as Superoxide Dismutase 2 (SOD2) or the cell cycle regulator protein p27 (Cdkn1b) by RT-qPCR would allow a downstream examination of IIS in these animals. If IIS is inhibited and increase in these genes expression would be expected.

Overall our data from animal models of pathological features of AD suggests a difference in endogenous IIS alteration in response to increasing tau pathology

compared with the changes seen in response to increasing amyloid pathology, although the *Igf1* expression increase is observed in both.

In the latest stage of AD pathology that we could examine, that being post mortem human brain tissue, another pattern of IIS change was observed (fig 3.9, C). No increase in *IGF1* was observed, with the only change in IIS signalling being an increase in pT-Akt levels. This differs from previous evidence of an observed decrease in Akt phosphorylation in the human AD brain (Steen et al., 2005), and increased IGF1 (Connor et al., 1997). As hypothesised, no increase was observed in p-ERK level in AD samples compared to non-AD controls. This difference to previous literature is likely a product of sample size, with our preliminary investigation only using 3 samples for each group, whereas most human data studies use hundreds of samples. Also, whilst data from mouse studies is examining differences in genetically and environmentally identical animals, data from humans is from genetically and environmentally heterogeneous samples, with the cause of death and comorbidities of samples unknown. Furthermore, *IGF1* expression can be regulated at levels other than expression level.

Overall, we have demonstrated that the IIS cascade is endogenously altered differently in response to different pathological components of AD. This characterisation has allowed the more appropriate timings of IIS modulating interventions to test our overall hypothesis in the future.

Chapter 4

Implications of increased *Igf1* expression on acute neurodegeneration

Introduction

The overall hypothesis of this thesis is that IIS modulating interventions could be exploited for therapeutic gain in neurodegenerative disorders, and potential provide novel therapeutic options. Investigating this overall hypothesis is simpler with regards to the timing of intervention in acute neurodegenerative diseases (e.g. stroke, TBI) compared to chronic neurodegenerative disorders (e.g. AD, PD), as neuronal cell loss occurs immediately following the noxious incident, and then at a slower rate in subsequent weeks. Interventions to ameliorate neuronal cell loss must therefore occur within this time frame. The most appropriate way to modulate IIS during this period that could modulate neuronal cell loss in acute neurodegenerative diseases must now be investigated.

Increased IGF1 protein and *IGF1* expression, particularly in astrocytes, has been observed in a multitude of both chronic and acute neurodegenerative diseases (Beilharz et al., 1998; Connor et al., 1997; Li et al., 1998; Madathil et al., 2010; Nieto-Sampedro et al., 1982; Sandberg Nordqvist et al., 1996; Walter et al., 1997; Yao et al., 1995). Crucially this increased IGF1 is proximal to the source of injury in acute neurodegenerative disorders (Beilharz et al., 1998; Madathil et al., 2010). How this increased IGF1 impacts on neurodegeneration however is unclear.

IGF1 can act as a survival factor in the adult brain. Exogenous administration of IGF1, or the overexpression of *IGF1*, is protective against neuronal cell death following a noxious stimulus in animal models of stroke and TBI (Carro et al., 2006; Guan et al., 2000; Guan et al., 1993; Johnston et al., 1996; Madathil et al., 2013). This pro-survival effect seems to have a dose response relationship however, where low levels of IGF1 administration elicited no neuroprotection against injury (Bergstedt and Wieloch, 1993; Johnston et al., 1996). Presumably the locally secreted IGF1 from astrocytes will be at low concentrations, meaning that interpreting the survival effect

of the observed endogenously raised astrocyte IGF1 is difficult to interpret in relation to these previous experiments.

IGF1 is a potent activating factor of signalling through the IIS cascade (Laviola et al., 2007). Reducing IIS signalling by genetic and pharmacological means however, has proved beneficial and neuroprotective in neurodegenerative disease models (Cohen et al., 2006; Cohen et al., 2009; Cooper et al., 2015; Freude et al., 2009; Killick et al., 2009). With increased astrocyte IGF1 presumably increasing signalling through the IIS cascade in the brain, it would appear to have the opposite of the above protective effect, and perhaps instead contribute to neurodegeneration.

There seems to therefore be a contradiction in the field, whereby pharmacologically and genetically lowering IIS signalling seems protective against neurodegeneration, and yet administering activators of this cascade also seem beneficial. A possible resolution to this conflict could be that an IGF1 resistant state and therefore reduced signalling through the cascade is beneficial, and that the exogenous administration of IGF1 thereby induces a resistant state. Whether this resistant state would be induced in such an acute time frame as that of the time that neuronal cell loss occurs in acute neurodegeneration, and whether local endogenous IGF1 release would be sufficient to stimulate this however, is unclear.

Whilst most of these attempts to define the benefit of alterations to the IIS cascade in neurodegeneration have focused on enforcing gross changes on the system, all have overlooked the possible endogenous effects caused by the local IGF1 increase in astrocytes proximal to the site of noxious stimuli. With the IIS cascade being heavily implicated in neuronal cell death and neurodegeneration, and the apparent ubiquity of the IGF1 increase in acute neurodegenerative disorders, this endogenous IGF1 increase could be modulated as a means of altering the IIS cascade to affect neurodegeneration. In this chapter we have investigated the implications of endogenous IGF1 increase on neurodegeneration.

Aims

The aim of this chapter is to study the effect that raised astrocyte Igf1 during neurodegeneration has on neurodegeneration itself. To understand the mechanism behind any association, we have investigated how changes in neuronal cell death and neuronal number relate to IIS signalling changes in both neurons and astrocytes.

Methods

To investigate the effect that raised Igf1 had on neurodegeneration in acute neurodegenerative disorders, we developed an *in vitro* model of acute neurodegeneration that allowed us to induce neuronal cell loss and an increase in astrocyte Igf1, and subsequently modulated this expression via *Igf1* siRNA knock down.

The design of this *in vitro* model of acute neurodegeneration was based on the neuron astrocyte bilaminar co-culture model outlined by Shimizu *et al*, whereby primary astrocyte and neuron cultures are grown separately until mature, and then combined in one well, by suspending a coverslip with primary neurons attached above an astrocyte culture grown in the bottom of the well (figure 4.1 A)(Shimizu et al., 2011). The source of these cells was not a rat however, but generated from postnatal mice, modified from the protocols of Schildge *et al* and the primary neuron protocol used by Dresbach *et al* (Dresbach et al., 2003; Schildge et al., 2013). The generation of primary astrocytes and primary neurons, as well as their adaptation into bilaminar co-cultures, is outlined in detail in the materials and methods chapter. Both primary neuron and astrocyte cultures were derived from dissected mouse cortices and hippocampi.

To model acute neurodegeneration in these cultures they were exposed to hypoxic conditions for 5 hours. Cell number, *Igf1* expression, and IIS signalling were then measured at 24 and 72 hours after the cessation of the hypoxic incident (figure 4.1 B)(**hypoxic cultures**). These factors were also measured in co-cultures kept in

normoxic conditions for comparison (**normoxic cultures**). In our knock down cultures, siRNA against *Igf1* was administered one hour prior to cultures entering hypoxic conditions, and for the same length of time in normoxic conditions, to examine any effect of knock down alone on cultures. In each plate wells were either treated with siRNA specific to the *Igf1* sequence (**knock down cultures**), or non-targeted siRNA as a control (**control cultures**). Therefore one plate was used for normoxic comparison, and a plate each for the 24 and 72-hour post hypoxia time points. On each plate were 2 wells to be lysed for RNA, 2 for protein, and one well for PFA fixation and DAPI staining (figure 4.1 B). This allowed a direct comparison between cell number, *Igf1* expression and IIS signalling level, in wells either under control of knock down conditions within the same plate. Comparisons following hypoxia (in the 24 and 72 hour post hypoxia plates) are made relative to the normoxic control cultures. This also allows inter-experiment variability in the density of neuronal cultures to be accounted for, allowing a more sensitive detection of changes within experiments.

To examine change in cell number and signalling through the IIS cascade in these cultures, we took cells for RNA, protein, and PFA fixed coverslips for DAPI staining (figure 4.1 C). To examine changes in signalling levels through the IIS cascade, we performed western blotting on our protein samples for specific activating phosphorylation sites on key members of the cascade, that being pS473 on Akt (pS-Akt) (Alessi et al., 1996), and pT202/pY204 and pT185/pY187 on ERK1/2 (p-ERK)(Canagarajah et al., 1997; Payne et al., 1991), and normalised these levels to total protein Akt and ERK1/2 levels. Western blotting for cleaved caspase 3 (CC3) was also performed on protein samples to examine levels of apoptosis. *Igf1* expression was assessed by RT-qPCR, and cell number was assessed by counting DAPI stained cells under a light microscope.

Hypotheses

1. The primary hypothesis in this chapter is that the endogenous Igf1 increase observed in acute neurodegenerative diseases contributes to neuronal cell death.

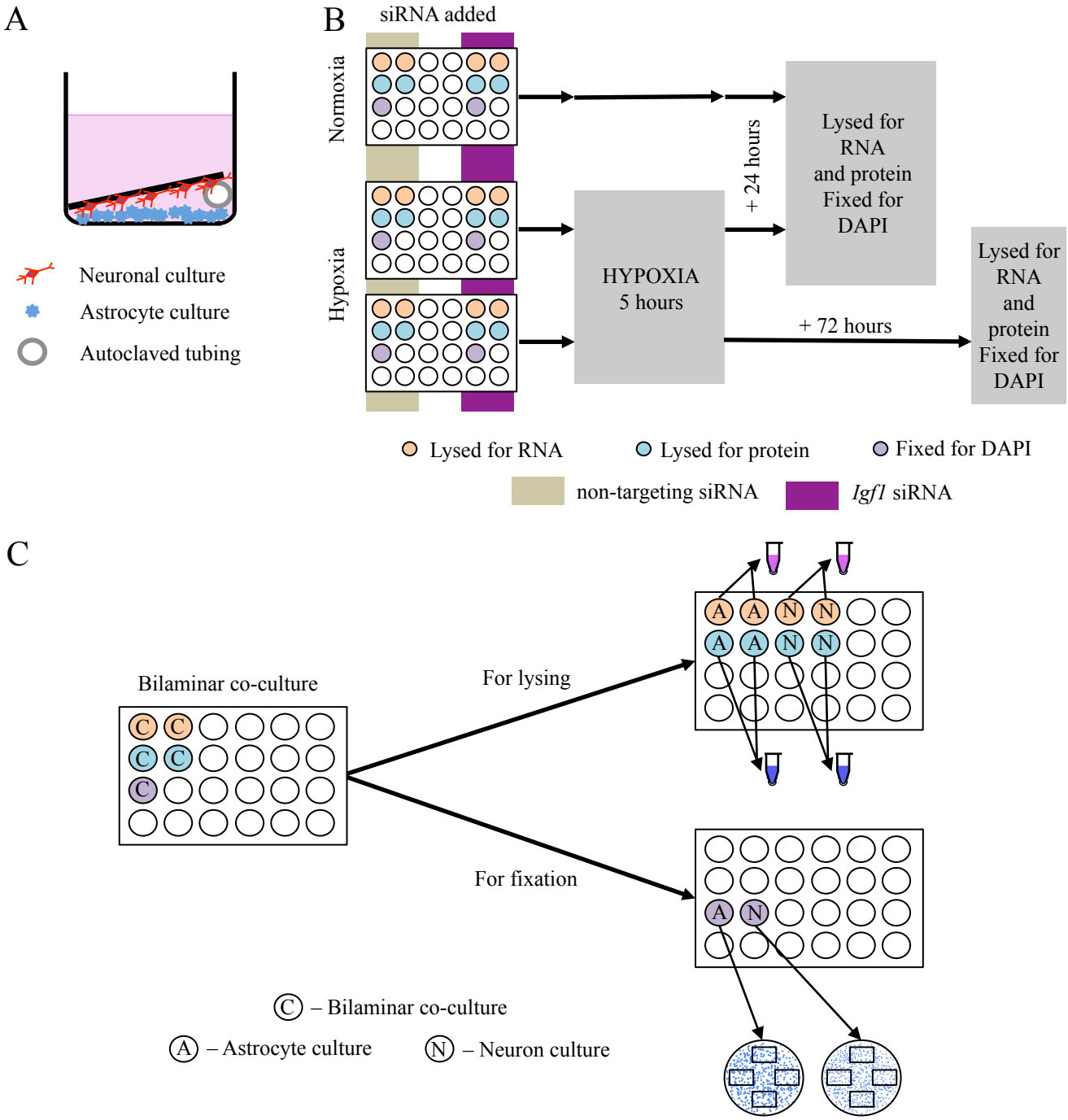

Figure 4.1. A diagrammatic representation of our *in vitro* model of acute neurodegeneration and our experimental layout. (A) Model of a well of a bilaminar co-culture. A cover slip with a primary neuronal culture is suspended over a primary astrocyte culture, allowing both to share the same media but be separated for analysis (B) Each experiment involved three plates, one under normoxic conditions, and two exposed to a hypoxic insult. These plates are processed at different times in relation to the cessation of hypoxia, with one post hypoxic plate and the normoxic plate taken for RNA protein and fixed for DAPI staining 24 hours after hypoxia, and the other hypoxia exposed plate taken 72 hours after. Each plate containing wells treated with either non-targeting siRNA or siRNA against *Igf1* (C) Plates were processed for analysis by first removing the neuronal and astrocyte cover slip to another plate for fixation with PFA, and subsequent staining with DAPI, whereby four areas of each cover slip are imaged at x10 magnification and cell counts made. The other four wells have half the media moved to another well in the same plate, the neuronal cover slip moved into the corresponding wells, with each well then lysed for RNA or protein, with two wells pooled for each.

2. We also hypothesise that neuronal cell death can be reduced by preventing the endogenous Igf1 increase.
3. The mechanism of Igf1 dependant neuronal cell death is through increased p-ERK levels in neurons via astrocyte Igf1 increasing neuronal IIS signalling.

Results

Developing an in vitro model of acute neurodegeneration

Although increased IGF1 is observed in astrocytes, and the main characteristic of neurodegenerative diseases is the gradual loss of neurons, changes in IIS have been observed in both cell types (Garwood et al., 2015; Talbot et al., 2012). To elucidate the effects that increased astrocyte IGF1 has on both astrocyte and neurons, we not only investigated the role of this cascade on neurodegeneration, but also on IIS levels in both neurons and astrocytes separately. We therefore developed an *in vitro* model where we could induce neurodegeneration and astrocyte *Igf1* expression, but separately analyse cell number change and IIS signalling levels in neurons and astrocytes.

Inducing an endogenous increase in astrocyte Igf1 expression in response to a noxious stimuli

Our first aim in developing our *in vitro* model of acute neurodegeneration accompanied by increased astrocyte Igf1 was to ensure that our noxious stimulus induced an increase in astrocyte Igf1. With astrocytes being shown to be the cell type responsible for endogenous IGF1 increase in neurodegenerative diseases, we initially applied our noxious stimulus of a 5-hour hypoxic insult to primary astrocyte cultures. To ensure that our stressful stimulus induced Igf1 increase in only astrocytes, we also exposed separate primary neuronal cultures to the same stressful stimulus, and measured the *Igf1* expression levels in both cultures via RT-qPCR. For comparison,

we kept some cultures in normoxic conditions, with future reference to *Igf1* expression change being relative to the levels seen in normoxic cultures measured via RT-qPCR. To aid in statistical analyse, raw expression levels were used for statistical tests. To emphasise this, in figure 4.2 we show graphs of both relative and raw *Igf1* expression changes. Subsequent figures will only show relative changes, but statistical analysis is always performed on raw expression data unless otherwise specified.

Previous work examining *Igf1* expression had shown that astrocyte expression increased 48 hours after traumatic head injury (Madathil et al., 2010) and 72 hours after hypoxic-ischaemic injury (Lee et al., 1996), whilst *Igf1* expression seemed to be slightly decreased immediately after injury in both cases. We therefore chose to look for changes in *Igf1* expression in our cultures 24 and 72 hours after the cessation of the hypoxic insult. Our expectation was to observe an increase in *Igf1* expression in the astrocyte culture, with no change, or a decrease in expression in the neuronal cultures, as seen in previous literature (Clawson et al., 1999).

In pure astrocyte and pure neuronal cultures no increase in *Igf1* expression was observed at either time point following the hypoxic incident (figure 4.2 A). Hypoxia was successfully induced however, as shown by the significant increase in hypoxia inducible factor 1A (*Hif1a*) transcription following the hypoxic incident (figure 4.2 B, +24 hours astrocytes $p=0.0155$, +72 hours astrocyte $p=0.05$, +24 hours neurons $p=0.0457$). This increase is in accordance with previous work showing an increase in *Hif1a* expression from low baseline expression levels following a hypoxic incident (Wiener et al., 1996). Under these experimental conditions, cell stress alone was insufficient to induce an increase in *Igf1* expression in either pure primary astrocytes or neurons.

Astrocytes and neurons are known to communicate in a variety of ways, for example via diffusible factors (Fields and Stevens-Graham, 2002). Furthermore, *Igf1* expression has been shown to be in proximity to the site of damaged and dying neurons in traumatic brain injury (Madathil et al., 2010). Considering this mode of astrocyte-neuron communication and the Madathil *et al* study, we postulated that diffusible factors from nearby stressed neurons was a requirement for astrocytes to

increase *Igf1* expression in response to a noxious stimulus. We therefore next modified a bi-laminar co-culture system from the protocol of Shimizu *et al*, allowing us to suspend a cover slip with primary neurons grown on it, above primary astrocytes grown on the bottom of the wells of a 24 well plate, whilst both cultures shared the same medium (Shimizu et al., 2011)(see figure 4.1, B).

This bi-laminar co-culture represents a system where astrocytes and neurons can co-exist and share the same medium and hence the same environment and factors, whilst being separable for analysis. To ensure that we do not miss an interaction due to a low dose of expressed neuronal factor, we carried out this experiment with bilaminar co-cultures containing neuronal cultures plated either at a density of 200,000 neurons/cm^2 or 500,000 neurons/cm^2. These bilaminar co-cultures were exposed to the same 5-hour hypoxic incident as was applied to single cultures previously, with cover slips then removed for separate neuronal and astrocytic *Igf1* expression analysis via RT-qPCR at both 24 and 72 hours post cessation of the hypoxic incident. Again a normoxic culture, in this instance a bilaminar co-culture, was kept and processed for comparison.

Astrocyte cultures in co-culture with high density neuronal cultures showed a significant 150% increase in *Igf1* expression at 72 hours post hypoxia (fig 4.2 C, p=0.0300). In the low-density cultures however, no significant increase in *Igf1* expression was shown at either time point post hypoxia (fig 4.2 D). High density neuronal cultures present in the co-culture showed a significant decrease in *Igf1* expression at 24 hours following the hypoxic incident, but no significant difference at 72 hours post hypoxia or in the low density cultures (figure 4.2 C D, p=0.0055). Overall, this indicates that not only are neurons required at the time of a noxious stimulus for the increased expression of *Igf1* in astrocytes, but also there is a dose response relationship, whereby a higher number of neurons lead to a larger increase in *Igf1* expression. With our success in mimicking the phenomenon of endogenously increased astrocyte *Igf1* expression in response to a noxious stimulus, we now have a model where we can manipulate this response and thereby see how it influences neurodegeneration. As only the higher density of neurons resulted in a significant increase in the level of *Igf1* expression, we continued all further experiments with this density of neurons.

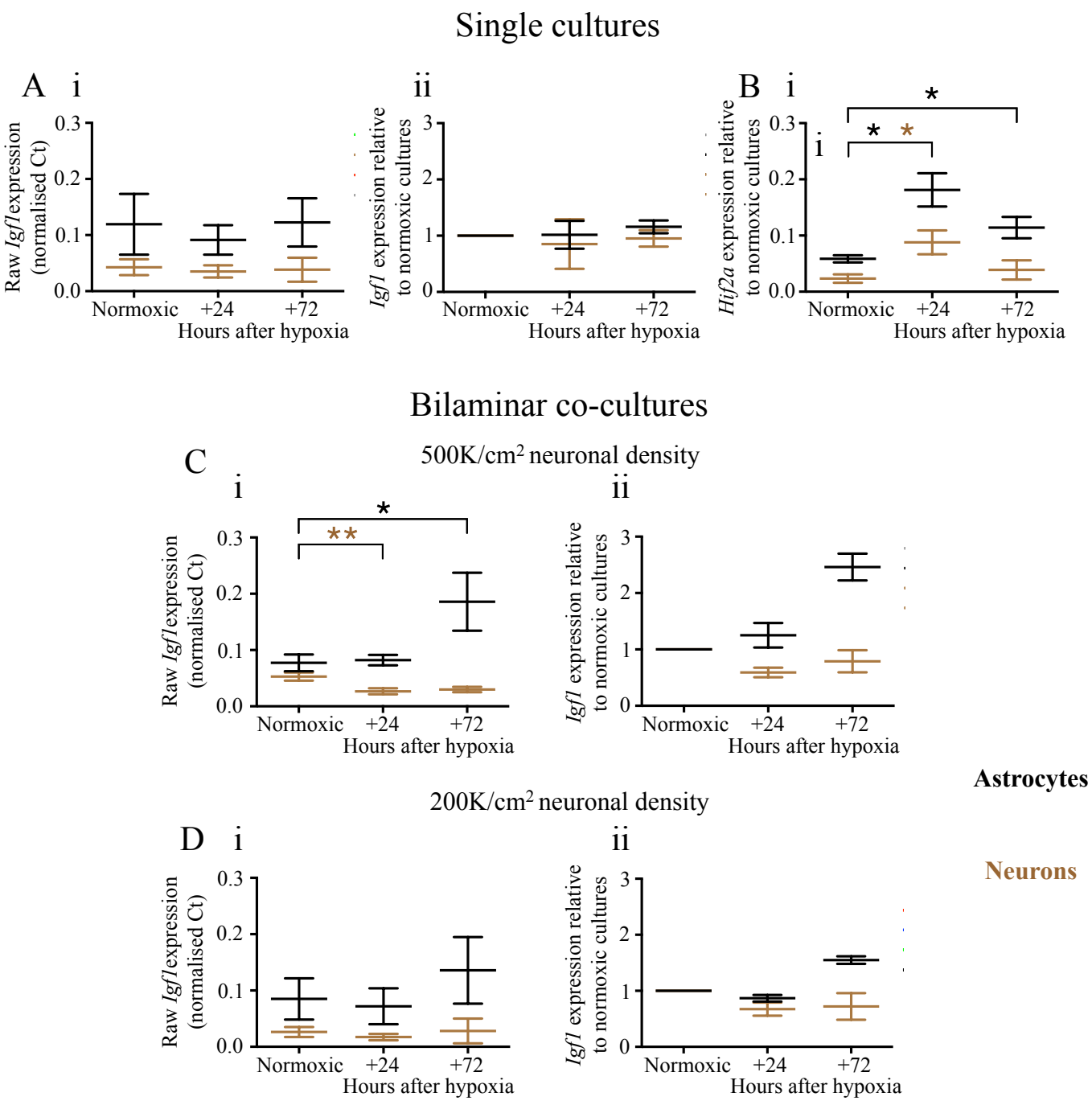

Figure 4.2. Changes in expression of *Igf1* and *Hif2a* in astrocytes and neurons in either single cultures of bilaminar co-cultures, either under normoxic conditions or following a 5 hour hypoxic incident as measured by RT-qPCR. In all: (i) raw RT-qPCR data of *Igf1* expression level relative to the housekeeping gene *Rps28*, (ii) relative RT-qPCR data of *Igf1* expression relative to the housekeeping gene *Rps28*, then relative to the ratio in normoxic conditions (A) *Igf1* expression does not change following a hypoxic incident in single astrocyte and neuronal cultures (B) *Hif2a* levels significantly increase in astrocytes and neurons following a hypoxic incident (C) *Igf1* expression significantly increases in astrocytes following a hypoxic incident when in a bilaminar co-culture with neurons at a density of 500K/cm^2 (D) A smaller and not significant increase in astrocyte *Igf1* expression is observed following a hypoxic incident when astrocytes are in a bilaminar culture with neurons plated at 200K/cm^2. Data shown is the mean +/- SEM. Student's t-test * $p<0.05$ ** $p<0.01$ *** $p<0.001$. Astrocytes in black, neurons in brown. A - n=4 cultures B – n=5 cultures C – n=3 cultures.

Characterising neurodegeneration and IIS change in our in vitro model

In order to assess neurodegeneration in co-cultures under the above conditions, we measured cell number and IIS signalling levels at +24 and +72 hours' following a hypoxic insult. Bilaminar cultures not exposed to hypoxia were used for comparison of IIS levels and cell number. Unless otherwise stated, changes reported are in relation to normoxic control cultures therefore.

A significant neuronal loss occurred at 24 hours and 72 hours post hypoxia, with a 30% and 40% decrease in neuronal number (figure 4.3 A, +24 hours p=0.0374, +72 hours p=0.0069). This was accompanied by a significant increase in Cleaved caspase 3 (CC3) levels, with a 160% increase at 72 hours post hypoxia (fig 4.3 B, p=0.0448).

Examining IIS changes following a hypoxic incident, we observed no significant increase in p-ERK levels in neurons at either time point post hypoxia (figure 4.3 C). Similarly we also saw no increase in pS-Akt levels in neurons at either time points following hypoxia (figure 4.3 A). This would suggest that the substantially increased astrocyte *Igf1* has not caused an increase in signalling through the IIS cascade in neurons, despite IGF1 also being a strong activator of Akt and ERK1/2 phosphorylation.

We then examined correlations between astrocyte *Igf1* change and neuron IIS change to examine interactions between these factors. If change in neuronal p-ERK level is plotted against changes in astrocyte *Igf1* expression, then a correlation between these levels exists (fig 4.4 A, p=0.0418). This indicates that an increase in *Igf1* expression leads to an increase in p-ERK levels, however the equation of the regression line is:

$$y = 0.1937x + 0.8043$$

This would mean that for a doubling of p-ERK level, an increase of 6.2 times the *Igf1* level observed in astrocytes under normoxic conditions would be required, and for a tripling of p-ERK levels, an 11 fold increase in *Igf1* expression would be required. Furthermore, plotting the change in neuronal pS-Akt levels against the change in astrocyte *Igf1* expression, we see no significant correlation.

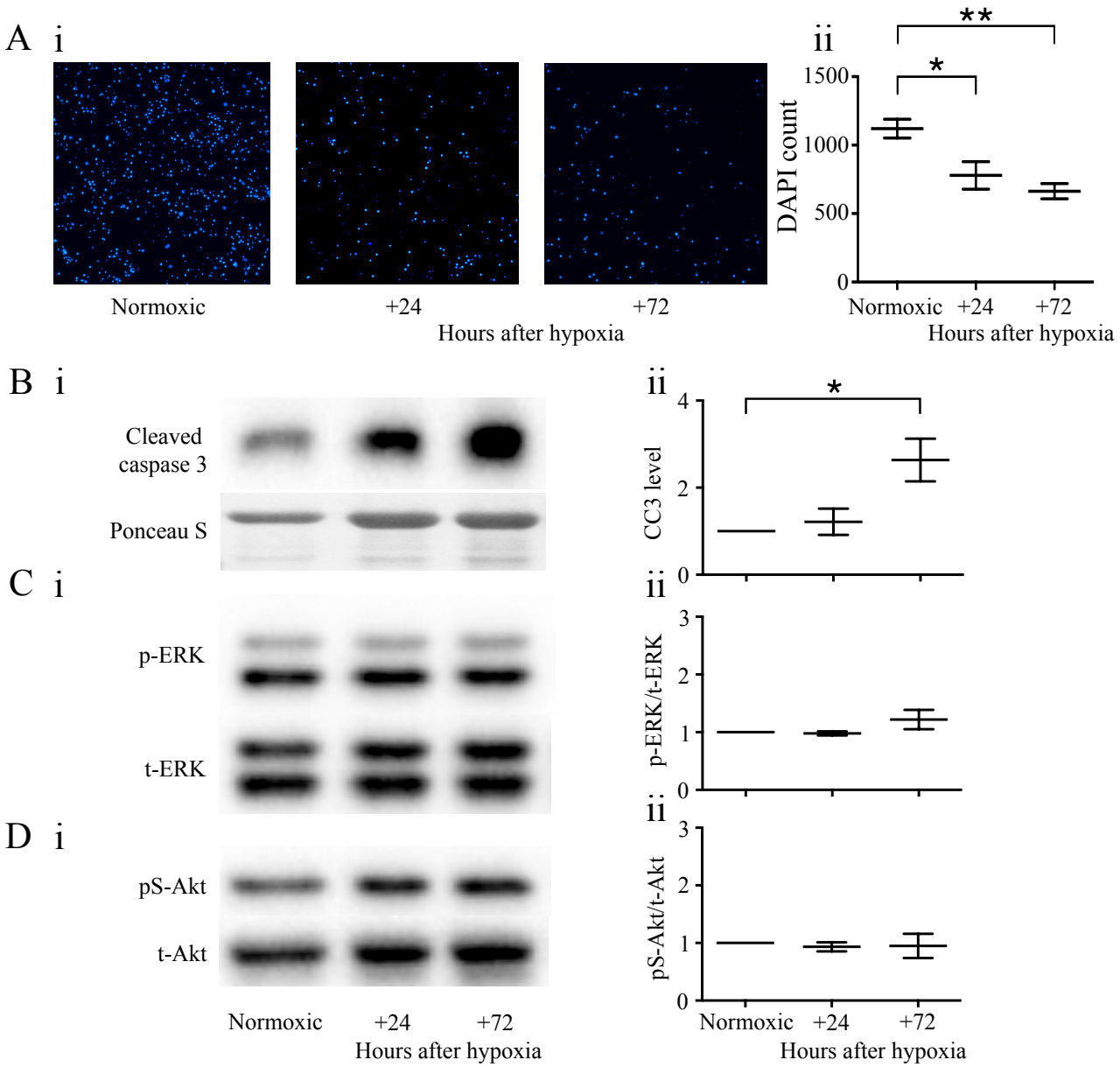

Figure 4.3. Bilaminar co-cultures of primary astrocytes and primary neurons when exposed to a 5 hour hypoxic incident, show profound neuron loss, an increase in apoptosis, but no change in ERK or AKT signaling. (A)(i) DAPI images of neuronal cultures separated from the bilaminar co-culture after being in normoxic conditions, or 24 and 72 hours after the cessation of hypoxic conditions and (ii) the graphical representation of this neuronal cell count. (B)(i, ii) Western blotting for CC3 shows that hypoxia causes an increase in apoptosis (C, D, i and ii) Western blotting showing no hypoxia induced changes in either pS-Akt or p-ERK levels. Data shown is the mean +/- SEM. Student's t-test * $p<0.05$ ** $p<0.01$ *** $p<0.001$. n=5 cultures.

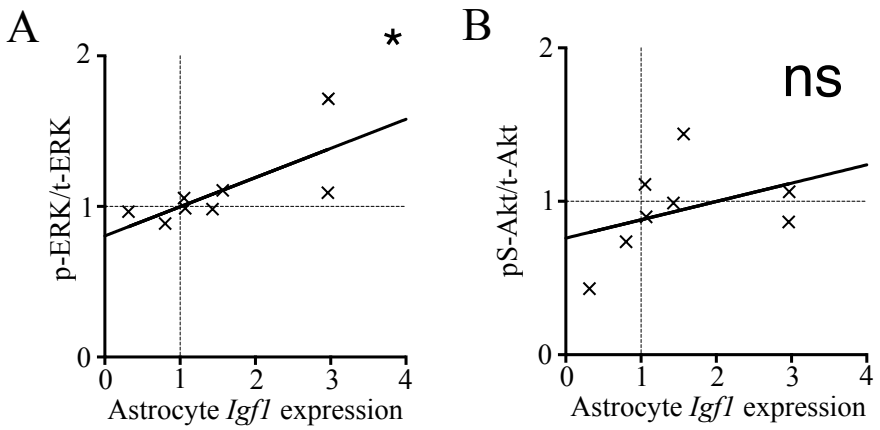

Figure 4.4. Correlations between change in astrocyte *Igf1* expression and changes in neuronal p-ERK and pS-Akt levels. (A) A significant interaction is seen between increased astrocyte *Igf1* levels and neuronal p-ERK levels (B) No significant association is observed increased astrocyte *Igf1* levels and neuronal pS-Akt levels. Pearson's R test * $p<0.05$, ns = not significant

With our co-culture model allowing the separation of astrocyte and neuronal cultures, we also examined the effect of increased astrocyte *Igf1* expression on IIS signalling and cell number in astrocytes. Astrocyte culture number under normoxic conditions, and 24 and 72 hours after hypoxia, was prone to substantial variability, with no overall pattern of an increase or decrease in astrocyte number with hypoxia (fig 4.5, A). There was however a significant increase in CC3 signal at 72 hours post hypoxia (fig 4.5 B, $p=0.0042$), indicating an increase in apoptosis at this time point in astrocytes, despite there being no decrease in astrocyte cell number at this time point.

Steady levels of p-ERK and pS-Akt were observed in astrocyte cultures under normoxic conditions and at both time points after hypoxia in astrocytes, with no significant difference between normoxic and hypoxic conditions (figure 4.5 C, D). We also observed no correlation between astrocyte *Igf1* increase and astrocyte p-ERK of pS-Akt level changes (figure 4.5 E, F). Despite no change in IIS signalling level or astrocyte cell number, we did see high levels of variability in astrocyte number in experiments, as well as occasional increases in pS-Akt levels in certain experiments.

We have therefore successfully identified an *in vitro* cellular model of induced acute neurodegeneration. Progressive neuronal cell loss following the short-term hypoxic incident is accompanied by increased astrocyte *Igf1* expression, allowing us to modulate the *Igf1* increase and investigate the effect this has on neuronal cell death and IIS changes.

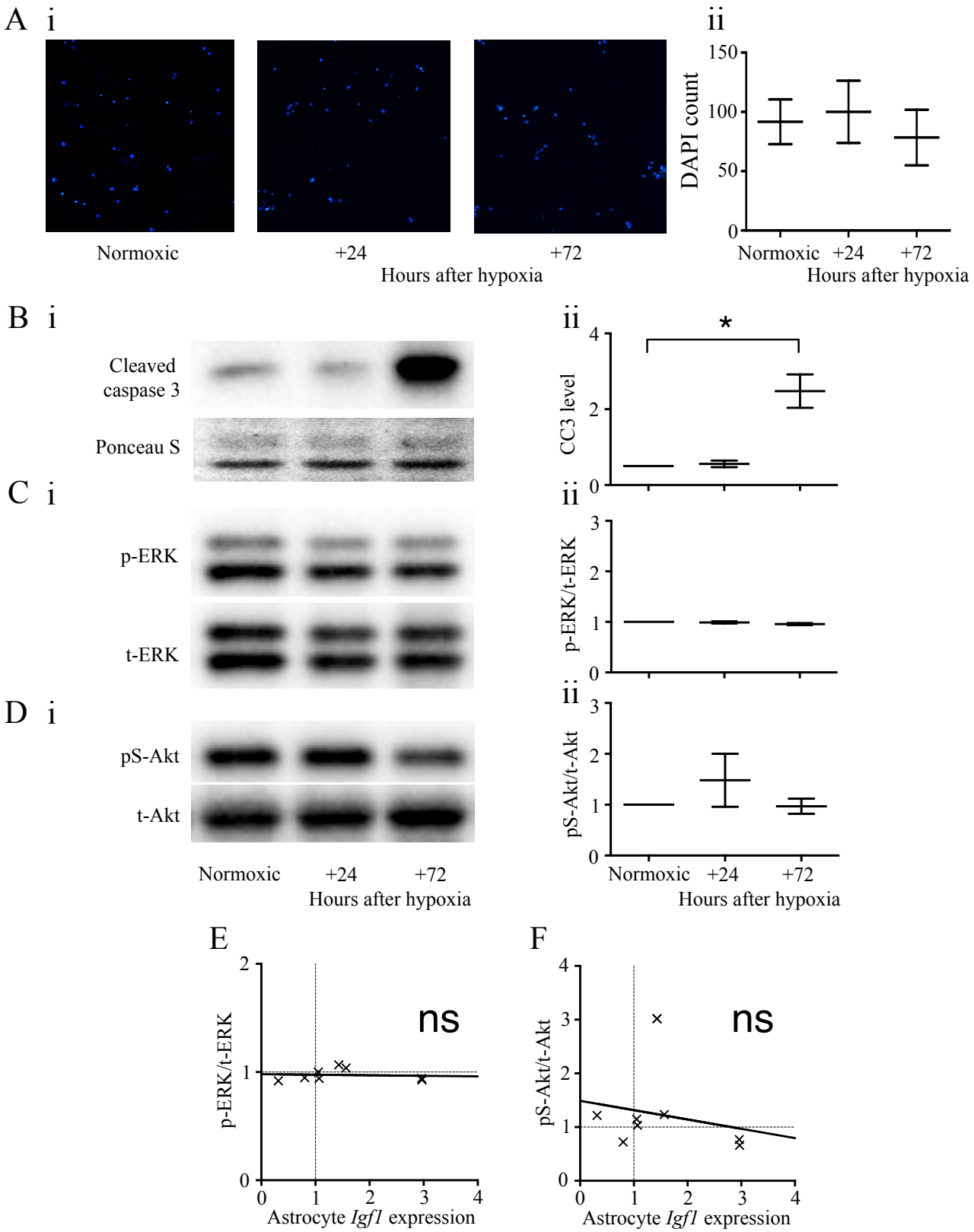

Figure 4.5. Characterization of cell loss and IIS signaling in astrocytes in a bilaminar co-culture under either normoxic conditions or at time points following a hypoxic incident. (A)(i) DAPI images of astrocyte cultures separated from the bilaminar co-culture after being in normoxic conditions, or 24 and 72 hours after the cessation of hypoxic conditions and (ii) the graphical representation of this astrocyte cell count. (B)(i, ii) Western blotting of CC3 shows that hypoxia causes an increase in apoptosis. (C, D, E, F) Western blotting showing no hypoxia induced changes in either pS-Akt or p-ERK levels, and no association between astrocyte *Igf1* and IIS signalling in astrocytes. Data shown in A-D is the mean +/- SEM. A-D, Student's t-test * $p<0.05$ ** $p<0.01$ *** $p<0.001$. E-F, Pearson's R test ns = not significant. n=4 cultures.

The role of endogenously increase Igf1 on neurodegeneration

In order to assess whether the increase in astrocyte *Igf1* expression was causal in the neuronal loss observed in these cultures, we compared bilaminar cultures with and without knock down of the *Igf1* gene.

Effects of Igf1 knock down during a hypoxic incident on neuronal cell loss and neuronal IIS signalling

Firstly we established that our siRNA succeeded in limiting *Igf1* expression increase under our experimental conditions by examining *Igf1* expression levels in our knock down cultures versus our control cultures via RT-qPCR. As shown in figure 4.6 B, there was a significant effect of siRNA treatment in *Igf1* expression in astrocytes with siRNA treatment, with a significant increase in expression in 72 hours post hypoxia control astrocytes but no other cultures (treatment p=0.0066, +72 hour post hypoxic control astrocytes vs normoxic control astrocytes p=0.0238).

The knock down of *Igf1* with siRNA caused a significant 15% loss of neurons compared to non-targeting siRNA in the absence of hypoxia (fig 4.6, C ii, p=0.0490). Therefore in order to understand the role of raised astrocyte *Igf1* in hypoxia induced neurodegeneration, we thus compared neuronal cell death after hypoxia in knock down and control cultures, relative to their own normoxic control conditions. When this was done, there was a significant effect of treatment on neuronal cell loss, with a significant reduction at 72 hours post hypoxia (fig 4.6 C iii, treatment effect p=0.0180, 72 hours cell loss p=0.0298). In control cultures there is a 40% reduction in neuronal number at 72 hours following hypoxia compared to control normoxic cultures, whereas in knock down cultures there is only a 10% reduction in neurons between knock down cultures 72 hours after hypoxia compared to knock down normoxic cultures.

This neuroprotective effect can be observed in a different way by plotting astrocyte *Igf1* expression increase against the percentage of neurons lost. When change in astrocyte *Igf1* expression levels and neuronal cell death levels at 72 hours post

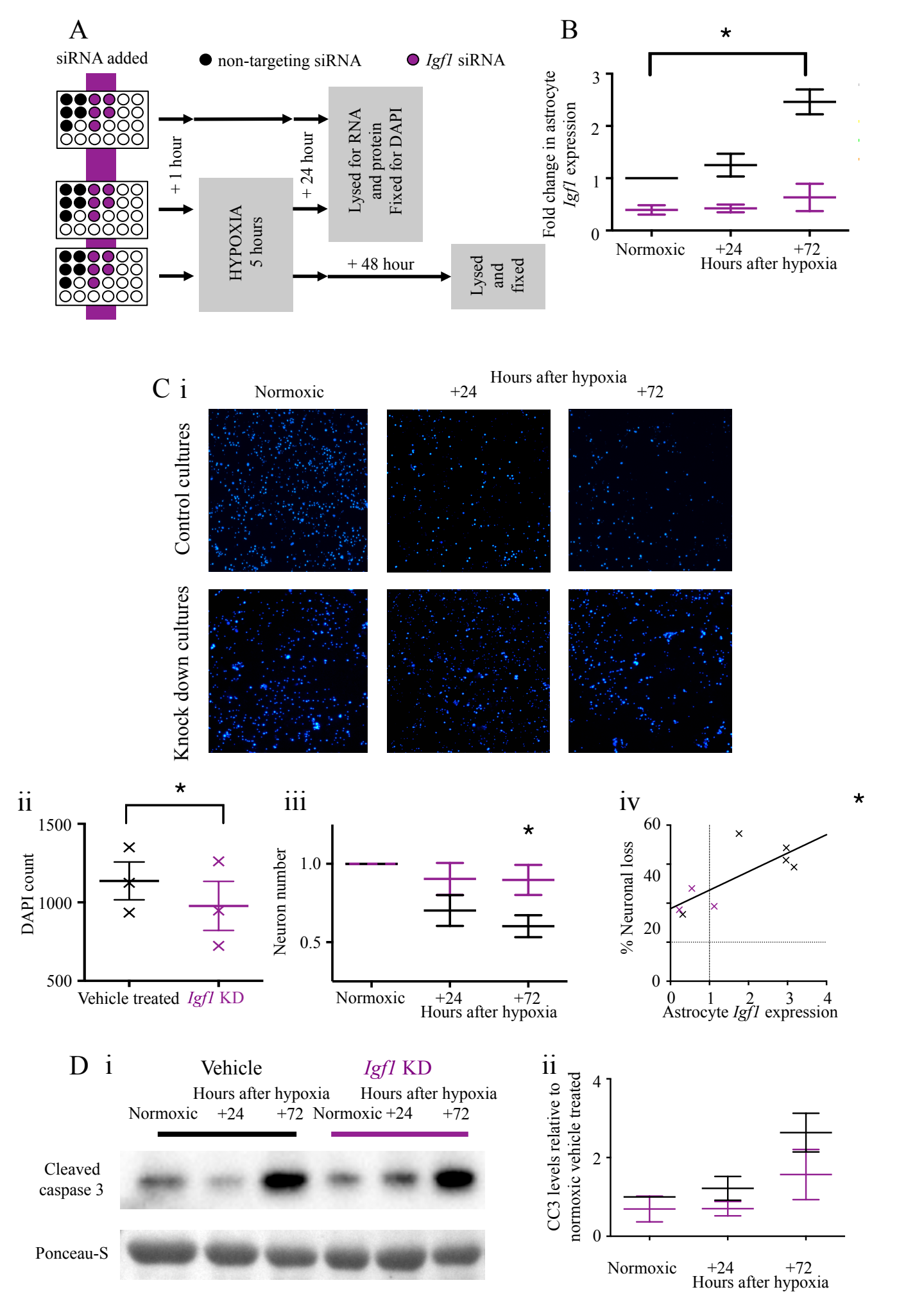
A
siRNA added
non-targeting siRNA
Igf1 siRNA
+ 1 hour
HYPOXIA
5 hours
+ 24 hour
Lysed for RNA
and protein
Fixed for DAPI
+ 48 hour
Lysed
and
fixed
B
*
Fold change in astrocyte
Igf1 expression
3
2
1
0
Normoxic
+24
+72
Hours after hypoxia
C i
Hours after hypoxia
Normoxic
+24
+72
Control cultures
Knock down cultures
ii
*
DAPI count
1500
1000
500
Vehicle treated
Igf1 KD
iii
*
Neuron number
1.0
0.5
Normoxic
+24
+72
Hours after hypoxia
iv
*
% Neuronal loss
60
40
20
0
0
1
2
3
4
Astrocyte Igf1 expression
D i
Vehicle
Igf1 KD
Hours after hypoxia
Hours after hypoxia
Normoxic
+24
+72
Normoxic
+24
+72
Cleaved
caspase 3
Ponceau-S
ii
CC3 levels relative to
normoxic vehicle treated
4
2
0
Normoxic
+24
+72
Hours after hypoxia

Figure 4.6. Knocking down and therefore preventing the increase in astrocyte *Igf1* expression, is mildly toxic to neurons, yet protects against hypoxia induced neuronal cell death. (A) Diagrammatic representation of the siRNA culture experiment (B) *Igf1* levels were decreased and prevented from rising in astrocytes following siRNA treatment, with a significant effect of treatment by 2-way ANOVA (C) Knocking down *Igf1* expression was slightly toxic, yet ameliorated hypoxia induced neuronal cell death (i) DAPI images of neuronal cultures under 10X magnification, in normoxic conditions and 24 and 72 hours after hypoxia, in control and knock down cultures (ii) Under normoxic conditions knocking down *Igf1* significantly reduces neuron number (iii) Accounting for this toxicity by plotting change in neuronal number relative to normoxic knock down cultures, a significant reduction in neuronal loss compared to control cultures is apparent (iv) When knock down and control culture data are plotted together, 72 hour post hypoxia neuronal loss significantly correlates with increased astrocyte *Igf1* expression at 72 hours (D) No change in CC3 level is observed with *Igf1* knock down. Data shown in all but C iv is the mean +/- SEM. C ii -Student's t-test, B Ciii Dii 2-way ANOVA, C iv, Pearson's R * $p<0.05$ ** $p<0.01$ *** $p<0.001$. Control cultures in black, knock down cultures in yellow. n=3 in each treatment.

hypoxia for knock down cultures (relative to normoxic knock down cultures) are pooled with the control cultures, a significant correlation is found (fig 4.6, C iv; $p=0.0287$). This suggests two things: that the normal level of *Igf1* expression in these cultures is required for normal neuronal health with a reduction in this being toxic, and secondly that the astrocyte *Igf1* increase following hypoxia is contributing to hypoxia induced neuronal cell death.

We next investigated the mechanism behind the observed Igf1-dependant neuronal cell death, by examining how *Igf1* knock down affected CC3 levels and IIS signalling following a hypoxic incident. In control cultures, CC3 levels were significantly increased 72 hours post following hypoxia. Despite *Igf1* knock down conferring neuroprotection, there was no reduction in CC3 levels in knock down cultures compared with control cultures at either time point following hypoxia, whether CC3 level change was measured relative to normoxic control culture levels, or normoxic knock down culture levels (fig 4.6, D). Similarly there was no effect of treatment on CC3 level. The lack of change in CC3 levels in normoxic knock down cultures compared to normoxic control cultures implies that the neurotoxicity of *Igf1* knock

down is not through apoptotic mechanisms. This also suggests that the neuroprotection observed following a hypoxic incident by blocking the astrocyte *Igf1* increase, is similarly not due to apoptotic neuronal cell death mechanisms.

We hypothesised that endogenous astrocyte *Igf1* increase not only contributes to neuronal cell death, but also does so via activation of the IIS cascade in neurons, thereby increasing p-ERK levels. As detailed earlier, there was no significant increase in p-ERK levels in neurons in control cultures following a hypoxic incident. Similarly there was no increase in p-ERK levels in knock down cultures at either time point following hypoxia, nor an effect of treatment (fig 4.7 A i). There was also no significant change in the p-ERK levels in knock down cultures compared to control cultures.

Examining further the relationships between astrocyte *Igf1* expression change, neuronal p-ERK change, and neuronal cell death, we examined correlations between these variables. Under control culture conditions a significant correlation exists between change in astrocyte *Igf1* expression and relative neuronal p-ERK level, however there is no correlation between these factors for the knock down cultures, when considered independently or when pool with control culture data (fig 4.7 A ii). When changes in neuronal p-ERK levels relative to normoxic knock down culture levels were plotted against the percentage of neurons lost relative to normoxic control numbers, a highly significant association was observed (fig 4.7 A iii, $p=0.0003$). This was not the case when examining this association in control cultures. This indicates that an increase in p-ERK levels is associated with increased neuronal cell death in knock down cultures, despite astrocyte *Igf1* being knocked down, and astrocyte *Igf1* not correlating with p-ERK levels.

Considering levels of phosphorylation at Akt in response to hypoxia under knock down conditions, there is similarly no significant change in pS-Akt level post hypoxia (figure 4.7 B). There was also no significant difference in pS-Akt levels between control cultures and knock down cultures, nor an effect of treatment. There was similarly no correlation between change in neuronal pS-Akt level and change in astrocyte *Igf1* expression level in knock down cultures (fig 4.7 B iii).

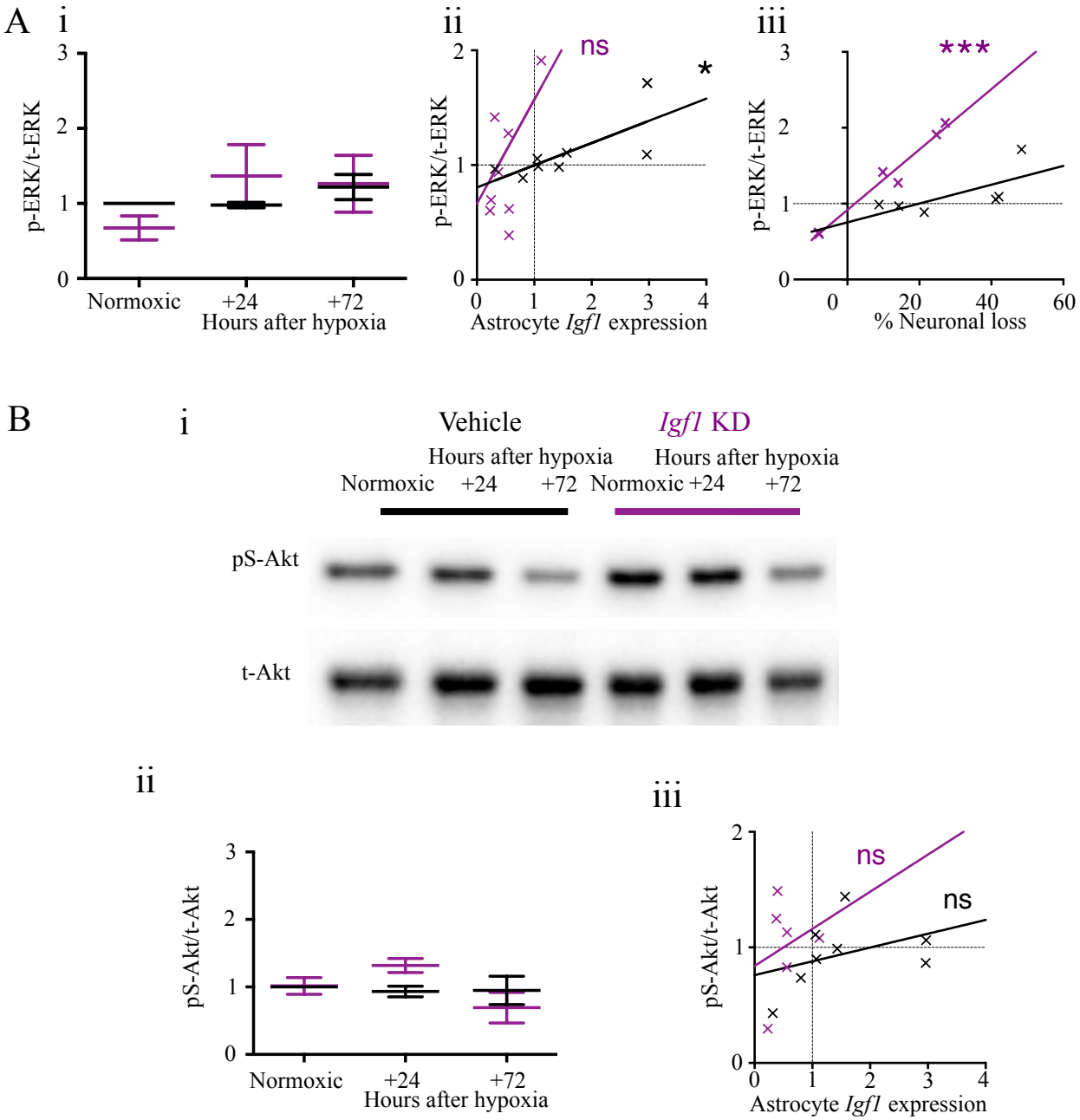

Figure 4.7. Changes in p-ERK and pS-Akt levels in neurons following a hypoxic incident in knocked down and control cultures. (A) Changes in neuronal p-ERK levels in knock down cultures were variable and not significantly different from the levels seen in control cultures (i) Graphical representation of changes in p-ERK levels in neuronal cultures. Due to variability in p-ERK levels no representative images were possible. (ii) A significant interaction is seen between increased astrocyte *Igf1* levels and neuronal p-ERK levels in control cultures, but no association between these two factors is observed in knock down cultures (iii) A highly significant association is shown between neuronal p-ERK and neuronal cell loss in knock down cultures. (B) There were no significant differences in pS-Akt levels in knock down cultures compared to vehicle treated cultures, (i) Western blots of knock down and control cultures (ii) Graphical representation of this (iii) No association is observed between increased astrocyte *Igf1* level and changes in neuron pS-Akt level. Data shown in A i and B ii is the mean +/- SEM. In A i and B ii, 2-way ANOVA. All others, Pearson's R * $p<0.05$ ** $p<0.01$ *** $p<0.001$. Control cultures in black, knock down cultures in yellow. n=3 in all

Effects of Igf1 knock down during a hypoxic incident on astrocyte number and IIS levels

With *Igf1* knock down proving to be acutely neurotoxic, we also examined astrocyte cell number change as well as astrocyte IIS levels in response to *Igf1* knock down. Despite variability in astrocyte number similar to that observed in our control cultures, no significant change in astrocytes number was observed under either normoxic conditions or at either time point following hypoxic conditions when *Igf1* was knocked down, and there was no effect of treatment (fig 4.8 A). This was the case whether change in astrocyte number was relative to normoxic control culture astrocyte number, or relative to normoxic knock down astrocyte number. Furthermore, no significant correlation was observed between astrocyte *Igf1* increase and change in astrocyte number (fig 4.8 A iii).

Levels of apoptosis as measured by CC3 level, were unchanged in astrocytes from knock down cultures relative to control cultures under normoxic conditions, and at both time points following hypoxia (fig 4.8 A iv). Similarly no significant difference in either p-ERK or pS-Akt was seen following *Igf1* knock down compared with control cultures, with no significant change in levels of either following hypoxia in knock down cultures (fig 4.8 B C).

These data suggests that astrocyte *Igf1* expression does not signal to astrocytes themselves via the IIS cascade, and that the increase in *Igf1* level does not affect astrocyte cell number or levels of astrocyte apoptosis.

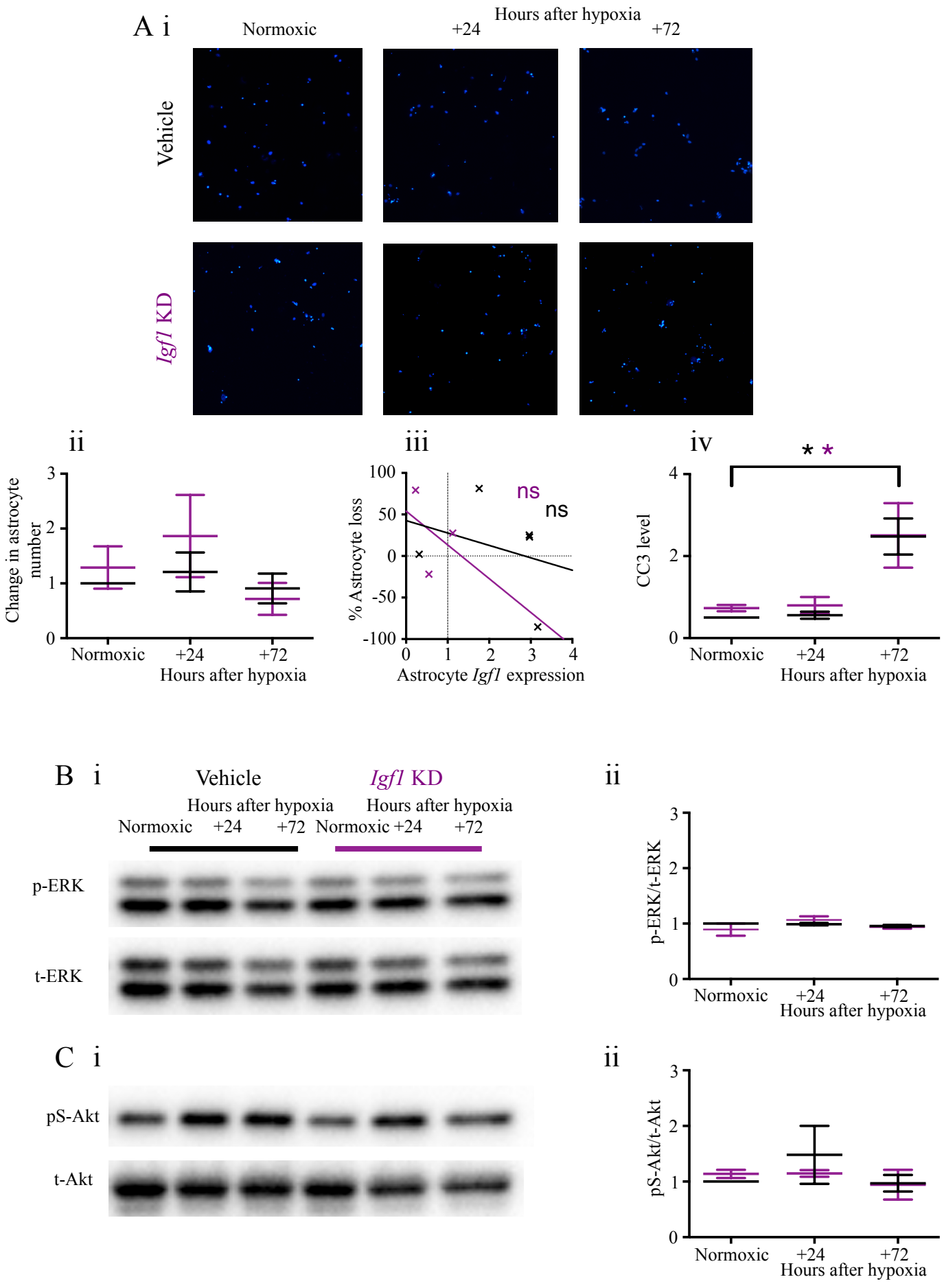
A i
Normoxic
Hours after hypoxia
+24
+72
Vehicle
Igf1 KD
ii
Change in astrocyte number
Normoxic
+24
+72
Hours after hypoxia
iii
% Astrocyte loss
ns
ns
Astrocyte Igf1 expression
iv
CC3 level
Normoxic
+24
+72
Hours after hypoxia
B i
Vehicle
Igf1 KD
Hours after hypoxia
Hours after hypoxia
Normoxic +24 +72 Normoxic +24 +72
p-ERK
t-ERK
ii
p-ERK/t-ERK
Normoxic
+24
+72
Hours after hypoxia
C i
pS-Akt
t-Akt
ii
pS-Akt/t-Akt
Normoxic
+24
+72
Hours after hypoxia

Figure 4.8. Knocking down and therefore preventing the increase in astrocyte *Igf1* expression, does not effect astrocyte number or IIS levels following a hypoxic incident. (A) There is no significant change in astrocyte number following *Igf1* knock down, but apoptosis is still increased 72 hours post hypoxic incident (i) DAPI images of astrocyte cultures under 10X magnification, in normoxic conditions and 24 and 72 hours after hypoxia, in control and knock down cultures (ii) graphical representation of this (iii) Plotting *Igf1* change against change in astrocyte number showed no association between these factors (iv) Despite no overall change in astrocyte number, increased apoptosis is present in both vehicle treated and siRNA treated cultures 72 post hypoxia (B)(C) p-ERK and pS-Akt levels did not change in control or knock down cultures following a hypoxic incident (i) Typical western blot images (ii) graphical representation of western blot data. Data shown is the mean +/- SEM, except A iii. 2-way ANOVA in all but Pearson R in A iii * $p<0.05$ ** $p<0.01$ *** $p<0.001$. Vehicle treated cultures in black, *Igf1* siRNA treated cultures in yellow. n=3 in each treatment.

Summary

This thesis aims to investigate whether alterations to the IIS cascade can be used to modulate neuronal cell death in neurodegenerative diseases. This chapter focuses on investigating how the increased levels of astrocyte Igf1 proximal to the source of injury in acute neurodegenerative diseases impacts on neuronal degeneration itself. Whilst overexpressing human *IGF1* in mouse astrocytes following a traumatic brain injury reduced neurodegeneration (Madathil et al., 2013), what effect the endogenous increase in astrocyte IGF1 had on neurodegeneration has until now remained unexplored. We investigated the consequence of this endogenous change by designing an *in vitro* model of induced neurodegeneration in a primary neuronal/astrocyte bilaminar co-culture.

This model showed increased expression of astrocyte *Igf1* and progressive neuronal cell loss following a short-term hypoxic insult. By preventing this astrocyte *Igf1* increase via siRNA administration at the time of hypoxic insult, we identified that *Igf1* increase during acute neurodegeneration contributes to neuronal cell death. This finding is at odds to previous findings of Igf1 being a protective factor, and therefore further work should be carried out to investigate this phenomenon further. The

mechanism by which Igf1 caused neuronal cell death, and therefore mechanisms behind the protective effect of its inhibition, was not as we had expected. The results of this chapter have therefore identified a novel potential mechanism of modulating the IIS cascade during acute neurodegeneration to ameliorate neuronal cell loss.

We had hypothesised that Igf1 would contribute to neuronal cell death, but we had also hypothesised that it would do so by increasing IIS signalling and therefore p-ERK levels in neurons, with increased p-ERK levels being shown in previous studies to be a neuronal cell death signal (Chen et al., 2009; Luo and DeFranco, 2006). Although gross significant changes in p-ERK levels were neither observed in vehicle treated or siRNA treated cultures following hypoxia, in vehicle treated cultures the increase in p-ERK level correlated with the change in astrocyte *Igf1*. When *Igf1* was knocked down, p-ERK levels in neurons still showed the capacity to increase, and furthermore correlated strongly with the levels of cell death in the cultures. This firmly suggests that IGF1 does not induce cell death via an increase in p-ERK levels, but rather signals through a different mechanism. Furthermore, there was no reduction in the levels of apoptosis when *Igf1* was knocked down, suggesting that the neuroprotective effect of preventing the endogenous *Igf1* increase during neurodegeneration, is through a different mechanism to both of those investigated.

Preventing Igf1 increase following a hypoxic insult proved to be neuroprotective, however our knock down of astrocyte *Igf1* was also mildly toxic to neurons under normoxic non-stressed conditions, masking the neuroprotective effect unless this initial toxicity is taken into consideration. This therefore represents a novel mechanism of neuronal cell death in acute neurodegeneration, and a novel opportunity to intervene in neuronal cell death via endogenous IIS modulation. The exploitation of this for possible therapeutic gain would depend heavily on being able to reduce the short-term increase in *Igf1* expression, whilst not lowering the expression beyond baseline levels. A potential way of doing this would be with IGF1R inhibitors, and titrating the dosage to give sufficient inhibition to block an increase but not limit baseline levels. Before this can be explored further however, an IGF1R receptor inhibitor would need to be investigated in the same cell culture model that we have used, to see if the same neuroprotection can be elicited that we have seen, but without causing neurotoxicity.

Chapter 5

Repurposing clinically approved IIS inhibitors to treat acute neurodegeneration

Introduction

Various studies have demonstrated that genetically decreasing signalling through the IIS cascade in animal models of chronic neurodegeneration can ameliorate and slow the onset of the pathology in these models, as well as reducing neuronal cell death (Cohen et al., 2006; Cohen et al., 2009; Cooper et al., 2015; Freude et al., 2009; Killick et al., 2009). Pharmacological inhibitors of this pathway have also shown beneficial effects when applied to animal models of neurodegenerative disease. Many of these inhibitors focus on the Ras-Raf-ERK branch of the IIS pathway, and it is inhibitors of this branch that we focus on in this chapter.

The clinically approved c-Raf inhibitor Sorafenib has been shown to ameliorate neuronal cell death in culture, and furthermore rescues working memory deficits in a mouse model of fAD (Echeverria et al., 2008; Echeverria et al., 2009). Ashabi *et al* have also demonstrated that using the experimental non-clinically approved MEK inhibitor U0126 can mitigate neurodegeneration in mice where Aβ fibrils were injected into their brains (Ashabi et al., 2013). Pharmacologically inhibiting the Ras-Raf-ERK pathway in chronic neurodegenerative diseases in humans could prove difficult however. With the long duration of neuronal cell loss, and common side effects associated with IIS inhibition, applying Ras-Raf-ERK inhibitors at the correct point in disease pathogenesis to ameliorate degeneration whilst limiting serious side effects, would be difficult. Acute neurodegenerative diseases have a far smaller window for therapeutic intervention however; meaning the timing for disease intervention is simplified, and the long-term side effects of IIS inhibitor treatment are mitigated by the reduced time frame of drug administration. Evidence showing that inhibition of the Ras-Raf-ERK cascade reduces infarct size and neurodegeneration in mouse models of

stroke when administered during or after the ischaemic incident, indicates that inhibitors of this cascade are a promising therapeutic target for acute neurodegenerative diseases (Gladbach et al., 2014; Namura et al., 2001; Wang et al., 2003).

An over activation in the proliferative Ras-Raf-ERK pathway is a frequent feature in many cancers. This has resulted in the development of many compounds to inhibit specific members of this pathway, with many of these being approved for human use as chemotherapy agents (Roberts and Der, 2007; Wellbrock et al., 2004). With pharmacological Ras-Raf-ERK inhibition seeming a promising approach to treat acute neurodegenerative disease, these anti-cancer drugs could potentially be repurposed for use in acute neurodegeneration. This chapter therefore investigates the possibility of repurposing drugs that inhibit the IIS cascade that are already approved for use in humans, for the alternative use of intervening in neuronal cell death cascades and preventing neurodegeneration.

Aims

This chapter investigates the possibility of repurposing the clinically approved MEK inhibitor Trametinib and B-Raf inhibitor Dabrafenib, for the alternative use of ameliorating neuronal cell death in acute neurodegenerative disease. We tested the proof of principle of the neuroprotective effects of our chosen inhibitor Trametinib in our developed model of acute neurodegeneration, before beginning testing it for efficacy in inhibiting Ras-Raf-ERK in the mammalian brain.

Methods

Initially to test our inhibitors for successful p-ERK level reduction in cells of the mammalian brain, we applied Trametinib and Dabrafenib to the media of primary neuronal and astrocyte cultures, modified from the protocols of Schildge *et al* and the primary neuron protocol used by Dresbach *et al* (Dresbach et al., 2003; Schildge et al., 2013). This allowed us to confirm that multiple cell types in the brain are inhibited by our drugs of choice, whilst also allowing us to test for feedback stimulation of the pathway that had been reported with some IIS

inhibitors previously (Anforth et al., 2012; Hatzivassiliou et al., 2010; Poulikakos et al., 2010).

To test the neuroprotective effects of Trametinib in an *in vitro* model of acute neurodegeneration, primary cultures were used to form the bilaminar co-cultures described in chapter 4. Trametinib was applied 1 hour prior to the 5 hour hypoxic incident, with cell number, *Igf1* expression, and IIS signaling measured at 24 and 72 hours after the cessation of the hypoxic incident, as well as in a culture under normoxic conditions for control comparison (figure 5.5 A) (**Trametinib treated**). Wells treated with the same volume of DMSO in the same experimental condition (normoxia or hypoxia) were used as a control (**vehicle treated**). Therefore, as in chapter 4, one plate was used for normoxic comparison, and a plate each for the 24 and 72-hour post hypoxia time points, with plates containing 2 wells to be lysed for RNA, 2 for protein, and one well for PFA fixation and DAPI staining (figure 5.5 A). Comparisons following hypoxia (in the 24 and 72 hour post hypoxia plates)(**hypoxic cultures**) are made relative to the normoxic control cultures (**normoxic cultures)**.

Cell number, and therefore neuronal cell death, was assessed by counting DAPI stained cells under a light microscope from neuronal cultures separated from the bilaminar co-cultures. We examine changes in signaling levels through the IIS cascade in these cultures, by western blotting for the activating phosphorylation sites pS473 on Akt (pS-Akt) (Alessi et al., 1996), and pT202/pY204 and pT185/pY187 on ERK1/2 (p-ERK)(Canagarajah et al., 1997; Payne et al., 1991), and normalised these levels to total protein Akt and ERK1/2 levels. Western blotting for cleaved caspase 3 (CC3) was also performed on protein samples to examine levels of apoptosis. *Igf1* expression was assessed by RT-qPCR. This allowed us to not only investigate the neuroprotective mechanisms of Trametinib administration to an *in vitro* model of acute neurodegeneration, but also investigate how this inhibition affected signaling through the IIS cascade in these cultures.

To investigate the administration of Trametinib to mice, we first assessed the toxicity of Trametinib on *ex vivo* mouse brain tissue by applying Trametinib for up to 14 days to the media of hippocampal organotypic brain slices from GFP expressing mice. We measured spine density on CA1 pyramidal neurons by imaging live slices using confocal microscopy, and also established Trametinib still inhibited MEK via western blotting in the same slices.

Trametinib was administered to mice via two mechanisms, via intracerebroventricular (ICV) injection, and via oral gavage. ICV was carried out by drilling a small hole in the skull over the ventricles, and lowering a needle into the ventricular space then injecting Trametinib, following the protocol of DeVos and Miller (DeVos and Miller, 2013). Oral gavage of Trametinib was given orally by gavage following standard procedures, and administered concurrently with intraperitoneal injection of Elacridar. All mice used were male wild type C57BL-6 strain, aged 4-6 months. For comparison, mice were also treated using the above methods, but with the same volume of vehicle, for comparison.

Throughout this chapter the level of inhibition through the Ras-Raf-ERK branch of the IIS cascade was established by western blotting for the above-mentioned activating sites on ERK1/2, and normalising by total ERK1/2 levels.

Hypotheses

1. We hypothesise that Trametinib will be neuroprotective when administered to our *in vitro* model of acute neurodegeneration, and therefore result in less neuronal cell death
2. This reduction in neuronal cell death will reduce astrocyte *Igf1* expression increase observed in non-treated bilaminar cultures
3. We also hypothesised that Trametinib will reduce p-ERK levels in the mammalian brain when administered orally to mice
4. We therefore hypothesise that Trametinib could be repurposed to treat acute neurodegeneration

Results

In vitro testing

IIS inhibition in primary neuronal and astrocyte cells using Trametinib and Dabrafenib

Variability has been shown between different cell lines with respect to their susceptibility to inhibition by IIS inhibitors (Gilmartin et al., 2011). To test the susceptibility of neurons and astrocytes to inhibition by Trametinib and Dabrafenib, primary cell cultures of neurons and astrocytes were treated with Trametinib and Dabrafenib. To then test these drugs in our bilaminar co-culture model to test for neuroprotection following a noxious insult, we also established the desired concentration of each drug to add to the media.

Initially neurons and astrocytes were treated once with each drug, with cells lysed for protein 24 hours after treatment. Trametinib or Dabrafenib was applied in rising concentrations of 0.1µM 1µM 10µM and 100µM, diluted in the culture medium. Control cultures were treated with the same volume of DMSO as the 100µM Trametinib wells, 15µl, without drug.

Trametinib treated astrocytes show a reduction of p-ERK in a dose dependent manner, with 95% inhibition achieved with the lowest dose of 0.1µM, rising to 98% inhibition at 10µM (figure 5.1, A B). Interestingly, the 100µM dose resulted in the death of the cells, indicating that there is a maximal dose for Trametinib before it is toxic to astrocytes, at least in culture. For Dabrafenib, lower concentrations of the drug did not inhibit ERK phosphorylation, with a slight increase observed, but reduction of 40% and 65% were seen at concentration of 10µM and 100µM. This inhibition is less than that caused by Trametinib administration, with a significantly higher concentration required to achieve a reduction in p-ERK. The lack of cell death in Dabrafenib treated cultures compared with cell death in 100µM treated Trametinib cultures, suggests we have not tested maximal concentrations of Dabrafenib in cultures.

For treated neurons, the same trend is seen, with increased concentrations of Trametinib and Dabrafenib negatively correlating with p-ERK levels (figure 5.1 C D). The reduction in

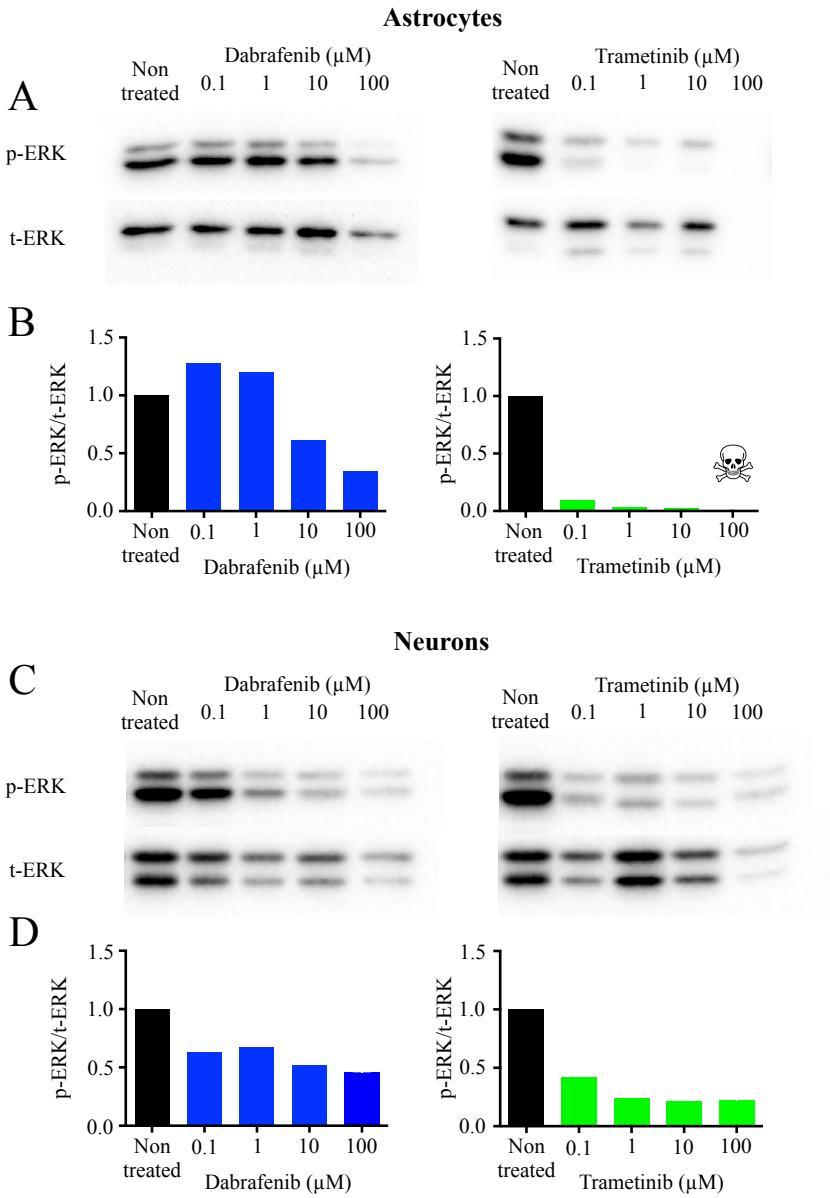

Figure 5.1. Trametinib and Dabrafenib potently inhibit p-ERK in both astrocyte and neuronal cells in culture. (A)(B) Trametinib potently inhibited astrocyte p-ERK levels with near complete ablation of observable phosphorylation with even the lowest dose (0.1μM), and cell death at the highest (100μM). Dabrafenib however increased phosphorylation levels at the two lower doses, with approaching 60% p-ERK reduction at the highest concentration of 100μM. (C)(D) A similar pattern was seen in neuronal cultures, albeit without culture death at the highest Trametinib dose, less ERK phosphorylation reduction for the same dose with Trametinib, and no increase in ERK phosphorylation at low doses with Dabrafenib administration.

phosphorylation levels from Trametinib treatment is not as severe in neuronal cultures as it was in astrocyte culture however, with only a 60% reduction with 0.1μM, increasing to 80% reduction with 100μM. Furthermore, the highest concentration of 100μM Trametinib did not cause the whole neuronal cultures to die whereas it did in astrocyte cultures. Dabrafenib treatment in neurons was again less potent than Trametinib treatment, with a maximal reduction in phosphorylation levels at the highest dose of 100μM of 55%. This would again imply that a higher concentration of Dabrafenib could be used if a more profound inhibition of p-ERK was desired in culture. Therefore both Dabrafenib and Trametinib successfully inhibit MEK and B-Raf in astrocyte and neuronal cultures.

Whilst previous work with Trametinib has raised no issues other than the usual side affects associated with chemotherapy agent administration, we were concerned with previous evidence that Dabrafenib treated patients have an increased incidence of squamous cell carcinoma. As this is thought to be due to a feedback increase in IIS signalling that has been observed with the long term administration of similar ATP-competitive Raf inhibitors in wild type B-Raf cells (Anforth et al., 2012; Hatzivassiliou et al., 2010; Poulikakos et al., 2010), and the patients we are aiming to repurpose to will be wild type for B-Raf, we carried out a longitudinal study in cultures to ensure that Dabrafenib did not increase IIS signalling in the brain.

When astrocyte cultures were treated with 100μM Dabrafenib every second day over the duration of 7 days, there was a different effect on ERK1 and ERK2 phosphorylation levels; with prolonged drug exposure leading to decreased ERK1 phosphorylation but increased ERK2 phosphorylation (figure 5.2). These changes were seen at all time points following the start of drug addition, but by 7 days the phosphorylation level of ERK1 had begun to return to approaching non-treated level, with the increase in ERK2 phosphorylation rising dramatically. Again as was shown earlier, 100μM of Dabrafenib appeared to reduce total ERK levels when compared to time matched sham treated cultures (figure 5.2). These results indicate that when wild type primary astrocytes are treated with a sufficient dose of Dabrafenib to reduce p-ERK levels to below 50% of normal levels, not only does this cause total ERK levels to decrease, but that it leads to the paradoxical increases in p-ERK2 levels. The lack of potency in reducing p-ERK levels, combined with its reduction of t-ERK levels and its paradoxical stimulation of ERK2 phosphorylation, makes Dabrafenib an unsuitable

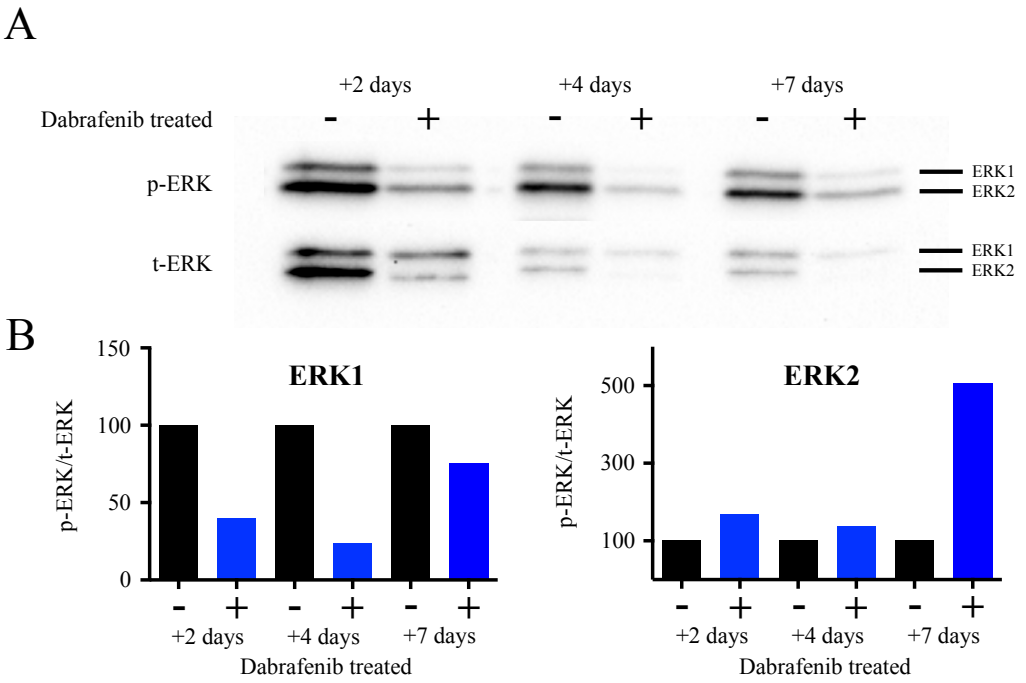

Figure 5.2. 100 µM Dabrafenib paradoxically inhibits ERK1 phosphorylation whilst increasing ERK2 phosphorylation when chronically applied to astrocyte cultures. (A) Western blots showing p-ERK and t-ERK levels in astrocyte cultures either treated with 100µM Dabrafenib or DMSO vehicle, for 2, 4, or 7 days. (B) 100µM Dabrafenib potently inhibited ERK1 phosphorylation after 2 and 4 days with less inhibition after 7 days, but resulted in increased ERK2 phosphorylation, most substantially after 7 days.

drug to test our hypothesis, and unsuitable for further consideration as a repurposable IIS inhibitor.

Whilst Dabrafenib appears to be unsuitable for testing our hypotheses, Trametinib is efficacious in both neurons and astrocytes *in vitro*. We therefore used Trametinib as our sole drug for investigating our hypothesis.

Trametinib is neuroprotective in a cellular model of hypoxia induced neuronal cell death

Using the same *in vitro* model of hypoxia induced acute neurodegeneration as used in chapter 4, we applied 10µM Trametinib one hour prior to the time of hypoxic insult, and investigated the possible neuroprotective properties of this drug by measuring neuronal cell number change and apoptotic markers between Trametinib treated cultures and cultures treated with

the same volume of DMSO vehicle (fig 5.3, A). Cell number and apoptosis levels were measured in cultures under normoxic conditions to see if Trametinib affected neuronal cell death independently of the stressful stimulus, and at 24 and 72 hours after the hypoxic incident. Similar data was also taken for astrocytes to investigate the role of IIS in astrocyte number change in response to a stressful stimulus. To gain further insight into the role that IIS plays in cell death, we lysed cells at the time points and conditions mentioned for protein and RNA also, allowing us to relate cell death to astrocyte *Igf1* gene expression levels, and levels of p-ERK and pS-Akt.

In bilaminar co-cultures treated with Trametinib, a near complete reduction in neuron p-ERK levels was achieved (figure 5.3 B). Hypoxia induced neuronal cell death and accompanying increase in apoptosis observed under vehicle treated conditions, is significantly reduced in cultures treated with Trametinib. A significant reduction in neuronal cell loss is observable at 72 hours post hypoxia, with a 15% and 22% loss of neurons at 24 hours and 72 hours post hypoxia with Trametinib treatment, compared to 30% and 40% lost in vehicle treated cultures (figure 5.3, $p=0.0149$). A significant effect of treatment on neuronal cell loss was also observed ($p=0.0187$). CC3 level in neurons is also significantly affected by Trametinib ($p=0.0081$), with a trend towards a reduction at 72 hours post hypoxia, ($p=0.0866$). Whereas *Igf1* knockdown was neuroprotective following the hypoxic incident, but neurotoxic under non-stressed conditions, no decrease in neuronal number was observed with Trametinib treated cultures under normoxic conditions. The reduction of neuronal cell loss and reduction of CC3 levels in neurons following a noxious stimulus when treated with Trametinib, strongly suggests that Trametinib is neuroprotective.

Whilst we hypothesised that Trametinib treatment would be neuroprotective, we also predicted that Trametinib treated cultures would reduce the magnitude of astrocyte *Igf1* increase due to the decrease in neuronal cell loss. Whilst we observed a trend towards an effect of treatment in astrocyte *Igf1* cultures ($p=0.0603$), this effect was an increase in astrocyte *Igf1* expression in Trametinib treated cultures under normoxic conditions and 24 hours after hypoxia (figure 5.4 A, $p=0.0357$, 0.0193). These increases in astrocyte *Igf1* expression in Trametinib treated cultures matched the magnitude of increase in *Igf1* expression seen 72 hours post hypoxia in vehicle treated cultures (~250% times normoxic vehicle treated *Igf1* expression level). Crucially as this *Igf1* increase is apparent even under normoxic conditions, it suggests that the increase is dependant on Trametinib administration

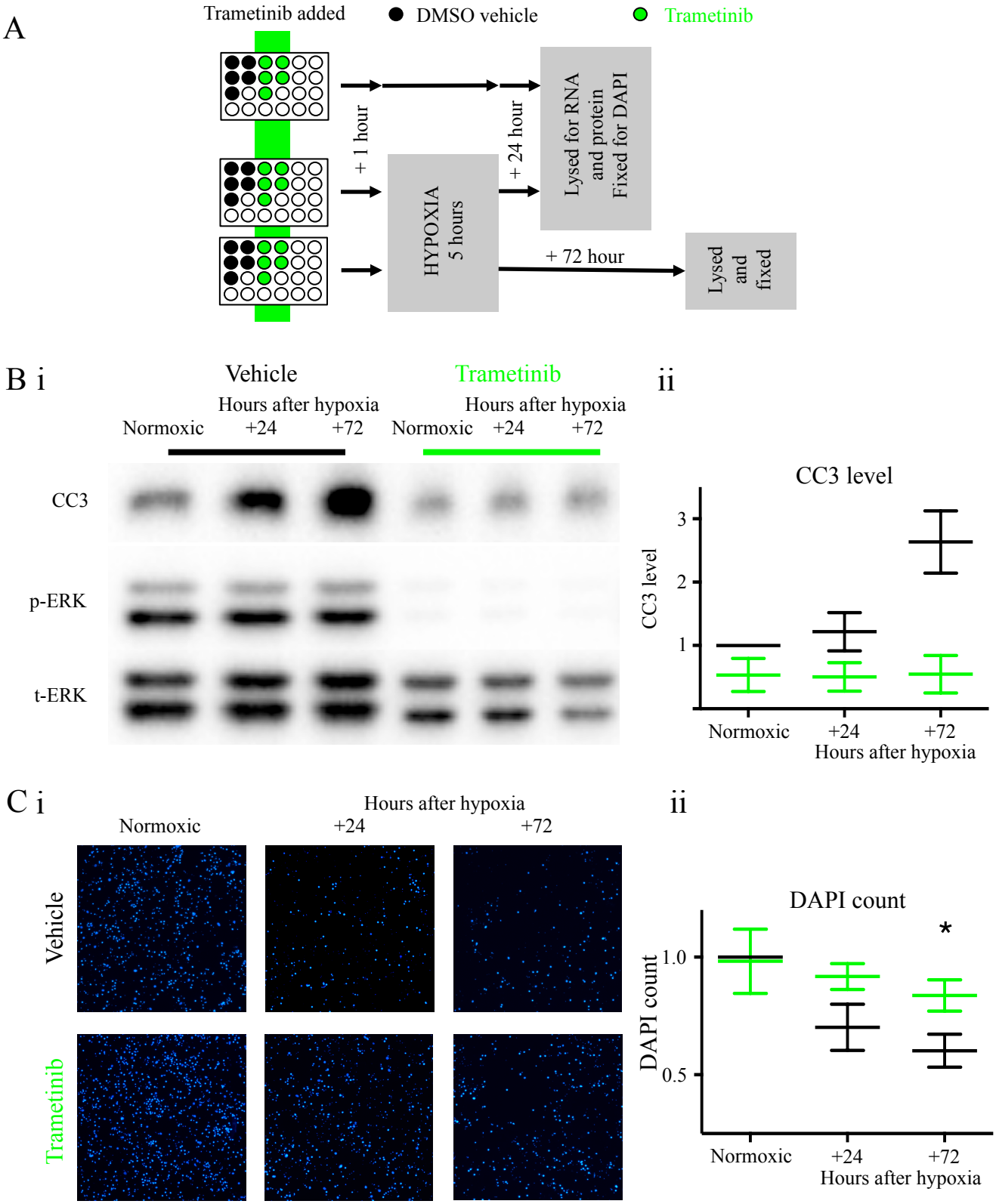

Figure 5.3. Trametinib administration to bi-laminar astrocyte-neuron co-cultures at the time of hypoxic stress, is neuroprotective. (A) Diagrammatic representation of Trametinib treatment experiments (B) Trametinib administration nearly completely reduced p-ERK levels in neuronal cultures, and reduced CC3 levels. (i) Western blots of p-ERK, t-ERK, and CC3 in Trametinib and vehicle treated cultures (ii) Graphical representation of western blot data (C) Neuronal loss following a hypoxic incident is significantly reduced 72 hours after the incident in Trametinib treated cultures (i) DAPI staining of neuronal cultures (ii) Graphical representations DAPI count data. Data shown is the mean +/- SEM. 2-way ANOVA * $p<0.05$ ** $p<0.01$ *** $p<0.001$. Vehicle treated cultures in black, Trametinib treated cultures in green. n=5 cultures.

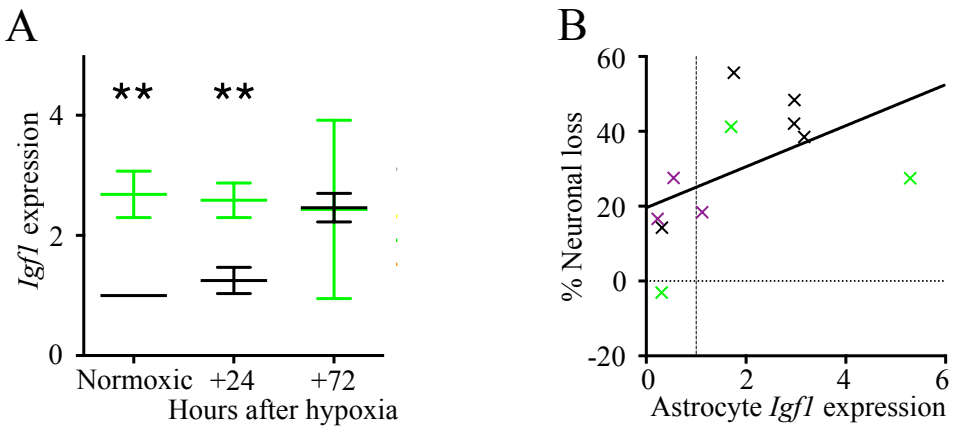

Figure 5.4. Trametinib application induces an increase in astrocyte *Igf1* expression, which does not correlate with neuronal cell death. (A) RT-qPCR for *Igf1* in astrocyte cultures from bilaminar co-cultures treated with Trametinib show a significant increase in *Igf1* expression in Trametinib treated cultures under normoxic conditions and at 24 hours post hypoxia. (B) No significant correlation between neuronal loss and *Igf1* expression was observed when data from *Igf1* siRNA (purple) vehicle treated (black) and Trametinib treated (green) cultures were pooled. Data in A mean +/- SEM, 2-way ANOVA, B Pearson's R test * $p<0.05$ ** $p<0.01$ *** $p<0.001$). n=5 cultures for Trametinib, n=5 for wild type, n=3 for KD.

rather than the hypoxic incident, thereby suggesting that decreased p-ERK levels induced an increase in *Igf1* expression in astrocytes to the same magnitude as a noxious insult.

In chapter 4 when pooled astrocyte *Igf1* expression at 72 hours post hypoxia from control cultures and *Igf1* knock down cultures was plotted against neuronal cell death, a positive correlation was seen, whereby higher *Igf1* expression was associated with higher neuronal death. When Trametinib treated data from 72 hours post hypoxia was also pooled with the other data the correlation was not significant (figure 5.4 B, $p=0.1115$). However, with increased astrocyte *Igf1* expression following a noxious stimulus being shown in chapter 4 to be neurotoxic, the increased astrocyte *Igf1* expression observed in Trametinib treated cultures could be a confounding variable in our examination of Trametinib as a neuroprotective agent, and could be limiting its neuroprotective potential. To establish if this induced *Igf1* expression increase has any effect on the usefulness of Trametinib as a neuroprotective agent, we carried out the same hypoxia insult on bilaminar co-cultures, but applied both Trametinib and siRNA against *Igf1*, to examine what effect Trametinib had without *Igf1* expression increase.

Combined Trametinib administration and Igf1 knock down is similarly neuroprotective in a cellular model of hypoxia induced neuronal cell death

Firstly we ascertained that astrocyte *Igf1* expression was successfully prevented from increasing in Trametinib+KD cultures, and found that there was a significant effect of treatment on astrocyte *Igf1* expression between Trametinib plus *Igf1* siRNA treated cultures than Trametinib treated alone (figure 5.5, p=0.0488). The Tramatinib+KD culture *Igf1* expression levels were similar to that of vehicle treated cultures. Similarly we also confirmed that neuronal p-ERK levels were reduced in Trametinib+KD cultures as was observed in solo Trametinib cultures (fig 5.5, C), with near complete reduction in p-ERK levels observed in neuronal cultures when treated with Trametinib+KD.

Cultures treated with Trametinib and *Igf1* siRNA showed decreased neuronal cell death compared to vehicle treated controls at +72 hours post hypoxia (figure 5.5 D, p=0.0335). The difference between Trametinib+KD cell loss at 24 and 72 hours post hypoxia, and that of either solo treatment, was not significantly different. This suggests that whilst the Trametinib+KD treated cultures were protected from neurodegeneration following a hypoxic incident by combined treatment, the neuroprotection of solo *Igf1* knock down and solo Trametinib treatment was not additive when combined. This further suggests that the increased astrocyte *Igf1* expression following solo Trametinib treatment did not limit the neuroprotection of Trametinib. Interestingly, no significant decrease in neuronal number was observed under normoxic conditions in Trametinib+KD cultures, in contrast to the loss of neurons in solo siRNA treated cultures. This suggests that the neurotoxicity of reduced *Igf1* expression under normoxic conditions is protected against by combined Trametinib treatment.

In Trametinib+KD treated cultures, the p-ERK reduction was once more accompanied by a near complete reduction in CC3 signal, with a highly significant effect of treatment (fig 5.6 A, p=0.0028.). This indicated that apoptosis was similarly reduced in Trametinib+KD treated cultures as in Trametinib solo treated. Unlike previous experiments, pS-Akt levels showed an increase in Trametinib+KD cultures compared to vehicle treated cultures, with a highly significant effect of treatment ($p<0.0001$), a trend towards an increase at 72 hours post hypoxia (p=0.0791), and a significant increase 24 hours post hypoxia (fig 5.6 B, p=0.0230).

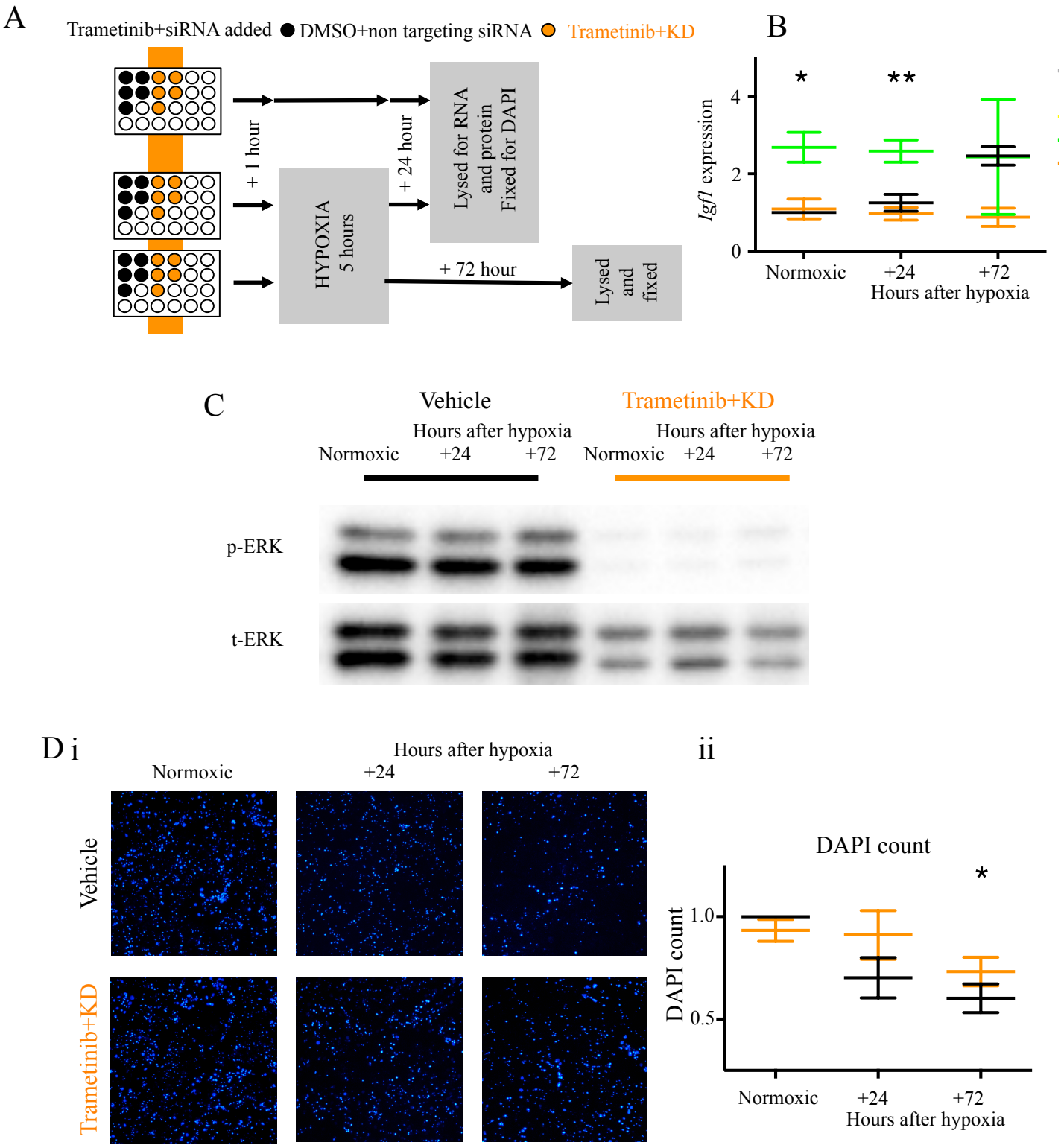

Figure 5.5. Combined Trametinib and *Igf1* siRNA administration to bi-laminar astrocyte-neuron co-cultures at the time of hypoxic stress, is similarly as neuroprotective as Trametinib treatment alone. (A) Diagrammatic representation of Trametinib+KD treatment experiments (B) *Igf1* siRNA treatment successfully and significantly reduces astrocyte *Igf1* expression when administered with Trametinib (C) Trametinib+KD administration reduces p-ERK levels in neuronal cultures (i) Western blots of p-ERK and t-ERK in Trametinib+KD and vehicle treated cultures (ii) Graphical representation of western blot data (D) Neuronal loss following a hypoxic incident is significantly reduced 72 hours after the incident in Trametinib +KD treated cultures (i) DAPI staining of neuronal cultures (ii) Graphical representations DAPI count data. Data shown is the mean +/- SEM. 2-way ANOVA* $p<0.05$ ** $p<0.01$ *** $p<0.001$. n=3 cultures.

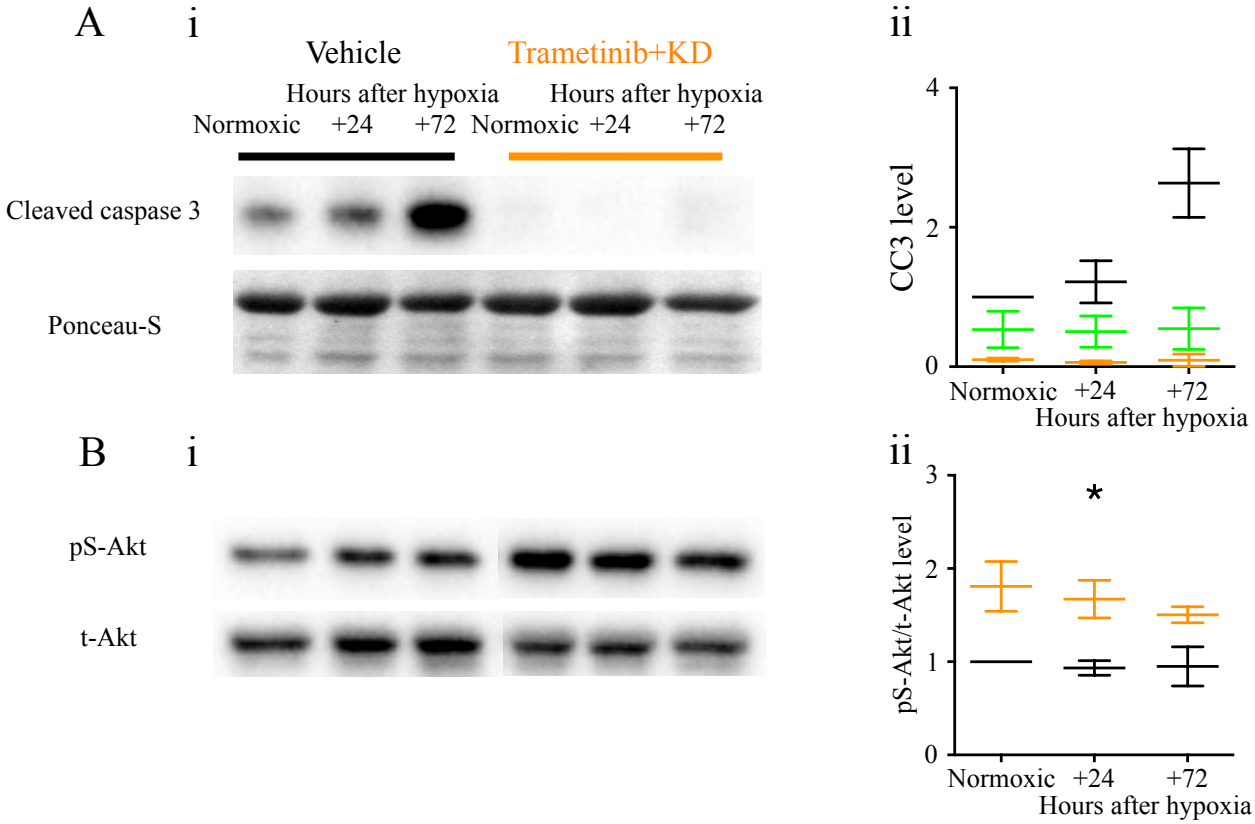

Figure 5.6. Changes in apoptosis and pS-Akt signaling in neurons following a hypoxic incident with Trametinib and *Igf1* siRNA treatment. (A) Levels of apoptosis in Trametinib+KD treated cultures are significantly reduced compared to vehicle treated cultures (i) Western blots of vehicle and Trametinib+siRNA treated neuronal cultures (ii) Graphical representation of this (B) pS-Akt are raised in Trametinib+KD cultures, with a significant increase at 24 hours post hypoxia (i) Western blots of vehicle and Trametinib +siRNA treated neuronal cultures (ii) Graphical representation of this. Data shown is the mean +/- SEM. 2-way ANOVA * $p<0.05$ ** $p<0.01$ *** $p<0.001$. Vehicle treated cultures in black, Trametinib treated cultures in green, Trametinib + *Igf1* KD treated cultures in orange. n=3 cultures.

Despite astrocyte *Igf1* increase following a noxious incident being neurotoxic, the increased astrocyte *Igf1* expression observed following Trametinib treatment does not limit the neuroprotection of the drug. Furthermore the neuroprotection from reducing *Igf1* expression and reducing p-ERK levels are not additive when combined.

The effect of Trametinib, and combined Trametinib and Igf1 siRNA administration on astrocytes in a cellular model of hypoxia induced neuronal cell death

One of the key advantages of our co-culture model is the ability to treat and manipulate the conditions in which the co-culture exists, but then be able to separate the cell types to analyse them separately. We therefore applied the same investigation of measuring changes in IIS signalling and change in cell number in the astrocyte cultures from our bilaminar co-cultures treated with Trametinib, Trametinib+KD, or control conditions.

In both Trametinib and Trametinib+KD treated cultures a near complete reduction in p-ERK levels was observed (fig 5.7, A). We also showed previously that a significant reduction in astrocyte *Igf1* expression was seen in Trametinib+KD cultures, whereas a significant increase in *Igf1* was observed in solo Trametinib treated cultures (figure 5.5 A). When either Trametinib or Trametinib+KD treatments were applied to the cultures at the time of the noxious incident, no change in astrocyte number at 24 or 72 hours post hypoxia was observed when change was relative to vehicle treated normoxic astrocyte cultures (figure 5.7 B). There was however a significant increase in astrocyte number in Trametinib and Trametinib+KD treated normoxic cultures compared to vehicle treated normoxic cultures (Trametinib $p=0.0495$. Trametinib+KD $p=0.0388$). As with the neurotoxicity observed following *Igf1* siRNA treatment (chapter 4), it may be that there is a change in cell number in Trametinib and Trametinib+KD treated cultures following hypoxic conditions when the change in number is relative to non-vehicle treated normoxic controls, thereby taking into account the change in cell number under normoxic conditions with treatment. However when analysis was carried out this way there was once again no significant change in astrocyte number following a hypoxic incident.

The reduction in p-ERK levels in astrocytes when treated with Trametinib or Trametinib+KD was accompanied by a reduction in CC3 levels, implying that apoptosis was reduced in these

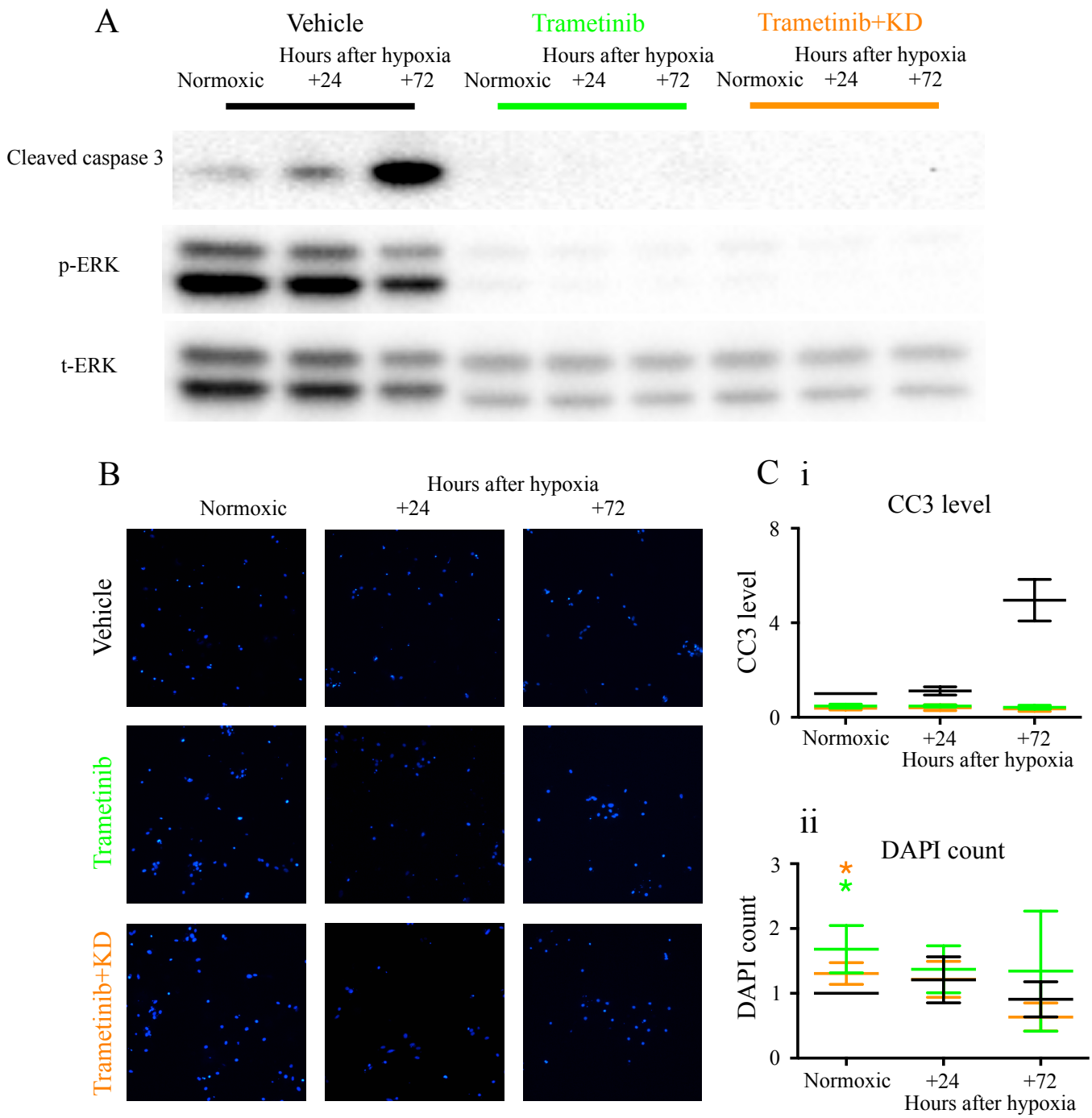

Figure 5.7. Trametinib and Trametinib+KD administration to bi-laminar astrocyte-neuron co-cultures at the time of hypoxic stress reduces apoptosis in astrocytes, and increases astrocyte number under normoxic conditions, but does not affect astrocyte number following hypoxia. (A) Western blots showing p-ERK, t-ERK, and CC3 levels in astrocyte cultures separated from bi-laminar co-cultures either treated with Trametinib, Trametinib + *Igf1* siRNA or DMSO and non-targeting siRNA, in either normoxic conditions, or 24 or 72 hours after a 5 hour hypoxic insult. Trametinib administration nearly completely reduced p-ERK levels, and significantly reduced CC3 levels. (B) DAPI staining in astrocyte cultures (C) Graphical representations of the (i) CC3 level and (ii) DAPI count between differently treated cultures. Data shown is the mean +/- SEM. 2-way ANOVA * $p<0.05$ ** $p<0.01$ *** $p<0.001$. n=5 cultures for Trametinib, n=3 cultures for Trametinib+KD.

Cultures. In Trametinib and Trametinib+KD treated cultures there was an effect of hypoxia on CC3 level, as well as an effect of treatment, and a significant interaction between these factors. Astrocyte pS-Akt levels were not significantly changed with Trametinib or Trametinib+KD treatment under normoxic or post hypoxic cultures (figure 5.8).

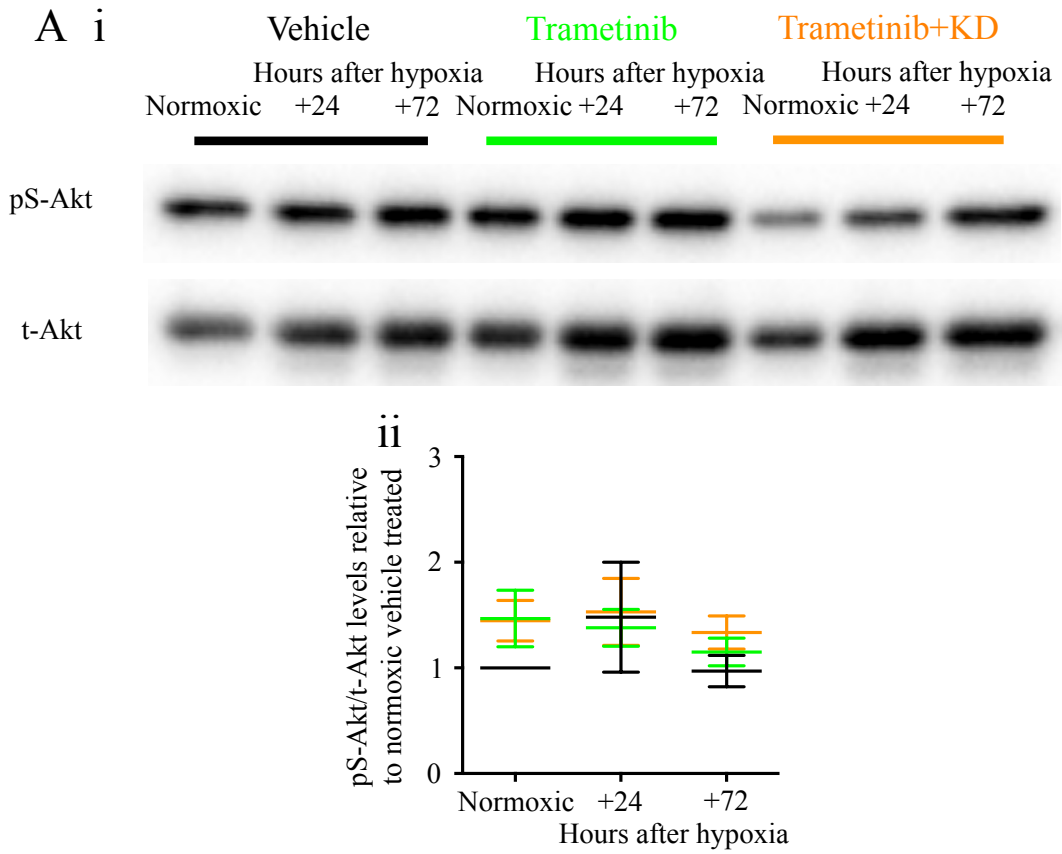

Figure 5.8. Changes in pS-Akt signaling in astrocytes following a hypoxic incident with Trametinib and combined Trametinib and *Igf1* siRNA treatment. (A) pS-Akt levels are not significantly altered in astrocytes from either Trametinib solo or Trametinib +KD cultures (i) Western blots of vehicle, Trametinib, and Trametinib+siRNA treated astrocyte cultures (ii) Graphical representation of this. Data shown is the mean +/- SEM. 2-way ANOVA * $p<0.05$ ** $p<0.01$ *** $p<0.001$. n=5 cultures for Trametinib, n=3 cultures for Trametinib+KD.

In vivo Trametinib administration in mice

We have successfully shown that Trametinib administration in a cellular model of acute neurodegeneration shows neuroprotective affects that are not limited by its induction of increased astrocyte *Igf1* expression. With our hypothesis of attenuating p-ERK levels being neuroprotective against neurodegeneration being supported by our *in vitro* model, we proceeded with investigating Trametinib *in vivo* administration in mice.

Safety assessment of Trametinib for in vivo application

It was necessary to establish that Trametinib was not toxic to intact brain tissue before *in vivo* experimentation could begin. To do this we used hippocampal organotypic slices, thin slices of mouse brain that preserve brain structures and circuitry, from GFP expressing mice. The 10% of glutamatergic neurons in these slices that express GFP allowed detailed observation of the morphology of neurons via confocal microscopy. With decreased dendritic arborisation and decreased spine number being indicative of neuronal stress and damage (Campana et al., 2008; Magarinos and McEwen, 1995), we investigated the toxicity of Trametinib administration on *ex vivo* brain tissue by measuring dendritic spine density and gross dendritic arborisation of CA1 neurons in the hippocampus when treated with Trametinib or the same volume of DMSO.

Organotypic slices were treated with 10μM Trametinib for up to 2 weeks, adding Trametinib to the culture medium every three days with control slices treated with the same volume of DMSO in otherwise parallel conditions. The brain slices were then taken for confocal imaging of CA1 pyramidal neurons of the hippocampus at 5 and 14 days from the start of Trametinib application, to examine changes in spine density and dendritic arborisation with treatment. These slices once imaged were then snap frozen and homogenised for protein, allowing us to quantify Trametinib inhibition of p-ERK levels in *ex vivo* brain tissue for up to 14 days.

Organotypic p-ERK levels were nearly undetectable in the Trametinib treated slices compared to vehicle treated slices (figure 5.9, A), yet confocal microscopy showed that not only did the neurons show comparable dendritic arborisation to the vehicle treated slices, but

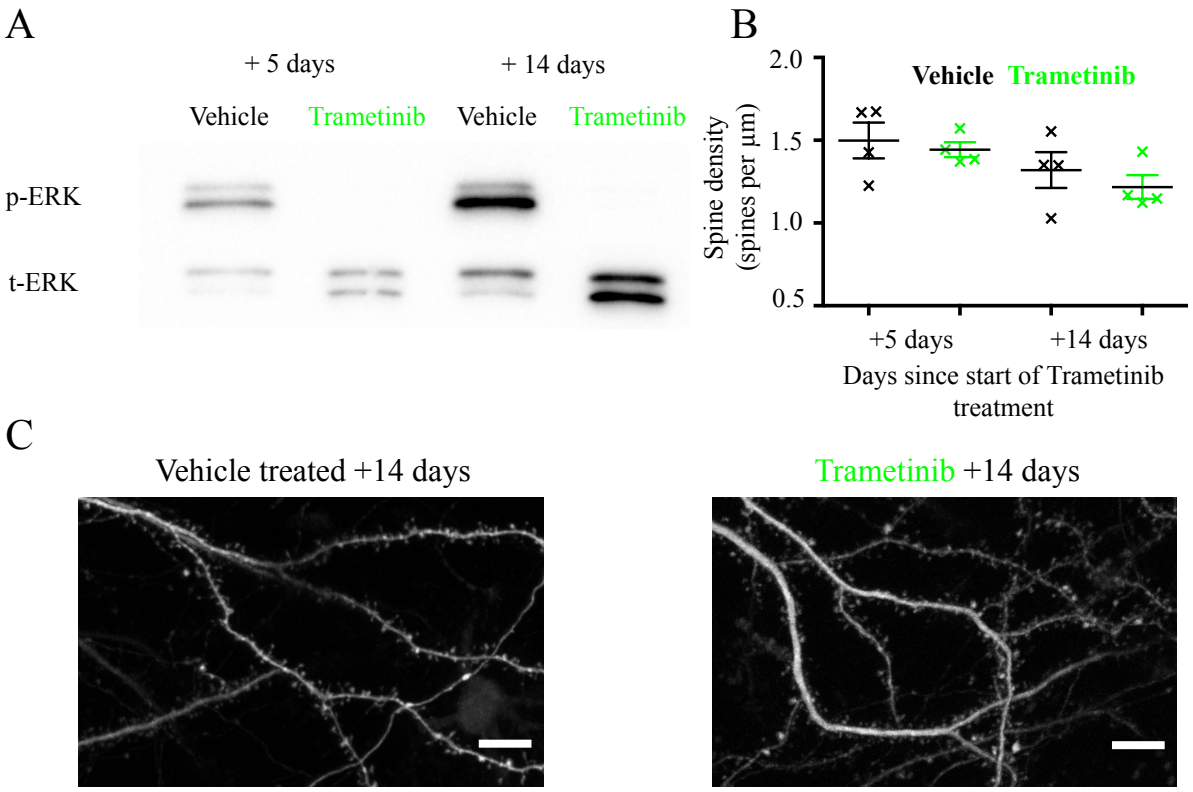

Figure 5.9. Trametinib reduces p-ERK levels in organotypic mouse brain slices without changing spine density or neuronal morphology. (A) 10µM Tram completely inhibits p-ERK levels in organotypic hippocampal slice preparations when treated for 5 and 14 days. (B)(C) Dendritic arborisation and spine density is unchanged between Trametinib and vehicle treated slices. Confocal images of organotypic cultures from *Thy1-GFP* expressing mice. Scale bar = 10µm. Data shown is the mean +/- SEM. Student's t-test. n=4 mice.

there similarly was no significant difference in spine density between the treatments (figure 5.9 B). It therefore seems that this dose of Trametinib is well tolerated by mouse brain tissue, and we therefore felt confident that *in vivo* procedures would not result in brain toxicity.

In vivo Trametinib application in adult mice

There is evidence to suggest that Trametinib shows poor brain bioavailability when administered orally in mice and humans (Vaidhyanathan et al., 2014). The mechanism limiting its brain bioavailability is the actions of the efflux protein P-glycoprotein (P-gp) but not the common breast cancer resistant protein (Bcrp) (Vaidhyanathan et al., 2016). P-gp (official gene name: *ABCB1* in humans, *Abcb1a* in mice) is an ATP dependant membrane bound transport protein found in epithelial cells throughout the body, and crucially is expressed in the luminal membrane of capillary endothelial cells in the brain (Schinkel, 1999). This suggests that it is the crossing of the blood brain barrier that acts as the limiting step in Trametinib's brain bioavailability. This would limit the brain bioavailability of all systemic administration routes of Trametinib; including oral, intravenous, and intraperitoneal administration. This initially poses a substantial problem, as these are the most feasible routes of administration in experimental animals. Overall however with repurposing of Trametinib for human administration in mind, oral administration is the only method for which Trametinib is currently approved for in humans (National Institute for Health and Clinical Excellence, 2016). A potential way to overcome this would be to co-administer Trametinib with an inhibitor of the efflux protein that limits its entry to the brain. Before oral administration is investigated however, we first wanted to establish that Trametinib was still efficacious at inhibiting the mammalian brain when administered directly to the intact brain.

With P-gp being expressed heavily in epithelial cells in the brain (fig 5.10), we administered Trametinib to the intact brain of 4-month old mice by intracerebroventricular injection; whereby a small volume of Trametinib (10 µl) in DMSO is injected directly into the ventricles of a mouse (DeVos and Miller, 2013). The same volume of DMSO vehicle was injected but containing no drug for control comparison. One group of mice received intracerebroventricular injections of Trametinib at 1mM, 100µM, and 10µM concentrations or DMSO vehicle, and were decapitated 24 hours after the injection, before cortex and hippocampal tissue was processed for western blotting to assess p-ERK levels. A second

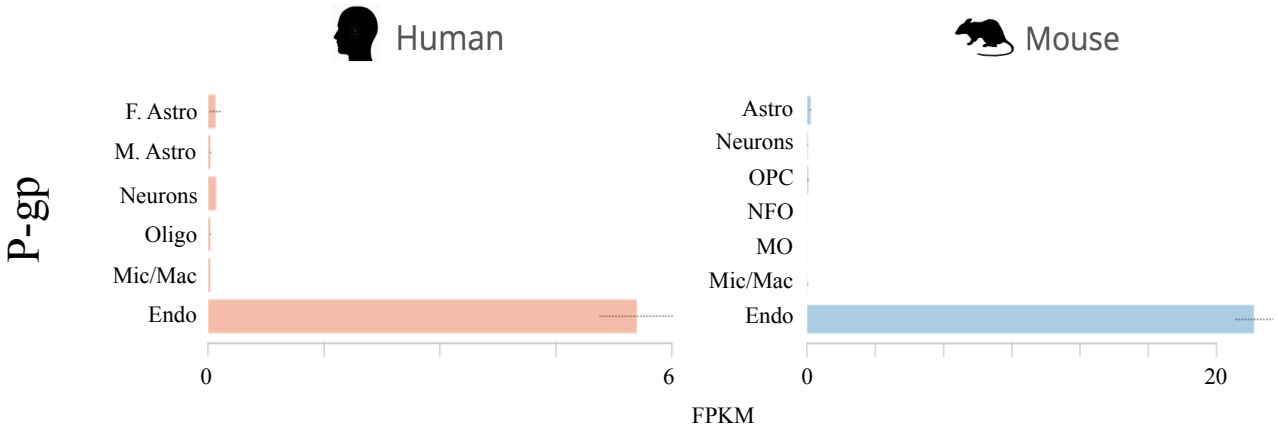

Figure 5.10. Expression levels of P-gp in the mouse and human brain. The efflux transporter P-gp that has been shown to limit the brain concentration of Trametinib, is nearly exclusively expressed in the epithelial cells of the human and mouse brain. Panels modified from http://www.brainrnaseq.org. F. Astro - Fetal Astrocytes, M. Astro – Mature Astrocytes, Oligo – Oligodendrocytes, Mic/Mac – Microglia/Macrophages, Endo – Endothelial, OPC – oligodendrocyte Precursor Cells, NFO – Newly Formed Oligodendrocytes, MO – Mature Oligodendrocytes. FPKM - Fragments per kilobase of transcript sequence per million mapped fragments

group of mice were injected with a concentration of 1mM of Trametinib or the same volume of DMSO intracerebroventricularly, and mice decapitated for analysis 1, 3, and 7 days after

injection. Usually when administering a drug, µg/kg is used as the measure of dosage. As we are dealing with a single organ however, and to avoid assumptions about whether the intracerebroventricularly injected drug remains in the brain or distributes around the whole body, we refrained from dosing based on a weight of tissue/animal and instead injected based on the concentrations mentioned above.

Intracerebroventricular injections of Trametinib produced no decrease in p-ERK levels in the cortex or hippocampus of injected mice at any time point or with any concentration of drug (figure 5.11). This data suggests that the intracerebroventricular injection of Trametinib did not succeed in reducing p-ERK *in vivo*.

The reason for this lack of effect is likely to be the actions of P-gp. We had assumed that by bypassing the blood brain barrier we would be able to administer Trametinib to the brain, avoiding the effects of P-gp, but this was not the case. To overcome this, we administered the P-gp inhibitor Elacridar at the same time as administering Trametinib, in an attempt to increase Trametinib's *in vivo* brain inhibition. Vaidhyanathan and Elmquist showed an increase in brain Trametinib concentration when administered in P-gp knock out mice, (Vaidhyanathan et al., 2014), and similarly showed that the brain concentration of the PI3K inhibitor GSK2126458, also reduced in its brain bioavailability by the P-gp transporter (as well as the Bcrp transporter), was successfully increased by combining GSK2126458 administration with the P-gp/Bcrp inhibitor Elacridar (Vaidhyanathan et al., 2016). Therefore we hypothesised that the brain bioavailability of Trametinib would be greatly increased with the co-administration of Elacridar.

To replicate previous studies that had success in administering Trametinib and Elacridar in mice, we administered Trametinib by oral gavage in animals fasted for 2 hours at a dose of 5mg/kg in a solution of 1% methocel/5%DMSO, with Elacridar administered by intraperitoneal (IP) injection at a dose of 10mg/kg in a solution of 30% microemulsion (6:3:1 ration of Kolliphor EL, Di-ethyl ether, Glyceryl trioctanoate; see methods), 30 minutes prior to Trametinib administration (Vaidhyanathan et al., 2014; Vaidhyanathan et al., 2016; van Waterschoot et al., 2009). Control animals were treated in the same way with vehicle solutions minus Trametinib and Elacridar. We were concerned with the half-lives of these drugs, so decided also on a shorter time between drug administration and animal decapitation. Animals were therefore killed 5 hours after Trametinib administration, and hippocampus and cortex tissue tested by western blotting for p-ERK and t-ERK levels.

Figure 5.12 shows that a significant 37% reduction in ERK1/2 phosphorylation was seen with Trametinib administration on its own (p=0.0089), but a far stronger reduction in p-ERK level was seen when Trametinib was combined with Elacridar (p=0.0011). Furthermore there is a significant difference between the solo Trametinib treated and Trametinib Elacridar dual treatment (p=0.0242). It is interesting to note that oral administration of just Trametinib in figure 5.12 succeeded in reducing p-ERK levels in the brain, whereas just Trametinib injected into the brain in figure 5.11 did not. This could be due to multiple factors, including the far higher dose given orally to account for the unknown permeability of the blood brain barrier, but also because of the shorter interval between administration of drug and quantification of p-ERK level in the brain, being 5 hours for oral administration and 24 hours for intracerebroventricular injection. Whilst solo Trametinib succeeded in reducing brain p-ERK level when given at a 5mg/kg dose by oral gavage, the reduction in p-ERK is lower than we would want to achieve in order to test our hypothesis. The reduction in phosphorylation seen when Trametinib was combined with Elacridar however was at the level we want to achieve over a long time period to test the effect of IIS reduction on neurodegeneration.

Unfortunately, despite our success in achieving *in vivo* p-ERK inhibition in the brains of mice, due to time constraints and the lack of access to an appropriate mouse model of acute neurodegeneration, testing the effects of Trametinib *in vivo* was not possible during my PhD studies, and will therefore be carried on further by my supervisor Dr Dervis Salih.

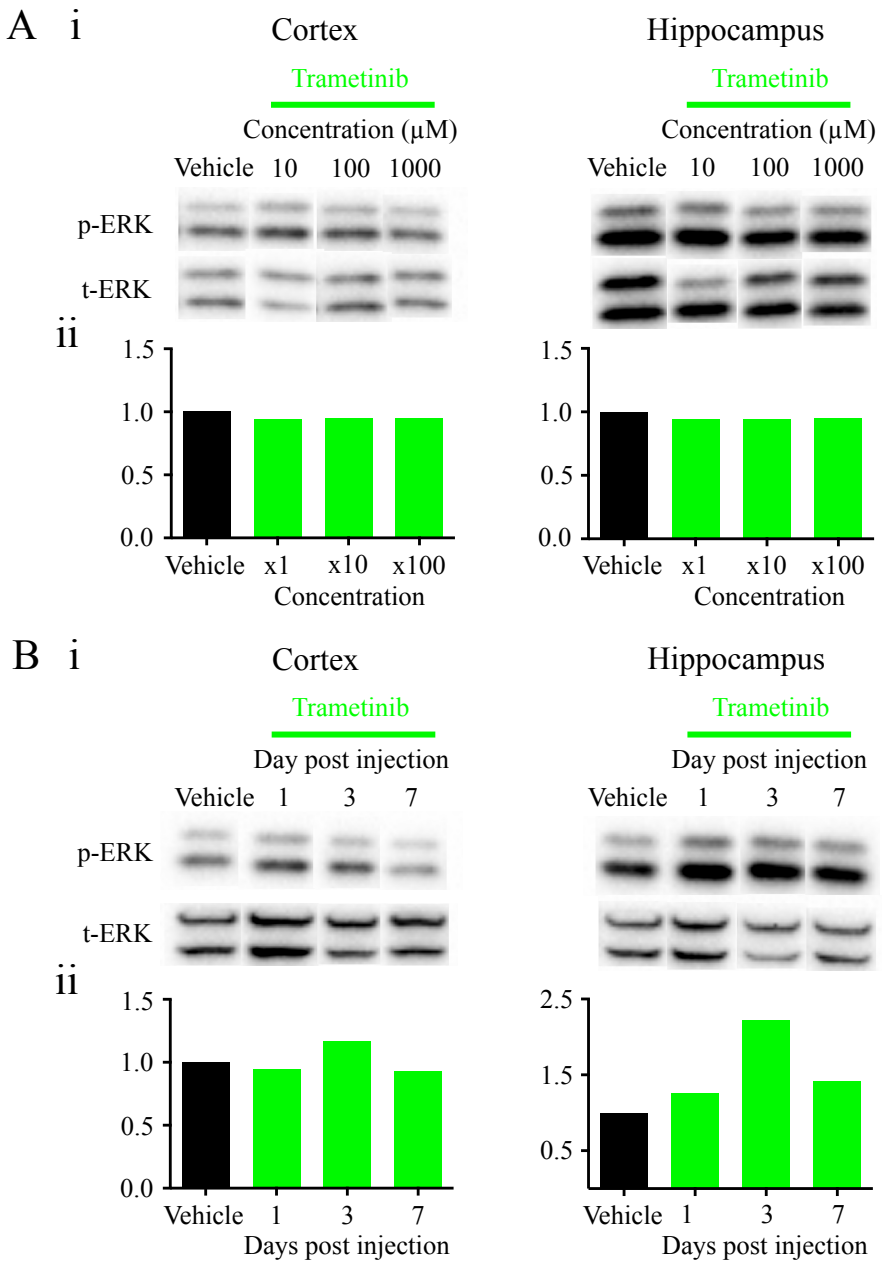

Figure 5.11. Injecting Trametinib intracerebroventricularly at a range of concentrations is ineffective at reducing p-ERK levels in the brains of wild type 4 month old mice, regardless of the duration between injection and p-ERK measurement. (A) When taken 24 hours after injection, 1.5mg/kg Trametinib failed to change p-ERK levels in the cortex or hippocampus (i) Western blot images of p-ERK and t-ERK from cortex and hippocampal (ii) Graphical representation of this (B) When 1.5mg/kg of Trametinib was injected intracerebroventricularly, and mice killed for analysis of cortex and hippocampus tissue to ascertain p-ERK levels, no change in p-ERK levels were observed in the cortex or injected mice at any time point, but an increase in p-ERK levels was observed in the hippocampus of injected mice, peaking at 3 days post injection (i) Western blot images of p-ERK and t-ERK levels in the hippocampus and cortex (ii) graphical representation of this.

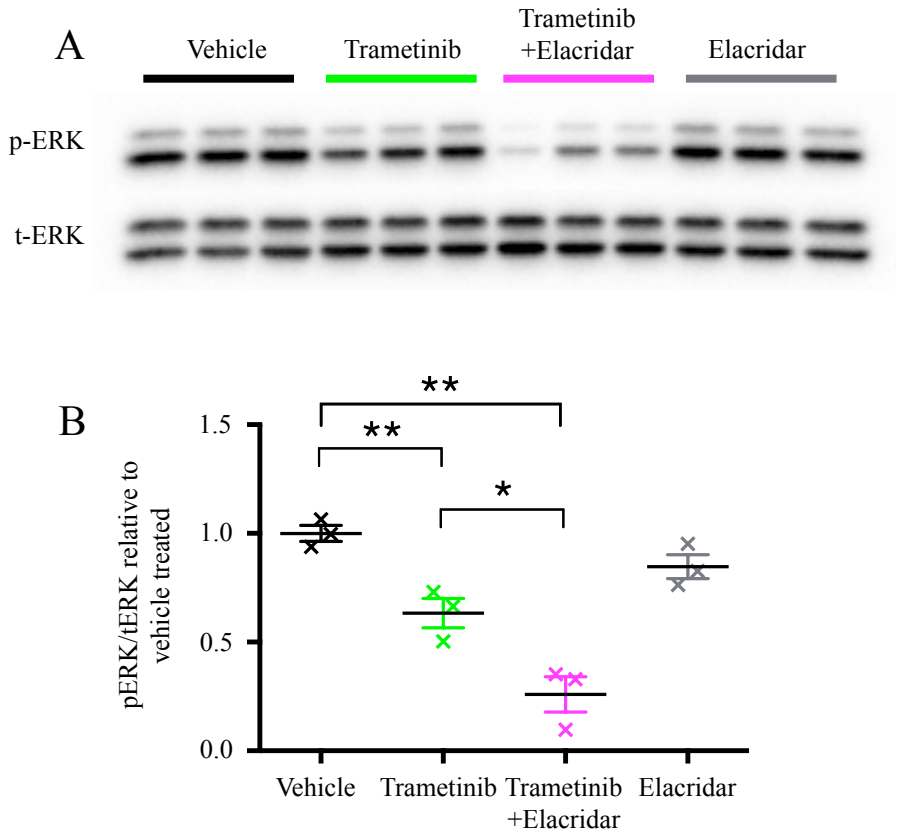

Figure 5.12. Co-administration of the P-gp inhibitor Elacridar with Trametinib increases brain MEK inhibition. 4-month old C57BL-6 mice were given either 5mg/kg oral Trametinib, 10mg/kg intraperitoneal Elacridar, both, or oral and intraperitoneal administration of the vehicles without any drug, with mice killed for analysis 5 hours after the Trametinib injection. Whilst Trametinib showed a significant decrease in p-ERK levels, when combined with the P-gp inhibitor Elacridar the reduction in p-ERK levels was greatly increased (A) Western blot images of p-ERK and t-ERK from the hippocampus of treated mice (B) Graphical representation of this. Data shown is the mean +/- SEM. Student's t-test * $p<0.05$ ** $p<0.01$ *** $p<0.001$. n=3 mice.

Conclusion

Previous studies have identified that pharmacological inhibitors of the IIS cascade are effective at reducing neurodegeneration in models of acute neurodegeneration. With the IIS cascade being frequently upregulated in cancers, many drugs have already been developed to inhibit IIS signalling to treat cancers, with many of these already being approved for use in humans. We therefore hypothesised that these clinically approved IIS inhibitors could be repurposed to intervene in the neurodegenerative process and potentially ameliorate neurodegeneration in acute neurodegenerative diseases.

Testing two clinically approved IIS inhibitors, we found that whilst Trametinib and Dabrafenib were potent inhibitors of the IIS cascade in both astrocyte and neurons in culture, long term administration of Dabrafenib showed paradoxical activation of ERK1/2 signalling in cultures with no B-raf mutations. Therefore we chose only to investigate our hypotheses with Trametinib.

Neuronal cell loss in our *in vitro* model of acute neurodegenerative disease was reduced by the application of Trametinib to cultures at the time of the hypoxia. This reduction in cell loss was accompanied by a reduction in CC3 signal, implying that apoptosis was similarly reduced by Trametinib treatment. We also hypothesised however that the endogenous astrocyte *Igf1* increase observed in these cultures following hypoxia, would be reduced by the neuroprotection of Trametinib. This was not the case however, with an increase in astrocyte *Igf1* expression in these cultures even under normoxic conditions. This raised the possibility that the *Igf1* induced neuronal cell death observed in chapter 4, could be limiting the neuroprotection of Trametinib. When Trametinib was applied at the same time as knocking down *Igf1* expression using siRNA however, no increase in neuroprotection was observed compared to those treated with Trametinib alone, implying that the Trametinib neuroprotection, and anti-*Igf1* neuroprotection are not additive.

With Trametinib showing proof of principle that it could ameliorate neurodegeneration, we then showed that Trametinib could be administered orally to decrease p-ERK levels in the brain. For Trametinib to be effective in the brain, inhibition of the efflux transporter P-gp with the co-administration of the P-gp inhibitor Elacridar at the same time as Trametinib administration was required. Combining these drugs lead to a potent reduction in p-ERK

levels in the hippocampus of wild type treated mice. With this successful inhibition of the IIS cascade in the brains of wild type mice, we are now in a position to apply this co-administration approach to mice modelling acute neurodegenerative disorders, to fully test our central hypothesis, that IIS inhibitors can be repurposed to provide neuroprotection in acute neurodegenerative diseases.

Chapter 6

Discussion

In this thesis I have investigated the therapeutic potential of modulating the IIS cascade in the brain in neurodegenerative diseases. Neurodegenerative diseases are a leading cause of mortality and disability in developed nations, and despite the variable pathologies of this group of diseases, they have a unifying factor – the irretrievable loss of neurons in the brain.

The IIS cascade is a molecular pathway able to modulate the rate of ageing in a range of organisms (Harrison et al., 2009; Holzenberger et al., 2003; Kenyon et al., 1993; Slack et al., 2015; Tatar et al., 2001), as well as modulate the progression of neurodegenerative diseases in experimental animals (Cohen et al., 2006; Cohen et al., 2009; Cooper et al., 2015). Endogenous changes in the IIS cascade have been observed in various neurodegenerative diseases (Bondy and Lee, 1993; Ferrer et al., 2001; Steen et al., 2005; Talbot et al., 2012). Furthermore, increased signalling at ERK1/2 has been implicated as a neuronal cell death mechanism, and has been observed in diseased neurons in the human neurodegenerative brain (Alessandrini et al., 1999; Almeida et al., 2005; Lu et al., 2008; Luo and DeFranco, 2006; Pei et al., 2002; Perry et al., 1999; Subramaniam et al., 2005; Zhu et al., 2002). This cascade therefore seems uniquely poised as a target to intervene in the neurodegenerative process. We have therefore investigated the feasibility of modulating this cascade for therapeutic benefit.

Targeting the IIS cascade has previously shown promising results, with the administration of IIS inhibitors decreasing infarct size in animal models of stroke and rescuing memory deficits in a mouse model of AD (Echeverria et al., 2009; Gladbach et al., 2014), and the overexpression of human *IGF1* in astrocytes leading to less neuronal cell death in a mouse model of TBI (Madathil et al., 2013). Whilst these results show promise, no IIS inhibitors have been taken to clinical trial for treating neurodegenerative diseases. Key questions need to be addressed in order to fully

exploit the possible therapeutic potential of targeting the IIS cascade to treat neurodegeneration.

We have focused on three areas demarcated into three results chapters addressing different questions about IIS modulation in neurodegeneration. Firstly, with the loss of neurons in chronic neurodegenerative diseases spanning years, to address the question of when IIS modulation would be most suitable as an approach to treat neurodegeneration in chronic neurodegenerative diseases, we characterised endogenous IIS changes in relation to different pathological components of AD. Chapter 3 therefore focused on characterising changes in the IIS cascade in mouse models of AD that model different disease components, and crucially occur at different times in the disease.

Secondly, although an overexpression of human *IGF1* in astrocytes has been shown to be neuroprotective following an acute neurodegenerative insult (Madathil et al., 2013), how the endogenous increase in astrocyte IGF1 effects neuronal cell death has never been considered. This is an important question, as this endogenous IGF1 increase is observed in multiple neurodegenerative diseases, and therefore seems to be a feature of neurodegenerative disease itself. Chapter 4 therefore addressed the endogenous *Igf1* response and its role in neuronal cell death, using a novel bilaminar co-culture model of acute neurodegeneration, and considers whether these phenomena could be exploited for novel therapeutic gain.

Finally in chapter 5, with experimental IIS inhibitors showing neuroprotective properties in mouse models of stroke, we investigate the repurposing of already clinically approved IIS inhibiting drugs to treat acute neurodegenerative diseases. This was done by establishing the suitability and practicality of using Trametinib to inhibit the IIS cascade in the mammalian brain, and also by testing the proof of principle in our *in vitro* model of acute neurodegeneration. By investigating these topics we have furthered the possible exploitation of the IIS cascade as a novel therapeutic target for improved therapeutic intervention in neurodegenerative diseases.

Endogenous changes in the IIS cascade in AD

To characterise IIS changes at different pathological stages of the chronic neurodegenerative disease AD in chapter 3, we examined changes in expression of *Igf1* and *IGF1,* and levels of phosphorylation at the activating phosphorylation sites of Akt and ERK1/2 (pS-Akt, pT-Akt, and p-ERK), in brain tissue from different aged APP-KI and TG4510 mice, and a preliminary investigation of human brain tissue. This allowed us to examine how IIS was changed in response to various pathological components of AD, that being rising amyloid beta and plaque levels in the APP-KI mice, rising phosphorylated tau and tau tangles in the TG4510 mice, and the very end stage of AD pathology with both advanced tau pathology and advanced amyloid pathology, in the post mortem human brain tissue.

This characterisation identified 3 different points in AD pathology where IIS was differently altered. In 2-month old APP-KI mice where amyloid pathology was limited to increased $A\beta_{40}$ and $A\beta_{42}$ levels and the very first detectable small amyloid plaques, substantial increases in Akt and ERK1/2 phosphorylation was observed, with over a ten times increase in p-ERK level in APP-KI cortical tissue. In the TG4510 hippocampus, Akt phosphorylation was decreased during both early tau pathology (hyperphosphorylated tau and tau pretangles), and very late stage tau pathology (tau tangles and substantial neuronal cell loss), albeit this reduction in phosphorylation was at pS-Akt in early, and pT-Akt in late tau pathology. Furthermore p-ERK levels were also increased in early tau pathology. Thirdly an increase at pT-Akt was observed in only fAD frontal cortex brain samples, but not sAD samples. Finally *Igf1* expression was increased in late stage tau pathology, as well as early and late (but not intermediate) amyloid pathology.

Timings of therapeutic IIS intervention in AD pathogenesis

The overall aim of characterising IIS during AD pathogenesis was to establish an appropriate time for therapeutic IIS modulation. It is useful to know that the majority of endogenous changes in the IIS cascade in AD pathogenesis occur at a very early

time point in both amyloid and tau pathological development, with limited changes in more advanced stages of pathology, including in human post mortem tissue. This would suggest that using IIS modulators at later stages of disease development would not be counteracted by endogenous IIS changes during disease development. However there is an indication of acquired IIS resistance in the APP-KI tissue could affect the efficacy of IIS interventions.

With *Igf1* increased in 2-month and 8-month tissue in the cortex of APP-KI mice, but p-ERK and pS-Akt levels only increased at 2-month, it seems that *Igf1* increases downstream IIS signalling in 2-month tissue but not in 8-month. This could be evidence of induced Igf1 insensitivity in the APP-KI mouse brain. Furthermore, the reduction in Akt phosphorylation in late stage TG4510 tissue, when *Igf1* expression was greatly increased, also suggests that this tissue may be insensitive to Igf1. This insensitivity would fit with human findings of an IGF1 resistant brain state (Talbot et al., 2012). However to verify this indication of acquired IIS insensitivity, as mentioned in chapter 3, an examination of downstream IIS gene expression should be undertaken, as well as possibly carrying *ex vivo* stimulation as was the case in human brain tissue (Bomfim et al., 2012). Overall it seems distinctly possible that APP-KI and TG4510 mice develop an Igf1 resistant brain state. Therefore when testing IIS modulators in AD, we must be vigilant of the possibility of acquired IIS resistance potentially limiting the efficacy of our treatments.

It would be interesting to investigate further the strong IIS change with the earliest amyloid pathology development, as if this IIS change impacts on disease progression, it could represent a novel site of disease intervention.

Phosphorylated ERK1/2 in AD

Our characterisation of IIS in different pathological stages of AD has also allowed us to examine the link between raised ERK1/2 phosphorylation and neuronal cell death. With previous literature implying raised p-ERK was associated with neuronal cell death signals, and increased p-ERK staining being shown in the neurons of the human

AD brain that contained tau tangles (Pei et al., 2002), we expected to observe increased p-ERK in tissue where neuronal cell death was occurring, primarily therefore TG4510 tissue and human AD tissue.

An increase in p-ERK was observed in 2.5-month TG4510 tissue, and a substantial 10 times increase was present in APP-KI tissue from the earliest beginnings of amyloid pathology. With no observable increase in neuronal cell death in the APP-KI model, it is highly unlikely that this increased p-ERK is associated with neuronal cell death. Similarly there is limited neuronal cell death at 2.5 months in TG4510 mice, especially compared to 8-month TG4510 tissue where no change in p-ERK level was observed. With no detectable difference in p-ERK levels in older TG4510 or human AD tissue, our data suggests that there is no increase in p-ERK levels during neuronal cell death, but there are earlier increases in p-ERK level that are likely not associated with neuronal cell death.

This is contrary to previous data suggesting increased p-ERK in tangle containing neurons in human AD (Pei et al., 2002), and data suggesting a role for increased p-ERK in neuronal cell death (Chen et al., 2009; Luo and DeFranco, 2006). This could be due to our detection method, western blotting, not being as sensitive as the immunohistochemistry employed in the previous study (Pei et al., 2002). Therefore whilst our evidence suggests no significant increase in p-ERK levels at times of neuronal cell loss, we would like to confirm this using immunohistochemistry in our tissue to investigate whether more subtle changes have occurred. However the clear change in young APP-KI tissue suggests that raised brain p-ERK levels are not always indicative of neuronal cell death.

One possible implication of the increased p-ERK observed in the 2-month APP-KI brain, is the role of ERK1/2 as a tau kinase. Increased $A\beta_{42}$ levels and amyloid plaques precede AD associated tau pathology in human AD, but what causes amyloid pathology to progress to tau hyperphosphorylation and tau tangles is unclear. With observations of increased p-ERK in tangle containing neurons in human AD (Pei et al., 2002), and it seeming that early amyloid pathology substantially increased p-ERK levels in our data, amyloid induced p-ERK increase could provide a link in the pathological progression of AD. With the beginnings of tau pathology in AD

occurring at a more advanced stage of amyloid pathology however, with plaques present, and the lack of increased p-ERK signal in later ages of APP-KI mice with more advanced plaque deposition, it seems unlikely that the increase in p-ERK levels observed in 2 month old APP-KI mice is responsible for initiating tau pathology. Furthermore, no increase in p-Tau levels were observed in characterisations of this mouse line (Saito et al., 2014). However, given the observation of increased p-Tau in other amyloid pathology mice (Howlett et al., 2008), perhaps if APP-KI mice are examined at an older age increased p-Tau may also be present.

Igf1 increase in AD

In both APP-KI and TG4510 mouse models, *Igf1* expression increased as the pathological components of the disease also increased, however no increase was observed in moderate pathology in 4-month APP-KI mice. This increased *Igf1* expression was corroborated by significantly higher levels of *Igf1* expression as shown from online databases of gene changes in multiple other mouse models of pathological components of AD, with *Igf1* being one of the most significantly increased genes in its expression compared to wild type mice (Matarin et al., 2015). Our work therefore corroborates raised astrocyte *Igf1* expression being a feature of the chronic neurodegenerative disease AD.

Consideration of whole tissue analysis and future experiments

The primary question addressed in this section was how IIS changes in the brain during AD pathogenesis. We addressed this question with techniques using whole brain lysates –western blotting and RT-qPCR. Whilst this is a useful way of examining this tissue for changes in gene expression and protein levels, the brain is composed of various cell types that will all contribute to the overall signal measured by whole lysate techniques. This cellular heterogeneity needs careful consideration in order to sensibly view our findings.

The overall signal measured by whole brain lysate techniques is contributed to by all cell types in the brain, with each cell type contributing a certain proportion to the signal based on the abundance of these cells and expression levels of genes in different cell types. Crucially, in neurodegeneration the relative proportion of these cells changes. For example the neuronal proportion is reduced from neurodegeneration, and the glial proportion increased by astrogliosis and microgliosis. Therefore whilst gene expression or protein level changes may be observed between our AD samples and wild type or non-diseased samples, in which cell types these changes occur is impossible to ascertain with the techniques we have used. Whether these changes represent true changes or rather are a product of a change in brain sample cell type proportions also means making firm assertions based solely on whole tissue lysate data hazardous. It is also very possible that significant changes in one cell type population may be offset by the opposing changes in another cell type population, and are therefore unobservable by these techniques.

To overcome these limitations, and allow us a more detailed investigation of individual cell type IIS changes in response to AD pathology, future experiments should be carried out. Firstly our western blot and RT-qPCR data could be normalised by neuronal, astrocyte, or microglial markers, to allow relative changes to specific cell types to be appreciated. Careful consideration of the markers would be needed however, utilising new identification of markers with greater specificity (Zhang et al., 2014). This should also be accompanied by immunohistochemistry replicating our western blot data, which would allow us to observe the cell types in question that changes occur in. Unfortunately this was not possible with the preparations of mouse and human tissue that we had available at the time of this thesis. Whilst flow cytometry may be a possible technique to separate changes in specific cell types, the cell separation phase of this technique may loose crucial data due to the extensive projections of the cell types in question. With these cell type specific experiments, a more detailed conclusion can be made about endogenous IIS changes in response to changing AD pathology.

Endogenously raised IGF1 in neurodegenerative disease

We directly tested the contribution of endogenous increases in *Igf1* on acute neurodegeneration by developing an *in vitro* model of acute neurodegeneration. This model showed progressive neuronal cell loss following a noxious insult, accompanied by an increase in astrocyte *Igf1* level. By comparing cultures with *Igf1* knocked down to those where *Igf1* increased following the hypoxic incident, allowed us to investigate the contribution of *Igf1* increases on neurodegeneration and IIS signalling in both astrocytes and neurons.

Astrocyte Igf1 contributes to neuronal cell death in acute neurodegeneration

We identified that cultures with *Igf1* knocked down showed less neuronal cell death following a hypoxic incident than cultures where astrocyte *Igf1* increased post hypoxia. This implies that the increased astrocyte *Igf1* following the hypoxic insult contributes to neuronal cell loss. This is unexpected given the Madathil *et al* overexpression findings, and would add an extra dimension to the dose response relationship between administered IGF1 concentration and neuroprotective effect seen in other papers, and emphasises the need to characterise endogenous changes (Madathil et al., 2013). To confirm this surprising result, we should carry out further control experiments to test this finding further.

Crucially a recovery experiment should be performed, whereby *Igf1* knock down is carried out, but a suitable concentration of Igf1 added to the media. If neuronal cell loss similar to noncoding-siRNA treated cultures was observed, then this would add substantial weight to our unusual finding. It would also be useful to repeat our experiment with either another siRNA against *Igf1,* or the addition of an Igf1R antibody to outcompete the binding of Igf1 to its receptor, in effect having the same effect as knocking down *Igf1*. By carrying out these further experiments, our unusual finding can be tested fully.

Our observation of the role of astrocyte *Igf1* in neuronal cell health is not as simple as it being neurotoxic however. *Igf1* knocked down cultures had fewer neurons under normoxic conditions, implying that a level of baseline astrocyte *Igf1* expression is required for neuronal cell maintenance. This would make the conversion of the observed neuroprotective effect to a clinically applicable intervention more complex, as evidently the degree of *Igf1* reduction is crucial to its effects on neurons.

Mechanism of Igf1 induced neurotoxicity

Whilst astrocyte *Igf1* increase seemed to signal to neurons as shown by the association between astrocyte *Igf1* increase and neuronal p-ERK increase, no significant increase in p-ERK or pS-Akt was observed in neurons following hypoxia. *Igf1* knockdown similarly did not affect p-ERK levels in neurons. Therefore the *Igf1* dependant neuronal cell death observed is unlikely to be via signalling through the IIS cascade.

We suspected this could be because *Igf1* is signalling in an autocrine manner to astrocytes, rather than in a paracrine fashion to neurons. In this circumstance I refer to autocrine as signalling amongst astrocytes or the single astrocyte that is increasing its expression of *Igf1* signalling solely to itself, whereas paracrine is signalling to another cell type, in this case neurons. p-ERK and pS-Akt levels not only did not change in astrocytes following an increase in *Igf1* expression, but any change did not correlate with *Igf1* increase. This strongly suggests that the increased *Igf1* expression in astrocytes does not signal through the IIS cascade to astrocytes, but does to neurons albeit weakly.

How astrocyte *Igf1* signals to neurons to cause neuronal cell death, whilst not doing so via IIS signalling, is unclear. One possibility is that we are missing changes in p-ERK or pS-Akt levels with the time points we picked, as Subramaniam *et al* showed early IGF1 supplementation caused an early increase in p-ERK after 15 minutes that was not present at later times, accompanied by increased pS-Akt 24 hours after injury and IGF1 addition (Subramaniam et al., 2005). However, these experiments applied

high levels of IGF1 immediately at the point of injury, whereas endogenously we do not observe *Igf1* increase until 72 hours post insult. Nonetheless it may be interesting to investigate earlier time points for IIS levels in our cultures.

It is also a possibility that Igf1 is not signalling via the IIS cascade. Our focus on the IIS cascade as the mediator of IGF1's effect on cells comes from the assumption that it signals via IGF1R. Hybrid IGF1R/insulin receptors exist, composed of a heterodimer of one IGF1R subunit and one insulin receptor subunit, and some are preferentially activated by IGF1 (Slaaby, 2015), however the formation of these in the brain and their physiological function is unknown. Furthermore IGF1 has also been shown to signal via other non-IIS means such as via Janus kinases (Gual et al., 1998), and c-Abl kinase (Genua et al., 2009). This furthers the possibility that IGF1 induced neuronal cell death is through non-IIS based mechanisms, making its exploitation as a neuroprotective options more difficult.

Furthermore whilst astrocyte Igf1 seems to signal only weakly through the IIS cascade to neurons and astrocytes, this may not be the case in the brain where far more cell types exist. With Igf1 being a proliferative factor, and microglial proliferating in cases of brain injury (Perry and Holmes, 2014), Igf1 increase could drive the proliferation of microglia. This would not explain the neurotoxic effects of *Igf1* increase in our model, but suggests that raised *Igf1* may have more physiological roles in neurodegeneration than was possible to observe in our *in vitro* model.

It is also very likely that Igf1 is not the only factor released from astrocytes in response to neuronal cell damage, but is a single factor in a whole milieu of chemokines and cytokines released in response to stress. It therefore seems that whilst we are modulating only one of these factors, that others may be responsible for or contribute to the neuronal cell loss observed, and that Igf1 in some way compounds this effect via non-IIS based means. Similarly we have been considering Igf1 change solely from its influence on p-ERK levels and its effect on neuronal cell death. Igf1 is implicated in many other neuronal functions, including synaptic function and plasticity in the adult brain (Llorens-Martin et al., 2009). Various studies have identified its effects of modifying neuronal excitation and synaptic transmission (Cao et al., 2011; Gazit et al., 2016), so whilst we were interested in Igf1's role in

neurodegeneration, it is clear that its physiological function in the brain is more complex than this.

Therefore it seems that increased IGF1 in acute neurodegenerative diseases could be contributing to neuronal cell death, but is not doing so via p-ERK dependant mechanisms. Further research is required to elucidate this observed phenomenon further before any firm conclusions can be made.

Trametinib as a repurposable IIS inhibitor for acute neurodegeneration

Despite increased IIS induced neuronal cell death seeming not to be present in our *in vitro* model of acute neuronal degeneration, abundant evidence exists that reducing IIS is neuroprotective in neurodegeneration. In particular, pharmacological application of IIS inhibitors to animal models of disease has been neuroprotective (Ashabi et al., 2013; Echeverria et al., 2009; Gladbach et al., 2014), yet the progression of these results to clinical trials has not yet taken place. We therefore investigated the neuroprotective effects of the already clinically approved drugs Trametinib and Dabrafenib, and the efficacy of using these drugs to inhibit the IIS cascade in the mammalian brain.

Identifying a suitable IIS inhibitor

Previous studies had indicated that Dabrafenib treatment to cells containing wild type as opposed to cells with a V600E B-raf mutation, might paradoxically lead to an increase in signalling through the Ras-Raf-ERK pathway (Anforth et al., 2012; Hatzivassiliou et al., 2010; Poulikakos et al., 2010). When testing Dabrafenib in primary astrocyte cultures, we found that ERK2 levels were in fact increased when Dabrafenib was repeatedly applied every 2 days for a week. With our aim being to investigate IIS inhibition this made Dabrafenib unsuitable for further investigation of our hypothesis. Trametinib on the other hand, proved effective at potently reducing p-ERK levels in primary neurons and astrocytes, and also had no toxic effects on *ex*

vivo organotypic brain slices when applied for 2 weeks. Trametinib was therefore used for testing our hypothesis.

Trametinib as a neuroprotective drug

When applied to our *in vitro* model of acute neurodegeneration, Trametinib reduced neuronal cell death following a hypoxic insult, indicating that inhibiting IIS with Trametinib is neuroprotective. Furthermore levels of apoptosis measured by CC3 were also reduced with Trametinib administration, indicating it is protective against apoptosis. This is interesting, as the neuronal cell death in our *in vitro* model was not accompanied by increased p-ERK levels, and therefore very unlikely to be p-ERK dependant. This is similarly shown in lifespan extension experiments, where reduced IIS leads to longer lifespans in a variety of organisms. The cause of death in these animals is not due to increased IIS, but rather it seems reducing IIS conveys a pro-health effect. It is highly likely therefore that this is also the case with Trametinib administration, where the neuroprotection is not by blocking p-ERK dependant neuronal cell death, but by a pro-health effect as a consequence of reduced p-ERK.

Based on this evidence of neuroprotection *in vitro,* we investigated the ability of Trametinib to inhibit IIS in the mammalian brain, for the eventual testing of neuroprotection in mouse models of neurodegeneration.

Trametinib use in the mammalian brain

Trametinib applied intracerebroventricularly (ICV) to the brain of wild type mice did not result in p-ERK reduction. Previous studies suggest that the efflux transporter P-glycoprotein (P-gp) limits the brain bioavailability of Trametinib (Vaidhyanathan et al., 2014; Vaidhyanathan et al., 2016). We therefore co-administered the P-gp inhibitor Elacridar with Trametinib in wild type mice, and found that p-ERK levels were substantially decreased in the brain. We did also see reductions with Trametinib treatment alone in these experiments, albeit smaller reductions than when combined

with Elacridar. In this experiment we examined p-ERK levels in the brain 3 hours after administration, rather than 24 hours at the earliest in the ICV experiments. Despite this, the greater brain p-ERK reduction when Trametinib was co-administered with Elacridar suggests that P-gp was limiting the brain bioavailability of Trametinib, but that P-gp does not fully prevent Trametinib's effect in the brain when measured a short duration after administration.

These results suggest that Trametinib has the potential to potently inhibit the IIS cascade in the brain, however it appears necessary to co-administer it with Elacridar to improve its brain bioavailability. As we were aiming to investigate the most clinically applicable use of IIS inhibitors to ameliorate neurodegeneration, we endeavoured to avoid co-administering a non-clinically available drug with Trametinib (Elacridar has been tested at phase I trial but no further (Kuppens et al., 2007)).

Mechanisms of IIS related cell death in acute neurodegeneration

Our findings have indicated that both reducing p-ERK levels and the astrocyte *Igf1* increase are neuroprotective in a cellular model of acute neurodegeneration. Not only do these data indicate a role of these factors in neuronal cell death, but they allow a mechanistic insight into how IIS may be implicated in neuronal cell death.

The role and interaction of phosphorylated ERK1/2 and raised Igf1 expression in neurodegeneration

Increased p-ERK levels have been implicated in neuronal cell death (Chen et al., 2009; Luo and DeFranco, 2006). IGF1 is a potent activator of the IIS cascade, in particular leading to increased p-ERK, and has been observed in acute neurodegeneration (Beilharz et al., 1998; Li et al., 1998; Madathil et al., 2010; Nieto-Sampedro et al., 1982). To investigate the trio of neuronal p-ERK increase, astrocytic *Igf1* increase, and neurodegeneration in acute neurodegenerative diseases, and the impact these factors have on one another, we manipulated the *Igf1* and p-ERK levels

in a culture model of neurodegeneration (figure 6.1). Put simply, by altering p-ERK and *Igf1* levels, we could address the question: does astrocyte *Igf1* increase cause neurodegeneration by increasing p-ERK levels?

Following a hypoxic insult in our culture model, *Igf1* expression increased in astrocytes, but p-ERK levels did not significantly increase in neurons. Whilst this change in astrocyte *Igf1* expression did correlate with neuronal p-ERK levels, the effect was weak; meaning only small increases in p-ERK resulted from substantial astrocyte *Igf1* expression increase. This correlation between astrocyte *Igf1* expression and neuronal p-ERK levels did not hold true when *Igf1* was prevented from increasing by knocking down *Igf1* using siRNA, with large increases in p-ERK levels still possible under low *Igf1* conditions. Furthermore, changes in neuronal p-ERK levels in hypoxia exposed siRNA treated cultures correlated very well with the level of neuronal cell death, suggesting that neuronal p-ERK level is still related to neuronal cell death level; even when neuronal death is reduced by knocking down *Igf1*. This heavily implies that the *Igf1* caused neuronal cell death is not dependant upon *Igf1* increasing p-ERK levels in neurons.

When p-ERK levels were lowered by Trametinib treatment, neuronal loss was reduced, but there was an increase in astrocyte *Igf1* expression (figure 6.1). Although we showed astrocyte *Igf1* expression levels were associated with neuronal cell death, this increased *Igf1* expression in Trametinib treated cultures was shown to not limit the neuroprotective effect of Trametinib, as shown by our combination of Trametinib with *Igf1* knockdown showing comparable levels of neuroprotection.

This suggests a detachment of the effects that neuronal p-ERK levels and astrocyte *Igf1* levels have on neuronal cell death, whereby decreased *Igf1* may lead to neuroprotection, but does not do so by lowering p-ERK levels. Increased neuronal p-ERK levels due to increased *Igf1* expression cannot therefore be the mechanism of action of the *Igf1* knockdown neuroprotective effect, meaning that other mechanisms must be responsible. This does show though, that reducing *Igf1* expression levels is not a sensible way of modulating neuronal p-ERK levels in an attempt to prevent p-ERK dependant neurodegeneration, meaning if p-ERK reduction is to be investigated

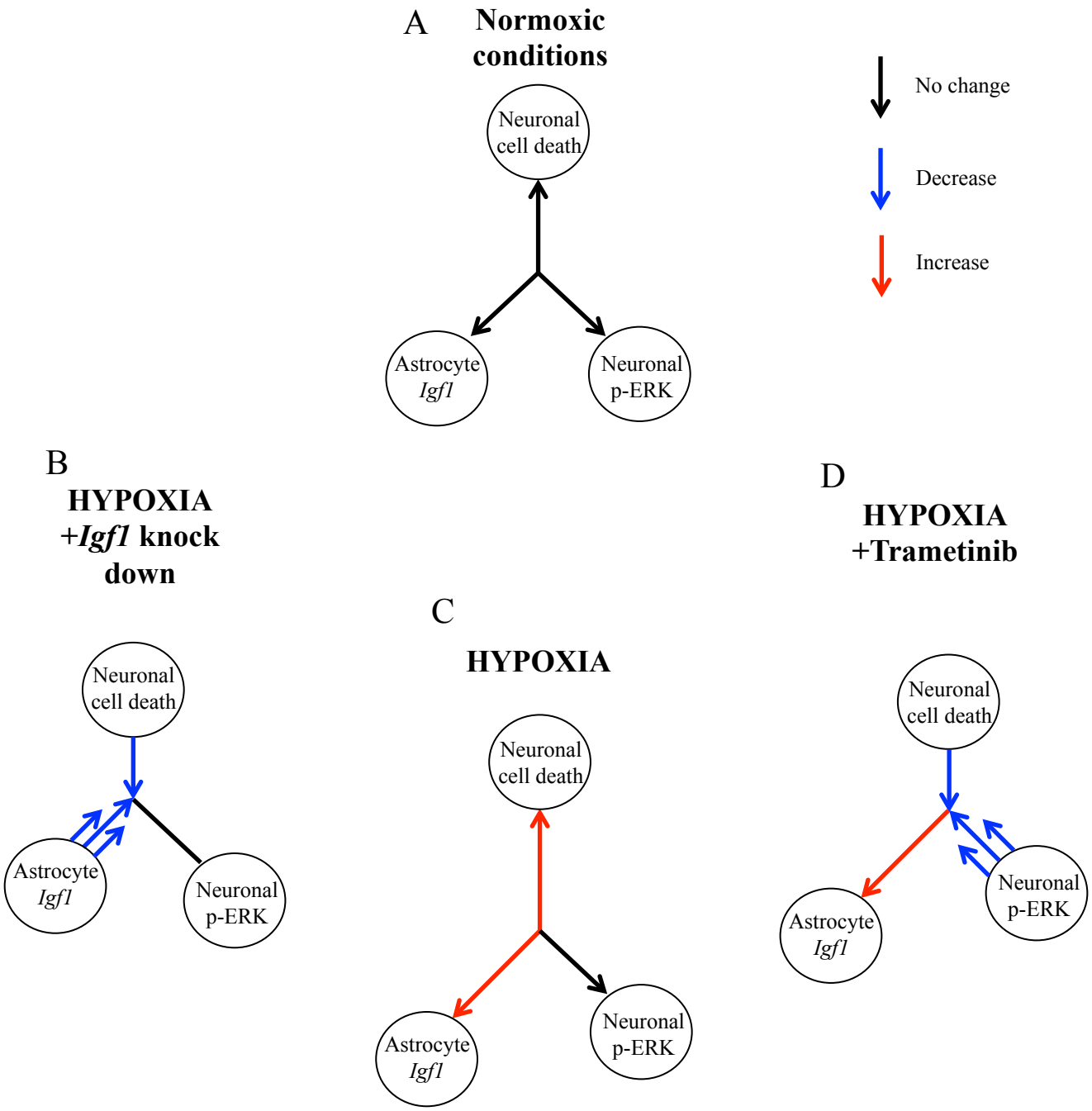

Figure 6.1. The relationship between astrocyte *Igf1* expression, neuronal p-ERK level, and neuronal cell death, under our experimental conditions. By modulating astrocyte *Igf1* increase and p-ERK levels in cultures during hypoxia, we were able to investigate the relationship between these factors and neuronal cell death. Whilst both neuronal p-ERK and astrocyte *Igf1* when reduced are neuroprotective, *Igf1* knockdown is not neuroprotective via reducing p-ERK levels. (A) Levels under normoxic conditions (B) Hypoxia and *Igf1* knock down (C) Hypoxia alone (D) Hypoxia with Trametinib administration. Black lines = no change, red lines = increase, blue lines = decrease.

as a neuroprotective mechanism, it has do done so through a more direct route, like Trametinib administration.

The weak correlation between astrocyte *Igf1* expression and neuronal p-ERK levels under hypoxic non-treated conditions could be a problem with our *in vitro* model however. Whilst it was possible to plate neuronal cultures at 500,000 neurons/cm^3, it was only possible to plate astrocytes at 120,000/cm^3. This imposes another difference between physiological conditions and our cell cultures therefore, as the proportion of astrocytes to neurons is higher *in vivo* than we could achieve *in vitro*. This could affect the relationship between the *Igf1* increase we observe in astrocytes and the change in p-ERK levels in neurons, as the change in *Igf1* level we see in astrocytes is relative, and therefore the actual protein amount that is released from the astrocyte layer is dependent upon the amount of astrocytes.

The potential for IIS inhibitors to treat neurodegeneration

IIS seems to be endogenously changed in acute and chronic neurodegenerative diseases, and IIS inhibition seems to be beneficial in both, indicating that the IIS cascade plays a key role in the neurodegenerative process. This has led us and others to suspect that the IIS cascade could be targeted to provide therapeutic gain to these diseases. Whilst the central tenant of both acute and chronic neurodegenerative diseases is undoubtedly the loss of neurons, the time frame that this happens over is very different. This time frame of neurodegeneration crucially effects how we can approach treatment in these diseases, as factors such as side effects of intervention, the endogenous IIS state of the brain, and the patient group, will differ between these two groups, and therefore effect the suitability of different approaches to treating these diseases. We must consider how our results combined with previous findings, affect the appropriateness of targeting the IIS cascade for therapeutic gain, and how it would be best to move forward with utilising this pathway in these diseases.

The appropriateness of our in vitro model of neurodegenerative disease

Using our previously described bilaminar co-culture model we developed an *in vitro* model of acute neurodegenerative disease. Using this model we identified acute *Igf1* increase as a contributing factor to neuronal cell loss, and also established that Trametinib application was neuroprotective. To move forward with these promising findings we must consider how applicable our model of acute neurodegenerative disease is.

The benefits of a model such as this are many, the most substantial of which is the ability to test our hypotheses about IIS and neurodegeneration in cell culture models before progressing to animal models. Our bilaminar co-cultures are also an improvement upon single cell cultures. In the brain neurons and astrocytes do not exist in isolation, but form contacts, interact, and influence each other during development, maturity, and in times of stress and disease. Therefore to study each cell type individually, whilst useful, ignored the interactions between cell types, and therefore limits the applicability to real life scenarios. To have both astrocytes and neurons in the same well therefore goes some way to replicate a more physiological scenario, however this model only accounts for 2 cell types of the brain, so is far from a complete *in vitro* model of the brain. Considering the involvement of microglia in neurodegeneration (Perry and Holmes, 2014), our bilaminar co-cultures should be viewed as an improved cellular model compared to single cell cultures, useful in particular for investigating interactions between neurons and astrocytes, but not a complete model of the brain.

The downsides of this model however are also plentiful. Astrocytes in our bilaminar co-cultures are likely to be very different from mature astrocytes in the brain. Whilst the neurons in primary neuronal cultures share many similarities with those found *in vivo*, such as morphological similarities, their capability of firing action potentials and undergoing complex cellular processes such as neural plasticity, similarities of this nature are less apparent in primary astrocyte cultures. The morphology of astrocyte in primary cultures is extraordinarily different from *in vivo,* with cultured astrocytes more similar to fibroblasts in size and shape than astrocytes. Also, perhaps most significantly, cultured cells are between 13 and 25 days old in our culture

experiments, and grown in a near 2D environment without the normal developmental cues that neurons microglia and the vasculature would provide. This all likely combines to give a young astrocyte phenotype, perhaps most similar to the developing nervous system, making interpreting changes in astrocyte physiology and number in our co-culture experiments difficult in relation to mature astrocyte *in vivo*.

These differences in astrocytes in culture does not undermine the benefit of their presence in our cultures however, as to begin to replicate physiological responses from neurons astrocytes must be present in proximity to them. This is especially evident in chapter 4, where to elicit the same kind of increase in *Igf1* expression that we see *in vivo* in astrocytes in response to damage, neurons must be present. This shows the benefit of a co-culture system, but to fully determine the role of Igf1 increase and Trametinib application on acute neurodegeneration, we must move towards animal models of these diseases.

IGF1 in chronic vs acute neurodegenerative diseases

Endogenous changes in the IIS cascade have been reported in both acute and chronic neurodegenerative diseases. These endogenous changes differ in different diseases, but with incomplete characterisation of IIS signalling levels in all neurodegenerative diseases, we are not in a position to conclusively say whether these differences are genuine or a consequence of sampling bias. Whilst some changes have been shown repeatedly, such as increased IGF1 levels, others such as increased p-ERK levels in neurons, have only been shown in a handful of diseases. Care must be taken not to over extrapolate these findings from one disease to many however.

We have shown that in our *in vitro* model of acute neurodegeneration, the increase in astrocyte *Igf1* contributes to neuronal cell death. This must not be interpreted as IGF1 increase in all neurodegenerative diseases contributing to neuronal cell death, as we cannot presume that the effects of a short term increase in astrocyte IGF1 is comparable to that observed in AD, where increased *IGF1* expression is presumably apparent for years. This is especially pertinent considering the well documented IIS

resistance in the chronic neurodegenerative disease AD (Talbot et al., 2012), suggesting that increased astrocyte IGF1 could have differing effects on IIS signalling and therefore pathology in chronic versus acute neurodegenerative diseases, despite its presence in both. Therefore whilst we showed in chapter 3 that *Igf1* expression increased in both mouse models of different pathological components of AD, we cannot then marry this with our findings in chapter 4 that raised *Igf1* expression in an acute model of neurodegeneration is neurotoxic. Therefore the implications of inhibiting *Igf1* increase, as a neuroprotective therapeutic strategy must currently only be considered with regard to acute neurodegenerative diseases until the role of raised IGF1 in chronic neurodegenerative diseases has been investigated directly.

With short term *Igf1* increase proving neurotoxic, and with acquired IIS resistance being demonstrated in human AD brain tissue, it could be that acquired IIS resistance is a protective mechanism of preventing a neurotoxic increase in signalling through the IIS cascade. Therefore the raised IGF1 observed in AD could be toxic, but is protected against by the acquired IIS resistance.

Inhibiting astrocyte Igf1 increase as a therapy in acute neurodegenerative disease

We have identified that *Igf1* increase during acute neurodegeneration may contribute to neuronal cell death. We established this by using siRNA to knock down *Igf1* mRNA, but this approach is not suitable for clinical application (Shim et al., 2012). Therefore not only should our next experiments attempt to block *Igf1* induced neuronal cell death in an animal model of acute neurodegeneration, but we should do so pharmacologically. Whilst a possible candidate for the pharmacological reduction of IGF1 increase is the IGF1R inhibitor Linsitinib, this is making the presumption that the neurotoxic affect of IGF1 is through the IGF1R, which given the lack of increase in ERK1/2 or Akt phosphorylation in our cultures is far from a certainty. To be able to investigate this further a suitable next step would be to apply Linsitinib to our *in vitro* model of neurodegeneration and attempt to replicate the neuroprotection we observed with *Igf1* knock down.

Given our evidence that knock down of *Igf1* under normoxic conditions was neurotoxic, to exploit the neuroprotection of preventing astrocyte *Igf1* increase whilst not lowering Igf1 signalling below normal levels may prove difficult. Another possible means of reducing this *Igf1* increase response would be to identify the molecular signal that leads to the increase. Given the necessity of neurons sharing the same media as astrocytes when the noxious stimulus is given, it would seem likely that the signal for astrocytes to increase *Igf1* expression is through a secreted factor from neurons. Therefore if the factor or factors responsible could be identified, this would provide alternative approaches to prevent the apparent Igf1 dependant neurotoxic effect in acute neurodegeneration.

Repurposing Trametinib as a neuroprotective agent

In our studies Trametinib has shown neuroprotective properties, and by combining its administration with the P-gp inhibitor Elacridar, we have shown that it has the capacity to reduce p-ERK levels in the brain. Whilst this means that we now have an approach where we can test the clinically available drug Trametinib in animal models of acute neurodegeneration to investigate the possibility of repurposing for these diseases, the use of the non-clinically approved drug Elacridar to achieve this would undoubtedly slow its progression to clinic if it proved efficacious.

With us proposing that Trametinib may be most suited to the treatment of acute neurodegenerative disorders, there is evidence to suggest that perhaps the Elacridar dependency may not be so severe in the chronic neurodegenerative disorder AD. Evidence showing a reduction in P-gp in mice modelling components of AD, AD patients, and indeed a reduction with age (Deo et al., 2014; Hartz et al., 2010; Silverberg et al., 2010; van Assema et al., 2012), gives hope that perhaps the necessity of Elacridar co-administered with IIS inhibitors may be less in sAD patients, and that Trametinib administration on its own may well be brain bioavailable in these patients. However, as discussed below, inhibiting IIS in chronic neurodegenerative diseases is more challenging than inhibiting IIS for acute neurodegenerative diseases. These P-gp

findings therefore are unlikely to impact on the repurposing of Trametinib without Elacridar to acute neurodegenerative diseases.

Side effects of IIS inhibition and the implications these have on repurposing

When repurposing a drug the new patient group must be stringently considered in order to ensure the drug is suitable. Inhibitors of the IIS cascade are predominantly used to treat cancers, with our drug of choice Trametinib specifically being used to treat metastatic melanoma. The side effects of Trametinib are many, and often serious. Essentially all patients taking combined Trametinib and Dabrafenib, or Trametinib as an individual treatment, experienced one clinically relevant adverse event during their course of treatment (Falchook et al., 2012; Infante et al., 2012; Robert et al., 2015). Of these events the most common in the combined therapy are pyrexia (53%) nausea (35%) and diarrhoea (32%), with skin rashes and dermatitis acneiform (49%) diarrhoea (34%) and peripheral oedema (26%) some of the most common events in solo drug treatment. Whilst these are undoubtedly unpleasant for the patients taking this medication, the high incidence of more serious events such as decreased heart ejection fraction (8%) and cutaneous squamous cell-carcinoma (1%) are far more concerning. Therefore the eventual repurposing of Trametinib in context of these side effects must be considered.

Symptoms such as these are far more acceptable as clinical outcomes in patients with terminal disorders such as metastatic melanoma, where the median survival from diagnosis is less than 1 year (Tsao et al., 2004). In chronic neurodegenerative disease patients where neuronal cell loss occurs over years, to elicit long-term neuroprotection Trametinib may be required to be administered for years to a patient. The side effects experienced from Trametinib would therefore be highly unlikely to be tolerable when administered for this duration, especially given the advanced age of the patient group. Unless a treatment regime could be devised to mitigate the majority of these side effects whilst maintaining the benefits, it seems unlikely that it would progress far as a neuroprotective agent for the long-term administration to chronic neurodegenerative disease patients. This is a problem experienced with many

discussions of life span extending therapies that target proliferative pathways such as IIS. Possible ways of maximising benefit whilst reducing harm would be by titrating the dose so that Trametinib proved efficacious at a suitably low dose to provide benefit with less side effects. Others would be regimes where Trametinib is administered at full dose for a short period of time before being withdrawn, with cycle repeated over a long period of time. This approach would be similar to an intermittent fasting paradigm that has conveyed many of the benefits of full fasting, but mitigated many of the side effects.

In acute neurodegenerative diseases however, the shorter duration of neuronal cell loss, and therefore shorter duration of required neuroprotection, would likely decrease the experienced side effects. This indicates that Trametinib administration would be suitable for repurposing to treat acute neurodegenerative diseases in humans. Stroke and TBI would therefore seem particularly well suited for the repurposing of Trametinib.

Alternative targets in the IIS cascade

Another possible way of avoiding the side effects of pharmacologically inhibiting the Ras-Raf-ERK cascade is to investigate the possibility of members of this pathway being more abundantly expressed, or exclusive expressed, in the brain as opposed to other tissues. This would allow the inhibition of these pathways to target neurodegeneration, whilst mitigating the substantial side effects of inhibiting this cascade elsewhere in the body. Identifying brain specific members of the cascade would therefore make therapeutic targeting of this pathway in neurodegenerative disease easier.

Using the Human Protein Atlas database to compile a list of genes that are expressed at a significantly higher level in brain tissue than other tissues (Uhlen et al., 2015), 381 genes were expressed at a level at least 5 times greater in the brain than all other tissues measured. Comparing this with a list of genes of proteins involved in MAPK signalling, identified 8 genes involved in MAPK signalling that were relatively overexpressed in the brain (figure 6.2). 7 of the 8 genes identified were too far

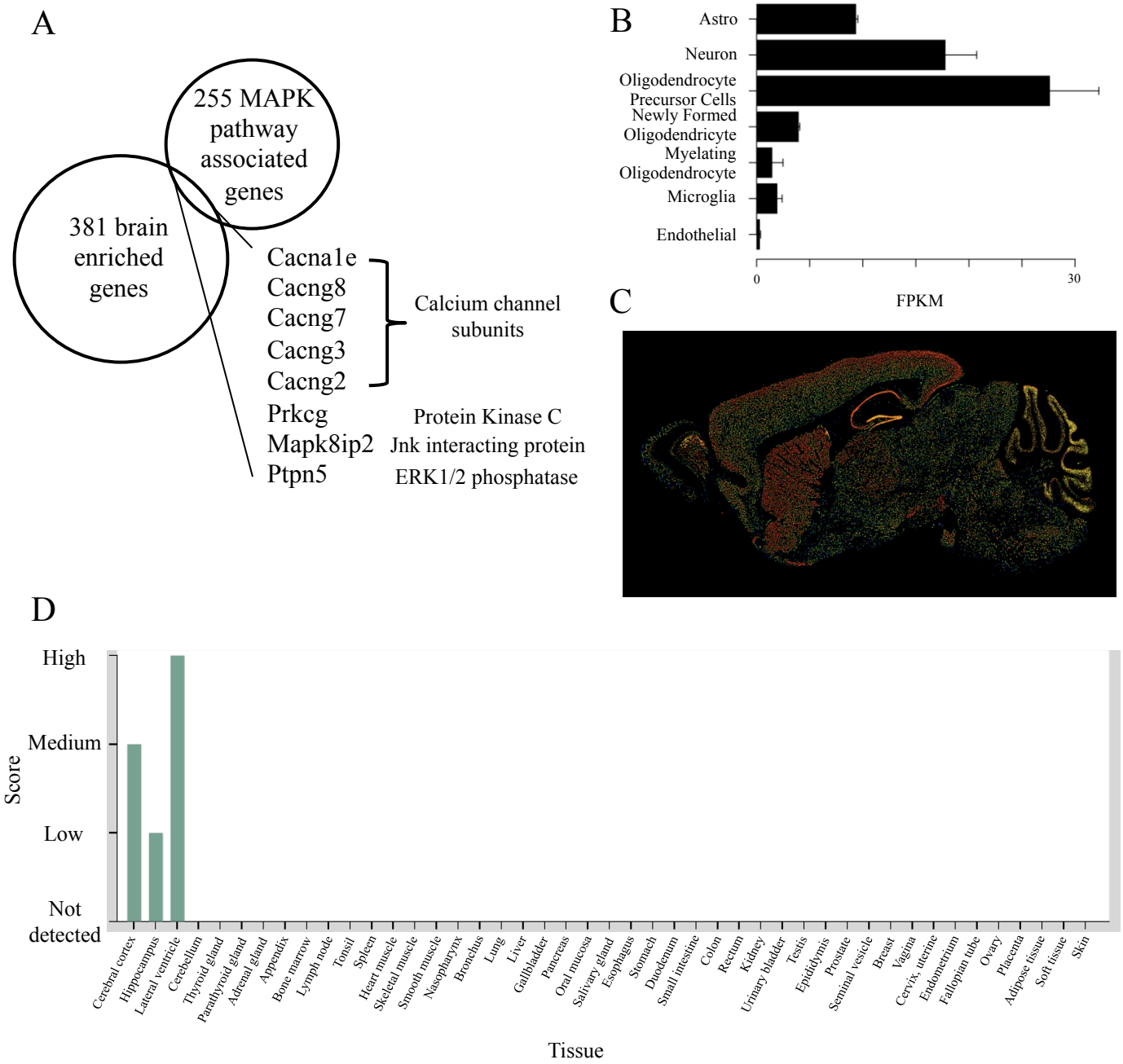

Figure 6.2. PTPN5 as a possible brain specific modulator of p-ERK levels. (A) Identification of brain enriched genes implicated in Ras-Raf-ERK signaling (B) *PTPN5* is expressed in multiple cell types in the brain, including neurons and astrocytes (C) Staining of brain expression of PTPN5 (D) Brain specificity of PTPN5 expression. Panel B modified from http://web.stanford.edu/group/barres_lab/brain_rnaseq.html, panel C modified from http://mouse.brain-map.org/, panel D modified from http://www.proteinatlas.org/. FPKM - Fragments per kilobase of transcript sequence per million mapped fragments.

upstream to specifically inhibit the Ras-Raf-ERK pathway without affecting multiple other cascades. The remaining gene Protein tyrosine phosphatase non-receptor type 5 (PTPN5; previously know as STEP) is a brain specific protein phosphatase, originally purified from striatum, but present at a high level of expression in all brain regions (Lombroso et al., 1991) (figure 6.2). Amongst its many substrates are p38, Fyn, PyK2, GluN2B, GluA2, and ERK1/2 (Moult et al., 2006; Munoz et al., 2003; Paul et al., 2003; Xu et al., 2012; Xu et al., 2009).

As this protein is a phosphatase, we would want to increase its effect, to reduce p-ERK levels. Activators of phosphatases are very difficult to design however, and currently none are known to exist. Furthermore previous work aiming to reduce PTPN5 using small molecular inhibitors have shown a positive effect on cognitive function in a triple transgenic mouse model of AD, thereby implying that decreasing PTPN5 action is beneficial in AD (Yang et al., 2012). Other evidence however suggests that decreasing the activity of PTPN5 has a detrimental effect on cell survival following focal cerebral ischemia in rats, and delays recovery from stressful stimuli (Deb et al., 2013). Therefore the potential role of PTPN5 in neurodegeneration is far from clear, but given its brain specificity, it seems worthy of further investigation.

Approaches to treating chronic neurodegeneration – the Alzheimer's disease problem

In this thesis we have identified that the use of a single IIS inhibitor may show efficacy in reducing neuronal cell death in neurodegenerative diseases, and have suggested that its use as a solo agent would be most appropriate for the treatment of acute neurodegenerative diseases where its long term side effects may be mitigated by the duration of its administration in these diseases. It brings us to a particularly pertinent question with regards to treating chronic neurodegenerative diseases however; are the methods and approaches currently used to approach chronic neurodegenerative disease treatment appropriate? AD has overwhelmingly received the greatest attention and man-hours in the attempt to devise improved therapeutic strategies for its treatment, and yet these have overwhelmingly failed to succeed, and is a perfect example of the problems encountered when attempting to treat chronic

neurodegenerative diseases. If biomedicine is to succeed in combatting AD and other chronic neurodegenerative diseases, then we must consider how we approach these diseases; this will be discussed here by considering AD.

Why some people develop sAD whilst others do not, especially in light of the possibility of high plaque brain load in cognitively functional patients (Braak et al., 2011), is unclear. Similarly the neuropathological features of dementia and sAD patients are extremely varied (Lam et al., 2013), and yet sAD patients in clinical trials are considered and crucially treated as one homogenous patient group. Risk factors associated with sAD development are extremely numerous and varied as well, making it seem highly likely that the reason different patients develop sAD varies, but can give rise to a similar clinical phenotype. With great patient heterogeneity why are we attempting to treat the patient group with a single treatment for all? It seems highly likely that different patients would be variably susceptible to different treatments, with it being possible that many of the recent failed phase III trials would prove efficacious for a particular AD patient group. Furthermore, recent evidence had cast doubt on even the disease pathogenesis is certain fAD patient populations, where the pathogenesis of disease has appeared far more straightforward than in sAD patients. With some patients with presenelin-1 mutations showing intact presenelin-1 activity, whilst others show a complete loss (Ben-Gedalya et al., 2015; Szaruga et al., 2015; Xia et al., 2015), evidence for heterogeneity in disease pathogenesis even amongst far simpler patient groups, would suggest that the mechanisms that give rise to the phenotype of AD are not consistent within patient groups, stressing that different treatments may work better for different patients.

With all this considered, it seems highly likely that for therapeutic developments to succeed in such a large variable patient group, and greater understanding of the pathological, genetic, and environmental heterogeneity of sAD patients is required. This would allow more targeted therapeutic approaches, which could open up possibilities for patients and lead to a vast improvement in AD patient care.

Conclusion

The IIS cascade seems critically implicated in neuronal cell death. In this thesis we have investigated how this implication could be exploited for therapeutic gain in treating neurodegenerative diseases by preventing neuronal cell death. Neurodegenerative diseases are a broad set of diseases however, split roughly into chronic and acute, with neuronal cell loss taking place over years or weeks respectively. The length of time that neuronal loss occurs over and therefore the length of time that clinical intervention would have to take place over, and the effect of inhibiting the IIS cascade systemically, mean that chronic and acute neurodegenerative diseases have to be considered separately in terms of disease intervention via the IIS cascade.

Chronic neurodegenerative diseases would be unlikely to be suitably treated by the application of IIS inhibitors over the duration of the neuronal loss. We therefore investigated times in the pathological development of AD that IIS changes are endogenously changes, and identified that there is an early strong increase in IIS signalling in response to rising amyloid pathology. How this early increase is implicated in disease progression is unknown, but investigating early inhibition of this rise would be an interesting way of modulating the earliest changes in relation to AD pathology. Otherwise, IIS based interventions in the chronic neurodegenerative disease pathogenesis may come down to titrating the dose of IIS inhibition to provide neuroprotection whilst mitigating peripheral side effects, or identifying brain specific means of intervening in the IIS cascade.

Acute neurodegenerative diseases seem the most susceptible to therapeutic IIS intervention, as the short duration of neuronal cell loss would reduce the duration of IIS inhibitor intervention, and therefore reduce the side effects as a consequence. Trametinib seems a potential option, having shown neuroprotective properties *in vitro*. However, the dependence of its brain IIS inhibition on the co-administration of Elacridar, means that the effect of P-gp inhibition on acute neurodegeneration would need to be investigated further to ensure that functional P-gp is not protective following an acute neurodegenerative insult.

Igf1 increase in acute neurodegenerative disease is another possible novel intervention strategy, with the prevention of this increase being neuroprotective. However, much work in *in vitro* models would be required with IGF1R inhibitors before this possible endogenous alteration could be therapeutically exploited.

Overall therefore, Trametinib seems an exciting novel treatment option for acute neurodegenerative diseases such as stroke and TBI, with potential promise to be had in modulating the endogenous increase in astrocyte *Igf1* increase observed during acute neuronal cell loss. Targeting chronic neurodegenerative diseases via the IIS cascade seems far more complex and fraught with complications.

References

Aarli, J.A. (2006). Neurological disorders : public health challenges (Geneva: World Health Organization).

Adams, H.P., Jr., del Zoppo, G., Alberts, M.J., Bhatt, D.L., Brass, L., Furlan, A., Grubb, R.L., Higashida, R.T., Jauch, E.C., Kidwell, C.*, et al.* (2007). Guidelines for the early management of adults with ischemic stroke: a guideline from the American Heart Association/American Stroke Association Stroke Council, Clinical Cardiology Council, Cardiovascular Radiology and Intervention Council, and the Atherosclerotic Peripheral Vascular Disease and Quality of Care Outcomes in Research Interdisciplinary Working Groups: The American Academy of Neurology affirms the value of this guideline as an educational tool for neurologists. Circulation *115*, e478-534.

Adolfsson, O., Pihlgren, M., Toni, N., Varisco, Y., Buccarello, A.L., Antoniello, K., Lohmann, S., Piorkowska, K., Gafner, V., Atwal, J.K.*, et al.* (2012). An effector-reduced anti-beta-amyloid (Abeta) antibody with unique abeta binding properties promotes neuroprotection and glial engulfment of Abeta. The Journal of neuroscience : the official journal of the Society for Neuroscience *32*, 9677-9689.

Alessandrini, A., Namura, S., Moskowitz, M.A., and Bonventre, J.V. (1999). MEK1 protein kinase inhibition protects against damage resulting from focal cerebral ischemia. Proceedings of the National Academy of Sciences of the United States of America *96*, 12866-12869.

Alessi, D.R., Andjelkovic, M., Caudwell, B., Cron, P., Morrice, N., Cohen, P., and Hemmings, B.A. (1996). Mechanism of activation of protein kinase B by insulin and IGF-1. The EMBO journal *15*, 6541-6551.

Almeida, R.D., Manadas, B.J., Melo, C.V., Gomes, J.R., Mendes, C.S., Graos, M.M., Carvalho, R.F., Carvalho, A.P., and Duarte, C.B. (2005). Neuroprotection by BDNF against glutamate-induced apoptotic cell death is mediated by ERK and PI3-kinase pathways. Cell death and differentiation *12*, 1329-1343.

Altman, J., and Das, G.D. (1965). Autoradiographic and histological evidence of postnatal hippocampal neurogenesis in rats. The Journal of comparative neurology *124*, 319-335.

Alzheimer's Association (2015). Clinical Trials results and new data analyses in Amyloid-related therapies from the Alzheimer's Association International Conference 2015.

Alzheimer's Disease International (2015). World Alzheimer Report 2015.

Amer, M.H., Al-Sarraf, M., Baker, L.H., and Vaitkevicius, V.K. (1978). Malignant melanoma and central nervous system metastases: incidence, diagnosis, treatment and survival. Cancer *42*, 660-668.

Amieva, H., Le Goff, M., Millet, X., Orgogozo, J.M., Peres, K., Barberger-Gateau, P., Jacqmin-Gadda, H., and Dartigues, J.F. (2008). Prodromal Alzheimer's disease: successive emergence of the clinical symptoms. Annals of neurology *64*, 492-498.

Anforth, R.M., Blumetti, T.C., Kefford, R.F., Sharma, R., Scolyer, R.A., Kossard, S., Long, G.V., and Fernandez-Penas, P. (2012). Cutaneous manifestations of dabrafenib (GSK2118436): a selective inhibitor of mutant BRAF in patients with metastatic melanoma. The British journal of dermatology *167*, 1153-1160.

Aronowski, J., and Zhao, X. (2011). Molecular pathophysiology of cerebral hemorrhage: secondary brain injury. Stroke; a journal of cerebral circulation *42*, 1781-1786.

Arriagada, P.V., Growdon, J.H., Hedley-Whyte, E.T., and Hyman, B.T. (1992). Neurofibrillary tangles but not senile plaques parallel duration and severity of Alzheimer's disease. Neurology *42*, 631-639.

Ashabi, G., Alamdary, S.Z., Ramin, M., and Khodagholi, F. (2013). Reduction of hippocampal apoptosis by intracerebroventricular administration of extracellular signal-regulated protein kinase and/or p38 inhibitors in amyloid beta rat model of Alzheimer's disease: involvement of nuclear-related factor-2 and nuclear factor-kappaB. Basic & clinical pharmacology & toxicology *112*, 145-155.

Avruch, J. (1998). Insulin signal transduction through protein kinase cascades. Molecular and cellular biochemistry *182*, 31-48.

Baird, N.A., Douglas, P.M., Simic, M.S., Grant, A.R., Moresco, J.J., Wolff, S.C., Yates, J.R., 3rd, Manning, G., and Dillin, A. (2014). HSF-1-mediated cytoskeletal integrity determines thermotolerance and life span. Science *346*, 360-363.

Barbieri, M., Rizzo, M.R., Papa, M., Boccardi, V., Esposito, A., White, M.F., and Paolisso, G. (2010). The IRS2 Gly1057Asp variant is associated with human longevity. The journals of gerontology Series A, Biological sciences and medical sciences *65*, 282-286.

Baura, G.D., Foster, D.M., Porte, D., Jr., Kahn, S.E., Bergman, R.N., Cobelli, C., and Schwartz, M.W. (1993). Saturable transport of insulin from plasma into the central nervous system of dogs in vivo. A mechanism for regulated insulin delivery to the brain. The Journal of clinical investigation *92*, 1824-1830.

Beilharz, E.J., Russo, V.C., Butler, G., Baker, N.L., Connor, B., Sirimanne, E.S., Dragunow, M., Werther, G.A., Gluckman, P.D., Williams, C.E.*, et al.* (1998). Co-ordinated and cellular specific induction of the components of the IGF/IGFBP

axis in the rat brain following hypoxic-ischemic injury. Brain research Molecular brain research *59*, 119-134.

Bekris, L.M., Yu, C.E., Bird, T.D., and Tsuang, D.W. (2010). Genetics of Alzheimer disease. Journal of geriatric psychiatry and neurology *23*, 213-227.

Ben-Gedalya, T., Moll, L., Bejerano-Sagie, M., Frere, S., Cabral, W.A., Friedmann-Morvinski, D., Slutsky, I., Burstyn-Cohen, T., Marini, J.C., and Cohen, E. (2015). Alzheimer's disease-causing proline substitutions lead to presenilin 1 aggregation and malfunction. The EMBO journal *34*, 2820-2839.

Benedict, C., Hallschmid, M., Hatke, A., Schultes, B., Fehm, H.L., Born, J., and Kern, W. (2004). Intranasal insulin improves memory in humans. Psychoneuroendocrinology *29*, 1326-1334.

Benedict, C., Hallschmid, M., Schultes, B., Born, J., and Kern, W. (2007). Intranasal insulin to improve memory function in humans. Neuroendocrinology *86*, 136-142.

Bergstedt, K., and Wieloch, T. (1993). Changes in insulin-like growth factor 1 receptor density after transient cerebral ischemia in the rat. Lack of protection against ischemic brain damage following injection of insulin-like growth factor 1. Journal of cerebral blood flow and metabolism : official journal of the International Society of Cerebral Blood Flow and Metabolism *13*, 895-898.

Bhat, N.R., and Zhang, P. (1999). Hydrogen peroxide activation of multiple mitogen-activated protein kinases in an oligodendrocyte cell line: role of extracellular signal-regulated kinase in hydrogen peroxide-induced cell death. Journal of neurochemistry *72*, 112-119.

Bird, T.D., Nochlin, D., Poorkaj, P., Cherrier, M., Kaye, J., Payami, H., Peskind, E., Lampe, T.H., Nemens, E., Boyer, P.J.*, et al.* (1999). A clinical pathological comparison of three families with frontotemporal dementia and identical mutations in the tau gene (P301L). Brain : a journal of neurology *122 (Pt 4)*, 741-756.

Bird, T.D., Stranahan, S., Sumi, S.M., and Raskind, M. (1983). Alzheimer's disease: choline acetyltransferase activity in brain tissue from clinical and pathological subgroups. Annals of neurology *14*, 284-293.

Birks, J. (2006). Cholinesterase inhibitors for Alzheimer's disease. The Cochrane database of systematic reviews, CD005593.

Bjedov, I., Toivonen, J.M., Kerr, F., Slack, C., Jacobson, J., Foley, A., and Partridge, L. (2010). Mechanisms of Life Span Extension by Rapamycin in the Fruit Fly Drosophila melanogaster. Cell metabolism *11*, 35-46.

Bomfim, T.R., Forny-Germano, L., Sathler, L.B., Brito-Moreira, J., Houzel, J.C., Decker, H., Silverman, M.A., Kazi, H., Melo, H.M., McClean, P.L.*, et al.* (2012). An

anti-diabetes agent protects the mouse brain from defective insulin signaling caused by Alzheimer's disease- associated Abeta oligomers. The Journal of clinical investigation *122*, 1339-1353.

Bondy, C., Werner, H., Roberts, C.T., Jr., and LeRoith, D. (1992). Cellular pattern of type-I insulin-like growth factor receptor gene expression during maturation of the rat brain: comparison with insulin-like growth factors I and II. Neuroscience *46*, 909-923.

Bondy, C.A. (1991). Transient IGF-I gene expression during the maturation of functionally related central projection neurons. The Journal of neuroscience : the official journal of the Society for Neuroscience *11*, 3442-3455.

Bondy, C.A., and Lee, W.H. (1993). Patterns of insulin-like growth factor and IGF receptor gene expression in the brain. Functional implications. Annals of the New York Academy of Sciences *692*, 33-43.

Bondy, C.A., Werner, H., Roberts, C.T., Jr., and LeRoith, D. (1990). Cellular pattern of insulin-like growth factor-I (IGF-I) and type I IGF receptor gene expression in early organogenesis: comparison with IGF-II gene expression. Molecular endocrinology *4*, 1386-1398.

Braak, H., Thal, D.R., Ghebremedhin, E., and Del Tredici, K. (2011). Stages of the pathologic process in Alzheimer disease: age categories from 1 to 100 years. Journal of neuropathology and experimental neurology *70*, 960-969.

Broughton, S., and Partridge, L. (2009). Insulin/IGF-like signalling, the central nervous system and aging. The Biochemical journal *418*, 1-12.

Burdick, D., Soreghan, B., Kwon, M., Kosmoski, J., Knauer, M., Henschen, A., Yates, J., Cotman, C., and Glabe, C. (1992). Assembly and aggregation properties of synthetic Alzheimer's A4/beta amyloid peptide analogs. The Journal of biological chemistry *267*, 546-554.

Campana, A.D., Sanchez, F., Gamboa, C., Gomez-Villalobos Mde, J., De La Cruz, F., Zamudio, S., and Flores, G. (2008). Dendritic morphology on neurons from prefrontal cortex, hippocampus, and nucleus accumbens is altered in adult male mice exposed to repeated low dose of malathion. Synapse *62*, 283-290.

Canagarajah, B.J., Khokhlatchev, A., Cobb, M.H., and Goldsmith, E.J. (1997). Activation mechanism of the MAP kinase ERK2 by dual phosphorylation. Cell *90*, 859-869.

Canals, S., Casarejos, M.J., de Bernardo, S., Solano, R.M., and Mena, M.A. (2003). Selective and persistent activation of extracellular signal-regulated protein kinase by nitric oxide in glial cells induces neuronal degeneration in glutathione-depleted midbrain cultures. Molecular and cellular neurosciences *24*, 1012-1026.

Cao, P., Maximov, A., and Sudhof, T.C. (2011). Activity-dependent IGF-1 exocytosis is controlled by the Ca(2+)-sensor synaptotagmin-10. Cell *145*, 300-311.

Carro, E., Trejo, J.L., Gerber, A., Loetscher, H., Torrado, J., Metzger, F., and Torres-Aleman, I. (2006). Therapeutic actions of insulin-like growth factor I on APP/PS2 mice with severe brain amyloidosis. Neurobiology of aging *27*, 1250-1257.

Carro, E., Trejo, J.L., Gomez-Isla, T., LeRoith, D., and Torres-Aleman, I. (2002). Serum insulin-like growth factor I regulates brain amyloid-beta levels. Nature medicine *8*, 1390-1397.

Chen, J., Rusnak, M., Lombroso, P.J., and Sidhu, A. (2009). Dopamine promotes striatal neuronal apoptotic death via ERK signaling cascades. The European journal of neuroscience *29*, 287-306.

Chen, Y.R., and Glabe, C.G. (2006). Distinct early folding and aggregation properties of Alzheimer amyloid-beta peptides Abeta40 and Abeta42: stable trimer or tetramer formation by Abeta42. The Journal of biological chemistry *281*, 24414-24422.

Citron, M., Oltersdorf, T., Haass, C., McConlogue, L., Hung, A.Y., Seubert, P., Vigo-Pelfrey, C., Lieberburg, I., and Selkoe, D.J. (1992). Mutation of the beta-amyloid precursor protein in familial Alzheimer's disease increases beta-protein production. Nature *360*, 672-674.

Clawson, T.F., Vannucci, S.J., Wang, G.M., Seaman, L.B., Yang, X.L., and Lee, W.H. (1999). Hypoxia-ischemia-induced apoptotic cell death correlates with IGF-I mRNA decrease in neonatal rat brain. Biological signals and receptors *8*, 281-293.

ClinicalTrials.gov (2016a). Clinical Trial of Solanezumab for Older Individuals Who May be at Risk for Memory Loss (A4).

ClinicalTrials.gov (2016b). Dominantly Inherited Alzheimer Network Trial: An Opportunity to Prevent Dementia. A Study of Potential Disease Modifying Treatments in Individuals at Risk for or With a Type of Early Onset Alzheimer's Disease Caused by a Genetic Mutation. (DIAN-TU).

ClinicalTrials.gov (2016c). Effect of Insulin Sensitizer Metformin on AD Biomarkers.

ClinicalTrials.gov (2016d). Metformin in Amnestic Mild Cognitive Impairment (MCI).

ClinicalTrials.gov (2016e). Prevention of Alzheimer's Disease by Vitamin E and Selenium (PREADVISE).

Cohen, E., Bieschke, J., Perciavalle, R.M., Kelly, J.W., and Dillin, A. (2006). Opposing activities protect against age-onset proteotoxicity. Science *313*, 1604-1610.

Cohen, E., Paulsson, J.F., Blinder, P., Burstyn-Cohen, T., Du, D., Estepa, G., Adame, A., Pham, H.M., Holzenberger, M., Kelly, J.W.*, et al.* (2009). Reduced IGF-1 signaling delays age-associated proteotoxicity in mice. Cell *139*, 1157-1169.

Connor, B., Beilharz, E.J., Williams, C., Synek, B., Gluckman, P.D., Faull, R.L., and Dragunow, M. (1997). Insulin-like growth factor-I (IGF-I) immunoreactivity in the Alzheimer's disease temporal cortex and hippocampus. Brain research Molecular brain research *49*, 283-290.

Cooper, J.F., Dues, D.J., Spielbauer, K.K., Machiela, E., Senchuk, M.M., and Van Raamsdonk, J.M. (2015). Delaying aging is neuroprotective in Parkinson's disease: a genetic analysis in C.elegans models. npj Parkinson's Disease *15022*.

Corcoran, N.M., Martin, D., Hutter-Paier, B., Windisch, M., Nguyen, T., Nheu, L., Sundstrom, L.E., Costello, A.J., and Hovens, C.M. (2010). Sodium selenate specifically activates PP2A phosphatase, dephosphorylates tau and reverses memory deficits in an Alzheimer's disease model. Journal of clinical neuroscience : official journal of the Neurosurgical Society of Australasia *17*, 1025-1033.

Coric, V., van Dyck, C.H., Salloway, S., Andreasen, N., Brody, M., Richter, R.W., Soininen, H., Thein, S., Shiovitz, T., Pilcher, G.*, et al.* (2012). Safety and tolerability of the gamma-secretase inhibitor avagacestat in a phase 2 study of mild to moderate Alzheimer disease. Archives of neurology *69*, 1430-1440.

Crews, L., Rockenstein, E., and Masliah, E. (2010). APP transgenic modeling of Alzheimer's disease: mechanisms of neurodegeneration and aberrant neurogenesis. Brain structure & function *214*, 111-126.

Czech, M.P. (1989). Signal transmission by the insulin-like growth factors. Cell *59*, 235-238.

Daughaday, W.H., Hall, K., Raben, M.S., Salmon, W.D., Jr., van den Brande, J.L., and van Wyk, J.J. (1972). Somatomedin: proposed designation for sulphation factor. Nature *235*, 107.

Davies, P., and Maloney, A.J. (1976). Selective loss of central cholinergic neurons in Alzheimer's disease. Lancet *2*, 1403.

de Bernardo, S., Canals, S., Casarejos, M.J., Solano, R.M., Menendez, J., and Mena, M.A. (2004). Role of extracellular signal-regulated protein kinase in neuronal cell death induced by glutathione depletion in neuron/glia mesencephalic cultures. Journal of neurochemistry *91*, 667-682.

De Strooper, B., Annaert, W., Cupers, P., Saftig, P., Craessaerts, K., Mumm, J.S., Schroeter, E.H., Schrijvers, V., Wolfe, M.S., Ray, W.J.*, et al.* (1999). A presenilin-1-

dependent gamma-secretase-like protease mediates release of Notch intracellular domain. Nature *398*, 518-522.

Deb, I., Manhas, N., Poddar, R., Rajagopal, S., Allan, A.M., Lombroso, P.J., Rosenberg, G.A., Candelario-Jalil, E., and Paul, S. (2013). Neuroprotective role of a brain-enriched tyrosine phosphatase, STEP, in focal cerebral ischemia. The Journal of neuroscience : the official journal of the Society for Neuroscience *33*, 17814-17826.

del Ser, T., Steinwachs, K.C., Gertz, H.J., Andres, M.V., Gomez-Carrillo, B., Medina, M., Vericat, J.A., Redondo, P., Fleet, D., and Leon, T. (2013). Treatment of Alzheimer's disease with the GSK-3 inhibitor tideglusib: a pilot study. Journal of Alzheimer's disease : JAD *33*, 205-215.

Deo, A.K., Borson, S., Link, J.M., Domino, K., Eary, J.F., Ke, B., Richards, T.L., Mankoff, D.A., Minoshima, S., O'Sullivan, F.*, et al.* (2014). Activity of P-Glycoprotein, a beta-Amyloid Transporter at the Blood-Brain Barrier, Is Compromised in Patients with Mild Alzheimer Disease. Journal of nuclear medicine : official publication, Society of Nuclear Medicine *55*, 1106-1111.

DeVos, S.L., and Miller, T.M. (2013). Direct intraventricular delivery of drugs to the rodent central nervous system. Journal of visualized experiments : JoVE, e50326.

Doble, A. (1996). The pharmacology and mechanism of action of riluzole. Neurology *47*, S233-241.

Dodge, J.C., Haidet, A.M., Yang, W., Passini, M.A., Hester, M., Clarke, J., Roskelley, E.M., Treleaven, C.M., Rizo, L., Martin, H.*, et al.* (2008). Delivery of AAV-IGF-1 to the CNS extends survival in ALS mice through modification of aberrant glial cell activity. Molecular therapy : the journal of the American Society of Gene Therapy *16*, 1056-1064.

Dominguez, J.M., Fuertes, A., Orozco, L., del Monte-Millan, M., Delgado, E., and Medina, M. (2012). Evidence for irreversible inhibition of glycogen synthase kinase-3beta by tideglusib. The Journal of biological chemistry *287*, 893-904.

Doody, R.S., Thomas, R.G., Farlow, M., Iwatsubo, T., Vellas, B., Joffe, S., Kieburtz, K., Raman, R., Sun, X., Aisen, P.S.*, et al.* (2014). Phase 3 trials of solanezumab for mild-to-moderate Alzheimer's disease. The New England journal of medicine *370*, 311-321.

Dresbach, T., Hempelmann, A., Spilker, C., Dieck, S.T., Altrock, W.D., Zuschratter, W., Garner, C.C., and Gundelfinger, E.D. (2003). Functional regions of the presynaptic cytomatrix protein Bassoon: significance for synaptic targeting and cytomatrix anchoring. Molecular and Cellular Neuroscience *23*, 279-291.

Duan, C. (2002). Specifying the cellular responses to IGF signals: roles of IGF-binding proteins. The Journal of endocrinology *175*, 41-54.

Dummer, R., Goldinger, S.M., Turtschi, C.P., Eggmann, N.B., Michielin, O., Mitchell, L., Veronese, L., Hilfiker, P.R., Felderer, L., and Rinderknecht, J.D. (2014). Vemurafenib in patients with BRAF(V600) mutation-positive melanoma with symptomatic brain metastases: final results of an open-label pilot study. European journal of cancer *50*, 611-621.

Echeverria, V., Burgess, S., Gamble-George, J., Arendash, G.W., and Citron, B.A. (2008). Raf inhibition protects cortical cells against beta-amyloid toxicity. Neuroscience letters *444*, 92-96.

Echeverria, V., Burgess, S., Gamble-George, J., Zeitlin, R., Lin, X., Cao, C., and Arendash, G.W. (2009). Sorafenib inhibits nuclear factor kappa B, decreases inducible nitric oxide synthase and cyclooxygenase-2 expression, and restores working memory in APPswe mice. Neuroscience *162*, 1220-1231.

Eisai (2012). Eisai presents first clinical data for BACE inhibitor E2609 at Alzheimer's Association International Conference 2012.

El-Ami, T., Moll, L., Carvalhal Marques, F., Volovik, Y., Reuveni, H., and Cohen, E. (2014). A novel inhibitor of the insulin/IGF signaling pathway protects from age-onset, neurodegeneration-linked proteotoxicity. Aging cell *13*, 165-174.

Falchook, G.S., Lewis, K.D., Infante, J.R., Gordon, M.S., Vogelzang, N.J., DeMarini, D.J., Sun, P., Moy, C., Szabo, S.A., Roadcap, L.T.*, et al.* (2012). Activity of the oral MEK inhibitor trametinib in patients with advanced melanoma: a phase 1 dose-escalation trial. The Lancet Oncology *13*, 782-789.

Fan, J.S., Huang, H.H., Chen, Y.C., Yen, D.H., Kao, W.F., Huang, M.S., Huang, C.I., and Lee, C.H. (2012). Emergency department neurologic deterioration in patients with spontaneous intracerebral hemorrhage: incidence, predictors, and prognostic significance. Academic emergency medicine : official journal of the Society for Academic Emergency Medicine *19*, 133-138.

Farias, S.T., Mungas, D., Reed, B.R., Harvey, D., and DeCarli, C. (2009). Progression of mild cognitive impairment to dementia in clinic- vs community-based cohorts. Archives of neurology *66*, 1151-1157.

Farlow, M., Arnold, S.E., van Dyck, C.H., Aisen, P.S., Snider, B.J., Porsteinsson, A.P., Friedrich, S., Dean, R.A., Gonzales, C., Sethuraman, G.*, et al.* (2012). Safety and biomarker effects of solanezumab in patients with Alzheimer's disease. Alzheimer's & dementia : the journal of the Alzheimer's Association *8*, 261-271.

Feigin, V.L., Lawes, C.M., Bennett, D.A., Barker-Collo, S.L., and Parag, V. (2009). Worldwide stroke incidence and early case fatality reported in 56 population-based studies: a systematic review. The Lancet Neurology *8*, 355-369.

Feng, G., Mellor, R.H., Bernstein, M., Keller-Peck, C., Nguyen, Q.T., Wallace, M., Nerbonne, J.M., Lichtman, J.W., and Sanes, J.R. (2000). Imaging neuronal subsets

in transgenic mice expressing multiple spectral variants of GFP. Neuron *28*, 41-51.

Ferrer, I., Blanco, R., Carmona, M., Ribera, R., Goutan, E., Puig, B., Rey, M.J., Cardozo, A., Vinals, F., and Ribalta, T. (2001). Phosphorylated map kinase (ERK1, ERK2) expression is associated with early tau deposition in neurones and glial cells, but not with increased nuclear DNA vulnerability and cell death, in Alzheimer disease, Pick's disease, progressive supranuclear palsy and corticobasal degeneration. Brain pathology *11*, 144-158.

Fields, R.D., and Stevens-Graham, B. (2002). New insights into neuron-glia communication. Science *298*, 556-562.

Fischer, P., Jungwirth, S., Zehetmayer, S., Weissgram, S., Hoenigschnabl, S., Gelpi, E., Krampla, W., and Tragl, K.H. (2007). Conversion from subtypes of mild cognitive impairment to Alzheimer dementia. Neurology *68*, 288-291.

Forlenza, O.V., Diniz, B.S., Radanovic, M., Santos, F.S., Talib, L.L., and Gattaz, W.F. (2011). Disease-modifying properties of long-term lithium treatment for amnestic mild cognitive impairment: randomised controlled trial. The British journal of psychiatry : the journal of mental science *198*, 351-356.

Forman, M., Palcza, J., Tseng, J., Leempoels, J., Ramael, S., Han, D., Jhee, S., Ereshefsky, L., Tanen, M., Laterza, O*., et al.* (2012). The novel BACE inhibitor MK-8931 dramatically lowers cerebrospinal fluid Aβ peptides in healthy subjects following single- and multiple-dose administration. Alzheimer's & Dementia: The Journal of the Alzheimer's Association *8*, P704.

Fox, N.C., Warrington, E.K., Freeborough, P.A., Hartikainen, P., Kennedy, A.M., Stevens, J.M., and Rossor, M.N. (1996). Presymptomatic hippocampal atrophy in Alzheimer's disease. A longitudinal MRI study. Brain : a journal of neurology *119 (Pt 6)*, 2001-2007.

Freude, S., Hettich, M.M., Schumann, C., Stohr, O., Koch, L., Kohler, C., Udelhoven, M., Leeser, U., Muller, M., Kubota, N*., et al.* (2009). Neuronal IGF-1 resistance reduces Abeta accumulation and protects against premature death in a model of Alzheimer's disease. FASEB journal : official publication of the Federation of American Societies for Experimental Biology *23*, 3315-3324.

Garwood, C.J., Ratcliffe, L.E., Morgan, S.V., Simpson, J.E., Owens, H., Vazquez-Villasenor, I., Heath, P.R., Romero, I.A., Ince, P.G., and Wharton, S.B. (2015). Insulin and IGF1 signalling pathways in human astrocytes in vitro and in vivo; characterisation, subcellular localisation and modulation of the receptors. Molecular brain *8*, 51.

Gazit, N., Vertkin, I., Shapira, I., Helm, M., Slomowitz, E., Sheiba, M., Mor, Y., Rizzoli, S., and Slutsky, I. (2016). IGF-1 Receptor Differentially Regulates Spontaneous and Evoked Transmission via Mitochondria at Hippocampal Synapses. Neuron *89*, 583-597.

Genentech (2012). Landmark Alzheimer's Prevention Trial.

Genua, M., Pandini, G., Cassarino, M.F., Messina, R.L., and Frasca, F. (2009). c-Abl and insulin receptor signalling. Vitamins and hormones *80*, 77-105.

Giannakopoulos, P., Herrmann, F.R., Bussiere, T., Bouras, C., Kovari, E., Perl, D.P., Morrison, J.H., Gold, G., and Hof, P.R. (2003). Tangle and neuron numbers, but not amyloid load, predict cognitive status in Alzheimer's disease. Neurology *60*, 1495-1500.

Gilmartin, A.G., Bleam, M.R., Groy, A., Moss, K.G., Minthorn, E.A., Kulkarni, S.G., Rominger, C.M., Erskine, S., Fisher, K.E., Yang, J.*, et al.* (2011). GSK1120212 (JTP-74057) is an inhibitor of MEK activity and activation with favorable pharmacokinetic properties for sustained in vivo pathway inhibition. Clinical cancer research : an official journal of the American Association for Cancer Research *17*, 989-1000.

Gladbach, A., van Eersel, J., Bi, M., Ke, Y.D., and Ittner, L.M. (2014). ERK inhibition with PD184161 mitigates brain damage in a mouse model of stroke. Journal of neural transmission *121*, 543-547.

Glenner, G.G., and Wong, C.W. (1984). Alzheimer's disease and Down's syndrome: sharing of a unique cerebrovascular amyloid fibril protein. Biochemical and biophysical research communications *122*, 1131-1135.

Goate, A., Chartier-Harlin, M.C., Mullan, M., Brown, J., Crawford, F., Fidani, L., Giuffra, L., Haynes, A., Irving, N., James, L.*, et al.* (1991). Segregation of a missense mutation in the amyloid precursor protein gene with familial Alzheimer's disease. Nature *349*, 704-706.

Gomez-Isla, T., Hollister, R., West, H., Mui, S., Growdon, J.H., Petersen, R.C., Parisi, J.E., and Hyman, B.T. (1997). Neuronal loss correlates with but exceeds neurofibrillary tangles in Alzheimer's disease. Annals of neurology *41*, 17-24.

Gomez-Isla, T., Price, J.L., McKeel, D.W., Jr., Morris, J.C., Growdon, J.H., and Hyman, B.T. (1996). Profound loss of layer II entorhinal cortex neurons occurs in very mild Alzheimer's disease. The Journal of neuroscience : the official journal of the Society for Neuroscience *16*, 4491-4500.

Grogan, K. (2012). Zeltia Alzheimer's drug tideglusib misses endpoints. In PharmaTimes Digital.

Gual, P., Baron, V., Lequoy, V., and Van Obberghen, E. (1998). Interaction of Janus kinases JAK-1 and JAK-2 with the insulin receptor and the insulin-like growth factor-1 receptor. Endocrinology *139*, 884-893.

Guan, J., Bennet, T.L., George, S., Waldvogel, H.J., Faull, R.L., Gluckman, P.D., Keunen, H., and Gunn, A.J. (2000). Selective neuroprotective effects with insulin-

like growth factor-1 in phenotypic striatal neurons following ischemic brain injury in fetal sheep. Neuroscience *95*, 831-839.

Guan, J., Williams, C., Gunning, M., Mallard, C., and Gluckman, P. (1993). The effects of IGF-1 treatment after hypoxic-ischemic brain injury in adult rats. Journal of cerebral blood flow and metabolism : official journal of the International Society of Cerebral Blood Flow and Metabolism *13*, 609-616.

Guardia-Laguarta, C., Pera, M., Clarimon, J., Molinuevo, J.L., Sanchez-Valle, R., Llado, A., Coma, M., Gomez-Isla, T., Blesa, R., Ferrer, I., *et al.* (2010). Clinical, neuropathologic, and biochemical profile of the amyloid precursor protein I716F mutation. Journal of neuropathology and experimental neurology *69*, 53-59.

Guise, S., Braguer, D., Carles, G., Delacourte, A., and Briand, C. (2001). Hyperphosphorylation of tau is mediated by ERK activation during anticancer drug-induced apoptosis in neuroblastoma cells. Journal of neuroscience research *63*, 257-267.

Gupta, R., Schumacher, H.C., Mangla, S., Meyers, P.M., Duong, H., Khandji, A.G., Marshall, R.S., Mohr, J.P., and Pile-Spellman, J. (2003). Urgent endovascular revascularization for symptomatic intracranial atherosclerotic stenosis. Neurology *61*, 1729-1735.

Haapasalo, A., and Kovacs, D.M. (2011). The many substrates of presenilin/gamma-secretase. Journal of Alzheimer's disease : JAD *25*, 3-28.

Haass, C., Kaether, C., Thinakaran, G., and Sisodia, S. (2012). Trafficking and proteolytic processing of APP. Cold Spring Harbor perspectives in medicine *2*, a006270.

Halagappa, V.K., Guo, Z., Pearson, M., Matsuoka, Y., Cutler, R.G., Laferla, F.M., and Mattson, M.P. (2007). Intermittent fasting and caloric restriction ameliorate age-related behavioral deficits in the triple-transgenic mouse model of Alzheimer's disease. Neurobiology of disease *26*, 212-220.

Hampel, H., Ewers, M., Burger, K., Annas, P., Mortberg, A., Bogstedt, A., Frolich, L., Schroder, J., Schonknecht, P., Riepe, M.W., *et al.* (2009). Lithium trial in Alzheimer's disease: a randomized, single-blind, placebo-controlled, multicenter 10-week study. The Journal of clinical psychiatry *70*, 922-931.

Han, V.K., Lund, P.K., Lee, D.C., and D'Ercole, A.J. (1988). Expression of somatomedin/insulin-like growth factor messenger ribonucleic acids in the human fetus: identification, characterization, and tissue distribution. The Journal of clinical endocrinology and metabolism *66*, 422-429.

Hardy, J.A., and Higgins, G.A. (1992). Alzheimer's disease: the amyloid cascade hypothesis. Science *256*, 184-185.

Harris, F.M., Brecht, W.J., Xu, Q., Mahley, R.W., and Huang, Y. (2004). Increased tau phosphorylation in apolipoprotein E4 transgenic mice is associated with activation of extracellular signal-regulated kinase: modulation by zinc. The Journal of biological chemistry *279*, 44795-44801.

Harrison, D.E., Strong, R., Sharp, Z.D., Nelson, J.F., Astle, C.M., Flurkey, K., Nadon, N.L., Wilkinson, J.E., Frenkel, K., Carter, C.S.*, et al.* (2009). Rapamycin fed late in life extends lifespan in genetically heterogeneous mice. Nature *460*, 392-U108.

Hartz, A.M., Miller, D.S., and Bauer, B. (2010). Restoring blood-brain barrier P-glycoprotein reduces brain amyloid-beta in a mouse model of Alzheimer's disease. Molecular pharmacology *77*, 715-723.

Hatzivassiliou, G., Song, K., Yen, I., Brandhuber, B.J., Anderson, D.J., Alvarado, R., Ludlam, M.J., Stokoe, D., Gloor, S.L., Vigers, G.*, et al.* (2010). RAF inhibitors prime wild-type RAF to activate the MAPK pathway and enhance growth. Nature *464*, 431-435.

Hawrylycz, M.J., Lein, E.S., Guillozet-Bongaarts, A.L., Shen, E.H., Ng, L., Miller, J.A., van de Lagemaat, L.N., Smith, K.A., Ebbert, A., Riley, Z.L.*, et al.* (2012). An anatomically comprehensive atlas of the adult human brain transcriptome. Nature *489*, 391-399.

Hemphill, J.C., 3rd, Greenberg, S.M., Anderson, C.S., Becker, K., Bendok, B.R., Cushman, M., Fung, G.L., Goldstein, J.N., Macdonald, R.L., Mitchell, P.H.*, et al.* (2015). Guidelines for the Management of Spontaneous Intracerebral Hemorrhage: A Guideline for Healthcare Professionals From the American Heart Association/American Stroke Association. Stroke; a journal of cerebral circulation *46*, 2032-2060.

Holzenberger, M., Dupont, J., Ducos, B., Leneuve, P., Geloen, A., Even, P.C., Cervera, P., and Le Bouc, Y. (2003). IGF-1 receptor regulates lifespan and resistance to oxidative stress in mice. Nature *421*, 182-187.

Howlett, D.R., Bowler, K., Soden, P.E., Riddell, D., Davis, J.B., Richardson, J.C., Burbidge, S.A., Gonzalez, M.I., Irving, E.A., Lawman, A.*, et al.* (2008). Abeta deposition and related pathology in an APP x PS1 transgenic mouse model of Alzheimer's disease. Histology and histopathology *23*, 67-76.

Huang, B.Y., and Castillo, M. (2008). Hypoxic-ischemic brain injury: imaging findings from birth to adulthood. Radiographics : a review publication of the Radiological Society of North America, Inc *28*, 417-439; quiz 617.

Hubbard, S.R. (1999). Structural analysis of receptor tyrosine kinases. Progress in biophysics and molecular biology *71*, 343-358.

Humpel, C. (2011). Identifying and validating biomarkers for Alzheimer's disease. Trends in biotechnology *29*, 26-32.

Hutton, M., Lendon, C.L., Rizzu, P., Baker, M., Froelich, S., Houlden, H., Pickering-Brown, S., Chakraverty, S., Isaacs, A., Grover, A.*, et al.* (1998). Association of missense and 5'-splice-site mutations in tau with the inherited dementia FTDP-17. Nature *393*, 702-705.

Hyder, A.A., Wunderlich, C.A., Puvanachandra, P., Gururaj, G., and Kobusingye, O.C. (2007). The impact of traumatic brain injuries: a global perspective. NeuroRehabilitation *22*, 341-353.

Infante, J.R., Fecher, L.A., Falchook, G.S., Nallapareddy, S., Gordon, M.S., Becerra, C., DeMarini, D.J., Cox, D.S., Xu, Y., Morris, S.R.*, et al.* (2012). Safety, pharmacokinetic, pharmacodynamic, and efficacy data for the oral MEK inhibitor trametinib: a phase 1 dose-escalation trial. The Lancet Oncology *13*, 773-781.

Irving, E.A., Barone, F.C., Reith, A.D., Hadingham, S.J., and Parsons, A.A. (2000). Differential activation of MAPK/ERK and p38/SAPK in neurones and glia following focal cerebral ischaemia in the rat. Brain research Molecular brain research *77*, 65-75.

Ittner, L.M., Ke, Y.D., Delerue, F., Bi, M., Gladbach, A., van Eersel, J., Wolfing, H., Chieng, B.C., Christie, M.J., Napier, I.A.*, et al.* (2010). Dendritic function of tau mediates amyloid-beta toxicity in Alzheimer's disease mouse models. Cell *142*, 387-397.

Jin, M., Shepardson, N., Yang, T., Chen, G., Walsh, D., and Selkoe, D.J. (2011). Soluble amyloid beta-protein dimers isolated from Alzheimer cortex directly induce Tau hyperphosphorylation and neuritic degeneration. Proceedings of the National Academy of Sciences of the United States of America *108*, 5819-5824.

Johnston, B.M., Mallard, E.C., Williams, C.E., and Gluckman, P.D. (1996). Insulin-like growth factor-1 is a potent neuronal rescue agent after hypoxic-ischemic injury in fetal lambs. The Journal of clinical investigation *97*, 300-308.

Kauwe, J.S., Cruchaga, C., Mayo, K., Fenoglio, C., Bertelsen, S., Nowotny, P., Galimberti, D., Scarpini, E., Morris, J.C., Fagan, A.M.*, et al.* (2008). Variation in MAPT is associated with cerebrospinal fluid tau levels in the presence of amyloid-beta deposition. Proceedings of the National Academy of Sciences of the United States of America *105*, 8050-8054.

Keane, M., Semeiks, J., Webb, A.E., Li, Y.I., Quesada, V., Craig, T., Madsen, L.B., van Dam, S., Brawand, D., Marques, P.I.*, et al.* (2015). Insights into the evolution of longevity from the bowhead whale genome. Cell reports *10*, 112-122.

Kenyon, C., Chang, J., Gensch, E., Rudner, A., and Tabtiang, R. (1993). A C. elegans mutant that lives twice as long as wild type. Nature *366*, 461-464.

Killick, R., Scales, G., Leroy, K., Causevic, M., Hooper, C., Irvine, E.E., Choudhury, A.I., Drinkwater, L., Kerr, F., Al-Qassab, H.*, et al.* (2009). Deletion of Irs2 reduces

amyloid deposition and rescues behavioural deficits in APP transgenic mice. Biochemical and biophysical research communications *386*, 257-262.

King, A.J., Arnone, M.R., Bleam, M.R., Moss, K.G., Yang, J., Fedorowicz, K.E., Smitheman, K.N., Erhardt, J.A., Hughes-Earle, A., Kane-Carson, L.S.*, et al.* (2013). Dabrafenib; preclinical characterization, increased efficacy when combined with trametinib, while BRAF/MEK tool combination reduced skin lesions. PloS one *8*, e67583.

Kitagawa, H., Warita, H., Sasaki, C., Zhang, W.R., Sakai, K., Shiro, Y., Mitsumoto, Y., Mori, T., and Abe, K. (1999). Immunoreactive Akt, PI3-K and ERK protein kinase expression in ischemic rat brain. Neuroscience letters *274*, 45-48.

Klegeris, A., Pelech, S., Giasson, B.I., Maguire, J., Zhang, H., McGeer, E.G., and McGeer, P.L. (2008). Alpha-synuclein activates stress signaling protein kinases in THP-1 cells and microglia. Neurobiology of aging *29*, 739-752.

Kojima, T., Kamei, H., Aizu, T., Arai, Y., Takayama, M., Nakazawa, S., Ebihara, Y., Inagaki, H., Masui, Y., Gondo, Y.*, et al.* (2004). Association analysis between longevity in the Japanese population and polymorphic variants of genes involved in insulin and insulin-like growth factor 1 signaling pathways. Experimental gerontology *39*, 1595-1598.

Kuppens, I.E., Witteveen, E.O., Jewell, R.C., Radema, S.A., Paul, E.M., Mangum, S.G., Beijnen, J.H., Voest, E.E., and Schellens, J.H. (2007). A phase I, randomized, open-label, parallel-cohort, dose-finding study of elacridar (GF120918) and oral topotecan in cancer patients. Clinical cancer research : an official journal of the American Association for Cancer Research *13*, 3276-3285.

Kurt, M.A., Davies, D.C., Kidd, M., Duff, K., and Howlett, D.R. (2003). Hyperphosphorylated tau and paired helical filament-like structures in the brains of mice carrying mutant amyloid precursor protein and mutant presenilin-1 transgenes. Neurobiology of disease *14*, 89-97.

Lam, B., Masellis, M., Freedman, M., Stuss, D.T., and Black, S.E. (2013). Clinical, imaging, and pathological heterogeneity of the Alzheimer's disease syndrome. Alzheimer's research & therapy *5*, 1.

Lambert, M.P., Barlow, A.K., Chromy, B.A., Edwards, C., Freed, R., Liosatos, M., Morgan, T.E., Rozovsky, I., Trommer, B., Viola, K.L.*, et al.* (1998). Diffusible, nonfibrillar ligands derived from Abeta1-42 are potent central nervous system neurotoxins. Proceedings of the National Academy of Sciences of the United States of America *95*, 6448-6453.

Laron, Z. (2001). Insulin-like growth factor 1 (IGF-1): a growth hormone. Molecular pathology : MP *54*, 311-316.

Lasagna-Reeves, C.A., Castillo-Carranza, D.L., Sengupta, U., Clos, A.L., Jackson, G.R., and Kayed, R. (2011). Tau oligomers impair memory and induce synaptic and

mitochondrial dysfunction in wild-type mice. Molecular neurodegeneration *6*, 39.

Laviola, L., Natalicchio, A., and Giorgino, F. (2007). The IGF-I signaling pathway. Current pharmaceutical design *13*, 663-669.

Lee, W.H., Wang, G.M., Seaman, L.B., and Vannucci, S.J. (1996). Coordinate IGF-I and IGFBP5 gene expression in perinatal rat brain after hypoxia-ischemia. Journal of cerebral blood flow and metabolism : official journal of the International Society of Cerebral Blood Flow and Metabolism *16*, 227-236.

Lennmyr, F., Karlsson, S., Gerwins, P., Ata, K.A., and Terent, A. (2002). Activation of mitogen-activated protein kinases in experimental cerebral ischemia. Acta neurologica Scandinavica *106*, 333-340.

Lesuisse, C., and Martin, L.J. (2002). Immature and mature cortical neurons engage different apoptotic mechanisms involving caspase-3 and the mitogen-activated protein kinase pathway. Journal of cerebral blood flow and metabolism : official journal of the International Society of Cerebral Blood Flow and Metabolism *22*, 935-950.

Li, S., Overman, J.J., Katsman, D., Kozlov, S.V., Donnelly, C.J., Twiss, J.L., Giger, R.J., Coppola, G., Geschwind, D.H., and Carmichael, S.T. (2010). An age-related sprouting transcriptome provides molecular control of axonal sprouting after stroke. Nature neuroscience *13*, 1496-1504.

Li, X.S., Williams, M., and Bartlett, W.P. (1998). Induction of IGF-1 mRNA expression following traumatic injury to the postnatal brain. Brain research Molecular brain research *57*, 92-96.

Lim, Y.Y., Ellis, K.A., Harrington, K., Pietrzak, R.H., Gale, J., Ames, D., Bush, A.I., Darby, D., Martins, R.N., Masters, C.L.*, et al.* (2013). Cognitive decline in adults with amnestic mild cognitive impairment and high amyloid-beta: prodromal Alzheimer's disease? Journal of Alzheimer's disease : JAD *33*, 1167-1176.

Lin, A.L., Poteet, E., Du, F., Gourav, R.C., Liu, R., Wen, Y., Bresnen, A., Huang, S., Fox, P.T., Yang, S.H.*, et al.* (2012). Methylene blue as a cerebral metabolic and hemodynamic enhancer. PloS one *7*, e46585.

Liu, J.L., Yakar, S., and LeRoith, D. (2000). Conditional knockout of mouse insulin-like growth factor-1 gene using the Cre/loxP system. Proceedings of the Society for Experimental Biology and Medicine Society for Experimental Biology and Medicine *223*, 344-351.

Llorens-Martin, M., Torres-Aleman, I., and Trejo, J.L. (2009). Mechanisms mediating brain plasticity: IGF1 and adult hippocampal neurogenesis. The Neuroscientist : a review journal bringing neurobiology, neurology and psychiatry *15*, 134-148.

Lois, C., Garcia-Verdugo, J.M., and Alvarez-Buylla, A. (1996). Chain migration of neuronal precursors. Science *271*, 978-981.

Lombroso, P.J., Murdoch, G., and Lerner, M. (1991). Molecular characterization of a protein-tyrosine-phosphatase enriched in striatum. Proceedings of the National Academy of Sciences of the United States of America *88*, 7242-7246.

Long, G.V., Trefzer, U., Davies, M.A., Kefford, R.F., Ascierto, P.A., Chapman, P.B., Puzanov, I., Hauschild, A., Robert, C., Algazi, A.*, et al.* (2012). Dabrafenib in patients with Val600Glu or Val600Lys BRAF-mutant melanoma metastatic to the brain (BREAK-MB): a multicentre, open-label, phase 2 trial. The Lancet Oncology *13*, 1087-1095.

Long-Smith, C.M., Manning, S., McClean, P.L., Coakley, M.F., O'Halloran, D.J., Holscher, C., and O'Neill, C. (2013). The diabetes drug liraglutide ameliorates aberrant insulin receptor localisation and signalling in parallel with decreasing both amyloid-beta plaque and glial pathology in a mouse model of Alzheimer's disease. Neuromolecular medicine *15*, 102-114.

Lu, K.T., Cheng, N.C., Wu, C.Y., and Yang, Y.L. (2008). NKCC1-mediated traumatic brain injury-induced brain edema and neuron death via Raf/MEK/MAPK cascade. Critical care medicine *36*, 917-922.

Luo, Y., and DeFranco, D.B. (2006). Opposing roles for ERK1/2 in neuronal oxidative toxicity: distinct mechanisms of ERK1/2 action at early versus late phases of oxidative stress. The Journal of biological chemistry *281*, 16436-16442.

Madathil, S.K., Carlson, S.W., Brelsfoard, J.M., Ye, P., D'Ercole, A.J., and Saatman, K.E. (2013). Astrocyte-Specific Overexpression of Insulin-Like Growth Factor-1 Protects Hippocampal Neurons and Reduces Behavioral Deficits following Traumatic Brain Injury in Mice. PloS one *8*, e67204.

Madathil, S.K., Evans, H.N., and Saatman, K.E. (2010). Temporal and regional changes in IGF-1/IGF-1R signaling in the mouse brain after traumatic brain injury. Journal of neurotrauma *27*, 95-107.

Magarinos, A.M., and McEwen, B.S. (1995). Stress-induced atrophy of apical dendrites of hippocampal CA3c neurons: involvement of glucocorticoid secretion and excitatory amino acid receptors. Neuroscience *69*, 89-98.

Magrassi, L., Leto, K., and Rossi, F. (2013). Lifespan of neurons is uncoupled from organismal lifespan. Proceedings of the National Academy of Sciences of the United States of America *110*, 4374-4379.

Mairet-Coello, G., Courchet, J., Pieraut, S., Courchet, V., Maximov, A., and Polleux, F. (2013). The CAMKK2-AMPK kinase pathway mediates the synaptotoxic effects of Abeta oligomers through Tau phosphorylation. Neuron *78*, 94-108.

Marler, J.R., Tilley, B.C., Lu, M., Brott, T.G., Lyden, P.C., Grotta, J.C., Broderick, J.P., Levine, S.R., Frankel, M.P., Horowitz, S.H.*, et al.* (2000). Early stroke treatment associated with better outcome: the NINDS rt-PA stroke study. Neurology *55*, 1649-1655.

Mashima, R., Hishida, Y., Tezuka, T., and Yamanashi, Y. (2009). The roles of Dok family adapters in immunoreceptor signaling. Immunological reviews *232*, 273-285.

Matarin, M., Salih, D.A., Yasvoina, M., Cummings, D.M., Guelfi, M.S., Paublete, R.M., Ali, S., Perona, M., Latcham, J., Fulleylove, M.*, et al.* (2015). A Genome-wide Database in Five Transgenic Mouse Models of Dementia; Gene Expression and Pathology in Different Brain Regions throughout Adult Life. Cell reports,
.

McShane, R., Areosa Sastre, A., and Minakaran, N. (2006). Memantine for dementia. The Cochrane database of systematic reviews, CD003154.

Milman, S., Atzmon, G., Huffman, D.M., Wan, J., Crandall, J.P., Cohen, P., and Barzilai, N. (2014). Low insulin-like growth factor-1 level predicts survival in humans with exceptional longevity. Aging cell *13*, 769-771.

Mittapalli, R.K., Vaidhyanathan, S., Dudek, A.Z., and Elmquist, W.F. (2013). Mechanisms limiting distribution of the threonine-protein kinase B-RaF(V600E) inhibitor dabrafenib to the brain: implications for the treatment of melanoma brain metastases. The Journal of pharmacology and experimental therapeutics *344*, 655-664.

Moult, P.R., Gladding, C.M., Sanderson, T.M., Fitzjohn, S.M., Bashir, Z.I., Molnar, E., and Collingridge, G.L. (2006). Tyrosine phosphatases regulate AMPA receptor trafficking during metabotropic glutamate receptor-mediated long-term depression. The Journal of neuroscience : the official journal of the Society for Neuroscience *26*, 2544-2554.

Munoz, J.J., Tarrega, C., Blanco-Aparicio, C., and Pulido, R. (2003). Differential interaction of the tyrosine phosphatases PTP-SL, STEP and HePTP with the mitogen-activated protein kinases ERK1/2 and p38alpha is determined by a kinase specificity sequence and influenced by reducing agents. The Biochemical journal *372*, 193-201.

Namura, S., Iihara, K., Takami, S., Nagata, I., Kikuchi, H., Matsushita, K., Moskowitz, M.A., Bonventre, J.V., and Alessandrini, A. (2001). Intravenous administration of MEK inhibitor U0126 affords brain protection against forebrain ischemia and focal cerebral ischemia. Proceedings of the National Academy of Sciences of the United States of America *98*, 11569-11574.

National Institute for Health and Clinical Excellence (2011). Donepezil, galantamine, rivastigmine and memantine for the treatment of Alzheimer's disease. In NICE technology appraisal guidance [TA217].

National Institute for Health and Clinical Excellence (2016). Trametinib in combination with dabrafenib for treating unresectable or metastatic melanoma.

Netchine, I., Azzi, S., Houang, M., Seurin, D., Perin, L., Ricort, J.M., Daubas, C., Legay, C., Mester, J., Herich, R.*, et al.* (2009). Partial primary deficiency of insulin-like growth factor (IGF)-I activity associated with IGF1 mutation demonstrates its critical role in growth and brain development. The Journal of clinical endocrinology and metabolism *94*, 3913-3921.

Nieto-Sampedro, M., Lewis, E.R., Cotman, C.W., Manthorpe, M., Skaper, S.D., Barbin, G., Longo, F.M., and Varon, S. (1982). Brain injury causes a time-dependent increase in neuronotrophic activity at the lesion site. Science *217*, 860-861.

Nishida, K., and Hirano, T. (2003). The role of Gab family scaffolding adapter proteins in the signal transduction of cytokine and growth factor receptors. Cancer science *94*, 1029-1033.

Nunes, M.A., Viel, T.A., and Buck, H.S. (2013). Microdose lithium treatment stabilized cognitive impairment in patients with Alzheimer's disease. Current Alzheimer research *10*, 104-107.

Obermeier, B., Daneman, R., and Ransohoff, R.M. (2013). Development, maintenance and disruption of the blood-brain barrier. Nature medicine *19*, 1584-1596.

Ozdinler, P.H., and Macklis, J.D. (2006). IGF-I specifically enhances axon outgrowth of corticospinal motor neurons. Nature neuroscience *9*, 1371-1381.

Patterson, K.R., Remmers, C., Fu, Y., Brooker, S., Kanaan, N.M., Vana, L., Ward, S., Reyes, J.F., Philibert, K., Glucksman, M.J.*, et al.* (2011). Characterization of prefibrillar Tau oligomers in vitro and in Alzheimer disease. The Journal of biological chemistry *286*, 23063-23076.

Paul, S., Nairn, A.C., Wang, P., and Lombroso, P.J. (2003). NMDA-mediated activation of the tyrosine phosphatase STEP regulates the duration of ERK signaling. Nature neuroscience *6*, 34-42.

Payne, D.M., Rossomando, A.J., Martino, P., Erickson, A.K., Her, J.H., Shabanowitz, J., Hunt, D.F., Weber, M.J., and Sturgill, T.W. (1991). Identification of the regulatory phosphorylation sites in pp42/mitogen-activated protein kinase (MAP kinase). The EMBO journal *10*, 885-892.

Pei, J.J., Braak, H., An, W.L., Winblad, B., Cowburn, R.F., Iqbal, K., and Grundke-Iqbal, I. (2002). Up-regulation of mitogen-activated protein kinases ERK1/2 and MEK1/2 is associated with the progression of neurofibrillary degeneration in Alzheimer's disease. Brain research Molecular brain research *109*, 45-55.

Perry, G., Roder, H., Nunomura, A., Takeda, A., Friedlich, A.L., Zhu, X., Raina, A.K., Holbrook, N., Siedlak, S.L., Harris, P.L., *et al.* (1999). Activation of neuronal extracellular receptor kinase (ERK) in Alzheimer disease links oxidative stress to abnormal phosphorylation. Neuroreport *10*, 2411-2415.

Perry, V.H., and Holmes, C. (2014). Microglial priming in neurodegenerative disease. Nature reviews Neurology *10*, 217-224.

Petersen, R.C., Smith, G.E., Waring, S.C., Ivnik, R.J., Tangalos, E.G., and Kokmen, E. (1999). Mild cognitive impairment: clinical characterization and outcome. Archives of neurology *56*, 303-308.

Pierce, A., Podlutskaya, N., Halloran, J.J., Hussong, S.A., Lin, P.Y., Burbank, R., Hart, M.J., and Galvan, V. (2013). Over-expression of heat shock factor 1 phenocopies the effect of chronic inhibition of TOR by rapamycin and is sufficient to ameliorate Alzheimer's-like deficits in mice modeling the disease. Journal of neurochemistry *124*, 880-893.

Pierre, M., and Nunez, J. (1983). Multisite phosphorylation of tau proteins from rat brain. Biochemical and biophysical research communications *115*, 212-219.
Poulikakos, P.I., Zhang, C., Bollag, G., Shokat, K.M., and Rosen, N. (2010). RAF inhibitors transactivate RAF dimers and ERK signalling in cells with wild-type BRAF. Nature *464*, 427-430.

Raghupathi, R. (2004). Cell death mechanisms following traumatic brain injury. Brain pathology *14*, 215-222.

Ramsden, M., Kotilinek, L., Forster, C., Paulson, J., McGowan, E., SantaCruz, K., Guimaraes, A., Yue, M., Lewis, J., Carlson, G., *et al.* (2005). Age-dependent neurofibrillary tangle formation, neuron loss, and memory impairment in a mouse model of human tauopathy (P301L). The Journal of neuroscience : the official journal of the Society for Neuroscience *25*, 10637-10647.

Rapoport, M., Dawson, H.N., Binder, L.I., Vitek, M.P., and Ferreira, A. (2002). Tau is essential to beta -amyloid-induced neurotoxicity. Proceedings of the National Academy of Sciences of the United States of America *99*, 6364-6369.

Rapoport, M., and Ferreira, A. (2000). PD98059 prevents neurite degeneration induced by fibrillar beta-amyloid in mature hippocampal neurons. Journal of neurochemistry *74*, 125-133.

Rinne, J.O., Brooks, D.J., Rossor, M.N., Fox, N.C., Bullock, R., Klunk, W.E., Mathis, C.A., Blennow, K., Barakos, J., Okello, A.A., *et al.* (2010). 11C-PiB PET assessment of change in fibrillar amyloid-beta load in patients with Alzheimer's disease treated with bapineuzumab: a phase 2, double-blind, placebo-controlled, ascending-dose study. The Lancet Neurology *9*, 363-372.

Roberson, E.D., Scearce-Levie, K., Palop, J.J., Yan, F., Cheng, I.H., Wu, T., Gerstein, H., Yu, G.Q., and Mucke, L. (2007). Reducing endogenous tau ameliorates amyloid

beta-induced deficits in an Alzheimer's disease mouse model. Science *316*, 750-754.

Robert, C., Karaszewska, B., Schachter, J., Rutkowski, P., Mackiewicz, A., Stroiakovski, D., Lichinitser, M., Dummer, R., Grange, F., Mortier, L.*, et al.* (2015). Improved overall survival in melanoma with combined dabrafenib and trametinib. The New England journal of medicine *372*, 30-39.

Roberts, P.J., and Der, C.J. (2007). Targeting the Raf-MEK-ERK mitogen-activated protein kinase cascade for the treatment of cancer. Oncogene *26*, 3291-3310.
Roche (2014). Roche announces phase II clinical results of crenezumab in Alzheimer's disease.

Saito, T., Matsuba, Y., Mihira, N., Takano, J., Nilsson, P., Itohara, S., Iwata, N., and Saido, T.C. (2014). Single App knock-in mouse models of Alzheimer's disease. Nature neuroscience *17*, 661-663.

Salloway, S., Sperling, R., Fox, N.C., Blennow, K., Klunk, W., Raskind, M., Sabbagh, M., Honig, L.S., Porsteinsson, A.P., Ferris, S.*, et al.* (2014). Two phase 3 trials of bapineuzumab in mild-to-moderate Alzheimer's disease. The New England journal of medicine *370*, 322-333.

Sandberg, A.C., Engberg, C., Lake, M., von Holst, H., and Sara, V.R. (1988). The expression of insulin-like growth factor I and insulin-like growth factor II genes in the human fetal and adult brain and in glioma. Neuroscience letters *93*, 114-119.

Sandberg Nordqvist, A.C., von Holst, H., Holmin, S., Sara, V.R., Bellander, B.M., and Schalling, M. (1996). Increase of insulin-like growth factor (IGF)-1, IGF binding protein-2 and -4 mRNAs following cerebral contusion. Brain research Molecular brain research *38*, 285-293.

Santacruz, K., Lewis, J., Spires, T., Paulson, J., Kotilinek, L., Ingelsson, M., Guimaraes, A., DeTure, M., Ramsden, M., McGowan, E.*, et al.* (2005). Tau suppression in a neurodegenerative mouse model improves memory function. Science *309*, 476-481.

Saver, J.L. (2006). Time is brain--quantified. Stroke; a journal of cerebral circulation *37*, 263-266.

Scheuner, D., Eckman, C., Jensen, M., Song, X., Citron, M., Suzuki, N., Bird, T.D., Hardy, J., Hutton, M., Kukull, W.*, et al.* (1996). Secreted amyloid beta-protein similar to that in the senile plaques of Alzheimer's disease is increased in vivo by the presenilin 1 and 2 and APP mutations linked to familial Alzheimer's disease. Nature medicine *2*, 864-870.

Schildge, S., Bohrer, C., Beck, K., and Schachtrup, C. (2013). Isolation and culture of mouse cortical astrocytes. Journal of visualized experiments : JoVE.

Schinkel, A.H. (1999). P-Glycoprotein, a gatekeeper in the blood-brain barrier. Advanced drug delivery reviews *36*, 179-194.

Schirmer, R.H., Adler, H., Pickhardt, M., and Mandelkow, E. (2011). "Lest we forget you--methylene blue...". Neurobiology of aging *32*, 2325 e2327-2316.

Shankar, G.M., Bloodgood, B.L., Townsend, M., Walsh, D.M., Selkoe, D.J., and Sabatini, B.L. (2007). Natural oligomers of the Alzheimer amyloid-beta protein induce reversible synapse loss by modulating an NMDA-type glutamate receptor-dependent signaling pathway. The Journal of neuroscience : the official journal of the Society for Neuroscience *27*, 2866-2875.

Shcheglovitov, A., Shcheglovitova, O., Yazawa, M., Portmann, T., Shu, R., Sebastiano, V., Krawisz, A., Froehlich, W., Bernstein, J.A., Hallmayer, J.F.*, et al.* (2013). SHANK3 and IGF1 restore synaptic deficits in neurons from 22q13 deletion syndrome patients. Nature *503*, 267-271.

Sherrington, R., Rogaev, E.I., Liang, Y., Rogaeva, E.A., Levesque, G., Ikeda, M., Chi, H., Lin, C., Li, G., Holman, K.*, et al.* (1995). Cloning of a gene bearing missense mutations in early-onset familial Alzheimer's disease. Nature *375*, 754-760.

Shim, M.S., Wong, S., and Kwon, Y., J. (2012). siRNA as a conventional drug in the clinic? Challenges and current technologies. Drug discovery today Technologies *9*, e71-e174.

Shimizu, S., Abt, A., and Meucci, O. (2011). Bilaminar co-culture of primary rat cortical neurons and glia. Journal of visualized experiments : JoVE.

Shipton, O.A., Leitz, J.R., Dworzak, J., Acton, C.E., Tunbridge, E.M., Denk, F., Dawson, H.N., Vitek, M.P., Wade-Martins, R., Paulsen, O.*, et al.* (2011). Tau protein is required for amyloid {beta}-induced impairment of hippocampal long-term potentiation. The Journal of neuroscience : the official journal of the Society for Neuroscience *31*, 1688-1692.

Silverberg, G.D., Messier, A.A., Miller, M.C., Machan, J.T., Majmudar, S.S., Stopa, E.G., Donahue, J.E., and Johanson, C.E. (2010). Amyloid efflux transporter expression at the blood-brain barrier declines in normal aging. Journal of neuropathology and experimental neurology *69*, 1034-1043.

Slaaby, R. (2015). Specific insulin/IGF1 hybrid receptor activation assay reveals IGF1 as a more potent ligand than insulin. Scientific reports *5*, 7911.

Slack, C., Alic, N., Foley, A., Cabecinha, M., Hoddinott, M.P., and Partridge, L. (2015). The Ras-Erk-ETS-Signaling Pathway Is a Drug Target for Longevity. Cell *162*, 72-83.

Solfrizzi, V., Panza, F., Colacicco, A.M., D'Introno, A., Capurso, C., Torres, F., Grigoletto, F., Maggi, S., Del Parigi, A., Reiman, E.M.*, et al.* (2004). Vascular risk

factors, incidence of MCI, and rates of progression to dementia. Neurology *63*, 1882-1891.

Solit, D.B., and Rosen, N. (2011). Resistance to BRAF inhibition in melanomas. The New England journal of medicine *364*, 772-774.

Soos, M.A., Field, C.E., and Siddle, K. (1993). Purified hybrid insulin/insulin-like growth factor-I receptors bind insulin-like growth factor-I, but not insulin, with high affinity. The Biochemical journal *290 (Pt 2)*, 419-426.

Sosa, L., Dupraz, S., Laurino, L., Bollati, F., Bisbal, M., Caceres, A., Pfenninger, K.H., and Quiroga, S. (2006). IGF-1 receptor is essential for the establishment of hippocampal neuronal polarity. Nature neuroscience *9*, 993-995.

Sperling, R., Salloway, S., Brooks, D.J., Tampieri, D., Barakos, J., Fox, N.C., Raskind, M., Sabbagh, M., Honig, L.S., Porsteinsson, A.P.*, et al.* (2012). Amyloid-related imaging abnormalities in patients with Alzheimer's disease treated with bapineuzumab: a retrospective analysis. The Lancet Neurology *11*, 241-249.

Stanciu, M., Wang, Y., Kentor, R., Burke, N., Watkins, S., Kress, G., Reynolds, I., Klann, E., Angiolieri, M.R., Johnson, J.W.*, et al.* (2000). Persistent activation of ERK contributes to glutamate-induced oxidative toxicity in a neuronal cell line and primary cortical neuron cultures. The Journal of biological chemistry *275*, 12200-12206.

Steen, E., Terry, B.M., Rivera, E.J., Cannon, J.L., Neely, T.R., Tavares, R., Xu, X.J., Wands, J.R., and de la Monte, S.M. (2005). Impaired insulin and insulin-like growth factor expression and signaling mechanisms in Alzheimer's disease--is this type 3 diabetes? Journal of Alzheimer's disease : JAD *7*, 63-80.

Sturchler-Pierrat, C., Abramowski, D., Duke, M., Wiederhold, K.H., Mistl, C., Rothacher, S., Ledermann, B., Burki, K., Frey, P., Paganetti, P.A.*, et al.* (1997). Two amyloid precursor protein transgenic mouse models with Alzheimer disease-like pathology. Proceedings of the National Academy of Sciences of the United States of America *94*, 13287-13292.

Subramaniam, S., Shahani, N., Strelau, J., Laliberte, C., Brandt, R., Kaplan, D., and Unsicker, K. (2005). Insulin-like growth factor 1 inhibits extracellular signal-regulated kinase to promote neuronal survival via the phosphatidylinositol 3-kinase/protein kinase A/c-Raf pathway. The Journal of neuroscience : the official journal of the Society for Neuroscience *25*, 2838-2852.

Subramaniam, S., and Unsicker, K. (2010). ERK and cell death: ERK1/2 in neuronal death. The FEBS journal *277*, 22-29.

Suh, Y., Atzmon, G., Cho, M.O., Hwang, D., Liu, B., Leahy, D.J., Barzilai, N., and Cohen, P. (2008). Functionally significant insulin-like growth factor I receptor mutations in centenarians. Proceedings of the National Academy of Sciences of the United States of America *105*, 3438-3442.

Szaruga, M., Veugelen, S., Benurwar, M., Lismont, S., Sepulveda-Falla, D., Lleo, A., Ryan, N.S., Lashley, T., Fox, N.C., Murayama, S.*, et al.* (2015). Qualitative changes in human gamma-secretase underlie familial Alzheimer's disease. The Journal of experimental medicine *212*, 2003-2013.

Talbot, K., and Wang, H.Y. (2014). The nature, significance, and glucagon-like peptide-1 analog treatment of brain insulin resistance in Alzheimer's disease. Alzheimer's & dementia : the journal of the Alzheimer's Association *10*, S12-25.

Talbot, K., Wang, H.Y., Kazi, H., Han, L.Y., Bakshi, K.P., Stucky, A., Fuino, R.L., Kawaguchi, K.R., Samoyedny, A.J., Wilson, R.S.*, et al.* (2012). Demonstrated brain insulin resistance in Alzheimer's disease patients is associated with IGF-1 resistance, IRS-1 dysregulation, and cognitive decline. The Journal of clinical investigation *122*, 1316-1338.

Taniguchi, S., Suzuki, N., Masuda, M., Hisanaga, S., Iwatsubo, T., Goedert, M., and Hasegawa, M. (2005). Inhibition of heparin-induced tau filament formation by phenothiazines, polyphenols, and porphyrins. The Journal of biological chemistry *280*, 7614-7623.

Tatar, M., Kopelman, A., Epstein, D., Tu, M.P., Yin, C.M., and Garofalo, R.S. (2001). A mutant Drosophila insulin receptor homolog that extends life-span and impairs neuroendocrine function. Science *292*, 107-110.

Terry, R.D., Masliah, E., Salmon, D.P., Butters, N., DeTeresa, R., Hill, R., Hansen, L.A., and Katzman, R. (1991). Physical basis of cognitive alterations in Alzheimer's disease: synapse loss is the major correlate of cognitive impairment. Annals of neurology *30*, 572-580.

Terwel, D., Lasrado, R., Snauwaert, J., Vandeweert, E., Van Haesendonck, C., Borghgraef, P., and Van Leuven, F. (2005). Changed conformation of mutant Tau-P301L underlies the moribund tauopathy, absent in progressive, nonlethal axonopathy of Tau-4R/2N transgenic mice. The Journal of biological chemistry *280*, 3963-3973.

The National Institute of Neurological Disorders and Stroke rt-PAStroke Study Group (1995). Tissue plasminogen activator for acute ischemic stroke. The National Institute of Neurological Disorders and Stroke rt-PA Stroke Study Group. The New England journal of medicine *333*, 1581-1587.

Tsao, H., Atkins, M.B., and Sober, A.J. (2004). Management of cutaneous melanoma. The New England journal of medicine *351*, 998-1012.

Tsubuki, S., Takaki, Y., and Saido, T.C. (2003). Dutch, Flemish, Italian, and Arctic mutations of APP and resistance of Abeta to physiologically relevant proteolytic degradation. Lancet *361*, 1957-1958.

Uhlen, M., Fagerberg, L., Hallstrom, B.M., Lindskog, C., Oksvold, P., Mardinoglu, A., Sivertsson, A., Kampf, C., Sjostedt, E., Asplund, A.*, et al.* (2015). Proteomics. Tissue-based map of the human proteome. Science *347*, 1260419.

Ullrich, A., Gray, A., Tam, A.W., Yang-Feng, T., Tsubokawa, M., Collins, C., Henzel, W., Le Bon, T., Kathuria, S., Chen, E.*, et al.* (1986). Insulin-like growth factor I receptor primary structure: comparison with insulin receptor suggests structural determinants that define functional specificity. The EMBO journal *5*, 2503-2512.

Vaidhyanathan, S., Mittapalli, R.K., Sarkaria, J.N., and Elmquist, W.F. (2014). Factors influencing the CNS distribution of a novel MEK-1/2 inhibitor: implications for combination therapy for melanoma brain metastases. Drug metabolism and disposition: the biological fate of chemicals *42*, 1292-1300.

Vaidhyanathan, S., Wilken-Resman, B., Ma, D.J., Parrish, K.E., Mittapalli, R.K., Carlson, B.L., Sarkaria, J.N., and Elmquist, W.F. (2016). Factors Influencing the Central Nervous System Distribution of a Novel Phosphoinositide 3-Kinase/Mammalian Target of Rapamycin Inhibitor GSK2126458: Implications for Overcoming Resistance with Combination Therapy for Melanoma Brain Metastases. The Journal of pharmacology and experimental therapeutics *356*, 251-259.

van Assema, D.M., Lubberink, M., Bauer, M., van der Flier, W.M., Schuit, R.C., Windhorst, A.D., Comans, E.F., Hoetjes, N.J., Tolboom, N., Langer, O.*, et al.* (2012). Blood-brain barrier P-glycoprotein function in Alzheimer's disease. Brain : a journal of neurology *135*, 181-189.

van Eersel, J., Ke, Y.D., Liu, X., Delerue, F., Kril, J.J., Gotz, J., and Ittner, L.M. (2010). Sodium selenate mitigates tau pathology, neurodegeneration, and functional deficits in Alzheimer's disease models. Proceedings of the National Academy of Sciences of the United States of America *107*, 13888-13893.

van Waterschoot, R.A., Lagas, J.S., Wagenaar, E., van der Kruijssen, C.M., van Herwaarden, A.E., Song, J.Y., Rooswinkel, R.W., van Tellingen, O., Rosing, H., Beijnen, J.H.*, et al.* (2009). Absence of both cytochrome P450 3A and P-glycoprotein dramatically increases docetaxel oral bioavailability and risk of intestinal toxicity. Cancer Res *69*, 8996-9002.

Vingtdeux, V., Giliberto, L., Zhao, H., Chandakkar, P., Wu, Q., Simon, J.E., Janle, E.M., Lobo, J., Ferruzzi, M.G., Davies, P.*, et al.* (2010). AMP-activated protein kinase signaling activation by resveratrol modulates amyloid-beta peptide metabolism. The Journal of biological chemistry *285*, 9100-9113.

Wadman, M. (2012). US government sets out Alzheimer's plan. Nature *485*, 426-427.

Walenkamp, M.J., Karperien, M., Pereira, A.M., Hilhorst-Hofstee, Y., van Doorn, J., Chen, J.W., Mohan, S., Denley, A., Forbes, B., van Duyvenvoorde, H.A.*, et al.* (2005).

Homozygous and heterozygous expression of a novel insulin-like growth factor-I mutation. The Journal of clinical endocrinology and metabolism *90*, 2855-2864.

Walter, H.J., Berry, M., Hill, D.J., and Logan, A. (1997). Spatial and temporal changes in the insulin-like growth factor (IGF) axis indicate autocrine/paracrine actions of IGF-I within wounds of the rat brain. Endocrinology *138*, 3024-3034.

Wang, J., Gallagher, D., DeVito, L.M., Cancino, G.I., Tsui, D., He, L., Keller, G.M., Frankland, P.W., Kaplan, D.R., and Miller, F.D. (2012). Metformin activates an atypical PKC-CBP pathway to promote neurogenesis and enhance spatial memory formation. Cell stem cell *11*, 23-35.

Wang, R., Jin, F., and Zhong, H. (2014). A novel experimental hypoxia chamber for cell culture. American journal of cancer research *4*, 53-60.

Wang, X., Wang, H., Xu, L., Rozanski, D.J., Sugawara, T., Chan, P.H., Trzaskos, J.M., and Feuerstein, G.Z. (2003a). Significant neuroprotection against ischemic brain injury by inhibition of the MEK1 protein kinase in mice: exploration of potential mechanism associated with apoptosis. The Journal of pharmacology and experimental therapeutics *304*, 172-178.

Wang, Z.Q., Chen, X.C., Zhou, L.F., Wu, D.C., Che, X.M., and Yang, G.Y. (2003b). Effects of extracellular signal-regulated kinase (ERK) on focal cerebral ischemia. Chinese Med J-Peking *116*, 1497-1503.

Wellbrock, C., Karasarides, M., and Marais, R. (2004). The RAF proteins take centre stage. Nature reviews Molecular cell biology *5*, 875-885.

Weroha, S.J., and Haluska, P. (2008). IGF-1 receptor inhibitors in clinical trials--early lessons. Journal of mammary gland biology and neoplasia *13*, 471-483.

West, M.J., Coleman, P.D., Flood, D.G., and Troncoso, J.C. (1994). Differences in the pattern of hippocampal neuronal loss in normal ageing and Alzheimer's disease. Lancet *344*, 769-772.

Wiener, C.M., Booth, G., and Semenza, G.L. (1996). In vivo expression of mRNAs encoding hypoxia-inducible factor 1. Biochemical and biophysical research communications *225*, 485-488.

Wischik, C., Bentham, P., Wischik, D., and Seng, K. (2008). Tau aggregation inhibitor (TAI) therapy with remberTM arrests disease progression in mild and moderate Alzheimer's disease over 50 weeks. In Alzheimer's Association International Conference on Alzheimer's Disease (Chicago, USA: Alzheimer's & Dementia).

Wischik, C.M., Edwards, P.C., Lai, R.Y., Roth, M., and Harrington, C.R. (1996). Selective inhibition of Alzheimer disease-like tau aggregation by phenothiazines. Proceedings of the National Academy of Sciences of the United States of America *93*, 11213-11218.

World Health Organisation (1992). The ICD-10 classification of mental and behavioural disorders : clinical descriptions and diagnostic guidelines (WHO).

Xia, D., Watanabe, H., Wu, B., Lee, S.H., Li, Y., Tsvetkov, E., Bolshakov, V.Y., Shen, J., and Kelleher, R.J., 3rd (2015). Presenilin-1 knockin mice reveal loss-of-function mechanism for familial Alzheimer's disease. Neuron *85*, 967-981.

Xu, J., Kurup, P., Bartos, J.A., Patriarchi, T., Hell, J.W., and Lombroso, P.J. (2012). Striatal-enriched protein-tyrosine phosphatase (STEP) regulates Pyk2 kinase activity. The Journal of biological chemistry *287*, 20942-20956.

Xu, J., Kurup, P., Zhang, Y., Goebel-Goody, S.M., Wu, P.H., Hawasli, A.H., Baum, M.L., Bibb, J.A., and Lombroso, P.J. (2009). Extrasynaptic NMDA receptors couple preferentially to excitotoxicity via calpain-mediated cleavage of STEP. The Journal of neuroscience : the official journal of the Society for Neuroscience *29*, 9330-9343.

Yamamoto, H., Saitoh, Y., Fukunaga, K., Nishimura, H., and Miyamoto, E. (1988). Dephosphorylation of microtubule proteins by brain protein phosphatases 1 and 2A, and its effect on microtubule assembly. Journal of neurochemistry *50*, 1614-1623.

Yang, C.H., Huang, C.C., and Hsu, K.S. (2012). A critical role for protein tyrosine phosphatase nonreceptor type 5 in determining individual susceptibility to develop stress-related cognitive and morphological changes. The Journal of neuroscience : the official journal of the Society for Neuroscience *32*, 7550-7562.

Yao, D.L., West, N.R., Bondy, C.A., Brenner, M., Hudson, L.D., Zhou, J., Collins, G.H., and Webster, H.D. (1995). Cryogenic spinal cord injury induces astrocytic gene expression of insulin-like growth factor I and insulin-like growth factor binding protein 2 during myelin regeneration. Journal of neuroscience research *40*, 647-659.

Zhang, Y., Chen, K., Sloan, S.A., Bennett, M.L., Scholze, A.R., O'Keeffe, S., Phatnani, H.P., Guarnieri, P., Caneda, C., Ruderisch, N.*, et al.* (2014). An RNA-sequencing transcriptome and splicing database of glia, neurons, and vascular cells of the cerebral cortex. The Journal of neuroscience : the official journal of the Society for Neuroscience *34*, 11929-11947.

Zhu, J.H., Kulich, S.M., Oury, T.D., and Chu, C.T. (2002). Cytoplasmic aggregates of phosphorylated extracellular signal-regulated protein kinases in Lewy body diseases. The American journal of pathology *161*, 2087-2098.